University of Southampton
Faculty of Medicine, Health & Life Sciences
School of Biological Sciences

The Regulation of Tetrapyrrole Biosynthesis in *Arabidopsis thaliana*

By

Patrick George Stephenson

Thesis for the degree of Doctor of Philosophy
May 2009

UNIVERSITY OF SOUTHAMPTON

ABSTRACT

FACULTY OF MEDICINE, HEALTH AND LIFE SCIENCES
SCHOOL OF BIOLOGICAL SCIENCES

Doctor of Philosophy

THE REGULATION OF TETRAPYRROLE BIOSYNTHESIS IN *ARABIDOPSIS THALIANA*

By Patrick George Stephenson

The biosynthesis of tetrapyrroles, such as haem and chlorophyll, is highly regulated at a number of levels and in a variety of ways. Regulation has been intensely studied in the early stages of biosynthesis, leading to the production of aminolaevulinic acid, but the branchpoint in the pathway, which separates the production of chlorophyll from that of haem and phytochromobilin, is much less understood. This study was undertaken to understand how the chelatase branchpoint is regulated during de-etiolation by a) photoreceptors following light exposure, b) the protein cues GUN4, FLU and OHP1 & 2, and c) hormone signals.

Expression profiles of the branchpoint genes indicated that *CHLH* and *GUN4* mRNA was significantly upregulated when *Arabidopsis* seedlings were transferred from a dark environment into red, far-red, blue or white light, indicating that these genes are important sites for regulation of the pathway. Through further expression analysis, the phytochrome and cryptochrome photoreceptors were shown to control this response. To further understand how the phytochrome signal is acting on these genes, the phytochrome-interacting *PIF1* and *PIF3* genes were studied more closely during de-etiolation. Expression of the *HEMA1* gene, and protochlorophyllide and chlorophyll accumulation in the *pif* mutants revealed a key requirement for these genes in negatively regulating the tetrapyrrole pathway as part of the circadian clock output. Mutant and overexpression lines for the *GUN4*, *FLU* and *OHP1* & *2* genes were used to assess the impact of these factors on the tetrapyrrole pathway. This implicated GUN4 and FLU as having major regulatory roles on both the chlorophyll and haem branches of the pathway. Although OHP1 & 2 showed only a minor regulation of the tetrapyrrole pathway, an essential role for these proteins in chloroplast development and/or protection in the light was demonstrated. Finally, bioinformatics analysis of the expression of chelatase branchpoint revealed *GUN4* as a key regulatory site for hormone signals. Further studies identified the hormone-regulated *MYB50* and *MYB61* genes as strong negative regulators of *GUN4* expression.

Additionally, a range mutants have been produced which retain expression of *HEMA1* during a far-red block of greening response and potentially have a role in the ROS-mediated plastid-to-nucleus signalling pathway. Backcrossing and phenotyping of these mutants has taken place to allow further genetic studies to follow.

TABLE OF CONTENTS

DECLARATION

I, PATRICK GEORGE STEPHENSON

Declare that the thesis entitled TETRAPYRROLE BIOSYNTHESIS IN *ARABIDOPSIS THALIANA* and the work presented in the thesis are my own, and have been generated by me as a result of my own original research. I confirm that:

- This work was done wholly or mainly while in candidature for a research degree at this University.
- Where any part of the thesis has previously been submitted for a degree or any other qualification at this University or any other institution, this has been clearly stated.
- Where I have consulted the published work of others, this is always clearly stated.
- Where I have quoted from the work of others, the source is always given. With the exception of these quotations, this thesis is entirely my own work.
- I have acknowledged all main sources of help.
- Where the thesis is based on work done by myself jointly with others, I have made clear exactly what was done by others and what I have contributed myself.
- Part of this work has been published as:

Stephenson P.G**.** and Terry M.J. (2008) Light signalling pathways regulating the Mg-chelatase branchpoint of chlorophyll synthesis during de-etiolation in *Arabidsopsis thaliana*. *Photochem. Photobiol. Sci.*, 7: 1243-1252.

Stephenson P.G., Fankhauser C. and Terry M.J. (2009) PIF3 is a repressor of chloroplast development. *Proc Natl. Acad. Sci. USA*, 106: 7654-7659.

Signed:.....
Date:.....

ACKNOWLEDGEMENTS

Firstly, thanks go to the BBSRC for funding this project. I would also like to thank Margaret Ahmad, Klaus Apel, Garry Whitelam, Enrico López-Juez, Peter Quail, Xing-Wang Deng and Christian Fankhauser for their generosity with seed stocks, and Mats Hansson, Dieter Soll and Trevor Griffiths for use of their antibodies. Thanks also to Alex McCormac for general advice and Anton Page for help with all aspects of electron microscopy.

I would like to thank my supervisor Matthew Terry for his guidance and expertise throughout my project; and, also from the Terry lab, I would like to thank Felix Jaffé for help with plasmid production and plant transformation, and Enrico Freschet for intellectual discussion.

A big thank you goes to Anna Masters for her help, support and understanding at the most stressful times. Finally, for financial support during my undergraduate and postgraduate years I would like to thank my mother, Rachel Stephenson; and thanks also go to my brothers for providing my competition.

ABBREVIATIONS

40S	40S subunit of ribosomal RNA
ABA	Abscisic acid
ABI	Abscisic acid insensitive
ACT	Actin
AK	Agrikola RNAi silencing line
ALA	Aminolaevulinic acid
BAR	Bialaphos resistance
Bc	Continuous blue light
bHLH	Basic helix-loop-helix
CAB	Chlorophyll a/b binding protein
CAO	Chlorophyll a oxygenase
CCA	Circadian clock associated
CHLD	D subunit of Magnesium chelatase
CHLH	H subunit of Magnesium chelatase
CHLI	I subunit of Magnesium chelatase
Chlide	Chlorophyllide
CHLM	Magnesium protoporphyrin methyltransferase
CO	Constans
COA	Coproporphyrinogen III oxidase
Col	Columbia ecotype
COP	Constitutive photomorphogenic
CRY	Cryptochrome
E	Efficiency
ELIP	Early light-inducible
EMS	Ethylmethane sulphonate
EOD	End of day
FC	Ferrochelatase gene
Fe-CHEL	Ferrochelatase enzyme
FHY	Far-red elongated hypocotyl
FLU	Fluorescent in blue light
FOR	Forward primer
FR HIR	Far-red high irradiance response

FR-BOG	Far-red block of greening
FRc	Continuous far-red light
GK	Gabi-Kat mutant line
GL	Glabrous
Glu-TR	Glutamyl-tRNA reductase enzyme
gPCR	Genomic polymerase chain reaction
GSA	Glutamate-1-semialdehyde aminotransferase
GUN	Genomes uncoupled
GUS	β-Glucuronidase enzyme
hemA	Glutamyl-tRNA reductase (*Hordeum vulgare*)
HEMA	Glutamyl-tRNA reductase gene
Het	Heterozygous
HiFi	High fidelity
HIR	High irradiance response
HO	Haem oxygenase
Hom	Homozygous
HY	Elongated hypocotyl
LAF	Long after far-red light
LB	Lysogeny broth
L*er*	Landsberg *erecta* ecotype
Lhcb	Light-harvesting chlorophyll a/b binding protein
LHCII	Light-harvesting complex II
LHY	Late elongated hypocotyl
LIL	Light inducible-like
LOV	Light, oxygen, or voltage responsive domain
Mg-CHEL	Magenesium chelatase
Mg-PMT	Magnesium-protoporphyrin IX methyltransferase
Mg-protoIX	Magnesium protoporphyrin IX
Mg-protoME	Magnesium-protoporphyrin IX monomethylester
miRNA	Micro RNA
MS	Murashige and Skoog
MYB	V-Myb avian myeloblastosis viral oncogene
NASC	Nottingham *Arabidopsis* Stock Centre
OHP	One helix protein

Pchlide	Protochlorophyllide
Pfr	Far-red light absorbing form of phytochrome
PHOT	Phototropin
PHY	Phytochrome
PIF	Phytochrome interacting factor
PIL	Phytochrome interacting factor-like
PLB	Prolamellar body
POR	Protochlorophyllide oxidoreductase
PPT	Phosphinothrycin
PQ	Plastoquinine
Pr	Red light absorbing form of phytochrome
ProtoIX	Protoporphyrin IX
PS	Photosystem
PSII	Photosystem II
qPCR	Quantitative real-time polymerase chain reaction
Rc	Continuous red light
REV	Reverse primer
ROS	Reactive oxygen species
RT-PCR	Reverse transcription polymerase chain reaction
SAF	Survivor after far-red light
Scp	Small CAB-like protein
SEP	Stress enhanced protein
siRNA	Short interfering RNA
SK	SALK mutant line
Taq	DNA polymerase enzyme isolated from *Thermus aquaticus*
TOC1	Timing of *CAB* expression
TPR	Tetratricopeptide repeat
TTG	Transparent testa glabrous gene
UBQ	Ubiquitin
uidA	β-glucuronidase gene
(V)LFR	(Very) Low fluence response
v/v	Volume per volume
w/v	Weight per volume
WLc	Continuous white light

WS	Wassilewskija ecotype
WT	Wild type
YLS8	Yellow leaf specific
ZTL	Zeitlupe

Chapter 1: Introduction

1.1 Seedling development and de-etiolation

In the model plant *Arabidopsis thaliana*, when a seedling is transferred from the dark to the light this signal is perceived and results in a change from skotomorphogenic growth to photomorphogenic growth, in a process known as de-etiolation. The morphological, molecular and biochemical changes that take place in a seedling subjected to this transition have been studied for many years and as a result much is known about this process. For example, it is well known that dark-grown (etiolated) dicotyledonous seedlings have elongated hypocotyls, small folded cotyledons, and undeveloped chloroplasts (proplastids or etioplasts). Conversely, transfer into the light inhibits hypocotyl elongation, and induces leaf expansion and differentiation, and chloroplast development (de-etiolation) (Mullet, 1988; Dale, 1988; Gruissem, 1989).

1.1.3 Chloroplast development

The development of the chloroplast is arguably the most important process in the plants life, as a fully etiolated seedling has only stored food resources to rely on for energy. As well as the requirement for the chloroplast as the main site of energy production through photosynthesis, a great many other metabolic functions occur in the plastid. They are responsible for the synthesis of fatty acids, aromatic amino acids, purine and pyrimidine bases, isoprenoids (such as carotenoids) and tetrapyrroles (such as haem and chlorophyll) (Lopez-Juez, 2007). As many of these functions are also required in non-photosynthetic tissues, this has been achieved through the differentiation of the proplastid into a range of different plastid types (figure 1.1; Whatley, 1978; Waters and Pyke, 2004).

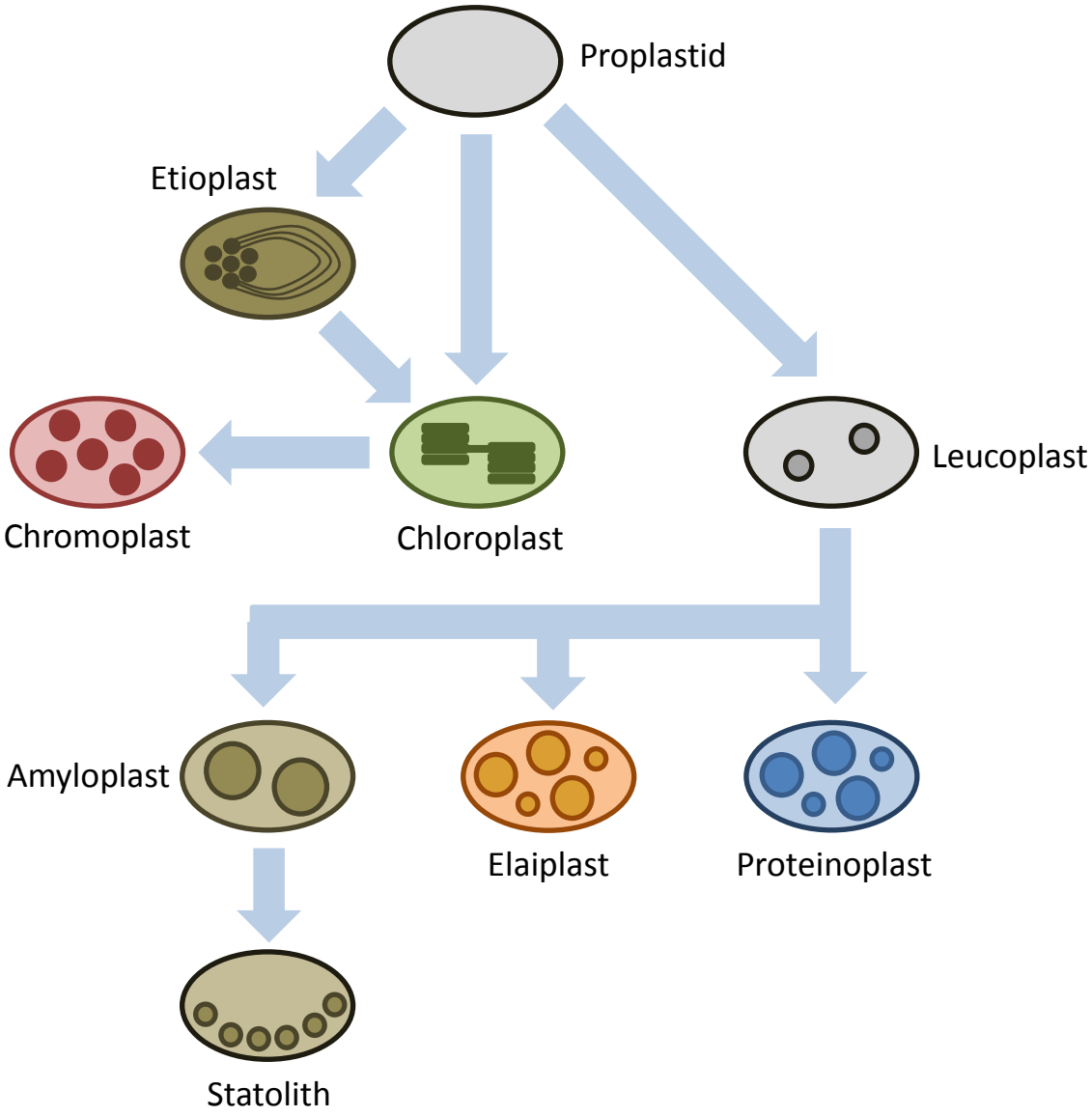

Figure 1.1 The development of different plastid types. The undifferentiated proplastid is directly able to form the etioplast, photosynthesising chloroplast (which is able to form the pigment-containing chromoplast) or partially-undifferentiated leucoplast. The leucoplast can differentiate into the protein containing proteinoplast, lipid storing elaiplast or the starch containing amyloplast, which in turn may then become the gravity-sensing statolith.

The chloroplast, whose origin is now relatively well understood, is believed to have developed from an endosymbiotic bacterium. However, while the genomes of *Nostoc* species, which are believed to be the closest relatives to the ancient chloroplast bacteria, contain approximately 5000 genes, the chloroplast contains only ca. 130 genes, of which 80 encode proteins (Martin *et al*., 2002; Lopez-Juez and Pyke, 2005). The missing genetic material has been transferred from the chloroplast to the nucleus at a rate of approximately one gene for every 16000 pollen grains in tobacco (Huang *et al*., 2003), and as a result tight control is required to ensure that the proteome of the chloroplast is maintained to ensure effective energy capture (discussed in section 1.6). In *Arabidopsis*, expression of the chloroplast genome is controlled by three polymerases: a plastid-encoded polymerase (PEP), which has been retained from the ancestral endosymbiont, and two nuclear encoded polymerases (NEP), one of which is also targeted to the mitochondria (Hedtke *et al*., 1997, 2000; Sato *et al*., 2003; Suzuki *et al*., 2004; Shiina *et al*., 2005). These genes appear to function in a sequential pattern, where the NEP are initially active in the transcription of plastid 'housekeeping' genes, resulting in the expression and synthesis of PEP, which is responsible for the transcription of photosynthesis-related genes (Hajdukiewicz *et al*., 1997). Interestingly, it appears that a precursor to tetrapyrrole synthesis, glutamyl tRNA, is partially responsible for the shift as it has been shown to bind and repress NEP (Hanaoka *et al*., 2005). Although PEP is plastid encoded, the nucleus is still in control of PEP-transcribed genes through the requirement of nuclear-encoded sigma factors which determine promoter specificity of the RNA polymerase (Isono *et al*., 1997).

1.1.3 Protein targeting and import

The transcription and translation of chloroplast genes in the nucleus poses the problem of targeting and import into the chloroplast. The movement of polypeptides across the envelopes is carried out by the Toc (translocon of the outer envelope of chloroplasts) and Tic (translocon of the inner envelope of chloroplasts) complexes, which are able to recognise an N-terminal 'plastid transit peptide' of 20-100 amino acids (Jarvis, 2008). Although these complexes are responsible for the movement of most chloroplast-targetted genes, not all plastid proteins are imported through Tic or

Toc. Envelope proteins, for example, do not contain transit peptides (Hofmann and Theg, 2005), and some inner envelope proteins have been shown to be routed by novel, Toc-independent pathways such as substrate-specific import (Nada and Soll, 2004).

Once in the stroma a second mechanism is required to target specific proteins to the thylakoid membrane. This translocation may be achieved through the ATP-dependent Sec pathway (Schuenemann *et al*., 1999), the Tat pathway which uses the photosynthetic pH gradient as the source of energy (Jarvis and Robinson, 2004), or spontaneous insertion (Jarvis and Robinson, 2004).

1.2 The tetrapyrrole pathway in plants

Tetrapyrrole synthesis is essential in all organisms. In non-photosynthesising organisms tetrapyrrole biosynthesis leads to the production of haem, a critical molecule responsible for many roles including energy transduction. Additionally, in higher plants and light harvesting bacteria the pathway provides chlorophyll, molecules that are essential for photosynthesis. Tetrapyrroles are also required for light perception, through the production of phytochromobilin. These linear molecules, produced from haem in the later stages of the biosynthesis pathway, are covalently attached to a range of phytochromes, thus producing a variety of photoreversible molecules required for red/far-red photo detection (see section 1.3.1.1 for a more detailed discussion). Finally, tetrapyrrole metabolism can generate sirohaem, a co-factor of nitrite and sulphite reductases, and vitamin B12 in bacteria (covered in detail by Tanaka and Tanaka, 2007).

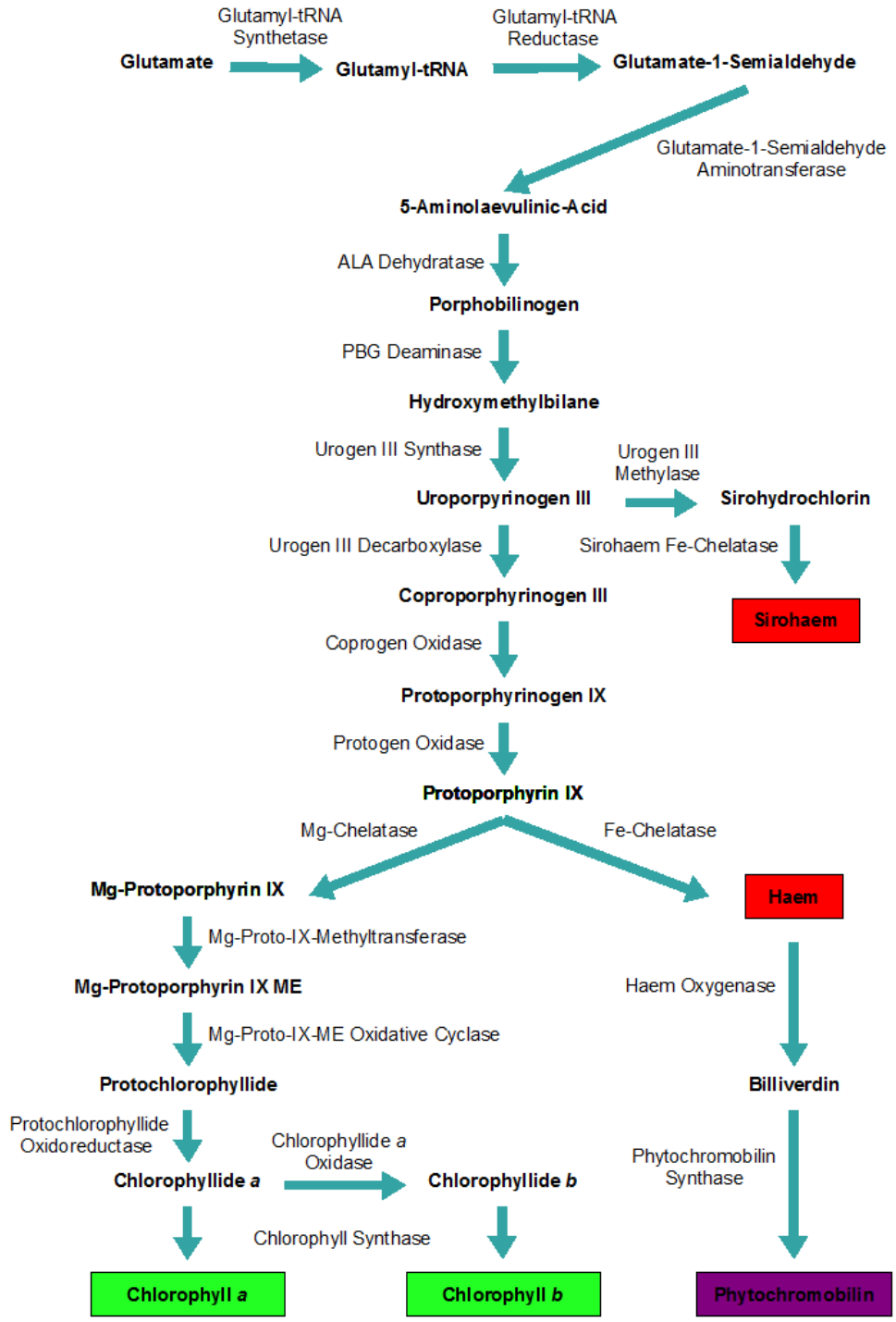

Figure 1.2 The tetrapyrrole biosynthesis pathway in *Arabidopsis thaliana*, leading to the synthesis of sirohaem, chlorophyll, haem and phytochromobilin. Synthesis of the initial precursor 5-aminolaevulinic acid (ALA) from glutamate occurs in three enzymic steps involving glutamyl-tRNA (encoded by the *HEMA* gene family). The pathway branches at uroporphyrinogen III to form Sirohaem, via Sirohydrochlorin. A second branch at protoporphyrin IX results in the formation of haem, through the action of the ferrochelatase enzyme; haem oxygenase and phytochromobilin synthase may then produce the phytochrome chromophore phytochromobilin. Alternatively, Mg-chelatase, a heterotrimer of three subunits (CHLD, CHLH and CHLI), can synthesise Mg-protoporphyrin IX from protoporphyrin IX which leads to the formation of chlorophyll. Tetrapyrrole intermediates are indicated in black and synthesis enzymes in grey.

1.2.1 ALA synthesis

5-Aminolaevulinic acid (ALA) is the first committed precursor in the tetrapyrrole biosynthesis pathway (Figure 1.2). In animals and α-proteobacteria ALA is produced by ALA synthase (ALS) from succinyl-coenzyme A and glycine in a one step condensation reaction known as the Shemin pathway (Radin *et al*., 1950; Sasaki *et al*., 1987). However, plants, algae, cyanobacteria, and green and purple sulphur bacteria generate ALA from glutamate in a two step reaction via the C5 pathway (Beale, 1999). Initially glutamate is ligated to $tRNA_{glu}$ by the enzyme glutamyl-tRNA synthetase (GTS) to produce glutamyl-tRNA. This is followed by a reduction reaction, catalysed by glutamyl-tRNA reductase (Glu-TR - encoded by the *HEMA* gene family), to produce glutamate-1-semialdehyde. Glutamate-1-semialdehyde is then transaminated by glutamate-1-semialdehyde aminotransferase (GSA - encoded by the *GSA* gene) to form ALA.

Failure of *HEMA1* antisense *Arabidopsis* plants to survive under normal growth conditions (Kumar and Soll, 2000), coupled with the fact that no ALS gene has yet been identified in plants, confirms their dependence on the C5-pathway for ALA synthesis. Interestingly, however, the protists *Euglena gracilis* (Mayer and Beale, 1992) and *Scenedesmus obliquus* (Drechsler-Thielmann *et al*., 1993) are known to use both the C5 and Shemin pathways to produce ALA.

1.2.2 Porphyrin synthesis

In the intermediate stages of tetrapyrrole synthesis two molecules of ALA are initially condensed to generate the first monopyrrole, porphobilinogen, by the enzyme porphobilinogen synthase. The sequential combination of two porphobilinogen molecules produces hydroxymethylbilane, which may then be cyclised to form the first cyclic porphyrin in the parthway, uroporphyrinogen III. Two different enzymes then act on uroporphyrinogen III: the first is S-adenosyl-L-methionine-dependent uroporphyrinogen III methyltransferase which is responsible for the production of sirohydrochlorin and ultimately sirohaem (Murphy *et al*., 1974). Alternatively uroporphyrinogen III decarboxylase can decarboxylate the acetate side chain of each porphyrin ring of uroporphyrinogen to form coproporphyrinogen III (Akthar, 1994).

Coproporphyrinogen III oxidase (COA) is then responsible for the production of protoporphyrinogen IX, and finally protoporphyrinogen IX oxidase catalyses protoporphyrin IX synthesis. Protoporphyrin IX is found at a branch point in the tetrapyrrole biosynthesis pathway.

1.2.3 Chlorophyll synthesis

The incorporation, or chelation, of Mg^{2+} into protoporphyrin IX is the first commited step in chlorophyll biosynthesis (reviewed in great detail by Tanaka and Tanaka, 2007). This reaction is mediated by the magnesium chelatase enzyme (Mg-CHEL), and is responsible for the production of Mg-protoporphyrin IX. Mg-protoporphyrin IX methyltransferase (Mg-PMT) and Mg-protoporphyrin IX-ME monomethyl ester cyclase (Mg-PCY) are then responsible for the production of protochlorophyllide (Pchlide). Pchlide is reduced by protochlorophyllide oxidoreductase (POR) to chlorophyllide (Chlide) *a*, which then forms chlorophyll *a* through the action of chlorophyll *a* synthase, and is subsequently partly converted to chlorophyll *b* by chlorophyll *a* oxygenase (CAO).

1.2.4 Haem synthesis

The chelation of Fe^{2+} ions into protoporphyrin IX, rather than Mg^{2+}, by the enzyme ferrochelatase (Fe-CHEL), leads to the production of protohaem (Dailey, 1990; Loeb, 1995; reviewed by Tanaka and Tanaka, 2007). Protohaem is then incorporated into numerous different haem proteins, or is modified further for the synthesis of other types of haem found in cytochrome *c* and terminal oxidases. Fe-CHEL activity has also been detected in the mitochondria of plant cells (Porra and Lascelles, 1968); however plastids are the major site of haem production (Cornah *et al*., 2002).

1.2.5 Phytochromobilin synthesis

Alternative to haem synthesis from protohaem is the production of phytochromobilin, a chromophore required for functional phytochrome molecules

(reviewed in detail by Davis, 2006). The action of two enzymes, haem oxygenase and phytochromobilin synthase, that work consecutively, produce phytochromobilin from protohaem. This molecule can then be bound to one of five phytochromes: phyA-E (discussed in more detail in section 1.3.1.1).

1.3 Regulation of tetrapyrrole biosynthesis in plants by light

1.3.1 Current understanding of *Arabidopsis* photoreceptors

1.3.1.1 The phytochromes

1.3.1.1.1 Phytochrome molecule discovery

It has been known for many years that a red light photoreceptor exists in plants and in the late 1950s the first phytochrome was detected and isolated (Butler *et al*., 1959). Although it was suspected that more than one phytochrome was required to mediate the many responses attributed to this photoreceptor, 30 years passed until the sequence was established for three of these phytochromes (*PHYA-C*) in *Arabidopsis* (Vierstra and Quail, 1986; Sharrock and Quail, 1989). Additionally, Sharrock and Quail (1989) suggested the presence of two other phytochromes (*PHYD* and *PHYE*) which were soon identified (Clack *et al*., 1994).

1.3.1.1.2 Phytochrome structure and mechanism of action

The phytochrome molecule consists of an apoprotein (designated phyA-E) and the linear tetrapyrrole phytochromobilin (the synthesis of which is described in section 1.2.5); binding of the apoprotein to the bilin molecule occurs spontaneously, in the absence of other proteins or co-factors (Lagarias and Lagarias, 1989). The region for binding has been mapped to a cysteine residue (in the GAF domain [derived from vertebrate cGMP-specific phosphodiesterases, cyanobacterial Adenylate cyclases, and Formate hydrogen lyase transcription activator FhlA]) in the N-terminal domain (Lagarias and Rapoport, 1980; Lamparter *et al*., 2001; Wu and Lagarias, 2000), while the adjacent PAS (derived from Period clock (PER) protein, Aromatic hydrocarbon Receptor Nuclear Translocator (ARNT), and SIngle Minded (SIM)) and PHY (domain

specific to plant phytochromes) domains are required for tuning the spectroscopic properties of the bound bilin (Wu and Lagarias, 2000). The C-terminus of the protein, on the other hand, contains two further PAS domains and a regulatory histidine kinase domain (Quail, 1997; Yeh and Lagarias, 1998; Montgomery and Lagarias, 2002).

Phytochrome signalling is intiated by the photoconversion of the phytochrome molecule from an inactive Pr (red (R) light-absorbing) form to the active Pfr (far-red (FR) light-absorbing) form. Transfer of dark (D) grown plant material to R light (660nm) causes Pr to be converted to Pfr and further transfer to FR light (most strongly at 730nm) causes Pr to be reformed (Butler *et al*., 1959). Although transfer back to D from R light also causes Pr to be formed, in a process known as D reversion, this is considerably slower than FR light exposure (Furuya and Shafer, 1996). Additionally, it has also been shown that phytochromes weakly absorb blue (B) light (Furuya and Song, 1994). The exact structural changes that take place have mostly been elucidated, and it has been demonstrated that R light triggers a "Z" to "E" isomerization in the C-15 double bond between the C and D rings of the chromophore, which is accompanied by rearrangement of the apoprotein backbone (figure 1.3) (Quail, 1997; Fankhauser, 2001).

Phytochromes may be separated into two distinct groups: light labile (type I) and light stable (type II) (Furuya, 1989). PhyA alone belongs to the type I group, and becomes rapidly degraded upon exposure to R, FR or white (W) light; phyB-E, on the other hand, remain stable upon transfer to light and belong to the type II group. Interestingly, one study has since demonstrated that continuous FR light treatment could be replaced by intermittent FR light pulses to induce some phyA responses. Analysis of these action spectra suggests that neither the dark-synthesised Pr form of PhyA, nor the Pfr form, produced from photoconversion, is active in inducing the signal. Instead the signal is thought to be produced during the phototransformation from Pfr to Pr (Shinomura *et al*., 2000). As a result, the different phytochrome family members produce responses to different fluence and irradiance treatments. The associated responses have been paired up with the phytochrome responsible in table 1.1, and the details of photosensory activity are summarised in table 1.2.

a)

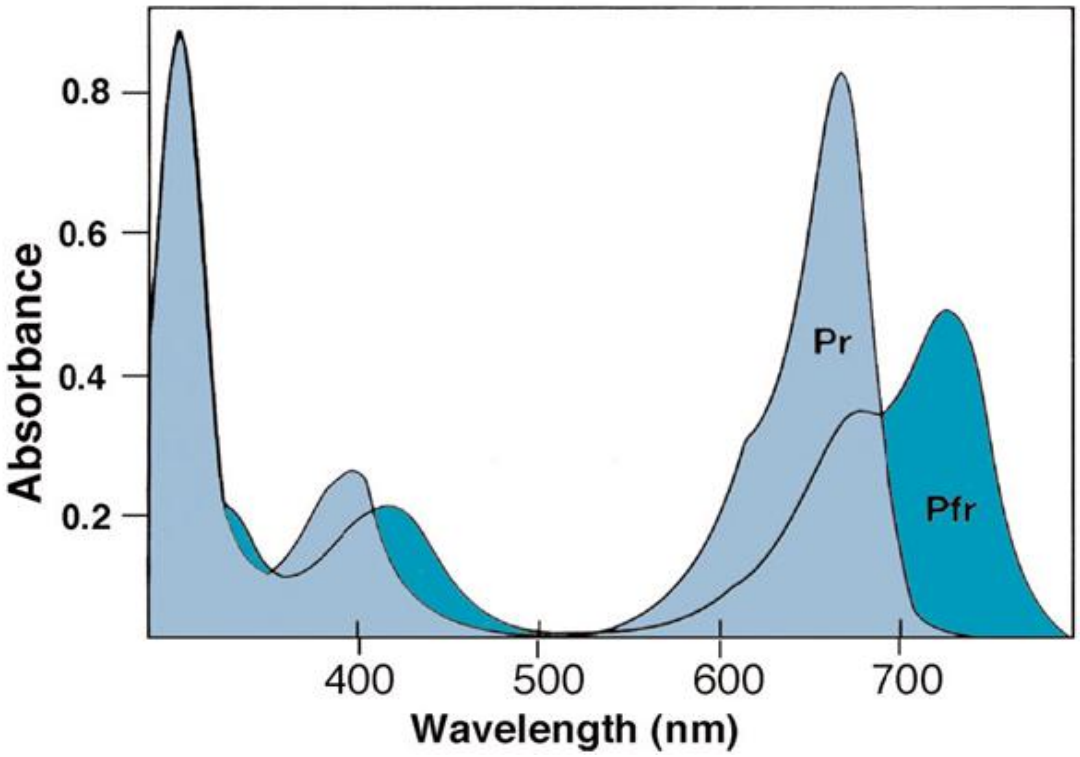

b)

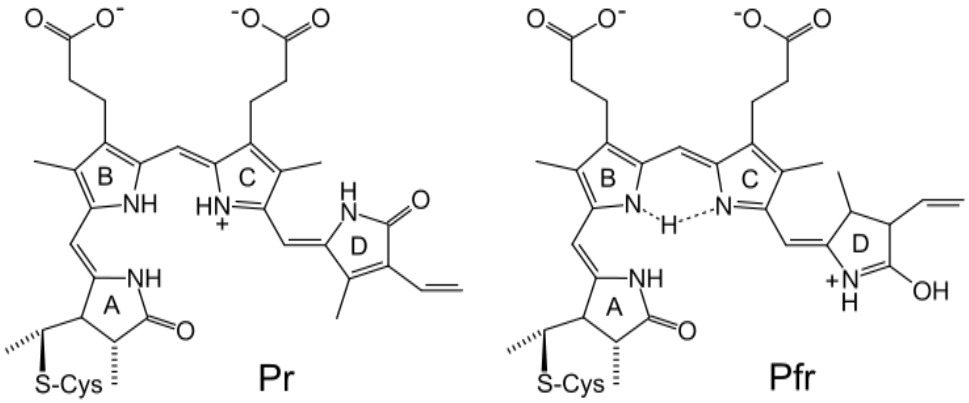

Figure 1.3 Photoconversion of phytochrome. The shift in phytochrome strucure from Pr to Pfr, following red light treatment, causes a shift in absorption spectrum resulting from a conformational change in the apoprotein-bound chromophore. a) Different absoption spectrums of the Pr and Pfr forms of phytochrome (from Wang and Deng, 2002a), b) conformational change in the phytochrome chromophore upon exposure to red light.

Table 1.1 The different responses of the phytochrome family members resulting from different fluences or irradiations (modified from Wang and Deng, 2002a).

Phytochrome Member	Photosensory Activity	Physiological Role
phyA	VLFR	Seed germination
	FR-HIR	Seedling de-etiolation under FRc; promote flowering
phyB	LFR	Seed germination under Rc
	R-HIR	Seedlong de-etiolation under Rc
	EOD-FR (R/FR Ratio)	Shade avoidance response (petiole and internode elongation, and flowering)
phyC	R-HIR	Seedling de-etiolation under Rc
phyD	EOD-FR (R/FR Ratio)	Shade avoidance response (petiole and internode elongation, and flowering)
phyE	LFR	Seed germination
	EOD-FR (R/FR Ratio)	Shade avoidance response (petiole and internode elongation, and flowering)

(VLFR = very low fluence response; LFR = low fluence response; HIR = high irradiance response; EOD-FR = end of day far red light response)

Table 1.2 Features of phytochrome photosensory activity (modified from Wang and Deng, 2002a).

Action	Fluence requirement	Photo reversibility
VLFR	0.1-1 µmol/m^2	No
LFR	1-1000 µmol/m^2	Yes
HIR	>1000 µmol/m^2	No

1.3.1.1.3 Phytochrome function

1.3.1.1.3.1 Seed germination and seedling de-etiolation

In the control of seed germination three phytochromes (phyA, phyB and phyE) have been implicated as having a role (Reed *et al*., 1994; Botto *et al*., 1996; Shinomura *et al*., 1996; Hennig *et al*., 2002). While phyA is known to input via the photo-irreversible VLFR response, and phyB through the photo-reversible LFR, the role of phyE is less well understood, although it has been speculated that it is required for phyA action (Hennig *et al*., 2002).

Following seed germination the rapid inhibition of hypocotyl extension and initiation of cotyledon expansion have been shown to be largely controlled by the

phototropin family (Folta and Spalding, 2001; see section 1.3.1.3 for a more detailed discussion), although the phytochromes have also been attributed a role. Under FR light light only phyA is active (Nagatani *et al*., 1993; Whitelam *et al*., 1993), while under R and W light although phyB gives the strongest phenotypic response phyA has been shown to be the major active phytochrome controlling gene expression, and double and triple mutant studies have also given a strong role to phyD (Neff and Van Volkenburgh, 1994; Johnson *et al*., 1994; Aukerman *et al*., 1997, Tepperman *et al*, 2004). Additionally, the *phyC* mutant has a longer hypocotyl and less expanded cotyledons under R light, and this is additive to the *phyA* mutant phenotype, but not *phyB* (Franklin *et al*., 2003a, 2003b; Monte *et al*., 2003).

1.3.1.1.3.2 Vegetative development

When under a canopy plants are exposed to a different ratio of R:FR light than when they are in the open. The phytochromes are able to perceive this difference, through a ratio of Pr:Pfr, and respond through various phenotypic changes including an increase in petiole length, early flowering, increase in length-to-width ratio of leaves, and an increase in stem length (Smith and Whitelam, 1997). Evidence of a constitutive shade avoidance phenotype in the *phyB* mutant (Lopez-Juez *et al*, 1992), and an enhanced phenotype in the *phyBphyD* or *phyBphyE* doubles, suggested these phytochromes as the main contributers to this response (Aukerman *et al*., 1997; Devlin *et al*., 1999). Additionally, a distinct role for phyE in regulating rosette leaf patterning was elucidated by studying the *phyAphyBphyE* triple mutant, which displayed elongated rosette internodes, a phenotype that was not apparent in the *phyAphyBphyD* triple (Devlin *et al*., 1998).

1.3.1.1.4 Phytochrome signalling

1.3.1.1.4.1 Phytochrome localisation

In *Arabidopsis* all five phytochromes migrate from the cytoplasm to the nucleus in a light-dependent manner, and this requires a Pr-to-Pfr conformational change (Kircher *et al*., 1999; Kircher *et al*., 2002; Sakamoto and Nagatani, 1996;

Yamaguchi *et al*., 1999). However, the kinetics of this tanslocation varies for the different phytochromes, for example only phyA is able to translocate under FR light, and the movement of phyA is much faster than the other phytochromes (Kircher *et al*., 2002; Nagy and Schafer, 2002).

Once in the nucleus, phytochromes have been shown to localise in distinct nuclear speckles which has been shown to be necessary for signalling, although the exact function remains elusive (Hisada *et al*., 2000; Kircher *et al*., 2002; Huq *et al*., 2003). However, import into the nucleus, requiring only a Pfr-Pr heterodimer, is not sufficient for localisation to the speckles, which requires a Pfr-Pfr homodimer (Chen *et al*., 2003). Additionally, the C-terminal PRD domain of the phytochrome has been shown to be required for this process, as *phyA* and *phyB* PRD mutants are nuclear imported but do not localise to speckles (Chen *et al*., 2003; Kircher *et al*., 2002; Yanovsky *et al*., 2002).

Recently the importance of the nuclear speckles was put into question when an N-terminal portion of phyB was fused to heterologous domains, producing a hypersensitive response to red light despite not forming nuclear bodies (Matsushita *et al*., 2003). However, the additional localisation of cry2 (Mas *et al*., 2000), COP1 (CONSTITUTIVE PHOTOMORPHOGENIC 1) (von Arnium *et al*., 1998), HY5 (ELONGATED HYPOCOTYL 5) (Ang *et al*., 1998), and LAF1 (LONG AFTER FAR-RED LIGHT 1) (Ballesteros *et al*., 2001; Mas *et al*., 2000) to the nuclear speckles has resulted in the theory that they may be used as sites of protein degradation.

1.3.1.1.4.2 Nucleus-located-phytochrome signalling in seedling photomorphogenesis

Microarray studies have revealed that among the functionally classifiable early light-responsive genes induced within 1 hour of far-red or red light exposure, 44% (for FR light) and 25% (for R light) encode transcription factors. Additionally, a second set of transcription factors is also repressed following light exposure (for example Tepperman *et al*., 2001, 2004), indicating the requirement for both instigation and suppression of signalling pathways at this time.

Nuclear-located light-responsive transcription factors are known to be highly important in the signalling of phytochrome responses, and transcriptional regulation, post-translational modification and degradation of these transcription factors are all important in the light-regulated control of development. Regulation of both positively and negatively acting transcription factors has been documented, although it is not always easy to determine which of these catagories a transcription factor falls into. PIF3, for example, has been widely debated to be both a positive and negative regulator of phytochrome signalling so that the current understanding is of a mechanistic duality, allowing both positive and negative functions (discussed in more depth in section 4.1) (Al-Sady *et al*., 2008).

Several basic mechanisms are involved in regulating transcription factor transcription, translation and activity in response to light. Firstly, transcription factor regulation is part of a large and complex network of light signalling inputs and outputs, resulting in the ability of various different photoreceptors to induce or repress their expression. Additionally, transcription factors may regulate their own synthesis, for example the *COMMON PLANT REGULATORY FACTOR 1* from parsley is light induced but has the ability to bind to both the LREs (light-responsive cis elements e.g. the G-box) and its own promoter (Weisshaar *et al*., 1991; Feldbrugge *et al*., 1994).

Secondly, ubiquitin-mediated degradation of light-signalling factors is widely acknowledged as a key mechanism in light signalling networks (Wei and Deng, 1996). One major component in this system is ring-finger type ubiquitin E3 ligase, COP1 (Suzuki *et al*., 2002a). COP1 is required for the degradation of positive regulators of photomorphogenesis in the dark via ubiquitylation and subsequent targeting by the 26S proteasome. Upon light exposure COP1 is excluded from the nucleus, thereby allowing photomorphogenesis to proceed (von Arnim and Deng, 1994; Seo *et al*., 2003; Yi and Deng, 2005). Thirdly, the bHLH (basic helix-loop-helix domain) and bZIP (basic leucine zipper domain) families of transcription factors may homo- or heterodimerize, and the ability and opportunity to do so allows the activation of different transcriptional networks (Jackoby *et al*., 2002; Toledo-Ortiz *et al*., 2003; Holm *et al*., 2002; Schindler *et al*., 2002; Zimmerman *et al*., 2004). Finally, phosphorylation of transcription factors can influence their ability to bind the LRE or

their subcellular location (Feldbrugge *et al*., 1994; Klimczak *et al*., 1992, 1995; Harter *et al*., 1994).

Mutations in the transcription factors *FAR1* (*FAR-RED IMPAIRED RESPONSE 1*), *FHY3* (*FAR-RED ELONGATED HYPOCOTYL 3*) and *LAF1* result is a hyposensitive response to far-red light, indicating a key role for these genes in phyA signalling. While *LAF1* is a member of the R2R3 domain MYB transcription factor family, *FAR1* and *FHY3* are novel transposon-derived transcription factors, which interact with each other, but all are specific to FR light (Hudson *et al*., 1999; Wang and Deng, 2002b; Hudson *et al*., 2003; Ballesteros *et al*., 2001). *HFR1* (*LONG HYPOCOTYL IN FAR-RED 1*) and *HY5* are also known to function in this pathway, although they are thought to a) function further downstream, as they affect a smaller subset of genes, and b) also respond to other wavelengths of light (Fairchild *et al*., 2000; Duek and Fankhauser, 2003; McCormac and Terry, 2002a). COG1 (COGWHEEL 1) and OBP3 (OBF4 BINDING PROTEIN 3), both Dof transcription factors, and MYC2, a bHLH transcription factor, are also required for correct regulation of photomorphogenesis (Park *et al*., 2003; Ward *et al*., 2005; Yadav *et al*., 2005).

Finally, a subset of bHLH transcription factors, known as PHYTOCHROME INTERACTING FACTORs (PIFs), interact directly, and specifically, with the Pfr form of phytochrome. PIF3, 4, 5 and 6 interact mainly with phyB, and PIF1 interacts with both phyA and phyB (Castillon *et al*., 2007; Monte *et al*., 2007). However, as stated previously, although a lot of work has been done to elucidate the exact role of the PIFs, it is proving difficult to separate their positive and negative-regulatory functions (covered in more detail in section 4.1). The functions and interactions of the above mentioned transcription factors is summarised in figure 1.4.

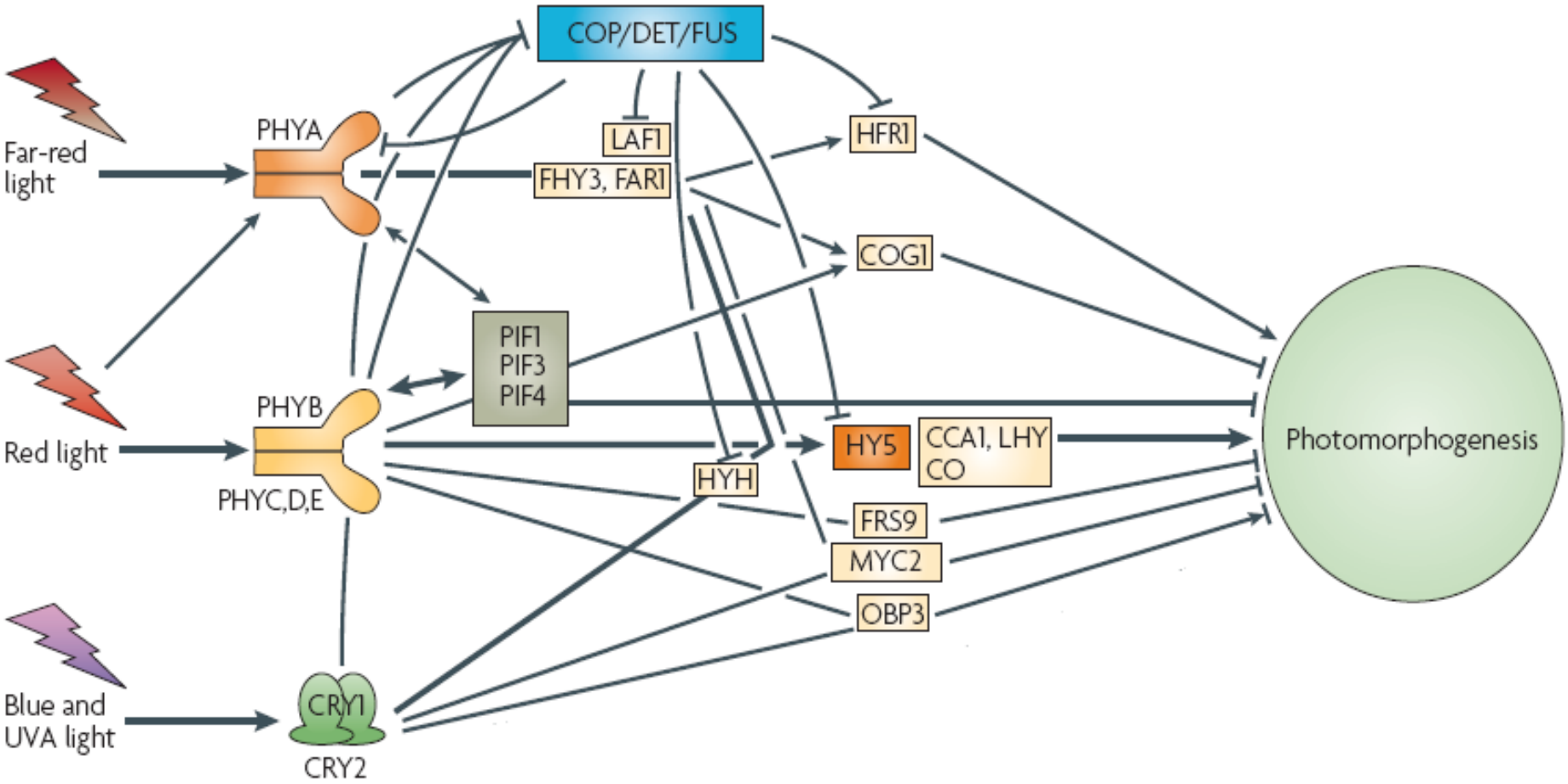

Figure 1.4 Tanscriptional networks for seedling photomorphogenesis in *Arabidopsis thaliana.* Formation of the functionally active Pfr form of phytochrome initiates a signalling cascade through the bHLH phytochrome interacting factors (PIFs) and and the circadian clock-input factor FHY3. The key transcription factor HY5 acts as a signal integration point of major branches downstream of both the phytochomes and cryptochromes, and the COP/DET/FUS ubiquitin signalling componants acts as light-inactivatible repressors of photomorphogenesis. Bold lines indicate convergence pathways. Adapted from Jiao *et al*., 2007.

1.3.1.1.4.3 Cytoplasm-located-phytochrome signalling

As PHYA does not contain a nuclear localisation signal (NLS), it has been shown that FHY1 (FAR-RED ELONGATED HYPOCOTYL 1) and FHL (FHY1-LIKE), which do contain NLS, and mutations in which severely impair phytochrome signalling, are required for phyA nuclear import (Whitelam *et al*., 1993; Desnos *et al*., 2001; Zeidler *et al*., 2001; Hiltbrunner *et al*., 2005, 2006; Zhou *et al*., 2005). Recently a double *fhy1fhl* mutant was produced (Rosler *et al*., 2007) which elucidated the function of cytoplasmic phyA, without any input from the nuclear localised phytochrome. Rosler *et al*. (2007) demonstrated effectively that phyA was no longer imported into the nucleus, yet the distinct phyA-mediated inhibition of hypocotyl gravitropism response, along with inhibition of hypocotyl extension in blue light and red-light mediated phototropic responses remained. This demonstrates that cytoplasmic phytochrome is able to produce a signal which is required to produce a subset of phytochrome responses.

1.3.1.1.5 Interactions of light and directional sensing

Gravity provides plant stems with a direction to orientate themselves when breaking through the soil surface in search of sunlight (negative gravitropism), and plant roots with a direction in which to seek water and nutrients (positive gravitropism). Additionally, other plant organs show intermediate gravitropic responses, growing perpendicular to the ground, and are able to change their growth in response to changing gravitropic signals (Hangarter, 1997). However, it has also been extensively shown that light, and in particular phytochrome-mediated signalling, is able to interact with gravitropic signalling. The exposure of *Arabidopsis* seedlings to R or FR light, for example, abolishes the negative gravitropism of the hypocotyl which is apparent in the D, or B or W light growth, and this response is controlled by phyA and phyB (Liscum and Hangarter, 1993; Poppe *et al*., 1996; Robson and Smith, 1996). It has been suggested that this gives an ecological advange by allowing plants to prioritise phototropic growth over gravitropic.

1.3.1.2 The cryptochromes

1.3.1.2.1 Cryptochrome discovery

The cryptochrome (cry) family of B/UV-A sensing photoreceptors is composed of three members, although the functional output is dominated by cry1 and cry2. The first member, originally named *HY4* (*ELONGATED HYPOCOTYL 4*) was identified in a mutant screen for *Arabidopsis* seedlings unable to inhibit hypocotyl elongation in white light (Koornneeff *et al*., 1980), and this result was later confirmed in a T-DNA screen for seedlings deficient in B/UV-A responses (Ahmad and Cashmore, 1993). The *hy4* mutant, later named *cryptochrome 1* (*cry1*), presented a near-etiolated phenotype under blue or UV-A light, but in contrast had a de-etiolated phenotype under R or FR light, and an intermediate response under W light. The *cry1* mutant was also later shown to be affected in anthocyanin accumulation and chalcone synthase gene expression (Ahmad *et al*., 1995). Conversely, plants over-expressing *CRY1* are hypersensitive to blue light and over accumulate anthocyanin (Lin *et al*., 1996). Sequence analysis of the *CRY1* protein showed sequence similarity to a rare class of flavoproteins, known as phytolyases, which mediate repair of UV-damaged DNA (Sancar, 1994).

Two other members, cry2 and cry3, have since been identified. Cry2, which is similar in structure to cry1, also mediates hypocotyl responses but is highly light labile and therefore shows a more discernible phenotype under low fluence blue light (Lin *et al*., 1998). Cry2, along with cry1, has also been shown to affect flowering time (Bagnall *et al*., 1996; Guo *et al*., 1998). Cry3, on the other hand, is less similar structurally and functionally to cry1. The CRY3 amino acid sequence is similar to *Synechocystis* CRY DASH (Drosophila-Arabidopsis-Synechocystis-Human) functioning as a transcriptional repressor (Brudler *et al*., 2003). Additionally, unlike CRY1 or CRY2, CRY3 lacks a C-terminal extension and contains a targeting sequence suggested to target the photoreceptor to mitochondria and/or chloroplasts (Kleine *et al*., 2003).

Like photolyases, cryptochromes contain two noncovalently bound chromophores, flavin adenine dinucleotide (FAD) as a key cofactor to carry out initial

biological function upon photoexcitation, and methenyltetrahydrofolate (MTHF) as a light-harvesting antenna to enhance biological efficiency. It has been shown that primary light reactions in cry1 involve intra-protein electron transfer from tryptophan and tyrosine residues to its flavin cofactor FAD (Giovani *et al*., 2003).

Cryptochrome family members have been identified in many other species, including tomato, pea and rice, which contain four, three and three cryptochromes, respectively (Perrotta *et al*., 2000; Matsumoto *et al*., 2003; Platten *et al*., 2005). In these species the cryptochromes show considerable homology, structure and function to those in *Arabidopsis*.

1.3.1.2.2 Cryptochrome signalling

The cryptochrome signalling mechanism was demonstrated through fusion of the C-terminal domain of either CRY1 (CCT1) or CRY2 (CCT2) to β-Glucuronidase (GUS), both of which display a constitutive photomorphogenic (COP) phenotype (Yang *et al*., 2000). Both CCT1 and CCT2 were shown to bind to COP1, a negative regulator of photomorphogenic responses (Deng *et al*., 1992; Wei *et al*., 1994), indicating that cry1 and cry2 signalling is mediated through negative regulation of COP1 by direct interaction (Yang *et al*., 2001; Wang *et al*., 2001). Additionally, removal of the N-terminal domain of CRY1 (CNT1) leads to a COP phenotype in darkness, and overexpression of the CNT in WT plants conferred a *cry1*-like phenotype (Sang *et al*., 2005) through a dominant-negative mechanism.

Following transfer to B light, but not R or FR light, both cry1 and cry2 become rapidly phosphorylated in the CCT region (Bouly *et al*., 2003; Shalitin *et al*., 2002). This phosphorylation requires the homodimerizarion of the cryptochrome molecule via CNT, and this interaction is required for signalling (Sang *et al*., 2005). Additionally, the crystal structure of cry3 revealed that it is normally present in a dimeric state (Klar *et al*., 2007), but it is currently not known whether this is required for function.

Genetic and biochemical studies have demonstrated that cryptochromes physically interact with phytochromes, and this is required for the regulation of

photomorphogenic development, floral initiation, and in the entrainment of the circadian clock in *Arabidopsis* (Casal and Mazzella, 1998; Somers *et al*., 1998; Neff and Chory, 1998; Mockler *et al*., 1999; Hennig *et al*., 1999; Ahmad *et al*., 1998; Mas *et al*., 2000).

1.3.1.2.3 Cryptochrome function

Cryptochromes have been shown to control many photomorphogenic responses within *Arabidopsis*, one of which became immediately obvious when a mutation in *cry2* was shown to be allelic to the late-flowering mutant *fha* (Guo *et al*., 1998). Although the *cry1cry2* double mutant only shows a similar delay in flowering to the *cry2* single mutant under W light, there was an increase in initiation time under B light suggesting that cry2 acts redundantly to cry1 in promoting flowering initiation (Mockler *et al*., 1999). The cryptochrome molecular function behind this response was later shown to be a role in stabilising CONSTANS (CO) protein level, in an antagonistic action to phyB, thereby maintaining the circadian clock output (Mockler *et al*., 1999; Valverde *et al*., 2004).

Recent studies have elucidated a role for the cryptochromes in controlling stomatal pore opening (Mao *et al*., 2005). While the *cry1cry2* double mutant displays a reduced capacity for stomatal opening under B light, and therefore an increased drought tolerance, *CRY1* over-expressing plants show a hypersensitive response in B light. Cryptochrome control was shown to be functioning through COP1, as stomata in the *cry1cry2cop1* triple mutant open as wide as those in the *cop1* single mutant, which shows a hypersensitive response (Mao *et al*., 2005). This study also highlighted a role for the cryptochromes in mediating B light-dependent random hypocotyl bending.

Finally, both cry1 and cry2 have been shown to function in *Arabidopsis* root growth control. As well as playing a major role in root chloroplast development (Usami *et al*., 2004), it has been demonstrated that cry1 is a positive regulator of primary root growth under B light, through the study of mutant and over-expressing plants. Conversely, cry2 was shown to act negatively in the control of primary root growth, indicating that cry1 and cry2 act antagonistically in this function (Canamero *et al*., 2006).

1.3.1.3 The phototropins

1.3.1.3.1 Phototropin discovery

Although B light-mediated phototropic responses in plants have been known and studied for over 200 years, the first phototropin, denoted *NONPHOTOTROPIC HYPOCOTYL 1* (*NPH1*), was not identified in *Arabidopsis* until relatively recently (Liscum *et al*., 1995). Following genetic and biochemical studies, which demonstrated the ability of *NPH1* to autophosphorylate under B light (Cristie *et al*., 1999; Briggs *et al*., 2001), it was renamed *PHOTOTROPIN 1* (*PHOT1*), and *PHOT2* was discovered soon after (Briggs *et al*., 2001a, 2001b, 2002).

The protein structures of the phototropins can be separated into two parts: a photosensory region at the N terminus, containing two very similar domains of ~110 amino acids designated LOV1 and LOV2, and a serine/ threonine kinase domain at the C terminus. LOV domains are members of the PAS domain superfamily associated with cofactor binding and mediating protein interactions (Taylor and Zhulin, 1999). However, they are most closely related with those domains which respond to external signals such as light, oxygen, or voltage, hence LOV (Huala *et al*., 1997). The phototropin LOV domains are capable of binding the cofactor flavin mononucleotide (FMN) and consequently function as B light sensors (Christie *et al*., 1999; Salomon *et al*., 2000), whereby stimulation of the LOV domain leads to autophosphorylation via the C-terminal kinase domain.

1.3.1.3.2 Phototropin function

The *Arabidopsis* phot1 and phot2 photoreceptors display both similar and distinct functions within the plant. Hypocotyl phototropism is controlled by both phot1 and phot2 under high intensity B light, however, under low intensities only phot1 has a role (Sakai *et al*., 2000, 2001). Phot1 and phot2 are also both required for chloroplast movement, however, under low light conditions phot1 is more responsible for movement towards the light source to maximise photosynthetic capacity, while under high light phot2 is more responsible for movement away from the light source to avoid photodamage (Sakai *et al*., 2001; Kagawa and Wada, 2000; Kagawa *et al*., 2001;

Jarillo *et al*., 2001a). The phototropins have also been attributed to controlling B light-mediated stomatal pore opening, although in this role both phot1 and phot2 contribute equally (Kinoshita *et al*., 2001). Finally, phototropins have been associated with ceasing hypocotyl growth and stimulating cotyledon expansion in de-etiolating seedlings (Folta and Spalding, 2001; Ohgishi *et al*., 2004).

1.3.1.4 Other *Arabidopsis* photoreceptors

1.3.1.4.1 The ZTL family

The ZTL family members, *ZEITLUPE* (*ZTL*), *FLAVIN-BINDING, KELCH REPEAT, F-BOX 1* (*FKF1*) and *LOV KELCH PROTEIN 2* (*LKP2*), are relatively recently discovered photoreceptors which are now known to be associated with the circadian clock (Somers *et al*., 2000; Nelson *et al*., 2000; Schultz *et al*., 2001; see section 1.3.5.1 for a more detailed discussion on the circadian clock). Recently, however, ZTL and FKF1 were shown to have B light-receptor activity required for the regulation of the central clock oscillation and photoperiodic flowering response, respectively (Kim *et al*., 2007; Sawa *et al*., 2007). ZTL family members have 70-80% amino acid identity between them, and have a LOV domain (similar in structure to those of the phototropins, and capable of binding an FMN), an F-box domain (for targeted protein ubiquitination and subsequent degredation) and six kelch repeat domains (for protein-protein interaction) (Somers *et al*., 2000; Nelson *et al*., 2000; Schultz *et al*., 2001).

Mutations in the *ZTL* gene have allowed some of the mechanisms, and targets, of ZTL control to be elucidated. The *ztl* mutant displays a long circadian cycle, as indicated by *CAB2* expression levels and cotyledon movement (Somers *et al*., 2000). This effect, which is mirrored in a *TOC1* over-expressing plant (Somers *et al*., 1998; Mas *et al*., 2003a; Makino *et al*., 2002), was later attributed to a decreased interaction between the ZTL and TOC1, resulting in higher levels of TOC1 in the *ztl* mutant (Mas *et al*., 2003b). In support, low over-expression of *ZTL* results in a shorter circadian period and high over-expression causes arhythmycity (Somers *et al*., 2004). This model was later enhanced when it was shown that ZTL interacts with GIGANTEA

(GI), a major influence on the circadian rhythm (Fowler *et al*., 1999; Yanovsky and Kay, 2003; Mizoguchi *et al*., 2005; Fujiwara *et al*., 2005a, 2005b; Niinuma *et al*., 2007), in a blue light-dependent manner (Kim *et al*., 2007), resulting in ZTL escaping degradation during *GI* oscillations.

Interestingly, although ZTL has been shown to function under B light, hypocotyl extension in the *ztl* mutant shows a hypersensitive response under R light, but a WT phenotype under B light (Somers *et al*., 2000). However, Jarillo *et al*. (2001b) demonstrated, in a yeast-two-hybrid screen, that ZTL can also interact with cry1 and phyB, which may be the cause of this curiosity.

While LKP2 has been suggested as having redundant function to ZTL, through the study of *lkp2* mutant and over-expressing plants (Imaizumi *et al*., 2005; Schultz *et al*., 2001), the *LKP1* gene appears to be functioning differently. FKF1 does not appear to participate in circadian clock regulation but has an important role for photoperiod recognition for proper flowering time regulation. The mechanism behind this has been linked to the appearance of *CO* transcript only when high levels of *LKP1* protein and light coincide, suggesting that FKF1 protein regulates *CO* transcription in a light-dependent manner (Imaizumi *et al*., 2003). This was later explained through the LKP1-dependent degradation of CDF1, a suppressor of *CO* transcription, possibly through a B light-induced direct interaction with GI (Imaizumi *et al*., 2005; Kim *et al*., 2007).

1.3.1.4.2 The PAS/LOV Protein (PLP)

The PLP protein has a PAS domain at its N-terminal region and an LOV domain at its C-terminal region. The PAS domain at the N-terminal region of PLP is different from the LOV domain because it does not contain the conserved cysteine residue that forms a covalent adduct with FMN on B light irradiation (Crosson *et al*., 2003). Interestingly, the *PLP* gene has three splice variants: *PLPA* (encoding a protein of 397 amino acids), *PLPB* (encoding a protein of 399 amino acids where two amino acids (Ser and Asn) are inserted into the LOV domain), and *PLPC* (encoding a protein of 358 amino acids where a frame shift causes deletion of 46 C-terminal amino acids and addition of the final seven amino acids) (Ogura *et al*., 2008).

PLPA and PLPB were shown to interact with *VTC*2 (*VITAMIN C-DEFECTIVE 2*), a paralog of *VTC2*, *VTC2L*, and *BLH10* (*BEL1-LIKE HOMEODOMAIN 10*), of which there are two splice variants: *BLH10A* and *BLH10B*. However, interaction with the latter three proteins is abolished under B light irradiation, despite protein levels remaining constant under these conditions (Ogura *et al*., 2008). Although there is currently no clear indication that the LOV domains of PLPA or PLPB bind a flavin molecule, thereby giving light-receptor activity, the effect of B light on their capacity to interact with their binding proteins suggest that these may be new B light receptors. Additionally, expression of *PLP* mRNA and protein was increased in response to drought, salt and ABA treatment, which, coupled with the nature of their binding proteins, suggests a drought-specific role for these receptors (Ogura *et al*., 2008).

1.3.2 The role of photoreceptors in regulating the tetrapyrrole pathway

Study into the regulation the tetrapyrrole pathway has focussed on two main areas: the production of ALA, where glutamyl-tRNA reductase (encoded by the *HEMA* gene) is under the most intense regulation; and the allocation of protoporphyrin IX to the chelatase enzymes at the branch point in the pathway. It is unsurprising that these stages are regulated at more than one level as the reduction of glutamyl-tRNA to produce glutamate-1-semialdehyde represents the first committed step in the tetrapyrrole pathway, and factors determining the requirements of haem vs. chlorophyll differ dramatically during the day and night.

Regulation of the tetrapyrrole pathway by photoreceptors, such as phytochromes and cryptochromes, has been intensely studied, not least because phytochromobilin, one of the two components required for a functional phytochrome molecule, is produced via the haem branch of the tetrapyrrole pathway. As discussed earlier, five known phytochrome molecules may be formed (phyA-E) which act as receptors to different wavelengths of light, and subsequently give different developmental and physiological responses (discussed in more detail in section 1.3.1.1).

The importance of the Glu-TR protein for the flow of metabolites through the pathway resulted in an initial emphasis on characterising HEMA expression. Ilag *et al*. (1994) demonstrated that HEMA1 specifically was light regulated in *Arabidopsis*, which was later confirmed in Barley (Bougri and Grimm, 1996). Additionally, McCormac *et al*. (2001) established that *HEMA1* expression was initially low in etiolated seedlings but could be dramatically elevated following exposure to irradiation by various light sources for 1 day, and in fact only 2 hours of irradiation was required. It was also confirmed that continuous irradiation by red, far-red or blue light produced an up-regulation of *HEMA1* expression, and that this response is controlled by both the phytochrome and cryptochrome photoreceptors (McCormac *et al*., 2001; McCormac and Terry, 2002a). However, in *Arabidopsis* two members of the *HEMA* gene family have been discovered. Interestingly, studies on the second *HEMA* gene, *HEMA2*, revealed no significant change in the abundance of transcripts following exposure to light (Tanaka *et al*., 1996; Chow *et al*., 1998; Nagai *et al*., 2007). This irregularity may be explained by the constitutive low expression of *HEMA2* in the roots and flowers, and almost undetectable levels in other parts of the plant (Kumar *et al*., 1996). Conversely, *HEMA1* is expressed throughout the plant, but expression is significantly enhanced in the cotyledons and hypocotyl following light exposure. This suggests that while *HEMA2* may be responsible for the maintenance of haem production in non-photosynthesising organs, *HEMA1* is the primary *HEMA* gene involved in de-etiolation in *Arabidopsis.* This conclusion is supported by evidence that *HEMA2* promotor activity is reduced in cotyledons when grown in media containing sucrose, in a light independent manner, while in *HEMA1* this is a light-dependent process (Ujwal *et al*., 2002).

Additionally, in barley (*Hordeum vulgare*) three *HEMA* genes have been discovered (Tanaka *et al*., 1997). While *Hem*A1 and *Hem*A2 show similar expression patterns to the Arabidopsis *HEMA1* gene, *Hem*A3 is similar to the *Arabidopsis HEMA2* gene.

1.3.3 The role of *PIF1* in regulating the tetrapyrrole pathway

Much of the transcriptional regulation of tetrapyrrole-synthesis genes that is modulated by phytochrome is thought to be directly controlled by phytochrome interacting factors. These proteins are known to both bind phytochrome and contain a bHLH domain, suggesting DNA binding capabilities and a function as transcription factors (Huq *et al*., 2004). Initial studies on the *pif1* mutant presented a bleached phenotype similar to the *flu* mutant (involved in regulating Glu-TR; discussed in more detail in section 1.5.1) when transferred to W light after >2 days D. Subsequently it was found that this bleached effect was caused by a twofold increase in the accumulation of Pchlide during the dark phase, in the mutant when compared with the wild-type. Excess Pchlide is known to result in the production of reactive oxygen species (ROS) upon exposure to light, which can be damaging to the cell/plastid (Reinbothe *et al*, 1996). Interestingly, when seedlings remained in darkness for longer there was found to be an increase in the severity of bleaching. This suggests that *PIF1* acts as a negative regulator of chlorophyll biosynthesis, acting to prevent excess Pchlide production during periods of extended darkness. Once transferred to the light phyA or phyB act to repress PIF1 activity, thereby promoting chlorophyll biosynthesis (Huq *et al*., 2004).

1.3.4 The phyA-mediated far-red block of greening response

It has been known for some time that the enzyme POR requires light in order to become active, most likely through the transfer of electrons from NADPH to Pchlide (Griffiths, 1991; Lebadev and Timco, 1998; Schoefs and Franck, 2003; Masuda and Takamiya, 2004). It is also known that in etioplasts, which contain an organised membrane system, the prolamellar body (PLB), the majority of the protein is POR (Ikeuchi and Murakami, 1983). After the onset of illumination POR becomes active and is able to convert the pools of Pchlide into chlorophyllide (Chlide). The growth of plants in continuous far-red light (FRc) results in a number of changes to the plastid which are characteristic of the FR high-irradiance response (FR HIR) including activating the transcription of chloroplast genes and replication of plastid DNA (Dubell and Mullet, 1995). However, *Arabidopsis* seedlings grown under these conditions cannot accumulate chlorophyll, and subsequent exposure to continuous

white light (Wc) caused seedlings to bleach and die (Barnes *et al*., 1995). This response is most pronounced when 2 or more days of FR pre-treatment are given and cannot be rescued through altering the amount of Wc treatment or including a D treatment before transfer to Wc. Interestingly, however, the addition of sucrose in the media gives the capacity to green (Barnes *et al*., 1996).

Further analysis of the plastids in FR exposed seedlings revealed that they did not contain a large, structured PLB; instead they had only a small number of prothylakoid membranes and stroma-located, electron-dense vesicles. However, in the *phyA* mutant normal PLBs developed (figure 1.5) (Barnes *et al*., 1996; McCormac and Terry, 2002b).

Additional studies noted that both the expression of POR genes and the accumulation of POR proteins were reduced in seedlings grown under FRc conditions. This response became more pronounced with increasing FRc exposure. Therefore it may be possible to conclude that the reduction in POR expression and protein levels under FRc light may lead to a reduction in PLBs, and therefore reduced chlorophyll production. However, it can also be seen that 1d D followed by 2 days FRc treatment allows the retention of some POR activity (~20%) and some PLB structure, which presumably would be capable of chlorophyll production. Therefore we must also focus on the difference between seedlings exposed to 1 day FRc compared to those exposed to 2 days FRc, namely the onset of vesicle formation. These vesicles may represent the onset of degradation of the plastid; therefore irreversible damage may occur which no longer allows POR activity. This is supported by the fact that vesicle formation did not occur in seedlings grown in the presence of sucrose, even after 4 days FRc treatment, which correlated with the presence of active POR proteins (Barnes *et al*., 1996).

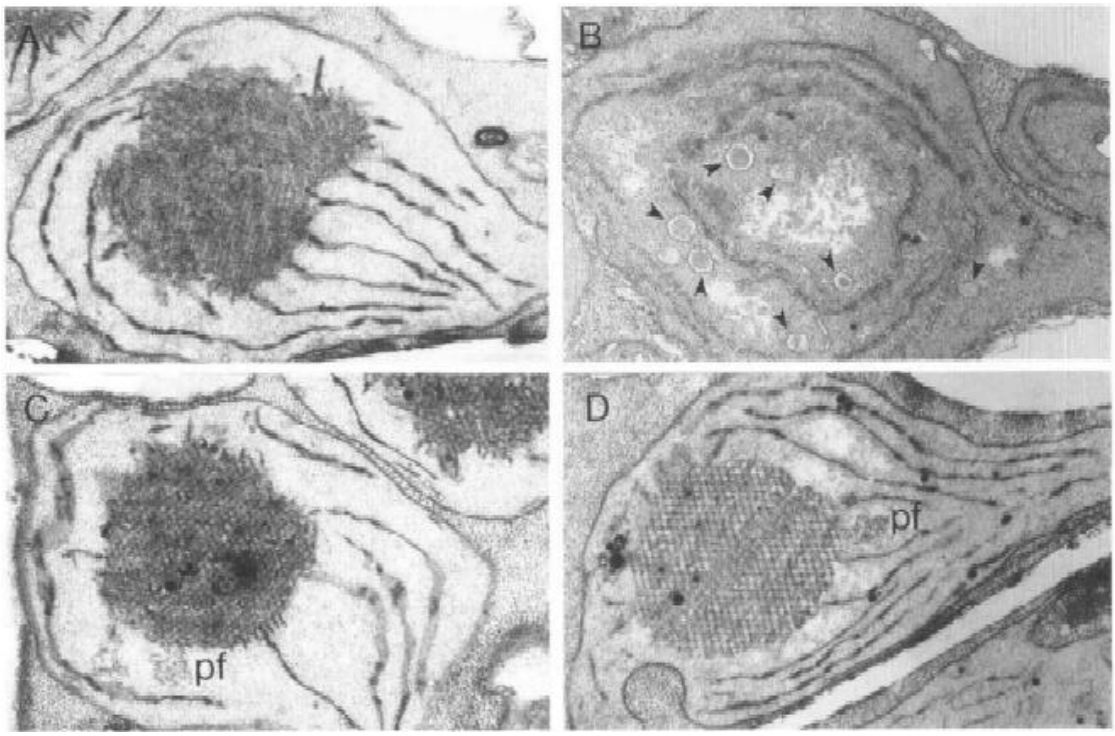

Figure 1.5 Plastids in mesophyll cells of cotyledons following a lethal far-red treatment. A) and B) L*er* in Dc and 1 day dark followed by 4 days FR. C) and D) phyA in Dc and 1 day dark followed by 4 days FR. Arrowheads indicate abberant vesicles. From Barnes *et al*., 1996.

1.3.5 Regulation by diurnal cycles and the circadian clock

1.3.5.1 The circadian clock

Circadian rhythms are driven by an endogenous clock brought about by autoregulatory negative feedback loops, primarily entrained by temperature and light inputs. The clock was previously thought to be simply based upon the negative interactions of the morning expressing transcription factors CCA1 (CIRCADIAN CLOCK ASSOCIATED 1) and LHY (LATE ELONGATED HYPOCOTYLS) and the evening expressing TOC1 (TIMING OF CAB EXPRESSION 1), and indeed they are of major importance (Schaffer *et al*., 1998; Wang and Tobin, 1998; Strayer *et al*., 2000; Harmer *et al*., 2000; Alabadi *et al*., 2001, 2002). It is now known, however, that the picture is far more complex (figure 1.6). In parallel to TOC1, EARLY FLOWERING 4 (ELF4), GIGANTEA (GI) and LUX ARRHYTHMO (LUX) are thought to form feedback loops with CCA1/LHY (Schaffer *et al*., 1998; Alabadi *et al*., 2001; Doyle *et al*., 2002; Mizoguchi *et al*., 2002, 2005; Kikis *et al*., 2005; Hazen *et al*., 2005; Onai and Ishiura, 2005). Additionally, there is another feedback loop involving CCA1/LHY and three TOC1 paralogues: PPR5, PPR7 and PPR9 (Farre *et al*., 2005; Nakamichi *et al*., 2005a, 2005b).

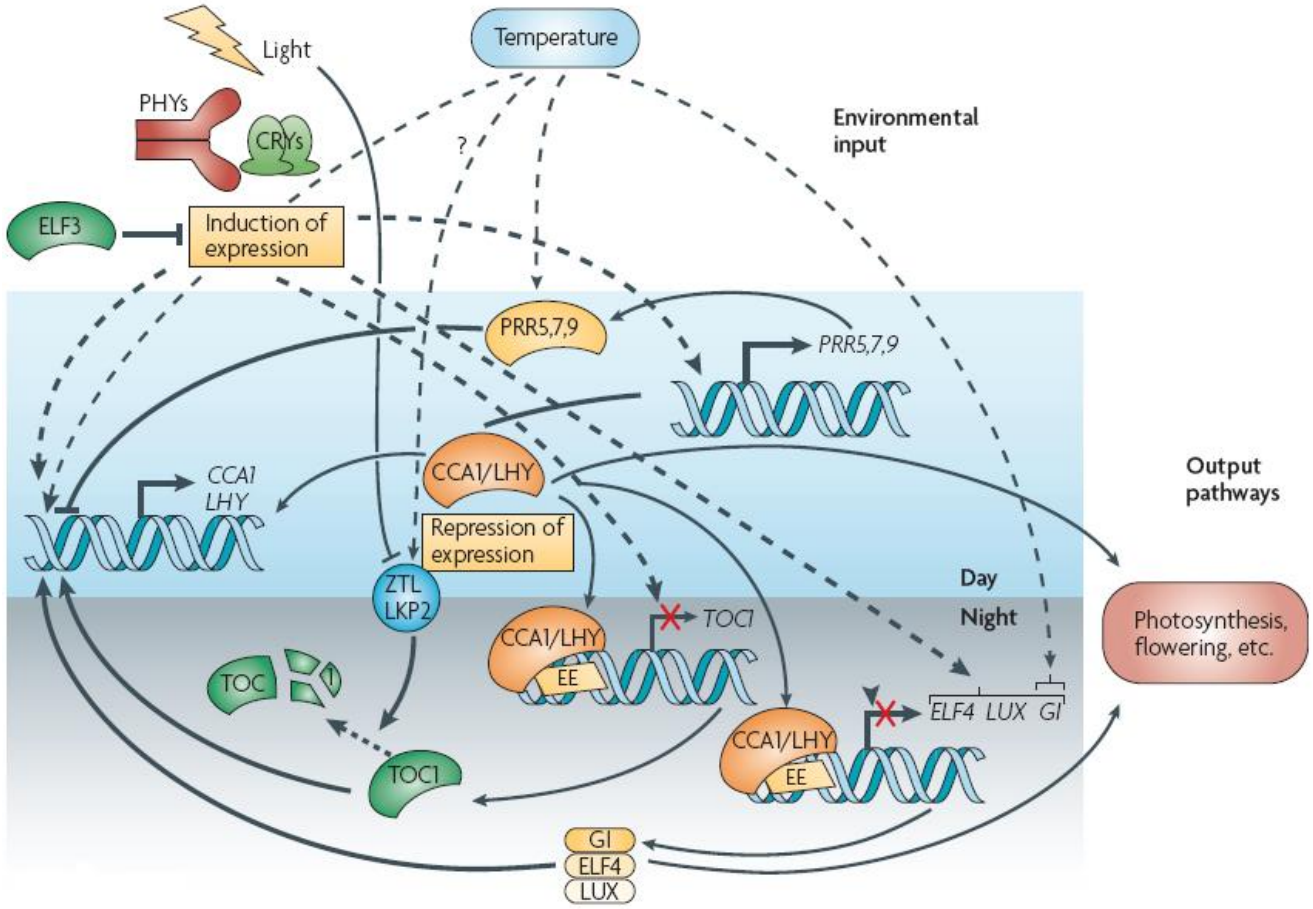

Figure 1.6 The role of light in regulating the circadian clock in *Arabidopsis thaliana.* The phytochrome, cryptochome and ZTL familys of phytoreceptors, as well as temperature, are required to initiate and reset the three feedback loops of the circadian clock (indicated by dashed lines), which require the action of central oscillators CIRCADIAN CLOCK ASSOCIATED 1 (CCA1) and LATE ELONGATED HYPOCOTYL (LHY). In the first loop, CCA1 and LHY repress TIMING OF CAB EXPRESSION 1 (TOC1) expression through binding to its promoter; conversely TOC1 acts as a positive regulator for CCA1 and LHY expression. In a similar second loop, CCA1 and LHY repress EARLY FLOWERING 4 (ELF4), GIGANTEA (GI) and LUX ARRHYTHMO (LUX) expression, which are responsible for the induction of CCA1 and LHY expression. Finally, in the third feedback loop, CCA1 and LHY positively regulate the expression of PRR5, PRR7 and PRR9, and these three proteins repress the expression of CCA1 and LHY. CCA1/LHY and ELF4/GI/LUX are then responsible for controlling the output pathways. The blue shaded area indicates the activities of different proteins during the subjective day, while the grey area indicates activities that peak during the subjective night. Aadapted from Jiao *et al*., 2007.

Light input into the clock has been intensely studied and it is now known that it is required for synchronisation at several points. As discussed previously, an array of photoreceptors are required for clock entrainment including phytochromes, cryptochromes and the ztl family. ELF3, a phyB-interacting protein, negatively affects R and B light input to multiple genes in the clock (Kikis *et al*., 2005; Liu *et al*., 2001; Covington *et al*., 2001), and FHY3 specifically gates phytochrome signalling to the clock (Allen *et al*., 2006). Yeast-2-hybrid assays have also indicated that PIF3 and PIL1 (PIF3-LIKE 1) are able to interact with TOC1 (Yamashino *et al*., 2003), although the *pif3* mutant does not exhibit any arhythmicity (Viczian *et al*., 2005; discussed in more detail in section 4.1). The ztl photoreceptor, on the other hand, forms part of the SCF complex which directly binds to TOC1 and targets it for degradation (Somers *et al*., 2000; Mas *et al*., 2003; Han *et al*., 2004).

1.3.5.2 Regulation of the tetrapyrrole pathway by diurnal cycles and the circadian rhythm

It has been shown previously that the capacity for ALA synthesis oscillates in barley leaves grown in cyclic (16 hour light / 8 hours dark) photoperiods, where the maximum is reached in the early hours of illumination, and shows a circadian rhythm when grown under constant light conditions (Kruse *et al*., 1997). Due to the fact that the levels of chlorophyll do not significantly fluctuate in plants grown under both cyclic photoperiods and constant light (Papenbrock *et al*., 1999), the change in the levels of ALA must be attributed to the need of the plant to remove photoreactive damaging or damaged compounds. For example, Pchlide may only be converted to Chlide during the day, due to the requirement of light for the activity of POR (Apel *et al*., 1980). Conversely, however, the levels of haem did show some fluctuation under both a cyclic photoperiod and constant light conditions (where levels peaked after the first hour and at 12 hours). Constant D conditions, however, produced a low, but stable, level of haem (Papenbrock *et al*., 1999). Therefore, it must also be true that the regulation of the chelatases plays a large role in the fate of protoporphyrin IX to ensure that the amounts of both chlorophyll and haem are fully controlled in the plant. Studies have shown that both Mg-CHEL and Fe-CHEL follow a pattern of expression and activity over a 24 hour period under cyclic and constant conditions. However, in

tobacco, for example, their levels of activity do not follow the same rhythm: while Mg-CHEL has the highest activity at the transition from dark to light, and a second smaller peak during the middle of the dark period, Fe-CHEL has its highest expression at the transition from light to dark (Papenbrock *et al*., 1999).

The development of a 'mini-array system' by Matsumoto *et al*. (2004), allowed the simultaneous, and accurate, analysis of many tetrapyrrole genes to asses their regulation in *Arabidopsis*. The previous discovery that chlorophyll and chlorophyll-binding proteins require close coordination with both themselves and the onset of light in order to produce a functional photosynthetic apparatus (Beator and Kloppstech, 1993), led the authors to apply much of their time to the study of regulation by circadian rhythms and diurnal cycles. From plants grown under 12 hour light / 12 hour dark cycles three clusters of genes became apparent: 1) regulation by both diurnal cycles and a circadian rhythm, 2) regulation by diurnal cycles alone, and 3) no apparent rhythm. Six genes were found in group 1, these were: *CHLH, CRD1, CAO, HEMA1, PORA* and *PORB*. The expression of the initial four genes coincided with each other and that of *Lhcb* (*LIGHT-HARVESTING CHLOROPHYLL* A/B *BINDING PROTEIN*), and was strongly induced by illumination. This suggests that they may be required at the onset of greening for the assembly of functional photosynthetic apparatus. Interestingly, while *PORA* and *PORB* were found to have synchronous expression with each other, their expression was slightly delayed compared to the other four genes and they were down- rather than up-regulated; this is perhaps down to the accumulation of POR proteins in etioplasts, which becomes largely unnecessary in the chloroplast.

The second group was made up of 19 genes, 16 of which were involved in the early stages of tetrapyrrole synthesis, up to the metal insertion step. These genes showed no rhythmic regulation under continuous light conditions, indicating their regulation by a diurnal cycle rather than a circadian rhythm. This regulation is likely to be due to the requirement for chlorophyll, and the necessity for the removal of phototoxic tetrapyrroles and replacement of damaged chlorophyll, during periods of illumination.

The final group is composed of various genes across the tetrapyrrole pathway

which presumably require no light regulation and are therefore either constitutively expressed, or are regulated by other environmental or internal cues.

1.4 Internal regulation of the tetrapyrrole pathway

1.4.1 The role of magnesium chelatase and ferrochelatase in regulating the tetrapyrrole pathway

The enormous changes in flux throught the two chelatase branches in the tetrapyrrole pathway must be carefully controlled and this cannot be accounted for entirely by changes in mRNA levels. It is therefore not surprising that the Mg-chelatase and Fe-chelatase enzymes have different structural and biochemical properties to maintain this regulation (summarised in table 1.3). Magnesium chelatase is comprised of three protein subunits, CHLI (38–42 kDa), CHLD (60–74 kDa) and CHLH (140–150 kDa) (Gibson *et al*., 1995; Jenson *et al*., 1996; Papenbrock *et al*., 1997). CHLI is an AAA+ ATPase (Neuwald *et al*., 1999; Fodje *et al*., 2001; Reid and Hunter, 2004), contains a Mg^{2+} binding site (Reid *et al*., 2003), and forms a stable complex with CHLD (Jenson *et al*., 1999). The third subunit, CHLH, binds porphyrins (Willows and Beale, 1998; Karger *et al*., 2001) and presumably contains the active site for chelation. Ferrochelatase, on the other hand, is made up of only one 36-42 kDa subunit and exists as either a monomer or homodimer (Walker *et al*., 1997; Suzuki *et al*., 2000; Suzuki *et al*., 2002b).

The kinetic properties of the two enzymes are also different. Firstly, Mg-chelatase has a threefold requirement for ATP: 1) ATP is required for metal insertion (Walker *et al*., 1997; Walker and Willows, 1997), 2) the formation of a complex between CHLD and CHLI is facilitated by ATP (Walker and Willows, 1997; Jenson *et al*., 2000), and 3) ATP has been shown to enhance the binding between ProtoIX and CHLH (Jenson *et al*., 2000). Interestingly, however, Fe-chelatase is inhibited by ATP. Secondly, Mg-chelatase has a much lower K_m for protoporphyrin IX than ferrochelatase (Cornah *et al*., 2002; Walker *et al*., 1997). This would suggest that during the day, when ATP levels are high, Mg-chelatase will be functioning and competing effectively for ProtoIX, and Fe-Chelatase will be inhibited. Conversely, in the dark, when ATP levels are low, Fe-chelation will be favoured.

Table 1.3 Comparison of the chelatases at the metal-insertion branch point of haem and chlorophyll synthesis (adapted from Cornah *et al*., 2002).

	Fe-Chelatase		**Mg-Chelatase**
Functional isoforms in higher plants	Ferrochelatase 1	Ferrochelatase 2	One[1]
Subunit composition	Monomer or homodimer	Monomer or homodimer	Heterotrimer (CHLD, CHLH, CHLI)
Subunit molecular weight	36-42 kDa	36-42 kDa	CHLI (38–42 kDa), CHLD (60–74 kDa) and CHLH (140–150 kDa)
K_m for protoIX	0.2-15.0 µM	Unknown	1-10 nM
K_m for metal ion	4.7 µM	Unknown	14.3 mM
Energy Requirement	None	None	ATP as substrate and for activation

[1] = Although the *Arabidopsis* genome encodes two *CHLI* genes that are 82% identical, *CHLH* and *CHLD* are single-copy genes.

Despite the requirement for all three subunits of Mg-chelatase to form a functional enzyme, it is the regulation of the *CHLH* subunit of Mg-Chlelatase that has been shown to be of key importance to the control of the chlorophyll branch of the tetrapyrrole pathway (Gibson *et al*., 1996; Papenbrock *et al*., 1999; Matsumoto *et al*., 2004), the regulatory role of the *CHLD* and *CHLI* subunits is less well understood. Currently, all evidence suggests that *CHLD* is unregulated at the transcription, translation and post-translation stages of synthesis. *CHLI*, on the other hand, was recently identified as a target of thioredoxin, which has been implicated in chloroplast protein degradation in response to light stress (Balmer *et al*., 2003). Additionally, it has been shown that CHLI acts as a chaperone for (and is required for the survival of) CHLD, and this association requires the ATPase activity of the I subunit (Lake *et al*., 2004).

Regulation of the ferrochelatase genes, *FC1* and *FC2*, is relatively well understood. The expression patterns of *FC1* and *FC2* are very similar to the *HEMA* genes (*HEMA2* and *HEMA1*, respectively; see section 1.3.2), suggesting that *FC2* is more responsible for haem production in photosynthetic tissues, while *FC1* is required in non-photosynthetic tissues (Miyamoto *et al*., 1994; Smith *et al*., 1994; Chow *et al*., 1998; Suzuki *et al*., 2002b). However, a recent study has shown that under stress conditions *FC1* is also induced in photosynthetic tissues, possibly to supply haem for defensive haemproteins outside plastids (Nagai *et al*., 2007).

Much debate has been given to the intracellular site of haem synthesis. Originally, a model for dual targeting of *FC1* to plastids and mitochondria was reported in *Arabidopsis* (Chow *et al*., 1997). However, mitochondrial localization of *FC1* was disputed since *FC1* and *FC2* were not imported into *Arabidopsis* mitochondria *in vitro* (Lister *et al*., 2001). Recently, it has been reported that in green algae *Chlamydomonas reinhardtii*, *FC* is encoded by a single gene and localized in chloroplasts (van Lis *et al*., 2005).

1.4.1.1 CHLH as an ABA recepter

Recently Shen *et al*. (2006) identified a protein which specifically binds ABA in a saturable manner, which they named *ABAR* (*ABA RECEPTOR*). While overexpression of *ABAR* caused an ABA hypersensitive response, RNAi lines were found to have significant ABA-insensitive phenotypes in seed germination, post-germination growth arrest and ABA-induced promotion of stomatal closure and inhibition of stomatal opening, and consequently were more sensitive to dehydration.

On the basis of sequencing information it was discovered that *ABAR* encoded for the H subunit of Mg-CHEL. Interestingly, however, further analysis led to the discovery that ABAR binds ABA independently of Proto IX, indicating that ABA signal perception might be distinct from Proto IX binding (Shen *et al*., 2006).

1.4.2 The role of Mg-PMT in regulating the tetrapyrrole pathway

To assess the impact of altered *CHLM* expression on the tetrapyrrole pathway, Alawady and Grimm (2005) produced antisense and overexpressing lines. It was apparent that low *CHLM* expression resulted in both low Mg-PMT synthesis and low chlorophyll content, and vice versa. However, reduced Mg-PMT activity also correlated with reduced Mg-chelatase activity and a low synthesis rate of 5-aminolevulinate, but with enhanced ferrochelatase activity. In contrast, high Mg-PMT activity led to inverse activity profiles, indicating a direct influence of Mg-PMT, in combination with Mg-chelatase, on the metabolic flux of ALA and the distribution of protoporphyrin into the branched pathway. They also showed that the modified

enzyme activities in tetrapyrrole biosynthesis in the transgenic plants could be explained by changes of certain corresponding mRNA contents, where increased 5-aminolevulinate synthesis and Mg chelatase activity correlate with enhanced transcript levels of the *HEMA*, *GSA*, and *CHLH*.

Conversely, Shepherd *et al*. (2005) demonstrated that the CHLH subunit of Mg-chelatase stimulates CHLM activity through the acceleration in formation and breakdown of an intermediate in the catalytic cycle of CHLM. Clearly, therefore, the synthesis and activity of CHLM is tightly linked with both the early stages of tetrapyrrole synthesis, and the first commited steps of chlorophyll synthesis.

1.4.3 The role of haem in regulating the tetrapyrrole pathway

Three main pieces of evidence support the hypothesis that ALA synthesis is inhibited by haem. The first of these comes from studies on plants treated with the herbicide 2,2'-dipyridyl, an inhibitor of ferrochelatase, which accumulated more Mg-protoporphyrin than control plants (Duggan and Gassman, 1974). This suggested that by blocking haem synthesis it is possible to disrupt the normal tight control of the production of chlorophyll intermediates.

Secondly, the mutants *aurea* and *yellow-green-2* of tomato, which have reduced haem breakdown due to defective phytochromobilin synthase and haem oxygenase genes respectively, were shown to have reduced chlorophyll levels, despite no block occurring in the chlorophyll synthesis pathway (Terry and Kendrick, 1999; Ryberg and Terry, 2002). This anomaly was again suggested to be due to the feedback inhibition of haem on ALA synthesis. Finally, during periods of rapid chlorophyll synthesis it has been noted that haem is concurrently turned over more rapidly (Castelfranco and Jones, 1975).

Subsequently it has been shown that disruption of ALA synthesis occurs at the stage of Glu-TR activity in higher plants, cyanobacteria and green algae. Exogenous haem can inhibit recombinant Glu-TR in barley (Pontoppidan and Kannangara, 1994), and this requires the N-terminal 30 amino acids of the enzyme (Vothknecht *et al*,

1998). Additionally, it has recently been shown by Vasieuskaya *et al*. (2005) that haem controls *HEMA* in *Chlamydomonas reinhardtii*. Here they concluded that regulation was either through the modulation of the amount of *HEMA* mRNA in a light-independent manner, or alternatively, haem may mediate the light induction of *HEMA*; studies are ongoing. Finally, the identification of a mutant (*ulf3*) capable of suppressing the *flu* phenotype, which normally resulted in dramatic increase in Pchlide production due to over-activity of Glu-TR (discussed in more detail in section 1.5.1), was the first genetic evidence for the role of haem in regulating Glu-TR (Goslings *et al*., 2004). The *ulf3* mutation was mapped to the *HY1* locus which encodes a haem oxygenase, giving the conclusion that increased levels of haem in the *hy1* mutant inhibit the activity of Glu-TR and suppress the synthesis of ALA.

1.5 External regulation of the tetrapyrrole pathway

1.5.1 The role of FLU in regulating the tetrapyrrole pathway

In a mutant screen, conducted by Meskauskiene *et al*. (2001), plants were selected for their inability to restrict the accumulation of Pchlide in the dark. These plants were described as resembling dark-grown seedlings that had been fed exogenous ALA (Meskauskiene *et al*., 2001), and they rapidly bleached and died following exposure to Wc light. This is presumably due to their high accumulation of Pchlide, which is known to become phototoxic at high levels, because plants could be rescued by germinating the seedlings under constant light.

In this initial study it was also concluded that FLU is a chloroplast protein that becomes tightly anchored to the chloroplast membrane following entry. Additionally, the FLU protein also contains a tetratricopeptide repeat (TPR) domain, and a coiled-coil motif, both of which are implicated in protein-protein interactions (Meskauskiene and Apel, 2002).

The potential for FLU to be involved in either of the two previously elucidated mechanisms of regulation of ALA synthesis, by light and haem, was discarded following further studies. Firstly, although *FLU* mRNA is shown to fluctuate between

etiolated and light-grown seedlings, its protein levels remain constant; and secondly, the *flu* mutant can partially rescue the inhibition of ALA synthesis found in the *hy1* (*haem oxygenase*) mutant (Goslings *et al*., 2004). Therefore, FLU was suggested as giving a third input into the regulation of *HEMA1*.

One current hypothesis places FLU as a bridge between Pchlide and Glu-TR, since Pchlide is thought to regulate Mg-CHEL and ALA synthesis in an unknown manner. It has since been shown that FLU does interact strongly with Glu-TR, but not with GSA-AT, and that this interaction required the TPR domain (Meskauskiene and Apel, 2002). However, there is as yet no evidence to suggest that FLU is controlled by Pchlide at the transcription, translation or post-translation level.

1.5.2 The role of GUN4 in regulating the tetrapyrrole pathway

The *GUN4* gene was originally found in a screen for mutants that maintained expression of *Lhcb* following exposure to the herbicide Norflurazon, which blocks plastid development, and therefore the plastid-to-nucleus signal (discussed in more detail in section 1.6.1). Five mutants were originally identified and became known as *genomes uncoupled 1-5 (gun1-5)* (Susek *et al*., 1993; Mochizuki *et al*., 2001). While *GUN1* encodes a chloroplast localized pentatricopeptide-repeat protein and either forms part of an independent retrograde plastid signal (Mochuzuki *et al*., 1996; Mochuzuki *et al*., 2001; McCormac and Terry, 2004) or appears later in the signalling cascade (Koussevitzky *et al*., 2007) (discussed in more detail in section 1.6.1.), *GUN2-5* have all been identified as being involved in tetrapyrrole biosynthesis. However, *GUN4* is the only one not to represent an enzyme of the pathway, where *GUN2*, *GUN3* and *GUN5* encode haem oxygenase, phytochromobilin synthase and the H subunit of Mg-chelatase, respectively (Mochuzuki *et al*., 1996; Mochuzuki *et al*., 2001).

In initial studies on *GUN4* it was found that this gene was only present in species that carry out oxygenic photosynthesis (one gene has been found, for example, in *Arabidopsis* and rice, while *Synechocystis* and *Nostoc* have three and four, respectively) (Larkin *et al*., 2003). Following analysis of the mutant in *Arabidopsis*,

which produced plants capable of developing a number of leaves and flower-like structures after 2 months on sucrose containing media, it was concluded that although GUN4 is required for chlorophyll synthesis under normal growth conditions, it is not essential (Larkin *et al*., 2003). Immunoblotting studies confirmed that GUN4 is localised to the chloroplast, and it was further hypothesised that it may be attached to the chloroplast membrane. This was supported by evidence that the protein sequence of GUN4 contains two distinct helical domains that resemble ARM or HEAT repeats, which have previously been associated with protein-protein interactions (Davison *et al*., 2005; Verdacia *et al*., 2005). Here, it is thought that GUN4 exists as a highly compact dimer.

The discovery that a *gun4/gun5* double mutant produced a more severe chlorophyll-deficient mutant than either a *gun4* or *gun5* mutant, and the copurification of GUN4 and CHLH, provided the first clues as to the role of GUN4 in tetrapyrrole regulation. *Synechocystis* was chosen as a system to test the hypothesis that GUN4 regulates Mg-chelatase. This provided evidence that when Mg-chelatase is pre-incubated with GUN4 it is more efficient and effective at producing Mg-deuteroporphyrin IX (the functional equivalent of Mg-protoporphyrin IX) from deuteroporphyrin IX (the functional equivalent of protoporphyrin IX) (Larkin *et al*., 2003).

Modeling of the GUN4 protein has since revealed that a cleft in its structure is capable of accommodating approximately half of a protoporphyrin IX molecule (Davison *et al*., 2005; Verdacia *et al*., 2005). Further studies suggested that GUN4 might become essential for Mg-protoporphyrin IX when Mg^{2+} is at low concentrations, where at 2 mM Mg^{2+} Mg-chelatase is virtually inactive in the absence of GUN4, but becomes almost fully active in its presence (Davison *et al*., 2005). Therefore, two possible functions of GUN4 are conceivable: it may be responsible for distributing protoporphyrin IX to both chelatases, or it may stabilise Mg-chelatase, effectively acting as a fourth subunit. However, some data also suggests that GUN4 may have other roles in the photosynthesising cell that are not restricted to chlorophyll biosynthesis, for example, GUN4 is present in a large pool as a monomer in the stroma, as well as a dimer attached to the chloroplast membrane, which is thought to be its functional form in terms of Mg-chelatase regulation (Wilde *et al*., 2004).

1.5.3 *SCP*s and the *LIL* genes

In green algae and higher plants light capture is achieved, in part, by antenna complexes consisting of three helix light harvesting chlorophyll *a*/*b* binding proteins (*LHC*), chlorophylls *a* and *b*, and carotenoids. In cyanobacteria and red algae, however, a water-soluble light-harvesting complex, known as the phycobilisome, is present, where phycobilins are covelently bound to the antenna polypeptides (Grossman *et al*., 1995). Although no direct *LHC* homologues were detected in cyanobacteria, Dolganov *et al*. (1995) discovered a single helix, high light inducible protein (HLIA), which is part of a five-member family of single helix, small CAB-like proteins (SCPA-E), and the prime candidates for *LHC* homologues (Funk and Vermaas, 1999). Interestingly, however, these SCP proteins show a higher similarity to relatives of LHC proteins in *Arabidopsis*, including the family of early light-induced proteins (ELIPs; Adamska, 1997, 2001; Montane and Kloppstech, 2000), the PsbS protein of PSII (Funk, 2001) and a small family of stress-enhanced proteins (SEPs) (Heddad and Adamska, 2000). In 2000 Jansson *et al*. identified an additional one helix protein (OHP) with considerable similarity to the SCP proteins.

In the cyanobacterium *Synechosystis* the five SCP proteins have been studied in some detail and their roles have been somewhat elucidated. Firstly, SCPA was shown to associate with the tetrapyrrole synthesis enzyme ferrochelatase (Jansson, 1999), and is required for its function. As yet, no similar partnership has been discovered in *Arabidopsis*, although a one helix domain is present at the C-terminal end of ferrochelatase II (Chow *et al*., 1998). SCPB and SCPE have both been shown to positively affect chlorophyll biosynthesis through alterations in Glu-TR activity (Xu *et al*., 2002), where, it was hypothesised that when chlorophyll was lacking a build up of SCPs would occur and result in activation of Glu-TR. Finally, SCPC and SCPD have been shown to associate with photosystem II (PSII) when damage occurs, and are thought to act as a temporary pigment resevoir (Promnares *et al*., 2006; Yao *et al*., 2007).

Interestingly, recently the ELIP2 protein in *Arabidopsis* was shown to regulate the tetrapyrrole biosynthesis pathway through regulation of the activity of both Glu-TR and Mg-Chelatase (Tzvetkova-Chevolleau *et al*., 2007), suggesting that ELIP2 could be orthologous to SCPB and SCPE, and Tzvetkova-Chevolleau *et al.* (2007)

similarly concluded that this was due to sensing of free chlorophyll. This mechanism would therefore have a twofold benefit: 1) prevent a build-up of free chlorophyll and the resulting oxidative stress, 2) prevent a lack of free chlorophyll, thereby maximising energy capture.

Conversely, very little has been done to investigate the role of *OHP1*, and whether it too may have a role in regulating tetrapyrrole biosynthesis. Current understanding characterises *OHP1*, and the more recently discovered *OHP2* (Andersson *et al*., 2003), as high light inducible, and expression occurs in a light intensity-dependent manner (Jansson *et al*., 2000; Andersson *et al*., 2003). Both proteins contain a single helix with most similarity to the first of the three LHC helices (Jansson *et al*., 2000; Andersson *et al*., 2003), and OHP1 contains both chloropyll and helix-helix binding sites (Jansson *et al*., 2000). OHP2 has been shown to localise with photosystem I (PSI) (Andersson *et al*., 2003), suggesting that it has a role in PSI protection in a similar manner to the proposed function of SCPC and SCPD in regards to PSII. The localisation and function of OHP1, on the other hand, has yet to be elucidated.

Finally, in the same screen, performed by Heddad and Adamska (2000), that found the *ELIP* genes in *Arabidopsis*, two other two helix proteins were identified. Given the increase in expression of these genes in response to high light, cold, heat, UV light, salt and desiccation treatment, they were named *STRESS ENHANCED PROTEINS* (*SEP*s). However, although both these proteins contain two helices, they are very dissimilar, showing only 14% identity and 32% similarity across their protein sequences, mostly due to the N-termini showing no conservation (Heddad and Adamska, 2000). Along with the ELIP proteins, though, they were both shown to be targeted to the chloroplast and be inserted in the thylakoid membrane. These genes therefore represent further members of the *SCP* family, and are most likely required to prevent damage to the photosynthetic apparatus during periods of stress.

1.6 Retrograde plastid signal transduction pathways

The chloroplast is originally derived from an endosymbiotic relationship between an ancestral plant cell and a photosynthesising cyanobacteria, and as such the chloroplast contains a genome of approximately 60-100 genes. However, the photosynthetic processes which take place within the chloroplast require many hundreds more genes to function correctly which are now found within the nucleus. The transcription of photosynthetic genes in both the chloroplast and nucleus consequently need to synchronise to both maximise the potential to capture energy and prevent the production of excess light reacting compounds, such as tetrapyrroles, which will become phototoxic. Additionally, it is understood that, as well as nuclear-derived signals; a signal originating from the chloroplast also exists.

This signalling from the chloroplast, known as the plastid retrograde signal, is now believed to take at least three forms: the tetrapyrrole intermediate, Mg-protoporphyrin IX (Mg-Proto); ROS; and a message derived from the plastid translational machinery.

1.6.1 The *gun* mutants and the role of Mg-protoporphyrin IX

Various pieces of evidence suggest Mg-protoporphyrin (Mg-proto), an intermediate of the tetrapyrrole pathway, as one retrograde signal. In early experiments using *Chlamydomonas reinhardii* it was found that chlorophyll biosynthetic intermediates block the expression of a variety of nuclear genes, such as the light-harvesting chlorophyll *a/b* binding protein of photosystem II (*Lhcb*) (Johanningmeier and Howell, 1984; Johanningmeier, 1988). The most effective method to block *Lhcb* accumulation was using conditions that caused an accumulation of Mg-proto. Thujaplicin, which abolishes Pchlide synthesis and causes the accumulation of porphyrins, and amitrole, which prevents normal prolamellar body development and results in Mg-proto accumulation, have both been shown to inhibit the light induction of *Lhcb* in plants (Oster *et al*., 1996; La Rocca *et al*., 2001).

Additionally, Mg-proto and Mg-protoporphyin IX monomethylester (Mg-protoMe) have been found to activate a heat- and light-responsive HSP70A promoter

fragment, but do not affect an HSP70A promoter fragment that is only responsive to heat. This suggests that Mg-proto and/or Mg-protoMe can activate transcription through a light-responsive *cis* element (Kropat *et al*., 1997). The discovery that Mg-proto and/or Mg-protoMe may be transported from the chloroplast in response to light to activate HSP70A has given support to the Mg-proto signal hypothesis (Kropat *et al*., 2000).

As mentioned earlier, a range of mutants termed *genomes uncoupled* (*gun*) were produced in the early 90s in which the plastid regulation of nuclear gene expression was disrupted (Susek *et al*., 1993). Interestingly, *gun2, 3 and 5* have all since been shown to disrupt enzymes in the tetrapyrrole biosynthetic pathway, and result in disrupted levels of Mg-proto. *GUN4*, on the other hand, has been elucidated as a regulator of Mg-chelatase, and therefore mutation also results in altered levels of Mg-proto. The *gun1* mutation, through *gun1/gun5* and *gun1/gun4* double mutant studies, has been shown to affect a different signalling pathway (Vinti *et al*., 2000; Mochizuki *et al*., 2001; McCormac and Terry, 2004). These studies have also revealed that *gun1* mutations do not affect tetrapyrrole metabolism.

The discovery that additional *CHLH* mutants show a *gun* phenotype, but mutants of *CHLI* (e.g. *cs* and *ch42*) do not, gave rise to the hypothesis that *CHLH* may also function as a tetrapyrrole sensor which is required for plastid-to-nucleus signalling (Mochizuki *et al*., 2001). This is supported by evidence that suggest *CHLH* binds porphyrins as a monomer, in the absence of the other Mg-chelatase subunits (Karger *et al*., 2001).

Interestingly, mutation of *LAF6*, a soluble ATP-binding cassette protein that localises to the chloroplast and has been implicated in the transport of proto, does not affect *Lhcb* levels. This data is slightly anomalous considering the *laf6* mutation results in a two-fold increase in proto levels, a photobleached phenotype and disruption of some nuclear gene expression (Moller *et al*., 2001). Therefore, although both *laf6* and *gun2-5* mutations affect tetrapyrrole metabolism, they appear to affect different signalling pathways. One possible explanation for this is that signalling may depend upon pathway flux, which is affected differently in these mutants.

Despite this body of evidence, two recent reports present evidence against the role of Mg-Proto as a retrograde plastid signal. To study the role of Mg-Proto Mochizuki *et al*. (2008) employed the *chlm*, *crd1*, and the *chlm crd1* double mutant, and double mutants of *chlm* and *crd1* with *gun1*, *gun4*, and *gun5*, as well as NF treated plants, all of which accumulate Mg-Proto and/or Mg-ProtoMe to different levels. They demonstrated that there was no correlation between an increase or reduction in Mg-Proto (or Mg-ProtoMe) accumulation with *Lhcb* expression.

At the same time, Moulin *et al*. (2008) showed that no Mg-Proto, or any other chlorophyll-biosynthesis intermediate, could be detected in NF-treated plants under conditions which were previously shown to repress nuclear gene expression. Conversely, when endogenous Mg-Proto levels were increased through supplementation with the ALA, the expression of nuclear-encoded photosynthetic genes was not repressed. They concluded that there was no correlation between nuclear-gene expression and any of the chlorophyll biosynthetic intermediates tested, but instead, it is possible that perturbation of tetrapyrrole synthesis may be resulting in localized ROS production, or an altered redox state of the plastid, which could mediate retrograde signaling.

1.6.2 Redox signals in chloroplast-to-nucleus communication

The redox state of cells is constantly changing, and this is further enhanced in a photosynthesising cell by the presence of the photosynthetic apparatus, which uses light-coupled electron flow to generate energy. Additionally, tetrapyrrole intermediates, such as Pchlide, are known to create reactive oxygen species (ROS) if exposed to light. Finally, under high irradiances redox signals are conveyed via the glutathione redox cycle which also results in the production of ROS. These three sources of redox unbalance have been suggested as a second plastid-to-nucleus signal (reviewed in Pfannschmidt *et al*., 2003).

The redox state of a cell is known to control gene expression in bacteria and is generally mediated by a two-component system such as the REGA-REGB system in *Rhodobacter capsulatus* (for a review see Bauer *et al*., 1999). Transcription,

translation and post-translational modification in the plastid are also known to be controlled by the redox state. Light intensity is translated into a redox signal, which the plant can then use to regulate photosynthetic gene expression. Potentially this signal could also be transmitted out of the plastid and affect gene expression in the nucleus.

In pea the transcription and translation of one nuclear-encoded gene, ferredoxin (*FED1*), has been shown to be controlled by photosynthetic electron transport (Petracek *et al*., 1998). Studies in *Dunaliella salina* have shown also that chlorophyll *a/b* ratios correlate directly with photosystem II (PSII) activation, regardless of whether changes resulted from varying light or temperature. In this study it was also discovered that *Lhcb* mRNA levels were controlled by the same signal (Maxwell *et al*., 1995).

More recently four tobacco *PSI* genes were studied in their ability to respond to redox signals. It was found that while *PSAD* and *PSAF* responded to changes in the redox signals originating between the plastoquinone (PQ) pool and PSI, *PETE* was regulated by the redox state of the PQ pool directly, and *PETH* was not affected by redox state changes (Pfannschmidt *et al*., 2001). The *cue1* mutant, in which the shikimate pathway is disrupted and therefore the production of aromatic compounds such as phenolic UV light protectants and PQ is reduced, has been used to show that redox poise affects *Lhcb* expression (Streatfield *et al*., 1999). This was concluded following the discovery that in the *cue1* mutant primary electron-accepting PQ of PSII is more transiently reduced, which correlated to the reduction in *Lhcb* mRNA.

Other researchers have argued that LHCII kinase, rather than PQ, is the primary redox sensor, following the discovery that LHCII protein phosphorylation and *Lhcb* transcript abundance positively correlate in winter rye (Pursiheimo *et al*., 2001).

1.6.3 The *GUN1* pathway

In the same screen that identified the genes *GUN2-5* another genomes uncoupled gene, *GUN1*, was identified. However, while *GUN2-5* all encode genes

involved in tetrapyrrole synthesis and have a function in the Mg-protoporphyrin IX retrograde signal, *GUN1* forms part of an independent chloroplast-to-nucleus signal (Mochuzuki *et al*., 1996, 2001; McCormac and Terry, 2004). The *gun1* mutant was initially shown to exhibit derepression of *Lhcb* expression following both NF treatment, which disrupts tetrapyrrole synthesis, and lincomycin treatment, which disrupts the plastid translation machinery (Susek *et al*., 1993). Although *GUN1* was suggested to be involved in both plastid gene expression and tetrapyrrole biosynthesis (Nott *et al*., 2006), microarray analysis identified only a small overlap in de-regulated genes in the *gun1* compared to *gun2* or *gun5* pathways (Strand *et al*., 2003), suggesting two separate but partially redundant pathways.

Recently the *GUN1* gene was discovered to encode a 918 amino acid polypeptide that is a member of the P-subfamily of pentatricopeptide repeat (PPR) containing proteins (Koussevitzky *et al*., 2007). The majority of the ~441 members of the PPR family are targeted to either mitochondria or plastids, where they are involved in processing, editing, stability and translation of RNA molecules. Additionally, GUN1 has a small mutS related (SMR) domain which is commonly found in proteins responsible for DNA repair.

The same report identified that GUN1 was both involved in a plastid gene expression (PGE) retrograde signal and the Mg-protoporphyrin IX mediated pathway, although acting downstream of the Mg-proto accumulation. Furthermore, in the role of plastid-to-nucleus signalling the *ABSCISIC ACID INSENSITIVE 4* (*ABI4*) gene was also found to have a function downstream of GUN1, although it is unlikely that ABA itself is the signal. ABI4 has also been shown to bind the *Lhcb* promotor and its core binding site, the CCAC motif, is considerably over-represented in the GUN1 and GUN2-5 signalling targets.

1.7 Project aims

The tetrapyrrole biosynthesis pathway has already been shown to be regulated at two main sites: the *HEMA1* gene and its protein product, Glu-TR, responsible for the synthesis of glutamate-1-semialdehyde in the first committed step, and the chelatase branchpoint separating the chlorophyll and haem/phytochromobilin synthesis pathways. The main focus of this project is the transcriptional and post-translational regulation at the branchpoint in the tetrapyrrole biosynthesis pathway in *Arabidopsis*. Although the initial point of regulation in the pathway has consequently been shown to control total flux through the pathway (e.g. McCormac *et al*., 2001), regulation of the branchpoint in the pathway is less well understood. The *GUN4* gene, originally identified in a screen for chloroplast-to-nucleus signalling mutants (Mochizuki *et al*., 2001; Larkin *et. al*., 2003) and a regulator of chlorophyll synthesis acting through the branchpoint enzyme Mg-chelatase, is of particular interest.

Quantitative RT-PCR will initially be employed to study the transcriptional regulation of the genes encoding the two enzymes at the branchpoint, Mg-chelatase and Ferrochelatase (*CHLD, CHLH, CHLI1* and *CHLI2*, and *FC1* and *FC2*, respectively), to elucidate the light regulation of these sites. Additionally, the *GUN4* gene and Magnesium protoporphyrin methyltransferase (*CHLM*), the next gene in the chlorophyll-synthesis pathway, will be analysed. This work will then be followed up with more in-depth analysis of the phytochrome-signalling pathway responsible for the regulation of *HEMA1* and any light-regulated branchpoint genes.

Transgenic analysis of the two tetrapyrrole pathway regulating proteins *GUN4* and *FLU* has yet to appear in the literature, and it would seem that the results from over-expression analysis will form a crucial part of our understanding of their role within the plant. Therefore plants containing overexpression constructs for these genes will be produced. In tandem it will also be important to learn the effect that disrupting the *GUN4* and *FLU* genes has on tetrapyrrole synthesis. As a result *gun4* and *flu* mutant plants will be analysed alongside WT seedling to assess their ability to de-etiolate effectively.

Recently, the *Synechocysis ScpB* and *ScpE* genes, which are homologous to

OHP1 from *Arabidopsis*, were shown to affect tetrapyrrole synthesis (Xu *et al*., 2002). Additionally, *ELIP2*, another member of the *LIL* (Light-Induced-Like) family, was shown to influence chlorophyll synthesis (Tzvetkova-Chevolleau *et al*., 2007). It will therefore be interesting to see the effect of *OHP1*, and the closely related gene *OHP2*, on the tetrapyrrole pathway. This will be achieved through analysis of both mutant and overexpressing lines for these genes.

Concurrently, a range of mutants has been produced in the Terry lab that retain expression of *HEMA1* following a far-red block of greening treatment, and are hypothesised to form part of the ROS retrograde plastid signalling network. These mutants, produced through simple EMS mutagenesis, require careful backcrossing should they be used for any further study. This action will be undertaken while making some preliminary analysis of the mutants, such as phenotypic analysis and allelic elucidation based on these observations.

Chapter 2: Materials and Methods

2.1 Basic physiology

2.1.1 Light treatments

For all physiology treatments, unless otherwise stated, broad-band white light (W) was provided by white fluorescent tubes (400 nm-700 nm = 110 µmol m^{-2} sec^{-1}). Narrow waveband sources were provided by LED displays in environmental control chambers (Percival Scientific Inc., Boone, IA, USA). Red light (R) corresponded to a peak at 669 nm (25 nm band-width at 50% of peak magnitude) with a fluence rate of 80 µmol m^{-2} sec^{-1}. Far-red light (FR) from the LEDs had a peak at 739 nm (25 nm band-width at 50% of peak magnitude) and was passed through a filter (#116; Lee Filters, Andover, UK) to remove $\lambda < 700$ nm to give a final fluence rate of 10 µmol m^{-2} sec^{-1} (23^{o}C). Blue light (B) had a peak at 470 nm (25 nm band-width at 50% of peak magnitude) and a fluence rate of 20 µmol m^{-2} sec^{-1} (23^{o}C).

2.1.2 Growth of seedling material

Prior to sowing, seeds were dried and stored at 4^{o}C for >1 week, as a stratification step to allow uniform germination. For each wild type and mutant line approximately 200 *Arabidopsis thaliana* seeds were surface sterilised using 10% (v/v) bleach for 20 minutes, before being washed three times using sterile water. Seeds were then sown onto autoclaved ½ MS (Murashige & Skoog, 1962) media (0.8% agar, 0% sucrose) in 55mm diameter plates, and sealed with parafilm. These were wrapped in tin foil and placed in a cold room (4^{o}C) for 48h, for stratification. Plates were (unless otherwise stated) routinely exposed to 2 hours W light to stimulate uniform germination, then re-wrapped in tin foil. Seedlings were then placed in a dark cabinet (23^{o}C) for 24h, for gene expression or hypocotyl analysis, or 48h, for pigment analysis. Seedlings were then treated with either W, R or FR light (as described in section 2.1.1), or remained in the dark. For the far-red block of greening response, following FR light treatment seedlings were exposed to W light for 24h. All plant lines and their corresponding WT backgrounds have been summarised in Table 2.1.

Table 2.1 Nomenclature and allelic labelling for all mutant plant lines used, and the original WT background used to generate them.

Mutant Line	Background (Ecotype)	Mutation Source	Acquired From	Reference
aba1-1	L*er*	EMS	NASC	Koornneef *et al*., 1982a
abi1-1	L*er*	EMS	NASC	Koornneef *et al*., 1984
abi2-1	L*er*	EMS	NASC	Koornneef *et al*., 1984
abi3-1	L*er*	EMS	NASC	Koornneef *et al*., 1984
abi4-102	*gl1-1* (Col)	EMS	NASC	Finkelstein *et al*., 1994 Laby *et al*., 2000
abi5-1	Ws	T-DNA	NASC	Finkelstein *et al*., 1994
cry1 (hy4-3)	Col-0	EMS	M. Ahmad	Ahmad *et al*., 1998
cry1cry2 (hy4-3fha1-1)	Col-0	EMS/EMS	M. Ahmad	Ahmad *et al*., 2002
cry2 (fha1-1)	Col-0	EMS	M. Ahmad	Ahmad *et al*., 1998
fhy1-1	L*er*	γ-Ray	G. Whitelam	Whitelam *et al*., 1993
fhy3-1	Col-0	EMS	G. Whitelam	Whitelam *et al*., 1993
flu-1	Col-0	EMS	K. Apel	Meskauskiene *et al*., 2001
gl1-1	L*er*	EMS	NASC	Koornneef *et al*., 1982b
gl2-1	L*er*	EMS	NASC	Koornneef *et al*., 1982b
gl3-1	L*er*	EMS	NASC	Koornneef *et al*., 1982b
gun4-1	Col-0	EMS	E. Lopez-Juez	Susek *et al*., 1993
myb50	Col-8	SALK	NASC	Alonso *et al*., 2003
myb61	Col	JI-SM	NASC	Tissier *et al*., 1999
ohp1-GK272	Col-2	Gabi-Kat	NASC	Rosso *et al*., 2003
ohp1-GK362	Col-2	Gabi-Kat	NASC	Rosso *et al*., 2003
ohp1-GK631	Col-2	Gabi-Kat	NASC	Rosso *et al*., 2003
ohp2-GK071	Col-2	Gabi-Kat	NASC	Rosso *et al*., 2003
phyA-1	L*er*	γ-Ray	G. Whitelam	Whitelam *et al*., 1993
phyAphyB (phyA-1phyB-1)	L*er*	γ-Ray/EMS	X-W. Deng	
phyB-1	L*er*	EMS	X-W. Deng	Koornneef *et al*., 1980
pif1-2	Col-0	T-DNA	P.H. Quail	Huq *et al*., 2004
pif1-101	Col-0	SAIL	C. Fankhauser	Sessions *et al*., 2002
pif1pif3 (pif1-101pif3-1)	Col-0/8	SAIL/SALK	C. Fankhauser	Alonso *et al*., 2003 Sessions *et al*., 2002
pif3-3	Col-0	SALK	P.H. Quail	Alonso *et al*., 2003 Monte *et al*., 2004
pif3-1	Col-8	SALK	C. Fankhauser	Alonso *et al*., 2003 Kim *et al*., 2003

Abbreviations: *aba* = abscisic acid deficient, *abi* = abscisic acid insensitive, Col = Columbia, *cry* = cryptochrome, *fhy* = far-red elongated hypocotyl, *flu* = fluorescent in blue light, Gabi-Kat = Gabi Kat T-DNA insertion lines, *gl* = glabrous, SAIL = GARLIC (SAIL) T-DNA insertion lines, *gun* = genomes uncoupled, L*er* = Lansberg *erecta*, *myb* = myeloblastosis, *ohp* = one helix protein, *phy* = phytochrome, *pif* = phytochrome interacting factor, SALK = SALK T-DNA insertion lines, JI-SM = John Innes Centre 'Suppressor Mutator' transposon insertion lines, Ws = Wassilewskija.

2.1.3 Growth and crossing of mature plants

For mature plant phenotyping and crossing experiments approximately 10 *Arabidopsis* seedlings were initially sown on soil in 8cm^2 pots. Pots were covered with

clear film wrap and treated with growth room conditions (16h/8h; light (80 µmol m^{-2} s^{-1})/dark; 23/20^{o}C). Following germination, the clear film wrap was removed and seedlings were separated to leave one seedling per pot. Plants phenotypes were recorded as indicated for individual experiments.

Due to the ease with which *Arabidopsis* self pollinates, for crossing purposes it is necessary to manually pollinate each plant to ensure a successful cross. For each mutant plant approximately four flowers were prepared, however, the first three flowers were ignored, as these are generally found to be infertile; crossing therefore commenced when more than six flowers had emerged. At this stage all unwanted flowers and leaves, and the terminal influorescence were removed, leaving four flowers with a fully developed stigma, but stamens that are yet to shed any pollen. Using optical glass magnifiers, each flower was carefully opened using fine forceps and the sepals, petals and stamens removed, being careful not to damage the stigma.

The emasculated flowers were marked using short strips of masking tape and left for 48 hours to allow the stigma to develop. During this period the plants were covered with a clear plastic bag to prevent pollination, and establish whether self-pollination has already occurred (a silique should not develop). After the 48-hour period each style had developed a characteristic "hairy/crowned" surface.

For the male (parental-line) parent an open flower that was visibly shedding pollen was chosen. Forceps were used to open the amputated flower, before brushing the exposed pollen on the pre-prepared style, and re-covering with a clear plastic bag. Plants were checked every 24 hours for the development of siliques, to allow the removal of the plastic bag and the silique to dry.

Siliques were harvested after approximately 3 weeks and transferred to vented eppendorf tubes for a further week, to allow them to dry completely. Seeds were then stratified for one week and planted to allow selfing.

2.2 Chlorophyll extraction and analysis

Two batches of 15 seedlings were harvested from each experimental plate and

weighed before freezing in liqued Nitrogen. Seedlings were homogenised in 1ml 80% acetone (v/v) using an Ultra-Turrax© T8 hand held homogeniser (IKA Labortechnik, Germany) and the suspension was vortexed thoroughly and spun at 13,000 g for 10 mins. Following extraction, samples were maintained in the dark at all times.

Absorbance was measured at 470nm, 647nm and 663nm, and data analysed using the formulae of Lichtenthaler (1987):

Total chlorophyll = (7.15*abs 663nm) + (18.71*abs 647nm)
Chlorophyll *a* = (12.25*abs 663nm) - (2.79*abs 647nm)
Chlorophyll *b* = (21.5*abs 647nm) – (5.1*abs 663nm)
Total carotenoids = ((1000*abs 470nm) – (1.82* chlorophyll *a*) – (85.02*chlorophyll *b*))/198

The results from the two extractions were then averaged and treated as one biological repeat.

2.3 Protochlorophyllide extraction and analysis

To extract protochlorophyllide (Pchlide), 0.1g of whole seedling material was homogenised using an Ultra-Turrax© T8 hand held homogeniser (IKA Labortechnik, Germany) in 1ml cold extraction solvent (acetone:0.1M NH_4OH, 90:10, v/v), as described previously (Terry and Kendrick, 1999). Samples were then centrifuged at 13,000 g in a bench-top microcentrifuge. The supernatant was kept and the pellet re-extracted with 0.75 ml fresh extraction solvent and the samples combined.

Pchlide was measured by relative fluorescence at 628 nm following exicitation at 440 nm, using a Hitatchi F-3010 fluorescence spectrophotometer (Hitatchi, Tokyo, Japan).

2.4 Protein extraction and immunoblotting

Total proteins were extracted from seedlings with 1.5 x (w/v) SDS extraction buffer (80 mM Tris-HCl (pH 8.8) containing 10% (w/v) glycerol, 10% (w/v) SDS, 5%

(v/v) 2-mercaptoethanol and 0.002% (w/v) bromophenol blue) by homogenising using an Ultra-Turrax© T8 hand held homogeniser (IKA Labortechnik, Germany) and centrifuging at 13,000 g for 10 min at 4^{o}C in a bench-top microcentrifuge. Proteins were separated using 9% SDS PAGE gels, with 4% stacking gels, and blotted onto Immobilon-P transfer membrane (Millipore, MA, USA) as described previously (Terry *et al*., 2001). Membranes were blocked at 4°C overnight in TBS (20mM Tris/HCl (pH 7.5) containing 167mM NaCl and 0.05% (v/v) Tween) with the addition of 5% (w/v) fat free milk powder, followed by three 1 min washes in TBS-Tween. The membrane was then incubated with polyclonal antibodies raised to CHLI, CHLH, Glu-TR or POR at a 1:1000 dilution in TBS-Tween at 37°C for 30 mins. After further washing, the membrane was incubated with goat anti-rabbit IgG conjugated to Alexa Fluor 680 (Invitrogen, CA, USA) in complete darkness at room temperature for 1h. Fluorescence was then measured using an Odyssey Infrared Imaging System (Li-Cor Biosciences, NE, USA) and data analysed using Odyssey v1.12 software.

2.5 RNA extraction

Prior to use all tips, eppendorfs, glassware, buffers, and solutions were autoclaved for 1.5 hours at 121^{o}C, and gloves were worn at all stages.

Approximately 500µg of whole seedling material was homogenised in 150µl phenol (pH 4.8) and 500µl 'RNA Miniprep' buffer (100mM NaCl; 10mM Tris pH 7.0; 1mM EDTA; and 1% SDS) using an Ultra-Turrax© T8 hand held homogeniser (IKA Labortechnik, Germany). Two hundred and fifty micro litres of chloroform was then added to each sample, and they were again vortexed thoroughly for 30 seconds. Following a spin in a microcentrifuge at 13,000 g for 5 min, the upper phase (approximately 500µl) was precipitated for 12 hours at 4^{o}C with 450µl 4M LiCl.

The precipitate was recovered by centrifugation in a microfuge at 13,000 g for 10 min. The pellet was then resuspended in 300µl DNase buffer (10mM Tris HCl pH 7.5; 2.5mM $MgCl_2$; and 0.5mM $CaCl_2$) and 1µl DNase, and incubated at 37^{o}C for 25 minutes. Five hundred micro litres phenol:chloroform:isoamyl (25:24:1, v/v/v) was then added. Samples were again vortexed thoroughly for 30 seconds and then centrifuged at 13,000 g for 5 min.

The upper phase was again retained, added to 750µl ethanol containing 5% (w/v) 3M NaAc (pH 5.5), mixed thoroughly, and precipitated for 1 hour at -20^{o}C. RNA was finally recovered in the pellet in a microfuge at 13,000 g for 5 min, air dried for approximately 1h, and resuspended in 30µl TE buffer (10mM Tris HCl (pH 8), 1mM EDTA).

The quantity and purity of samples was determined on a 'Nano-Drop' ND-1000 spectrophotometer (Thermo Fischer Scientific, DE, USA). One micro litre of RNA sample was loaded onto the sample pedestal and absorbance was measured over the range 200-300nm. Absorbance at 260nm allows the determination of RNA quantity, and the absorbance at 280nm (ratio of OD_{260nm}/OD_{280nm}) allows the determination of protein and carbohydrate contamination. Samples were stored at -80^{o}C until required.

2.6 Reverse transcription reaction

First strand complementary DNA (cDNA) was prepared from total RNA. One µg of oligo $(dT)_{12-18}$ (500µg/ml) primer (Invitrogen, CA, USA) was added to 1µg of RNA diluted in a total of 11µl of RNAse-free sterile water. This was incubated at 70^{o}C for 10 min to allow primer binding, followed by a 2 min chill on ice. Four micro litres of 5x first strand buffer (Invitrogen, CA, USA), 2 µl of 0.1M DTT (Invitrogen, CA, USA) and 1 µl 10mM dNTP mix (10mM of each dATP, dGTP, dCTP and dTTP at neutral pH) (Promega, UK) was added, and incubated at 42^{o}C for 2 minutes. One micro litre (two hundred units) of superscript reverse transcriptase (Invitrogen, CA, USA) was added, mixed by pipetting, and incubated at 42^{o}C for 50 minutes. The reaction was stopped by heating to 70^{o}C for 15 minutes.

2.7 Primer design

Where possible primers were designed to span an intron, to allow the recognition of contaminating genomic DNA. Additionally, qRT-PCR primers were specifically designed to give a product size of 50-250bp. All primers used and their sequences are shown in Table 2.2.

Table 2.2 Primer names and sequences used for all aspects of PCR.

Name	Sequence (3'- 5')
35S FOR	CATTTGGAGAGGACCTCGACTCT
40S FOR	GGCGACTCAACCAG
40S REV	CGGTAACTCTTCTGGTAACGA
AT1G75690 FOR (1)	GCCACGTGAACAAATCTTAGC
AT1G75690 REV (1)	ATCGTCCTTGAACTCCCTGAC
AT1G75690 FOR (2)	TCTTATCCCCGAATCAAAGC
AT1G75690 REV (2)	CTCCTCCACCAAGCTCTACG
ACT2 FOR	CTTGCACCAAGCAGCATGAA
ACT2 REV	CCGATCCAGACACTGTACTTCC
CHLD FOR	CCACATCAGATACGGATACGG
CHLD REV	GTCAGCATTGTACTCTATGCGCTC
CHLH FOR	CTGGTCGTGACCCTAGAACAG
CHLH REV	GATTGCCAGCTTCTTCTCTG
CHLI1 FOR	CGGTTATGAATGTAGCCACTG
CHLI1 REV	CTTGCCCTACTATAGCTGC
CHLI2 FOR	CAGATCTCGTTACCATGTC
CHLI2 REV	GGCATAGCTTCATCTCATC
CHLM FOR	AGCCGGGGTCGACAGTACAACAATC
CHLM REV	ACCGGCCAAGGATCTATCTTCAGTC
CAO FOR	CTTGGATTGGCGTGCTCG
CAO REV	CGGAACCGGACCAGAAACATTC
ELIP1 FOR	ATCAGTCTTCGCCGGTGGAT
ELIP1 REV	GCAAGTGTCAAGATCGCTGTT
ELIP2 FOR	CTGCTCCTTCCGGTGTATTG
ELIP2 REV	ACTAGAGTCCCACCAGTGACGTA
FC1 FOR	CACCGACTTAGCTGATGCAGTGATAG
FC1 REV	CCCACATCAGCTTATTAGAGCTGGTG
FC2 FOR	GCTACTTCATCAAACCGGCTTC
FC2 REV	GCATCAGTTATGTGGCGAA
FLU Clone FOR	CACCAAAAAAATGGCGGCGCTTATCCG
FLU Clone REV	GTCAGTCTCTAACCGAGC
FLU Clone REV [Stop]	TCAGTCAGTCTCTAACCGAGC
FLU FOR	GTGACAAGTCTCGAGCTCCAG
FLU REV	CAAGAGGTGTAGCCATCTGAAG
GLK1 FOR	GTATTCCTCTTCAGCTTCTTCC
GLK1 REV	CTCCTAACTGTTCCACTGCCTC
GLK2 FOR	CTAATACTCCGGCGTCTGCTCA
GLK2 REV	CAATAGCTGCATCTATGCTCTCAT
GK LB REV	ATATTGACCATCATACTCATTGC
GK RB FOR	GTGGATTGATGTGATATCTCC
GUN4 Clone FOR	CACCAAAAAAATGGCGACCACAAACTCTCTC
GUN4 Clone REV	GAAGCTGTAATTTGTTTTAAACAC
GUN4 Clone REV [Stop]	TCAGAAGCTGTAATTTGTTTTAAACAC
GUN4 FOR	TCCCTCAAACAACCCACTTC
GUN4 REV	GAGGAGGTGGAAGAAGCAGA
GSA FOR	CTTCACCAGCTTCTAACCGA
GSA REV	CTCATTTCCATCAATGTCCCA
HEMA1 FOR	CAAGAACTCTGCAGCTGATC
HEMA1 REV	CCATTCAGCTTCAGGTATAGC
Lhcb2.1 FOR	GTGACCATGCGTCGTACCGTC
Lhcb2.1 REV	CTCAGGGAATGTGCATCCG
LIL3 FOR	CACCGCCGCCGTCTCCGTGG
LIL3 REV	CCCAATGACTCATCATCATC
LIL3-Like FOR	ATGTCTATATCCATGGCG

Table 2.2 Continued.

LIL3-Like REV	CTGTTGATGAATCTGGCTC
M13 REV	CAGGAAACAGCTATGAC
MYB50 FOR	GCACTGTCTCTGGACAGGATC
MYB50 REV	TGTAAGAAAATTAATTAATTGG
MYB50 REV (2)	GACCACCAAAAGAGAAGGC
MYB61 FOR	TGTTAGCTTTGCACAGCATTG
MYB61 REV	TCTGAAATTCCCAGTTTGGTG
OHP1 Clone FOR	CACCAAAAAAATGAGCTCGTCGCCGTTATC
OHP1 FOR	ATGAGCTCGTCGCCGTTATC
OHP1 REV	TTATAGAGGAAGATCGAGTCC
OHP1 UTR FOR	GGCGAAATATGAATGGATCGG
OHP2 Clone FOR	CACCAAAAAAATGTCAGTAGCTTCACCGAT
OHP2 FOR	ATGTCAGTAGCTTCACCGAT
OHP2 REV	TTATTCCAAGTCTAGAATGC
PORA FOR	GGACTTGGCGTCTTTGGACAGC
PORA REV	GCCGTTGGCTGATAGACTGCG
SK LB (b)	GCGTGGACCGCTTGCTGCAACT
SK RB	GACAGGATATATTGGCGGGTA
SPM (32) RB	TAGAATAAGAGCGTCCATTTTAGAGTGA
YLS8 FOR	TTACTGTTTCGGTTGTTCTCCA
YLS8 REV	CACTGAATCATGTTCGAAGCAA

2.8. Quantitative polymerase chain reaction (qPCR)

qPCR is a technique which employs DNA binding fluorophores to visualise DNA amplification in a 'real-time' manner. In this case SYBR Green, an interchelator of dsDNA, was used.

2.8.1 qPCR process

Quantitative PCR was carried out using the DyNAmo SYBR Green kit according to the manufacturers instructions (Finnzymes, Finland). The concentration of sample components are show in Table 2.3. These were loaded into a 96 well plate (MJ Research, MA, USA) and sealed with clear caps (MJ Research, MA, USA). The plate was then vortexed briefly, and spun at 2,000xg for 2 min. The PCR conditions were as outlined in Table 2.4. Following this a melting curve was conducted. Here samples were heated from 60-95^{o}C, with a fluorescence reading taken every 0.2^{o}C. qPCR was run on a Opticon DNA Engine Continuous Fluorescence Detector (GRI, Braintree, UK) using the Opticon Monitor III program.

Table 2.3 Reagent concentrations used for different PCR reactions.

Reaction Reagent	Semi-quantitative PCR	gPCR	qPCR	HiFi PCR
	Concentration			
Template DNA	10ng	10ng	2.5ng	10ng
Primer A	1µM	1µM	0.3 µM	1µM
Primer B	1µM	1µM	0.3 µM	1µM
Taq Master Mix	1X	1X	-	-
SYBR-Green Master Mix	-	-	1X	-
PBR Buffer	-	-	-	1X
$MgSO_4$	-	-	-	1.5mM
dNTPs	-	-	-	200µM
HiFi Taq	-	-	-	2.5U
dH_2O	To 20µl	To 20µl	To 10µl	To 20µl

Table 2.4 Cycle conditions used for different PCR reactions.

Temperature (^oC)	Semi-quantitative PCR	gPCR	qPCR	HiFi PCR
	Duration			
95	3 min	3 min	10 min	3 min
95	30 sec	30 sec	15 sec	30 sec
Annealing	(54-62^{o}C)[1] 30 sec	(56^{o}C) 30 sec	(60^{o}C) 1 min	(56^{o}C) 30 sec
72	1 min	1 min 30 sec	-	-
68	-	-	-	1 min
go to step 2	24-32 cycles	35 cycles	39 cycles	29 cycles
72	5 min	5 min	10 min	-
68	-	-	-	5 min

[1] = the annealing temperature used in semi-quantitative PCR varied for each primer pair; see section 2.9 for details.

2.8.2. qPCR analysis

Firstly the melting curve was used for the detection of secondary products and primer dimers, highlighted by the presence of more than one peak. Provided that only one peak was detected then analysis can be conducted.

Analysis relied upon the presence of a control/constitutive gene (e.g. *40S*), both a control condition and an experimental condition (e.g dark vs. light), and an efficiency value being calculated. Efficiency, relating to the efficiency of the primers, was calculated through the construction of a standard curve. For this a preliminary plate was run containing a series dilution of template DNA (e.g. 1, 0.33, 0.11, 0.0369, 0.0123, 0.00409, 0.00136, 0.000454), and run under the conditions previously described. This was repeated three times and the mean cycle threshold value of the

three was taken. The mean cycle threshold value was then plotted against the Log cDNA concentration and the efficiency of the primer pair could be calculated using the slope of the amplification in the equation:

$$\text{Efficiency} = (10^{(-1/\text{slope})})$$

If the reaction was run under perfect conditions, efficiency should be 2 (i.e. doubling of DNA product after each cycle), but values of 1.5-2.1 are acceptable. Experimental results were analyzed based on the C(t) value (the point at which the fluorescence crosses a pre-determined threshold value), using the following equation:

$$\text{Relative expression} = \frac{(E_{\text{target}})^{\Delta C(t)\text{target (control – sample)}}}{(E_{\text{reference}})^{\Delta C(t)\text{reference (control – sample)}}}$$

These expression ratios were then used to assess gene expression under experimental conditions. Primer pairs used for all qPCR analysis and their expected product sizes are shown in Table 2.5.

Table 2.5 Primer pairs and their expected product sizes used in qPCR.

Primer Sets	**Product Size**
40S FOR + 40S REV	435bp
CAO FOR + CAO REV	364bp
CHLD FOR + CHLD REV	302bp
CHLH FOR + CHLH REV	319bp
CHLI1 FOR + CHLI REV	111bp
CHLI2 FOR + CHLI2 REV	207bp
CHLM FOR + CHLM REV	298bp
FC1 FOR + FC1 REV	311bp
FC2 FOR + FC2 REV	368bp
FLU FOR + FLU REV	270bp
GSA FOR + GSA REV	224bp
GUN4 FOR + GUN4 REV	80bp
HEMA1 FOR + HEMA1 REV	121bp
Lhcb2.1 FOR + Lhcb2.1 REV	246bp
OHP1 FOR + OHP1 REV	333bp
PORA FOR + PORA REV	108bp
PP2A FOR + PP2A REV	61bp
SAND Family FOR + SAND Family REV	61bp
YLS8 FOR + YLS8 REV	66bp

2.9 Semi-quantitative polymerase chain reaction

All semi-quantitative PCR reactions were carried out using Biomix PCR Mastermix (Bioline, MA, USA) in 0.2ml thin walled tubes (Thermo Fischer Scientific, DE, USA) and run on an MJ Research DNA Engine thermal cycler (MJ Research, MA, USA) using the conditions outlined in Table 2.3 and the cycles outlined in Table 2.4.

The annealing temperature of a primer pair in the amplification was determined by using a temperature gradient in the PCR reaction. Multiple reactions were set up for each primer pair and the temperature of the primer annealing step was varied over a temperature range between 54^{o}C – 62^{o}C. This determined the annealing temperature with the maximal amplification of the chosen gene, without the amplification of secondary products. For the majority of cases the annealing temperature corresponded to approximately 3^{o}C below the primer T_M.

The number of cycles required for each primer pair was determined using multiple reactions. Samples were run as normal but after 19-26 cycles one sample was removed and stored on ice, before being replaced for the final elongation step. Primer pairs and their expected product sizes for all semi-quantitative PCR reactions are shown in Table 2.6.

Table 2.6 Primer pairs and their expected product sizes used in sqPCR.

Primer Sets	Product Size
40S FOR + 40S REV	435bp
AT1G75690 FOR (2) + AT1G75690 REV (2)	559bp
ELIP1 FOR + ELIP1 REV	408bp
ELIP2 FOR + ELIP2 REV	541bp
LIL3 FOR + LIL3 REV	627bp
LIL3-Like FOR + LIL3-Like Rev	760bp
MYB50 FOR + MYB50 REV (2)	264bp
MYB61 FOR + MYB61 REV	804bp
OHP1 FOR + OHP1 REV	333bp
OHP2 FOR + OHP2 REV	519bp

2.10 Genomic PCR (gPCR)

For all mutant lines gPCR was carried out using Biomix PCR Mastermix (Bioline, MA, USA) in 0.2ml thin walled tubes (Thermo Fischer Scientific, DE, USA) and run on a an MJ Research DNA Engine thermal cycler (MJ Research, MA, USA) using the buffer concentrations outlined in Table 2.3 and the cycles outlined in Table 2.4. Primer pairs and their expected product sizes are shown in Table 2.7.

Table 2.7 Primer pairs and their expected product sizes used in gPCR.

Primer Sets	Insert	Product Size
35S FOR + FLU Clone REV Stop	FLU pMDC32	1042bp
35S FOR + GUN4 Clone REV Stop	GUN4 pMDC32	892bp
35S FOR + OHP1 REV	OHP1 pMDC32	424bp
35S FOR + OHP2 REV	OHP2 pMDC32	610bp
AT1G75690 FOR (1) + AT1G75690 REV (1)	SALK_018350	1049bp
GK RB FOR + OHP1 REV	GK272	471bp
GK RB FOR + OHP1 REV	GK362	422bp
GK RB FOR + OHP1 REV	GK631	785bp
GK RB FOR + OHP2 REV	GK071	473bp
MYB50 FOR + MYB50 REV	SALK_035416	1051bp
MYB50 FOR + SK LB REV	SALK_035416	587bp
MYB61 FOR + MYB61 REV	SM_3_30853	1060bp
OHP1 FOR + GK LB REV	GK272	137bp
OHP1 FOR + GK LB REV	GK362	334bp
OHP1 FOR + OHP1 REV	GK272/362	488bp
OHP1 UTR FOR + GK LB REV	GK631	77bp
OHP1 UTR FOR + OHP1 REV	GK631	615bp
OHP2 FOR + GK LB REV	GK071	579bp
OHP2 FOR + OHP2 REV	GK071	519bp
SK RB FOR + AT1G75690 REV	SALK_018350	958bp
SK RB FOR + MYB50 REV	SALK_035416	769bp
SPM (32) RB FOR + MYB61 REV	SM_3_30853	553bp

2.11 Gel electrophoresis

Semi-quantitative and genomic PCR products were assessed on a 1% (w/v) agarose/TAE (40mM Tris /acetate (pH 8.0), 1mM EDTA) gel, containing 1.5µl Ethidium Bromide for DNA detection. This was set at room temperature for approximately 1h. Ten micro litres of amplified sample DNA was loaded into the gel wells, following PCR. Additionally, 5µl of DNA Hyperladder I (Bioline, MA, USA) was loaded to assess the product size (figure 2.1). Gels were run at 120 volts using a

Powerpac 200 (Biorad, CA, USA) for 45 min in 1% (v/v) TAE buffer, before visualising under UV light.

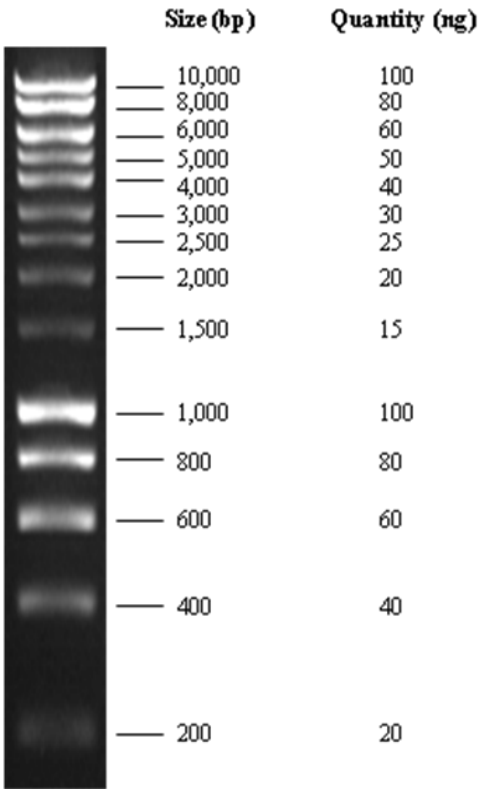

Figure 2.1 Size and quantity of DNA making up the DNA Hyperladder I (Bioline, MA, USA) used for analysis of agarose gels throughout this report.

2.12 Gene cloning and transformation

2.12.1 Primer design, gene cloning and Entry Vector™ generation

As the Gateway™ (Invitrogen, CA, USA) system was being employed to produce transformation vectors, all forward cloning primer were designed to contain the sequence CACCAAAAAAA immediately prior to the start of the desired sequence. Primers for the coding DNA sequence (CDS) of a gene were either designed with or without a stop codon, depending upon whether they were intended for use with a vector containing a tag or not. Primer pairs used for cloning, and their product sizes, are outlined in Table 2.8.

Table 2.8 Primer pairs and their product sizes used for the cloning of DNA products for transformation.

Primer Sets	Product Size
GUN4 Clone FOR + GUN4 Clone REV Stop	892bp
FLU Clone FOR + FLU Clone REV Stop	1045bp
OHP1 Clone FOR + OHP1 REV [Stop]	424bp
OHP2 Clone FOR + OHP2 REV [Stop]	610bp

Sequences were amplified from cDNA, produced as described in section 2.6, using High Fidelity (HiFi) Taq (Invitrogen, CA, USA), to ensure accurate amplification, using the protocols outlined in Table 2.3 and 2.4.

Following gel electrophoresis to confirm the PCR product was the correct size, it was quantified on an 'Nano-Drop' ND-1000 spectrophotometer (as described in section 2.5; Thermo Fischer Scientific, DE, USA) immediately prior to cloning into the Entry Vector™ (Invitrogen, CA, USA) according to the manufacturer's instructions (Invitrogen, CA, USA): 25ng of PCR product was combined with 1µl salt solution, 1µl of TOPO® (Entry) vector and dH_2O to a final volume of 6µl. This reaction mix was incubated at room temperature for 5 mins and then 2µl added to a vial of One Shot® chemically competent *E.coli* cells, mixed gently and incubated on ice for 15 min. The cells were heat shocked for 30 sec at 42^{o}C and transferred back to ice. Two hundred and fifty micro litres of LB broth was added to the cells and were then shaken at 37^{o}C for 1h. Cells were then spread on freshly prepared LB agar plates containing 50µg/ml kanamycin and incubated at 37^{o}C overnight.

Five colonies from any successful transformations were dipped into a PCR reaction containing primers as outlined in Table 2.9 and then onto a freshly prepared numbered LB agar plate containing 50µg/ml kanamycin. The PCR reaction was run as outlined in Table 2.3 and Table 2.4.

Table 2.9 Primer pairs, and their product sizes, used for confirmation of accurate Entry vector cloning.

Primer Sets	Product Size
GUN4 Clone FOR + M13 REV	1066bp
FLU Clone FOR + M13 REV	1219bp
OHP1 Clone FOR + M13 REV	598bp
OHP2 Clone FOR + M13 REV	784bp

Any accurate clones were then cultured in 5ml LB broth containing 50µg/ml kanamycin overnight, and DNA extracted using a Mini-prep kit (Qiagen, CA, USA) as described by the manufacturer. Correct insert location and orientation was confirmed using both PCR and sequencing (Geneservice, Oxford, UK). PCR was conducted using the conditions outlined in Table 2.3 and 2.4.

2.12.2 Expression vector construction

The LR Clonase™ reaction was carried out according to the manufacturer's instructions (Invitrogen, CA, USA): 100ng Entry Vector™ was added to 100ng pMDC32 destination vector and TE buffer (pH 8) to a final volume of 8µl.

Two µl of LR Clonase™ II enzyme (previously thawed on ice) was added to the reaction mix, vortexed briefly, centrifuged briefly to collect the contents and incubated at 25^{o}C for 1 hour. To terminate the reaction, 1µl of Proteinase K enzyme was added to the reaction which was then incubated at 37^{o}C for 10 mins. 1µl of fresh LR reaction was then transferred into 50µl of One Shot® OmniMAX™ 2 T1 phage-resistant cells (Invitrogen, CA, USA), incubated on ice for 20 mins, heat-shocked at 42^{o}C for 30 secs and immediately transferred back to ice. 250µl of LB broth was added to the cells before incubating at 37^{o}C with shaking for 1 hour, and then spread on freshly prepared LB agar plates containing 50µg/ml Kanamycin antibiotic outlined and incubated at 37^{o}C overnight.

Five colonies from any successful transformations were dipped into a PCR reaction containing primers as outlined in Table 2.11 and then into freshly prepared numbered LB agar plates containing 50µg/ml kanamycin antibiotic. PCR was performed according to the conditions in Table 2.3 and 2.4.

Restriction enzyme digest was conducted according to manufacturer's instructions (Promega, WI, USA): 1µl enzyme was added to 2µl 10x reaction buffer and 500ng plasmid, and finally dH_2O was added to a final volume of 20µl. This reaction mix was incubated at the temperature indicated in Table 2.10, and run on a gel electrophoresis with expected band sizes also shown in Table 2.10.

2.12.3 *Agrobacterium* transformation

DNA was extracted from transformed *E.coli* using a Mini-prep kit according to the manufacturer's instructions (Qiagen, CA, USA) and quantified by 'Nano-Drop' ND1000 spectrophotometer (as described in section 2.5; Thermo Fischer Scientific, DE, USA). Two hundred nano grams of plasmid was then transferred to a 1.5ml Eppendorf tube containing 50µl GV3101 *Agrobacterium* cells. Following gentle mixing, cells were transferred to 2mm electroporation cuvettes (Cell Projects, Kent, UK) and pulsed at 1.8 volts for 10ms. Cells were then transferred to 1.5ml eppendorf tubes containing 250ml LB broth and incubated at 30^{o}C for 2 hours before being spread on LB agar plates containing 25µg/ml gentamycin, 50µg/ml kanamycin and 25µg/ml rifampicilin. They were then cultured at 30^{o}C for 2 days.

Table 2.10 Restriction enzymes used for the confirmation of correct and accurate destination vectors. Negative-result band sizes are shown in brackets.

Vector	Restriction Enzyme	Product sizes	Temperature
GUN4 pMDC32	Xho1	1094, 2199, 7587 (1094, 3070, 7587)	37^{o}C
FLU pMDC32	Xho1	114, 821, 1094, 1417, 7587 (1094, 3070, 7587)	37^{o}C
OHP1 pMDC32	Xho1	1094, 1790, 7587 (1094, 3070, 7587)	37^{o}C
OHP2 pMDC32	Xho1	1094, 1976, 7587 (1094, 3070, 7587)	37^{o}C

Three colonies from each plate were shaken in 10ml LB broth containing 25µg/ml gentamycin, 50µg/ml kanamycin and 25µg/ml rifampicilin for two days. Five millilitres of this culture was used to confirm the presence of the insert through DNA extraction using a Mini-prep kit (Qiagen, CA, USA) and PCR, conducted using the primers outlined in Table 2.11.

Table 2.11 Primer sets used to confirm presence of vectors in *Agrobacterium*.

Primer Sets	Expected Band Size
35S FOR + GUN4 Clone REV Stop	892bp
35S FOR + FLU Clone REV Stop	1042bp
35S FOR + OHP1 REV Stop	424bp
35S FOR + OHP2 REV Stop	610bp

2.12.4 *Arabidopsis* transformation

Following confirmation of a positive PCR result the remaining 5ml of the Agrobacterium culture was added to 500ml LB broth containing 25µg/ml gentamycin, 50µg/ml kanamycin and 25µg/ml rifampicilin, and shaken for 30 hours at 30^{o}C. Cultures were then centrifuged at 2,000xg for 5 mins, supernatant removed and autoclaved, and cells resuspended in 400ml dH_2O containing 5% (w/v) sucrose. The absorbance of a 1ml aliquot at 600nm was used to determine the concentration of cells, with suitable readings in the range of 0.6-1.0. Silwet L-77 (van Meeuwen Chemicals BV, The Netherlands), at a concentration 0.05% (v/v), was added to Agrobacterium immediately prior to dipping plant material. The aerial parts of approximately 6 week old *Arabidopsis* plants (T1) were dipped in the Agrobacteria culture for 20 sec with agitation. The flowers of dipped plants were separated, pots placed on their side and placed in an area of low light overnight. Plants were placed upright the following morning and seeds collected when dry.

2.12.5 Selection of transformants

Seeds collected following the transformation procedure were plated on ½ MS media containing 1% (w/v) sucrose and 25µg/ml hygromycin antibiotic (Sigma, MO, USA). Plates were initially incubated at 4^{o}C for 2 days, then treated with 110 µmol m^{-2} sec^{-1} W light (23^{o}C) for 2h to induce germination, placed in the dark at 23^{o}C for 2 days and then left in 110 µmol m^{-2} sec^{-1} continuous white light (23^{o}C) for approximately 2 weeks, until positive transformants (T2) became visible. Seedlings that survived were transferred to soil and allowed to self fertilise. Seeds collected from the T3 plant were then plated on ½ MS, 1% (w/v) sucrose media containing 25µg/ml hygromycin, and the survival ratio noted.

2.13 Transmission electron microscopy

Cotyledon samples were dissected out under green safe light and placed in fixative comprising 3% (v/v) glutaraldehyde and 4% (v/v) formaldehyde in 0.1M Pipes buffer (pH 7.2). This primary fixation was carried out at room temperature for 2h in total darkness. Specimens were then rinsed in 0.1M Pipes buffer, postfixed in

1% (w/v) buffered osmium tetroxide for 1h, rinsed in buffer, dehydrated and embedded in Spurr resin following standard procedures. Silver sections were cut on a Leica OMU 3 ultramicrotome, stained with uranyl acetate followed by Reynold's lead citrate stain and viewed on a Hitachi H7000 transmission electron microscope (Hitachi Ltd., Tokyo, Japan). At least two independent samples were viewed for each genotype and experimental condition, and photographs were taken of representative plastids. Dissection and fixing of samples was carried out by members of the Biomedical Imaging Facility, Southampton, UK.

2.14 Note on Nomenclature and Statistical Analysis

The debate regarding correct representation of gene/protein/mutant gene symbols is ongoing, and consequently there is no absolutely accepted system. In this report symbols are used for both higher plants and bacteria. For plant symbols the following formats have been applied: genes symbols are uppercase and italicised, proteins symbols are uppercase not italicised, and mutant gene symbols are lowercase and italicised. For bacterial symbols the following formats have been applied: gene symbols have the first letter uppercase and italicised, proteins symbols are have the first letter uppercase not italicised, and mutant gene symbols are all lowercase and italicised. Although in the majority of cases these correspond to the originating author's format, in some situations they may have been changed to maintain consistency.

For all statistical analysis, unless otherwise stated, a Student's *t* test was performed. Where appropriate figures are marked with asterisks to indicate a statistically significant result or the P value is given in the text.

Chapter 3: Regulation at the Chelatase Branchpoint of the Tetrapyrrole Pathway

3.1. Introduction

3.1.1. Light-mediated changes in expression of branchpoint genes

In all organisms the tetrapyrrole pathway is of primary importance due to its role in the production of haem for incorporation into hemoproteins, with diverse biological functions including the transport of diatomic gases, chemical catalysis, diatomic gas detection, and electron transfer. However, in photosynthesising organisms the tetrapyrrole pathway is required for at least one other essential function: the synthesis of chlorophyll. The branch in the pathway that separates the synthesis of these two compounds occurs with the substrate protoporphrin IX.

At this stage two enzymes may act on protoporphyrin IX: Mg-chelatase or ferrochelatase. When assessing the activity and requirements of these two enzymes (summarised in Cornah *et al*., 2003), it seems clear that the ferrochelatase enzyme is required to function at all times in order to provided energy to the cell. The Mg-chelatase enzyme, on the other hand, is specifically required only when either a) light energy has become available and chlorophyll synthesis must begin, or b) there is a shortfall in chlorophyll accumulation. This means that the plant is able to optimise energy harvesting through chlorophyll reserves, without wasting energy on excess synthesis. In order to maximise the potential for this process the genes encoding the three subunits of the Mg-chelatase enzyme (*CHLD*, *CHLH* and *CHLI*) must be regulated effectively at both the gene and protein level. Additionally, this regulation appears to extend further with the presence of the *GUN4* gene. Discovered in a mutant screen for plastid signalling mutants (Susek *et al*., 1993), GUN4 has since been shown to function as a critical regulator of chlorophyll synthesis. Larkin *et al*. (2003) described that GUN4 can bind both the substrate and product of the Mg-chelatase enzyme, protoporphyrin IX and Mg-protoporphyrin IX, and the H subunit of this enzyme. Additionally, the presence of GUN4 with the Mg-chelatase enzyme *in vitro* lowered the K_m of protoporphyrin IX binding, therefore increasing the rate of Mg-protoporphyrin IX production when protoporphyrin IX is limiting.

Previous work has focussed on understanding regulation at the early stages of the tetrapyrrole pathway and has shown that while the *GSA* gene is largely unregulated by light, *HEMA1* is regulated under blue (B), far-red (FR), red (R) and white (W) light (McCormac *et al*., 2001; McCormac and Terry, 2002a). This regulation has been attributed to the phytochrome family of photoreceptors under FR and R light, and the cryptochrome family under B light (McCormac and Terry, 2002a). Additionally, it has been shown that *HEMA1* is regulated by sugars, hormones, the plastid retrograde signal and the circadian rhythm, and Glu-TR (the product of the *HEMA1* gene) is also regulated by haem negative feedback and the *FLU* protein (summarised in figure 3.1; see sections 1.3, 1.4 and 1.5 for a more detailed discussion). As Glu-TR is responsible for the first committed step of tetrapyrrole biosynthesis, these studies suggest the importance of one key regulatory site in the pathway. Based on this information, and the important role of GUN4 proposed from more recent publications (Davison *et al*., 2005; Verdacia *et al*., 2005) highlighting the GUN4 crystal structure and its role in chlorophyll synthesis, this study was undertaken to understand the key regulatory genes in the chelatase branch of the pathway.

To do this the expression of all the genes encoding the Mg- and Fe-chelatase enzymes (*CHLD*, *CHLH*, *CHLI1*, *CHLI2*, *FC1* and *FC2*; see sections 1.2.3 and 1.2.4), and the *GUN4* gene, will be studied. Additionally, *CHLM* (encoding the next enzyme in the chlorophyll branch, Mg-protoporphyrin IX methyltransferase (see sections 1.2.1 and 1.2.3), will also be included to assess regulation post-branchpoint. Further to this, and in a similar manner to McCormac and Terry (2002), it will be interesting to understand any light regulation in terms of the photoreceptors involved (see sections 1.3.1.1 and 1.3.1.2). Therefore the *phyA*, *phyB*, *phyAphyB* double, *cry1*, *cry2* and *cry1cry2* double mutants will be employed, as well as the phytochrome signalling mutants *fhy1*, *fhy3*, *pif1* and *pif3*.

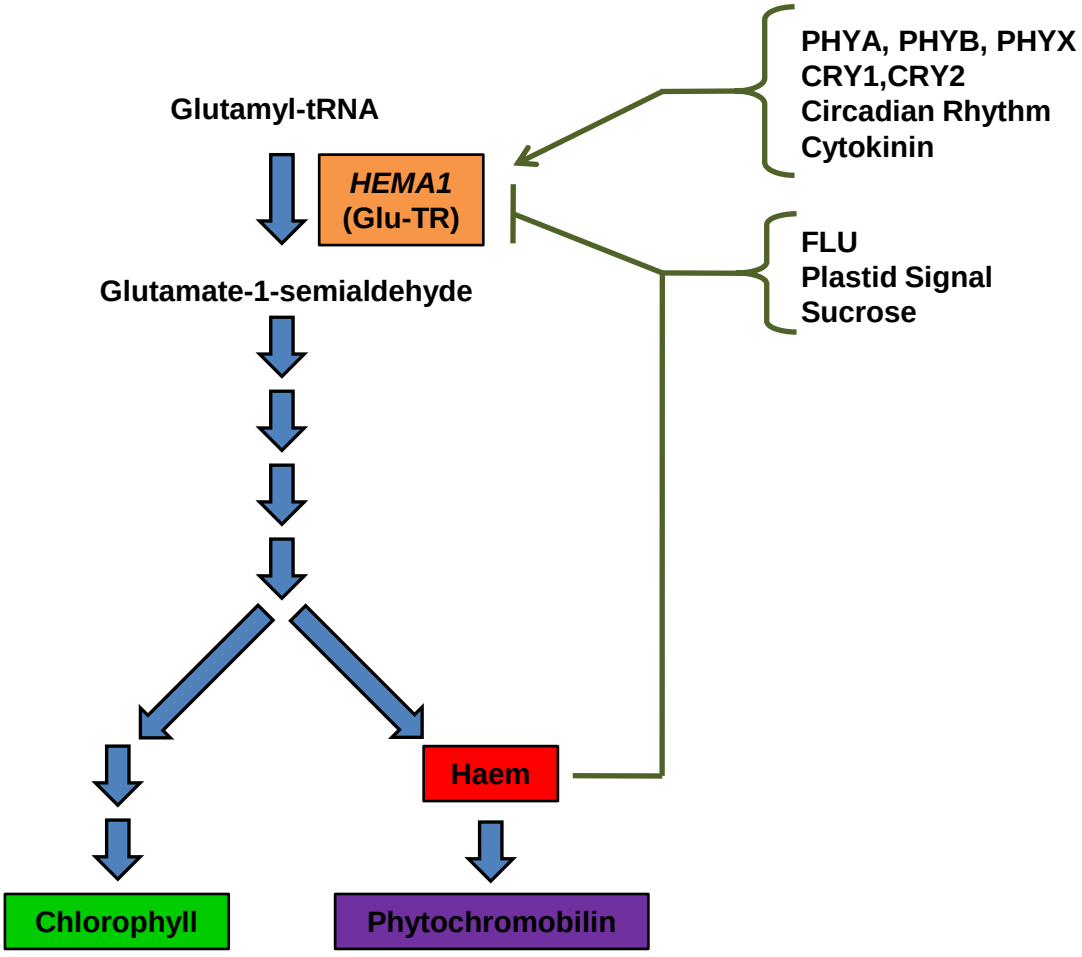

Figure 3.1 Regulation of the *HEMA1* gene and the Glu-TR protein product, required for the synthesis of ALA in the tetrapyrrole pathway. The phytochrome and cryptochrome photoreceptors, circadian rhythm, and cytokinin hormone induce expression of *HEMA1*. Sucrose and the plastid signal inhibit expression of *HEMA1*, and haem negative feedback and the FLU protein inhibit Glu-TR activity.

3.1.2. Bioinformatics approach to understanding the regulation of branchpoint genes

Bioinformatics tools, such as with the Genevestigator™ package (Zimmerman *et al*., 2005) and ConPred II membrane protein prediction program (Arai *et al*., 2004), are powerful methods used as early indicators of expression patterns and protein structure. Although these methods rely on microarray data and prediction, both of which are often unreliable, they offer the advantage of data mining to quickly flag potential points of regulation, which may then be investigated further.

As well as aiding in the determination of light induction of the branchpoint genes, the Genevestigator™ program was employed in this study to investigate the response of these genes to a wide range of stimuli, including temperature, hormones and mutations. Any interesting results can then be followed up through direct analysis by RNA extraction and PCR.

3.2. Results

3.2.1. Development of RNA extraction method

In order to conduct precise and reliable RT- and real time RT-PCR experiments it is essential that the RNA extraction method used is reliable. A number of commonly used methods were tested including using the 'RNA Mini-prep' provided by Qiagen (Qiagen, CA, USA), the 'TriZole' solution provided by Invitrogen (Invitrogen, CA, USA), and a number of variations on the protocol outlined by Verwoerd *et al* (1989).

Both the 'RNA Mini-prep' and the 'TriZole' method produced unreliable RNA in terms of the quality and quantity produced in each sample (data not shown), these methods were therefore not pursued further. On the other hand the two methods based on the Verwoerd *et al* (1989) protocol produced much higher quantities of RNA.

Firstly, the 'primary extraction method' was based over a three day period, uses relatively high quantities of solutions and plant material, and requires a DNase step for removal of contaminating DNA. This method often produced high quality RNA, however, it was also very time consuming and occasionally the DNA removal step caused some RNA to become degraded, apparently without removing the DNA (figure 3.2c). Additionally, this extraction method sometimes failed to produce any RNA (figure 3.2a).

The 'secondary extraction method', which was a similar technique but relied upon lower quantities of solutions and plant material, and was based over only one day, was also found to produce high quantities of RNA. Moreover, this RNA was both non-degraded (figure 3.2b) and exempt of any DNA contamination (figure 3.2d). Consequently the 'secondary extraction method' was used throughout the remainder of the project.

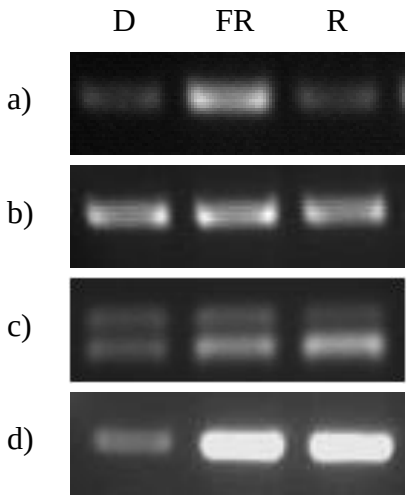

Figure 3.2 Comparison on the effectiveness of different RNA extraction methods.
a) Expression of *40S* rRNA in L*er* WT using the 'primary extraction method'. Seedlings were grown for 2d in the dark and then received 16h red (R; 80 µmol m^{-2} s^{-1}), far-red (FR; 10 µmol m^{-2} s^{-1}), or remained in the dark. b) Expression of *40S* rRNA in L*er* WT using the secondary extraction method. c) Expression of *Lhcb2*1* in L*er* WT using the primary extraction method. d) Expression of *Lhcb2*1* in L*er* WT using the secondary extraction method.

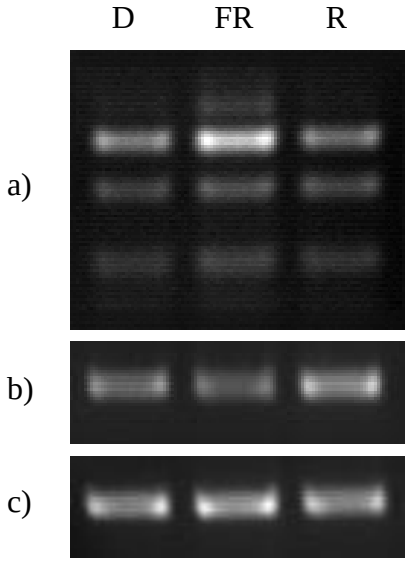

Figure 3.3 Comparison of the efficiency of the control genes *UBQ10* (a), *ACT2* (b) and *40S* rRNA (c) following 2d dark and 16h red (R), far-red (FR) or dark (D) treatment.

3.2.2. Selection of appropriate control genes

In order to gain sufficiently reliable data it is essential that all results are compared to appropriately regulated control genes. Genes were chosen based on a number of criteria. Firstly, they must be constitutively expressed under the experimental conditions used. They should preferably contain introns, to allow for the comparison against genomic DNA, in order to assess the presence of contaminating DNA. Finally, the primer design must be possible to prevent the amplification of other genes in the family.

For the purpose of control genes *ACT2* (*ACTIN 2*), *40S* rRNA and *UBQ10* (*UBIQUITIN 10*) were initially considered, however, each had disadvantages. Using the primers outlined in Czechowski *et al*. (2005) *UBQ10* expression was found to be constitutive but the primers tended to amplify many *UBQ* genes (figure 3.3a), which was confirmed through a BLASTN search against the primer sequences. Secondly, *ACT2* was tested using primers designed in the primer3 online programme (Rozen and Skaletsky, 2000). The presence of introns and confirmation, by BLASTN search, that only one product was amplified made this a perfect candidate. Unfortunately, however, although considered to show high constitutive expression by Czechowski *et al.* (2005), experiments have demonstrated that under some conditions *ACT2* is differently regulated (figure 3.3b). Finally, *40S* rRNA was considered using the primer sequences outlined in McCormac and Terry (2004). This gene was found to be both constitutively expressed and only one product was detected (figure 3.3c), however, as *40S* rRNA contains no introns the absence of contaminating DNA could not be confirmed.

To identify additional control genes the use of lesser known normalization genes was considered. Czechowski *et al*. (2005) have tested a wide range of genes with the aim to produce primer sequences for superior reference genes. These genes were placed into categories based on how constitutive their expression was under different conditions. For the purpose of the current study genes most constitutive under diurnal cycles, a light series and a complete developmental series were chosen. Three candidate genes came out of this screen: *PDF2* (*At1g13320* - a PP2A subunit), a *SAND* family member (*At2g28390*) and *YLS8 (At5g08290* - encoding a protein

involved in mitosis). Although all genes showed a considerably superior level of constitutive regulation over a range of light treatments (data not shown), *YLS8* was chosen for use in future studies as it is expressed more highly than either the *SAND* family member or *PDF2*. (figure 3.4). Consequently, for all future studies both *40S* rRNA and *YLS8* were both utilised as control genes, although data is presented based on normalisation to one gene only.

3.2.3. Regulation of *Lhcb2.1* over the initial 24 hours of de-etiolation

Having established an effective RNA extraction protocol, and determined effective control genes, it was important to ensure that the treatment conditions (in this case for light-induced gene expression) were acting as expected. The light inductive properties of the *Lhcb/CAB* family of genes has been extremely widely studied (for example McCormac and Terry, 2002a) and therefore one of these genes, *Lhcb2*1*, was chosen as a positive control. Expression of *Lhcb2*1* was assessed over the initial 24 hours of seedling de-etiolation under continuous far-red (FRc), red (Rc), blue (Bc) and white (Wc) light, using real-time PCR, in WT *Arabidopsis* seedlings, and additionally in the *phyA* and *phyB* mutants under FRc and Rc light, respectively (figure 3.5).

Under all light conditions *Lhcb2*1* is induced quickly and strongly, and expression is entirely knocked out in the *phyA* mutant under FR light and considerably reduced in the *phyB* mutant under R light. This confirms that a) the treatment conditions used in this study are able to induce light-regulated genes in the expected manner, and b) the phytochrome mutants do not respond to the treatment, indicating only the specified wavelengths are present. It should also be noted that during this qPCR analysis (and generally throughout this report) that technical replications never exceeded 10% expression error and biological replications very rarely exceeded 25% expression error, and in such cases it has been highlighted.

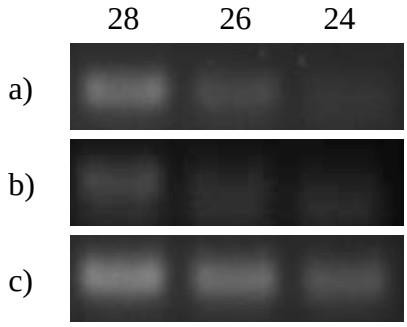

Figure 3.4 Comparison of the levels of expression of new control genes. Control genes were tested for band intensity following 28, 26 or 24 rounds of PCR with a 62 ^{o}C annealing temerature. a) *PDF2*, b) *SAND* family member, c) *YLS8*.

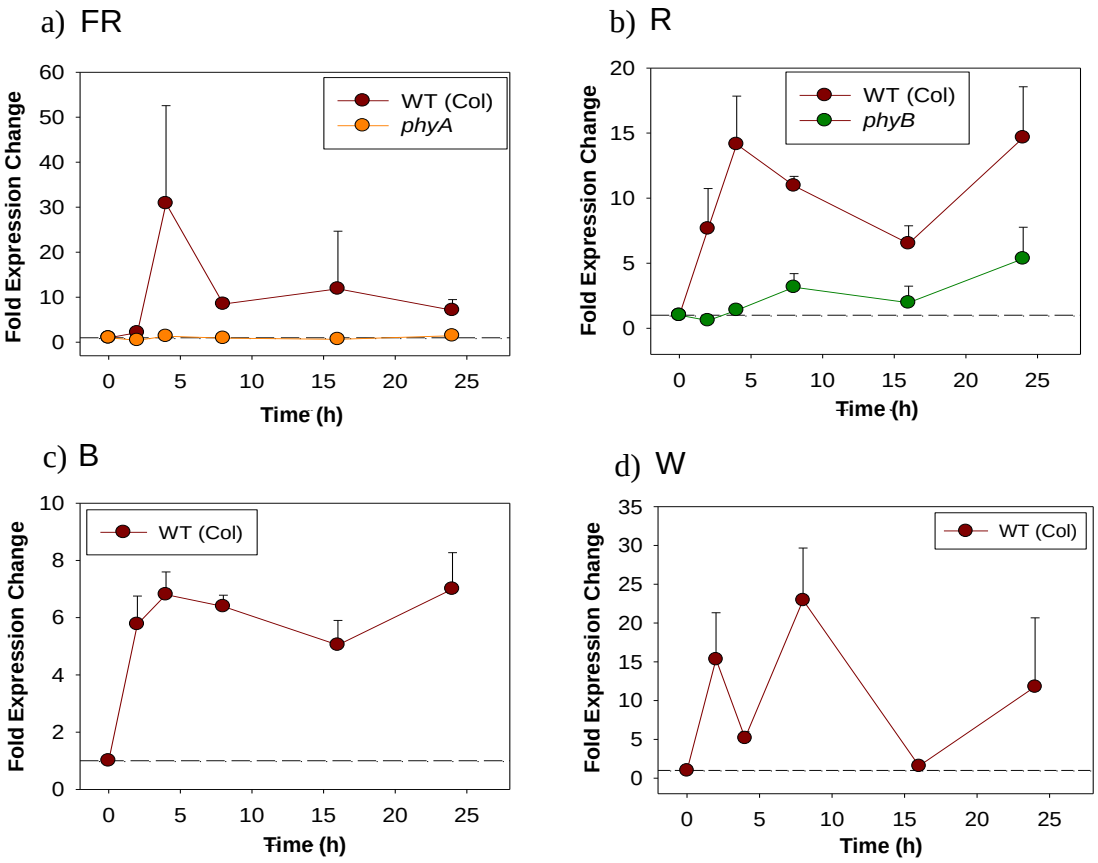

Figure 3.5 Induction of *Lhcb2*1* under different light conditions. Expression of *Lhcb2*1* was assessed under far-red (a), red (b), blue (c) and white (d) light in WT and phytochrome mutant seedlings over the initial 24 hours of de-etiolation, following 2d dark treatment; analysed by real-time PCR. Dashed line = expression constant. Values are mean ± SE of 3 independent experiments.

3.2.4. Regulation of the tetrapyrrole branchpoint genes during the early stages of de-etiolation

3.2.4.1. Regulation of gene expression by far-red light

Under FRc light, the *CHLH* gene was rapidly upregulated with a 12 fold induction after 4h ($p = 0.007$) (Figure 3.6). Expression then fell rapidly at 8h before rising again at 16h and 24h. In contrast *CHLD*, *CHLI1* and *CHLI2* showed very little induction by FRc with expression never exceeding about 2 fold higher than dark controls. Ferrochelatase genes also showed only a very weak light response with *FC2* peaking at about 3.5 fold induction following 8 hours treatment and *FC1* showing no response to FRc at all (Figure 3.6). The expression profile of *GUN4* was very similar to that of *CHLH* with a peak at 4h (8 fold; $p = 0.003$) followed by a rapid reduction at 8h and then a rise towards 24h, although in this case the second peak of expression was more modest than for *CHLH*. Under FRc *CHLM* also showed a similar profile to *CHLH* and *GUN4* with a very strong, 17 fold ($p = 0.049$), induction at 4h followed by a slight increase in expression from 8h to 24h. However, the peak in expression at 4h contains considerable error which might suggest either a problem with qPCR efficiency or error, or that this peak is very short lived and has been missed in one of the biological replicates.

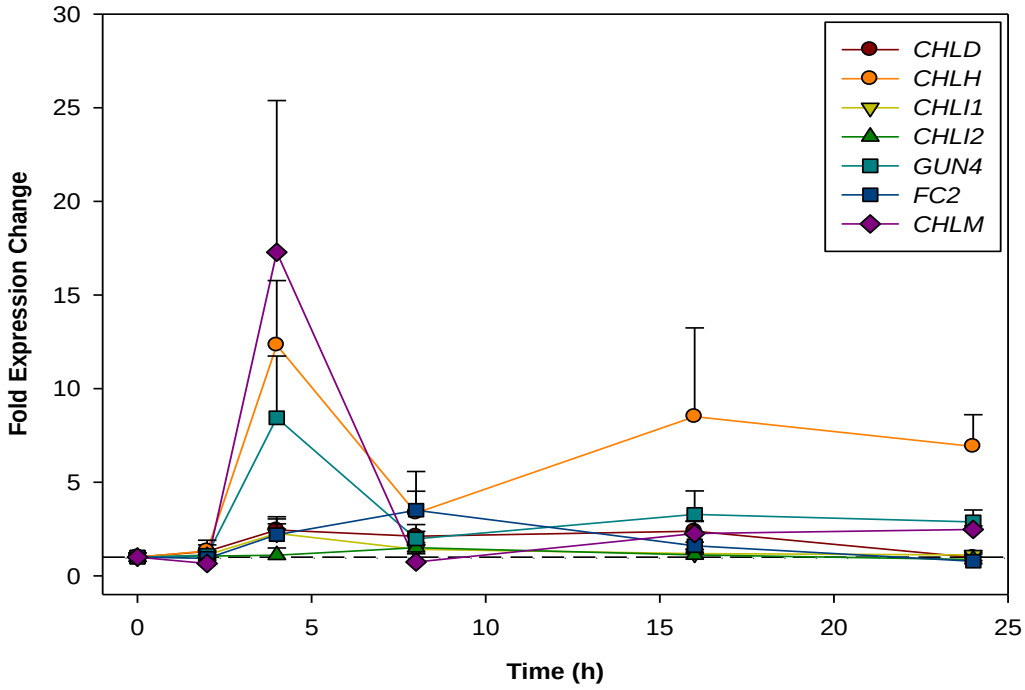

Figure 3.6 Far-red light induction of tetrapyrrole genes using real-time PCR, normalised to *40S* rRNA, over the initial 24 hours of irradiation, following 2d dark treatment. Dashed line = expression constant. Values are mean ± SE of ≥3 independent experiments.

In *Arabidopsis* the response to FRc is thought to be exclusively mediated by phyA (Whitelam *et al*., 1993; Casal *et al*., 2003; Franklin *et al*., 2005). To confirm that the FRc regulation of gene expression observed here was also under the control of phyA we further analysed the expression of *GUN4* (figure 3.7a) and *CHLH* (figure 3.7b) after 4h FRc in a *phyA* mutant background. For both genes expression was almost completely abolished in the *phyA* mutant indicating that FRc-induction of *CHLH* and *GUN4* is under phyA control. A previous study had also demonstrated that the phytochrome signalling mutants, *fhy1* and *fhy3*, had a major role in the regulation of *HEMA1* under FRc and Rc (McCormac and Terry, 2002a). The mutants were originally isolated in screens for long hypocotyls under FRc (Whitelam *et al*., 1993) and both proteins have well established roles in phyA signalling under FRc. FHY1 is required for nuclear import of phyA (Hiltbrunner *et al*., 2005) while FHY3 is one of an unusual class of transposase-derived transcription factors required for phyA-mediated activation of gene expression under FRc (Lin *et al*., 2007). To determine whether *FHY1* and *FHY3* were required for expression of *CHLH* and *GUN4* in FRc the induction of these genes in the *fhy1* and *fhy3* mutants was examined. In both mutants there was a complete loss of *CHLH* and *GUN4* expression after 4h FRc (figure 3.7) indicating an important role for *FHY1* and *FHY3* in FRc-mediated regulation of *CHLH* and *GUN4* expression.

Finally, as is discussed in section 1.3, there is currently great debate as to whether the *PIF* genes act positively or negatively as phytochrome signalling factors. To help answer this question, the expression of *GUN4* and *CHLH* was examined in the *pif1* and *pif3* mutants following 4 hours FRc treatment (figure 3.7). In both mutants the induction of *CHLH* and *GUN4* was considerably knocked down compared to WT, with the least induction occurring in the *pif1* mutant, suggesting a positive-regulatory role. These mutants and their role within the plant are, however, discussed in more detail in chapter 4.

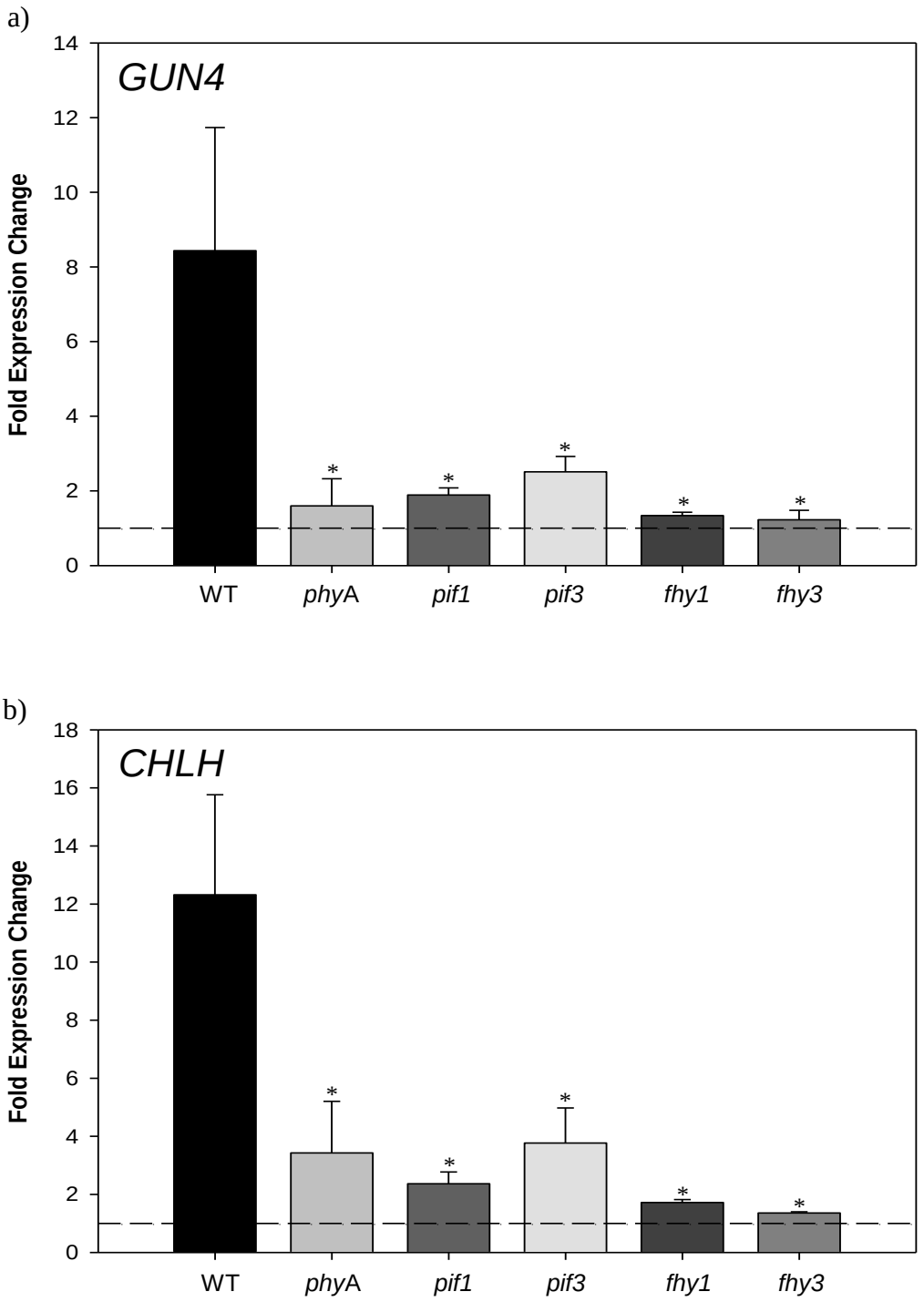

Figure 3.7 Expression induction of *GUN4* (a) and *CHLH* (b) in WT, phytochrome mutant and phytochrome-signalling mutant backgrounds following 2d dark and 4h far-red light treatment. Dashed line = expression constant. The level of significance with which the mutant data differs from WT is indicated: * = P = <0.05. Values are mean ± SE of ≥3 independent experiments.

3.2.4.2. Regulation of gene expression by red light

The relative response of the eight genes to continuous Rc light was similar to that observed under FRc with the *CHLH*, *GUN4* and *CHLM* genes all showing a strong induction of transcript (Figure 3.8). The other genes tested showed very little response to the light treatment at all with an almost 3 fold induction of *CHLI1* after 24h Rc being the largest response observed. The pattern of the light response of *CHLH*, *GUN4* and *CHLM* to Rc was, however, very different from that seen in FRc. The *CHLH* and *GUN4* genes again showed a strikingly similar expression profile with both induced within 2h Rc with an initial peak at this point and then a further peak after 8h ($p = 0.043$ and 0.022 for *CHLH* and *GUN4*, respectively) (figure 3.8). The expression of both genes declined at 16h before showing their strongest inductive response after 24h ($p = <0.001$ for both *CHLH* and *GUN4*). In contrast to this the *CHLM* gene was strongly induced after 16h Rc ($p = 0.03$) with no significant induction observed until after 8h Rc. This pattern might be the result of some variation in the qPCR efficiency between biological replicates, as indicated by the increase in error bar size at the 8h time point. Therefore, care should be taken before analysing this pattern in too much detail.

Subsequently, the expression of *CHLH* and *GUN4* at the two major peaks of expression (8h and 24h) was examined in the *phyB* mutant and the *phyAphyB* double mutant (figures 3.9 and 3.10). Induction by Rc was abolished in the *phyB* mutant in all cases, except for *CHLH* after 24h where it appears that phyA also contributes to the response (figure 3.10b). A small contribution of phyA to Rc-induction of tetrapyrrole-synthesis genes has been noted before (McCormac and Terry, 2002a). In this previous study it was also observed that Rc-induction of *HEMA1* was repressed in *fhy1* (about 50%) and *fhy3* (75%) while induction of *Lhcb* expression was hardly changed (25% repression in *fhy3* only) (McCormac and Terry, 2002a). Here, the expression of *CHLH* and *GUN4* was reduced in *fhy1* at both 8h and 24h, although this was only statistically significant at the 24h timepoint (Figures 3.9a and 3.10b). Similarly, expression of *CHLH* and *GUN4* unaffected at 8h in *fhy3*, but there was a slight increase in expression following 24 hours.

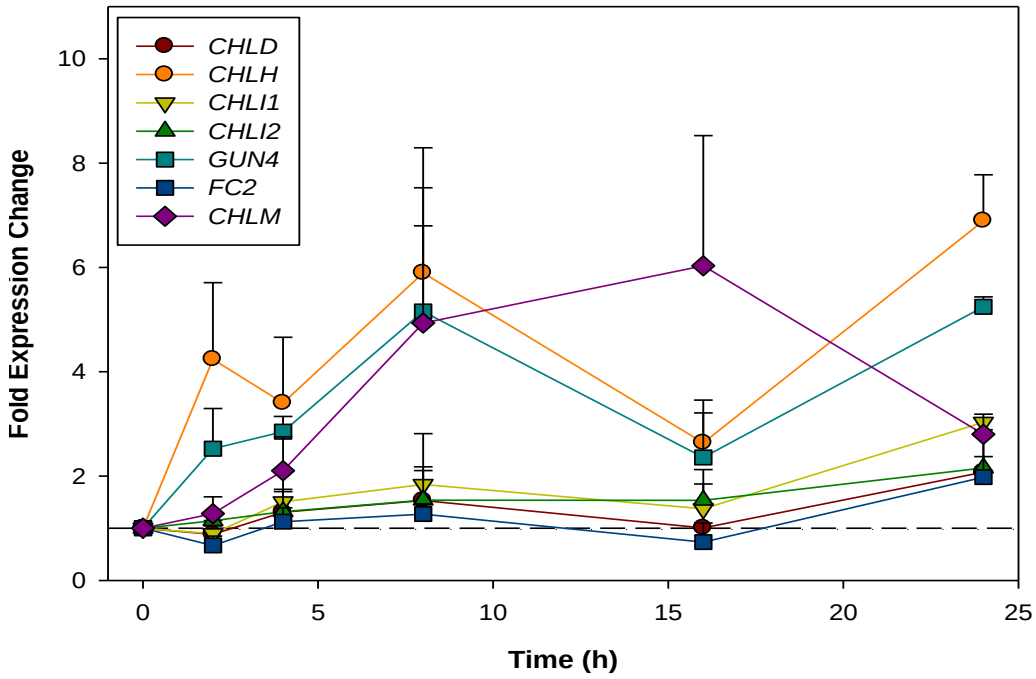

Figure 3.8 Red light induction of tetrapyrrole genes using real-time PCR, normalised to *40S* rRNA, over the initial 24 hours of irradiation, following 2d dark treatment. Dashed line = expression constant. Values are mean ± SE of ≥3 independent experiments.

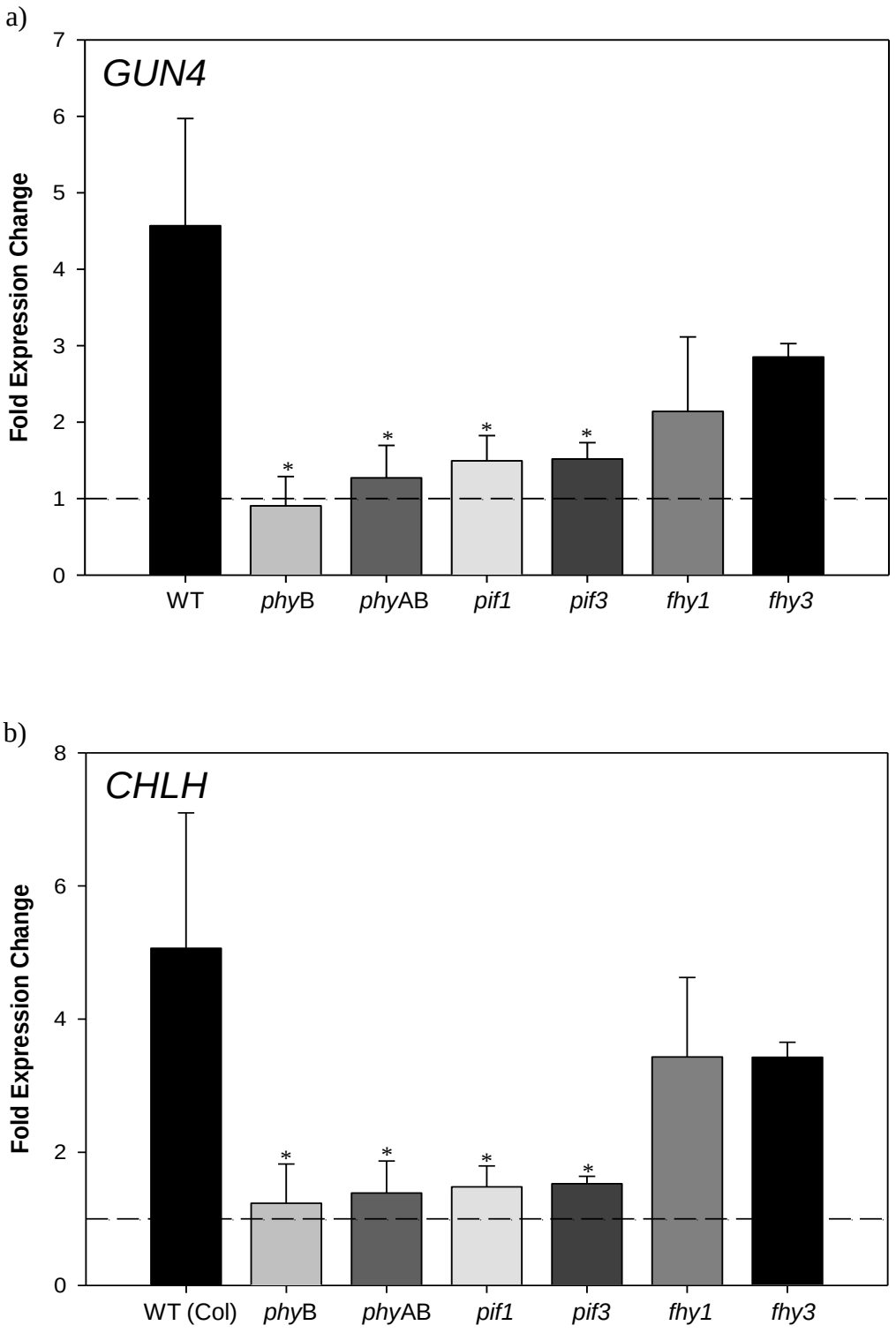

Figure 3.9 Expression induction of *GUN4* (a) and *CHLH* (b) in WT, phytochrome mutant and phytochrome-signalling mutant backgrounds following 2d dark and 8h red light treatment. Dashed line = expression constant. The level of significance with which the mutant data differs from WT is indicated: * = P = <0.05. Values are mean ± SE of ≥3 independent experiments.

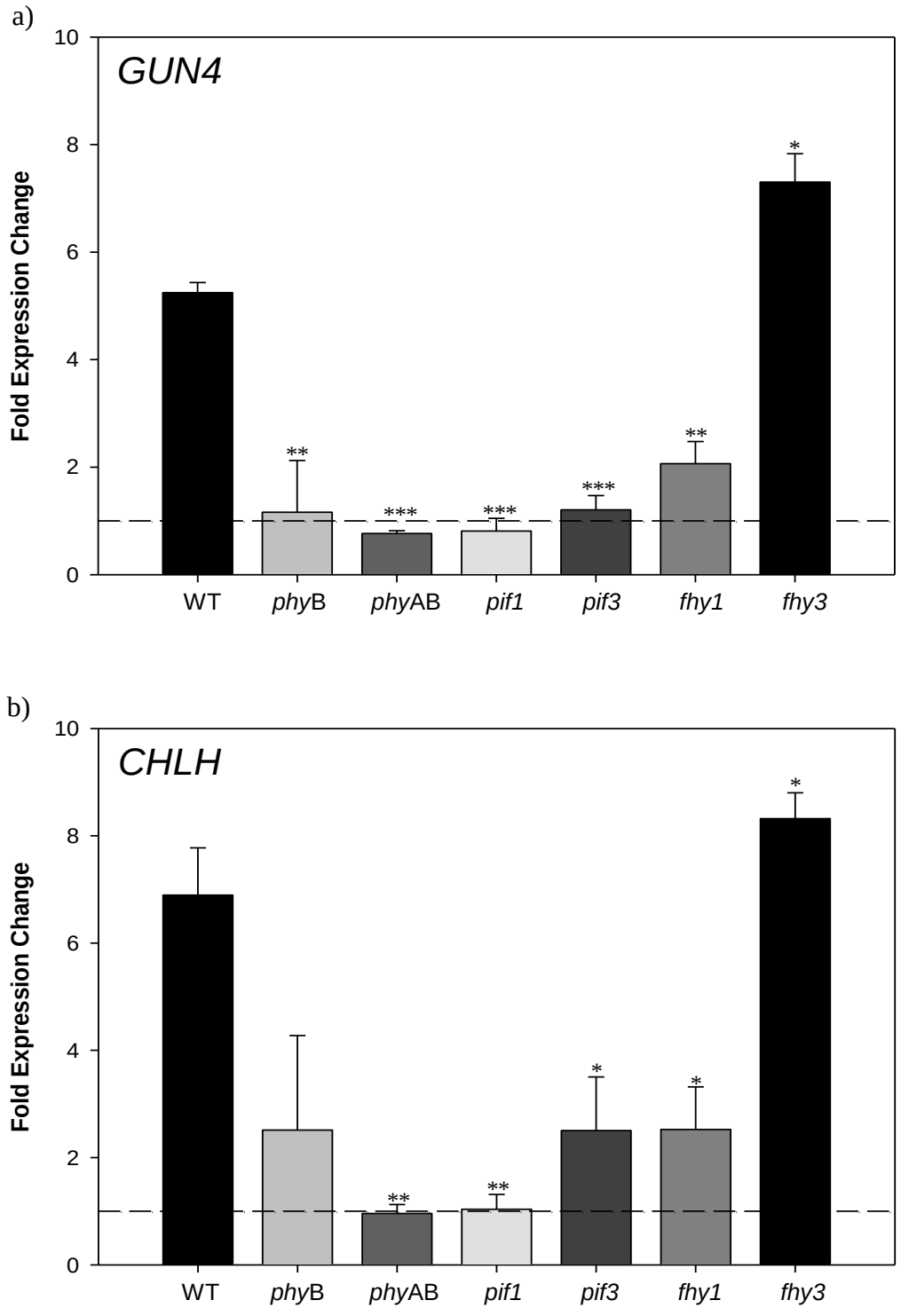

Figure 3.10 Expression induction of *GUN4* (a) and *CHLH* (b) in WT, phytochrome mutant and phytochrome-signalling mutant backgrounds following 2d dark and 24h red light treatment. Dashed line = expression constant. The level of significance with which the mutant data differs from WT is indicated: * = P = <0.05, ** = P = <0.01, *** = P = <0.005. Values are mean ± SE of ≥3 independent experiments.

Again expression in the *pif1* and *pif3* mutants was studied at the highest points of induction for *GUN4* and *CHLH* (8 and 24h). For *GUN4* the induction was entirely knocked out in both the *pif1* and *pif3* mutants, while induction was only knocked out in the *pif1* mutant for *CHLH*, with 2.5 fold induction remaining in the *pif3* mutant (figure 3.10). This data is, however, discussed in more detail in chapter 4.

3.2.4.3. Regulation of gene expression by blue light

Under Bc light there was, again, a clear similarity in the pattern of *CHLH* and *GUN4* expression (figure 3.11). The expression of both genes peaked after 2h (~6- and 5-fold for *CHLH* and *GUN4*, respectively; $p = <0.001$ for both *CHLH* and *GUN4*), before falling at 8h and then recovering at 16 and 24h ($p = 0.001$ and <0.001 at 24h for *CHLH* and *GUN4*, respectively). This pattern is suggestive of a circadian pattern of regulation, where expression is highest at the earliest timepoint and then again following approximately 24h of light treatment. The *CHLD* and *CHLI2* genes again showed little or no response to Bc with just a small (2 fold) peak at 4h, while *FC2* peaked quite strongly (>3 fold) at 4h (figure 3.11). In contrast to the situation in FRc and Rc, *FC1* also showed a small peak in expression, in this case after 2h (figure 3.11). Another difference observed under Bc was that *CHLI1* and *CHLM* showed a similar expression pattern. Again in contrast to the situation in FRc and Rc, under Bc the expression of both genes increased steadily from 2-24h to give ~5 fold and 4 fold induction respectively at the final time point ($p = 0.049$ and 0.001 at 24h for *CHLI1* and *CHLM* , respectively) (figure 3.11).

To identify the photoreceptors mediating Bc regulation of *CHLH* and *GUN4* at the 2h and 24h peaks of expression phytochrome and cryptochrome photoreceptor-deficient mutants were used. At 2h, expression of *GUN4* was unaffected in the *cry1cry2* double mutant, but completely abolished in *phyA* (and *phyAphyB*) indicating that this early B response is under the control of phyA (figure 3.12a). The situation was similar for *CHLH* except that expression was reduced by a third in *cry2* and the *cry1cry2* double mutant indicating that cry2 also has a role at this stage (figure 3.12b). At 24h the relative contribution of phyA was reduced for both genes. The expression of *GUN4* was equally affected by the *phyA* and *cry2* mutants while *CHLH* expression was most reduced in the *cry1cry2* double mutant (figure 3.13).

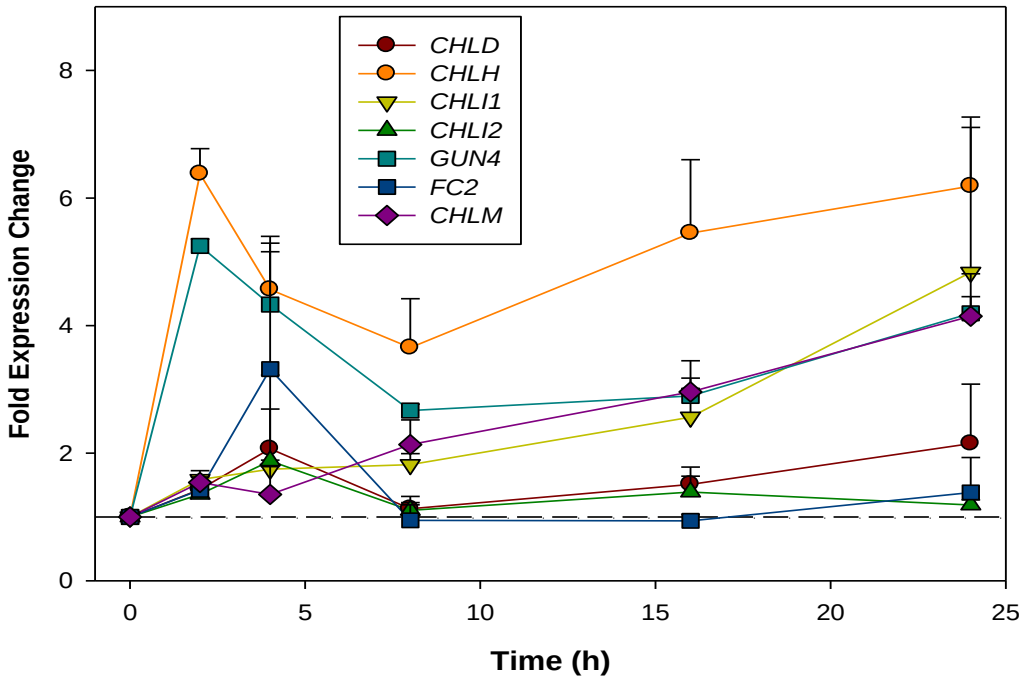

Figure 3.11 Blue light induction of tetrapyrrole genes using real-time PCR, normalised to *40S* rRNA, over the initial 24 hours of irradiation, following 2d dark treatment. Dashed line = expression constant. Values are mean ± SE of ≥3 independent experiments.

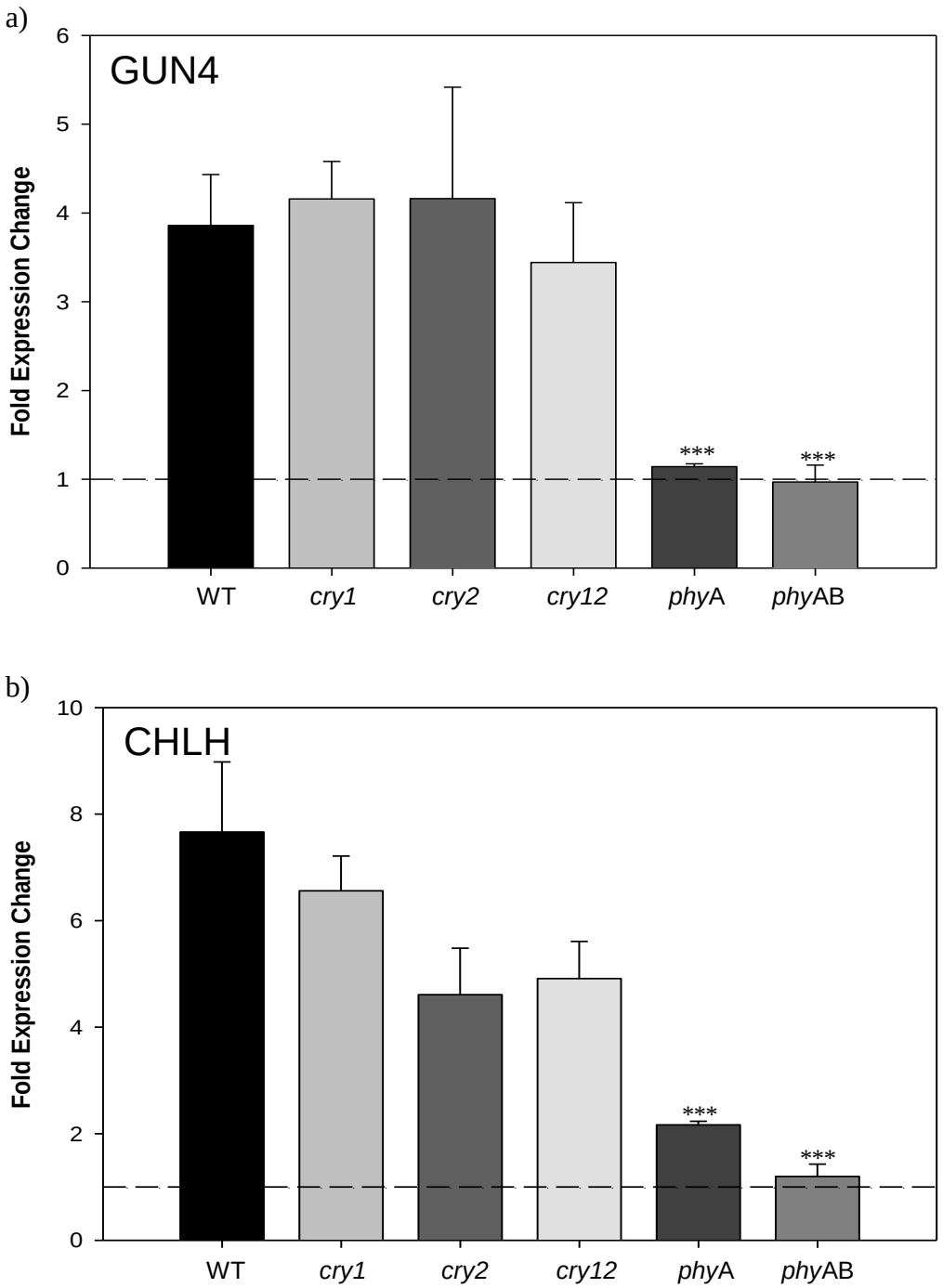

Figure 3.12 Expression induction of *GUN4* (a) and *CHLH* (b) in WT, cryptochrome mutant and phytochrome mutant backgrounds following 2d dark and 2h blue light treatment. Dashed line = expression constant. The level of significance with which the mutant data differs from WT is indicated: *** = P = <0.005. Values are mean ± SE of ≥3 independent experiments.

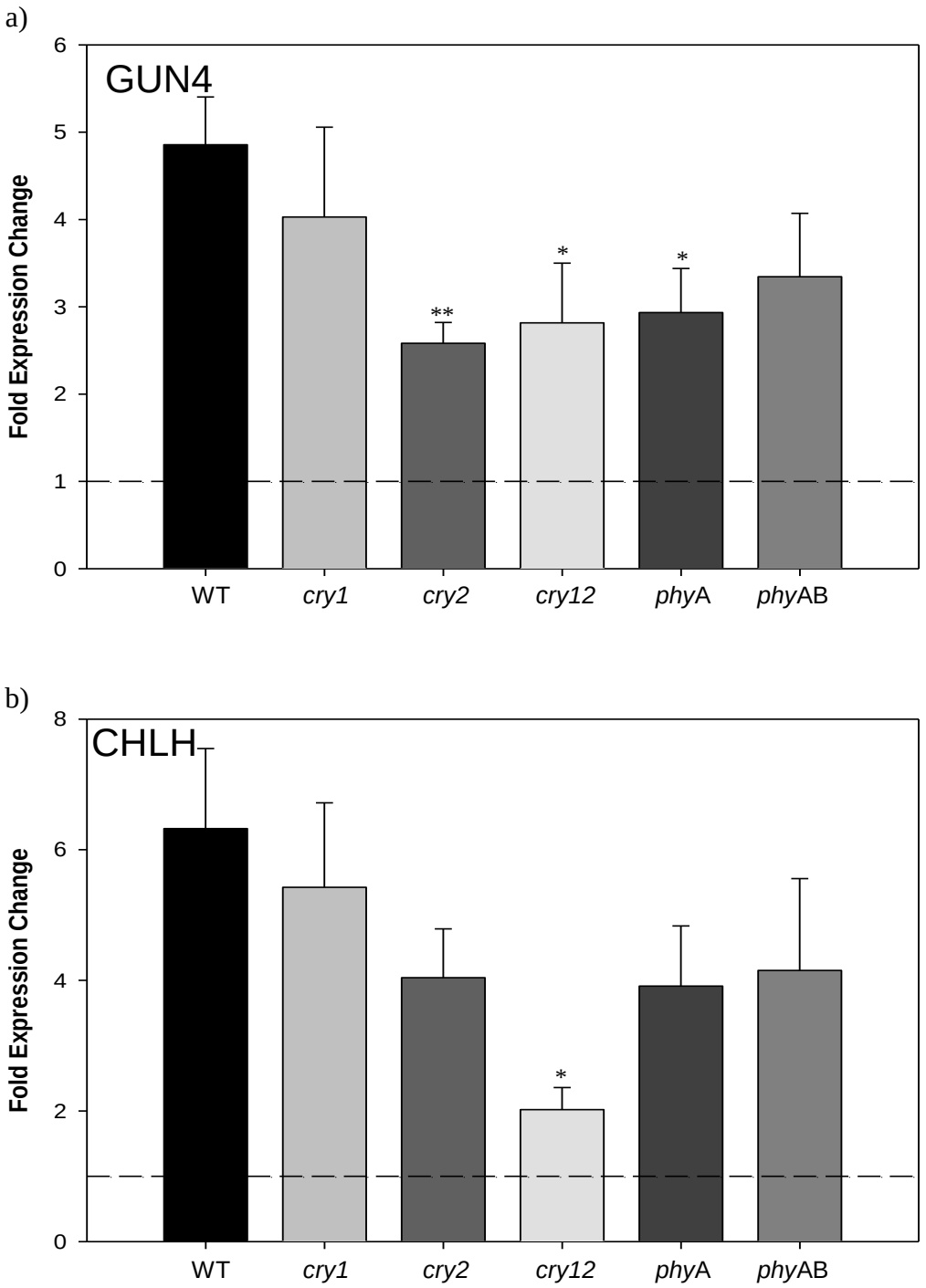

Figure 3.13 Expression induction of *GUN4* (a) and *CHLH* (b) in WT, cryptochrome mutant and phytochrome mutant backgrounds following 2d dark and 24h blue light treatment. Dashed line = expression constant. The level of significance with which the mutant data differs from WT is indicated: * = P = <0.05, ** = P = <0.01. Values are mean ± SE of ≥3 independent experiments..

3.2.4.4. Regulation of gene expression under white light

Figure 3.14 shows the timecourse of expression for the genes encoding chelatase and chelatase-related proteins over 24h continuous white light (Wc). It might be expected that these patterns would correspond approximately to the combined effects of Rc and Bc as the fluorescent Wc sources used contain very little FR. This is broadly the case although the relative contribution of Bc is greater as the monochromatic experiments were performed with 20 μmol m^{-2} sec^{-1} Bc and 80 μmol m^{-2} sec^{-1} Rc. Again the expression patterns of *CHLH* and *GUN4* were very similar with a 2h peak ($p = <0.001$ for both *CHLH* and *GUN4*) followed by a minimum at 16h and a second increase already apparent by 24h (figure 3.14). This expression pattern is strongly indicative of a circadian pattern of regulation, which is likely to have been stimulated immediately following light exposure, and indeed this may also be the case for all light treatments in this study. Therefore it is possible that the initial peak in expression in all these treatments is due to direct light responses, while the other, less regular peaks, are down to the circadian clock. Under Wc, *CHLD*, *CHLI1*, *CHLI2*, *FC1* and *FC2* all showed a small peak at 2h (4h for *CHLI1*) with ~2-3 fold induction with only *CHLI1* showing a moderate rise also at 24h. Interestingly, the *CHLD*, *CHLI2* and *FC2* genes in fact showed a small down regulation, particularly at 16 and 24h. As observed before, the expression profile of *CHLM* was quite different to the other genes with a strong transient induction peaking at 8h and a second peak apparent by 24h (figure 3.14).

3.2.5. Regulation of the tetrapyrrole branchpoint genes during the later stages of de-etiolation

The induction in expression of *GUN4* and *CHLH* over the initial 24 hours of light treatment suggests a key regulatory role for these genes during early de-etiolation. To further understand the regulation at the branchpoint over an extended period, to assess whether *CHLH* and *GUN4* are required later in development, the timecourse was extended to include 48, 72 and 120 hours of light treatment (figure 3.15).

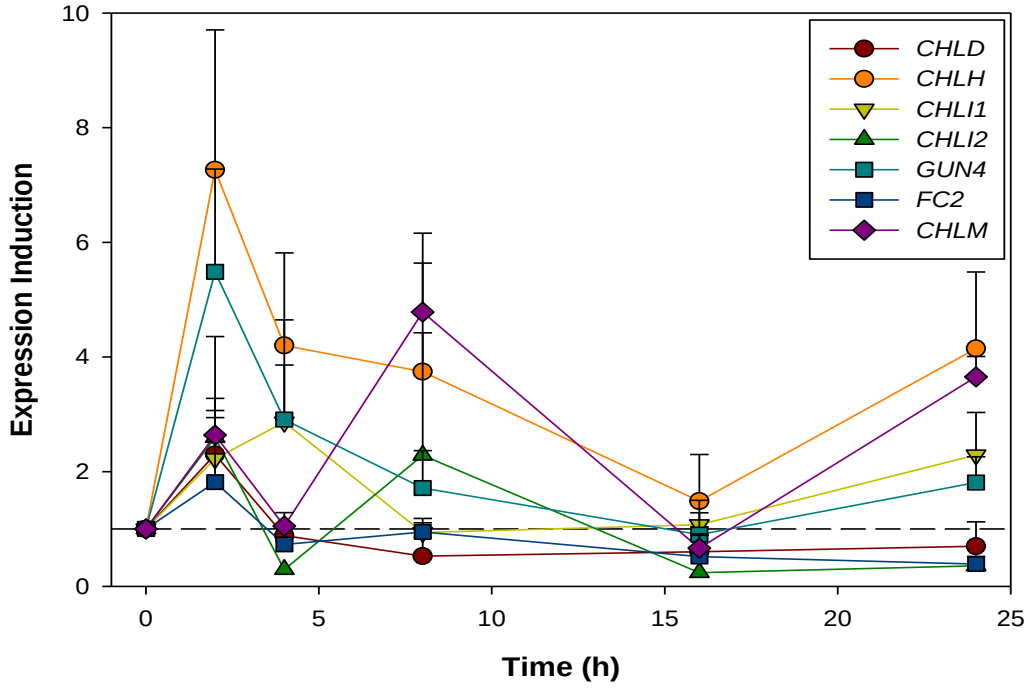

Figure 3.14 White light induction of tetrapyrrole genes using real-time PCR, normalised to *40S* rRNA, over the initial 24 hours of irradiation, following 2d dark treatment. Dashed line = expression constant. Values are mean ± SE of ≥3 independent experiments.

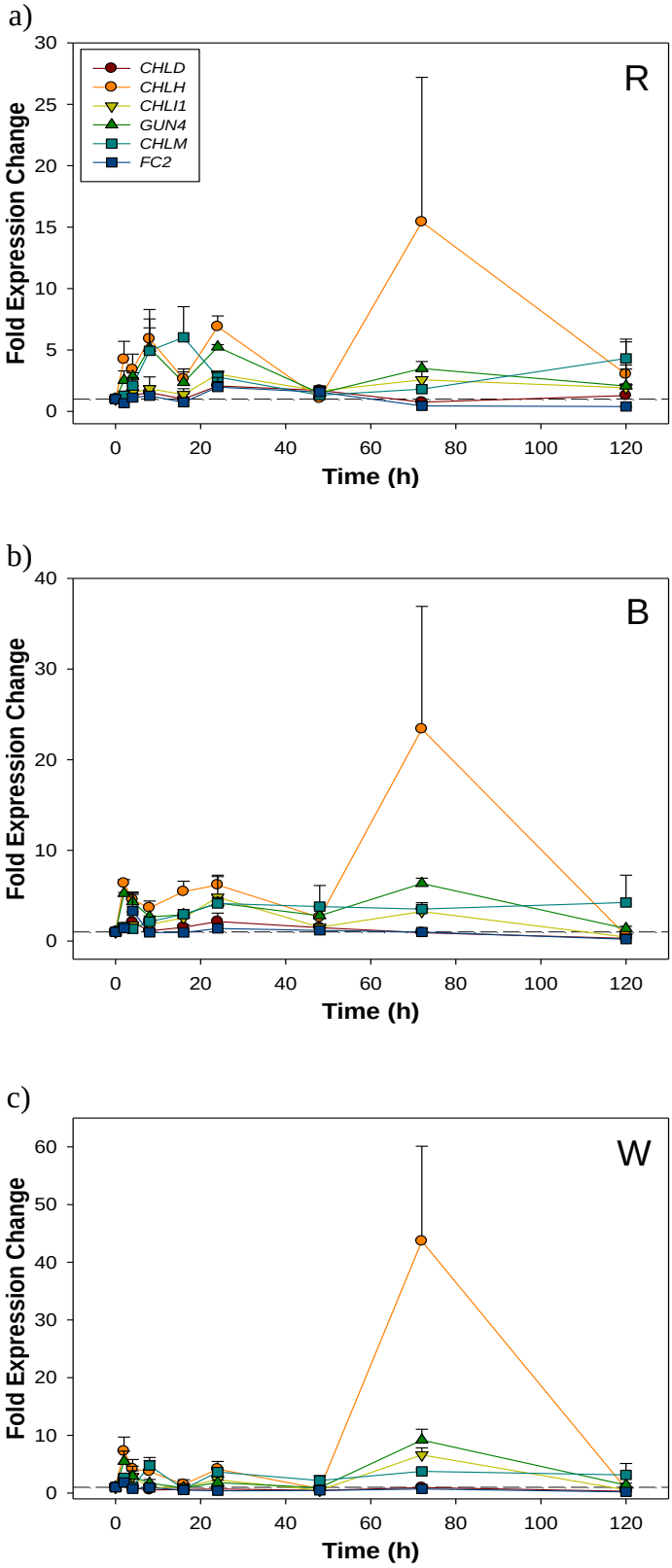

Figure 3.15 Induction of tetrapyrrole genes following extended light treatment. Expression of tetrapyrrole genes using real-time PCR, normalised to *40S* rRNA, over the initial 120 hours of growth under red (a), blue (b) and white (c) light, following 2d dark treatment. Dashed line = expression constant. Values are mean ± SE of 3 independent experiments.

It is strikingly apparent from this data that, although *GUN4* maintains a similar level of induction over 5 days to that of 24 hours (reaching peaks of 4, 6 and 9 fold under Rc, Bc and Wc, respectively), *CHLH* expression is dramatically induced following 72 hours of all light treatments (reaching peaks of 15 ($p = 0.101$), 23 ($p = 0.052$) and 43 ($p = 0.013$) fold under Rc, Bc and Wc, respectively). While *CHLM* maintains strong light inductive properties throughout all light treatments, *CHLI1* remains moderately light induced, and *CHLD* and *FC2* expression is unaffected by the extended treatments.

3.2.6. Regulation of gene expression under green light

The discovery that some of the chelatase genes, and particularly *CHLD*, are downregulated after receiving white light treatment, but are not downregulated following any other light treatments, suggested the input of another wavelength. Previous studies have suggested that green light can act positively on hypocotyl extension (Folta, 2004) and can negatively affect the transcription of photosynthetic genes (Dhingra *et al*., 2006). Therefore, expression of *CHLD* was compared to that of *CHLH* using both RT- (figure 3.16a) and qRT-PCR (figure 3.16b) under green light.

Although there is a large variation in the two samples taken and there is no significant regulation in either direction, on average there does not appear to be any downregulation of *CHLD* following green light treatment. Expression remains relatively stable over the 4h period studied, where levels fluctuate between 1 and 2 fold induction. *CHLH* expression, on the other hand, is induced following ca. 1h light treatment suggesting that green light is able to partially regulate expression of these genes in a similar manner to the other wavelengths tested.

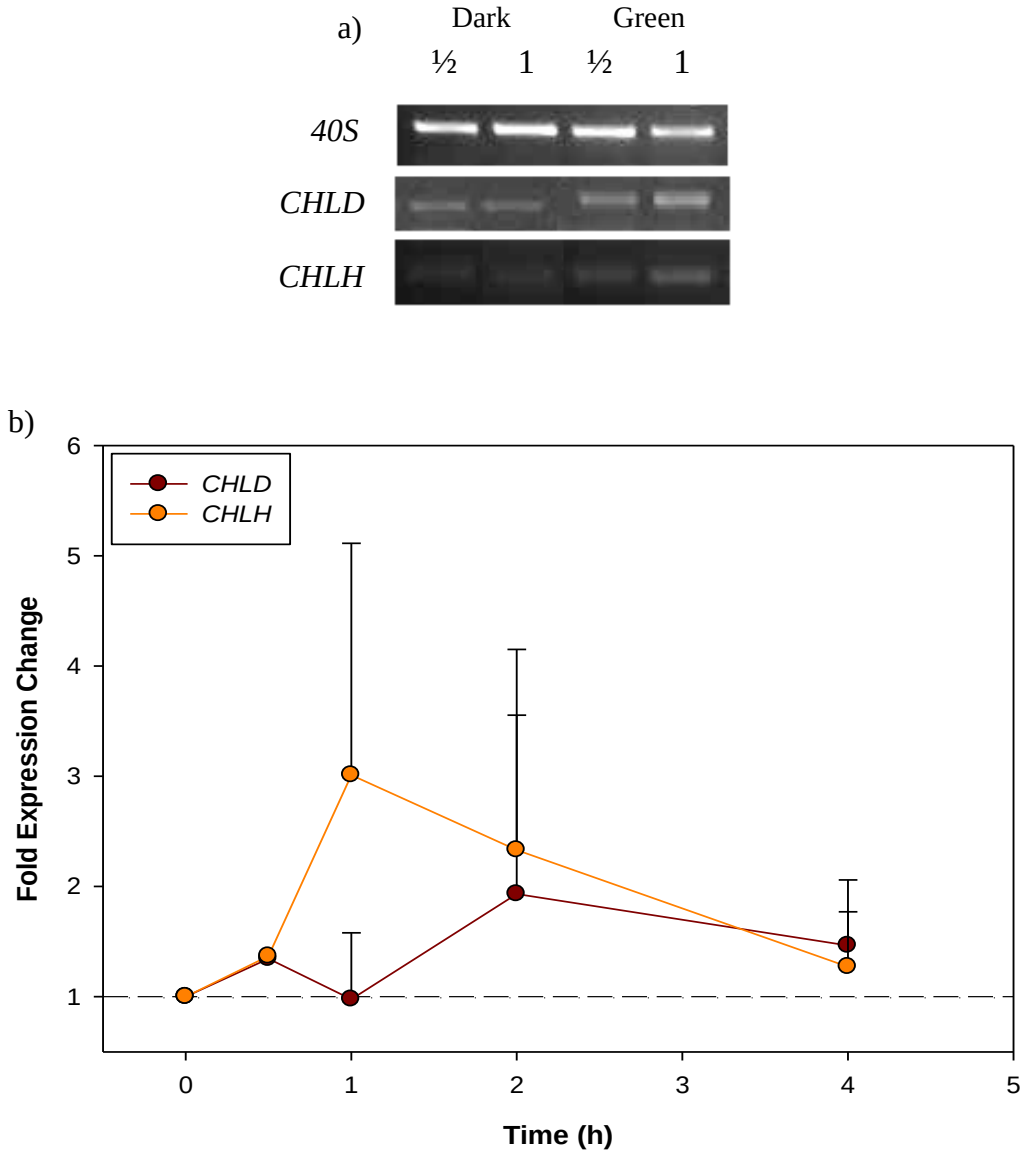

Figure 3.16 Induction of *CHLD* and *CHLH* by RT-PCR (a) and real-time PCR (b) following 2d dark and up to 4h green light (~20 treatment. Dashed line = expression constant. Values are mean ± SE of 3 independent experiments.

3.2.7. Regulation of CHLH and CHLI protein levels

The data above indicate a clear regulation of Mg-chelatase expression by light at the level of transcript abundance. To test whether these results were relevant to expression of the enzyme subunits themselves CHLH and CHLI protein levels were determined by western blot analysis. Figure 3.17 shows a time course for expression of CHLH and CHLI in darkness (D) and in seedlings transferred to white (Wc), red (Rc) and far-red (FRc) light.

In dark-grown seedlings CHLH protein was undetectable, but increased steadily following all light treatments, and was clearly detectable by 8h. These results are broadly consistent with the transcript data for *CHLH* which showed a strong early peak of expression at 2–8 h. The expression profile for CHLI protein was, however, quite different. Expression was easily detectable in dark-grown seedlings and remained constant over the 24h dark treatment. Under all light conditions tested there was gradual increase in expression that was clearly visible by 16 h. This result is also consistent with the expression data for *CHLI1* and *CHLI2*, which showed only a moderate increase in response to these light regimes.

3.2.8. Bioinformatics approach to the analysis of *GUN4* gene expression

3.2.8.1. The effect of mutation and stimuli

The light regulation of *GUN4* and the genes encoding the chelatase enzymes provides a strong basis to understand how tetrapyrrole intermediates are regulated between the chlorophyll and haem branches. However, *HEMA1* has been extensively shown to be regulated by a wide range of stimuli (figure 3.1) and it is not unlikely that *CHLH* and/or *GUN4*, the key light-regulatory sites at the branchpoint, are controlled similarly. Concordantly, a bioinformatics study was undertaken to highlight treatments which result in alterations in tetrapyrrole gene expression to further understand regulation of the pathway. All gene probes under study were checked for their specificity prior to analysis, and then imported into the Genevestigator ™ program (Zimmerman *et al*., 2005) based on 22k microarray chips.

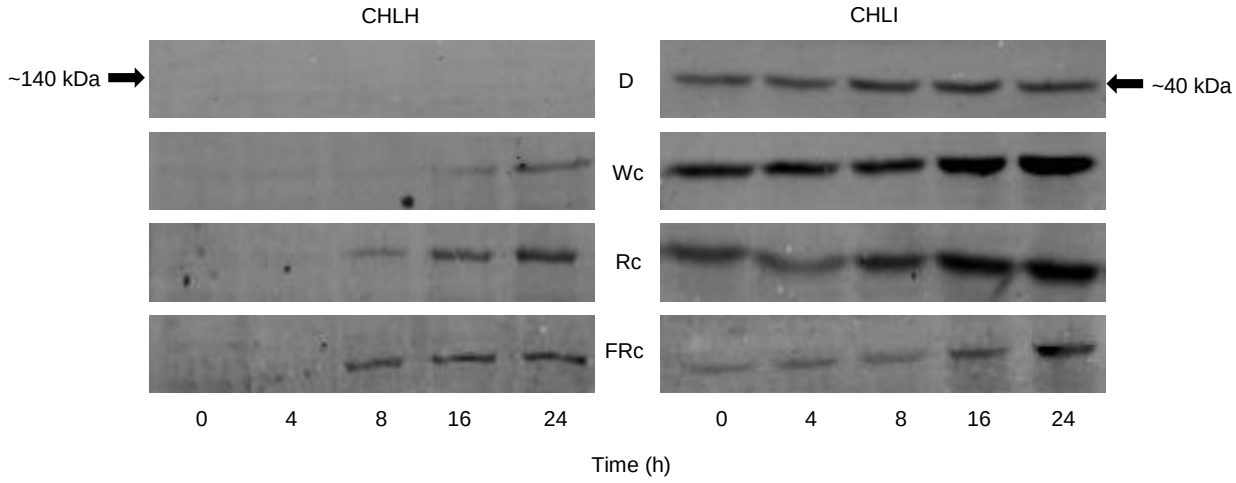

3.17 Expression of CHLH and CHLI proteins following 2d dark pretreatment and up to 24h dark (D), white (Wc; 110 µmol m^{-2} s^{-1}), red (Rc; 80 µmol m^{-2} s^{-1}) or far-red (FRc; 10 µmol m^{-2} s^{-1}) light treatment. One of two repeat experiments, with similar results, is shown.

a)

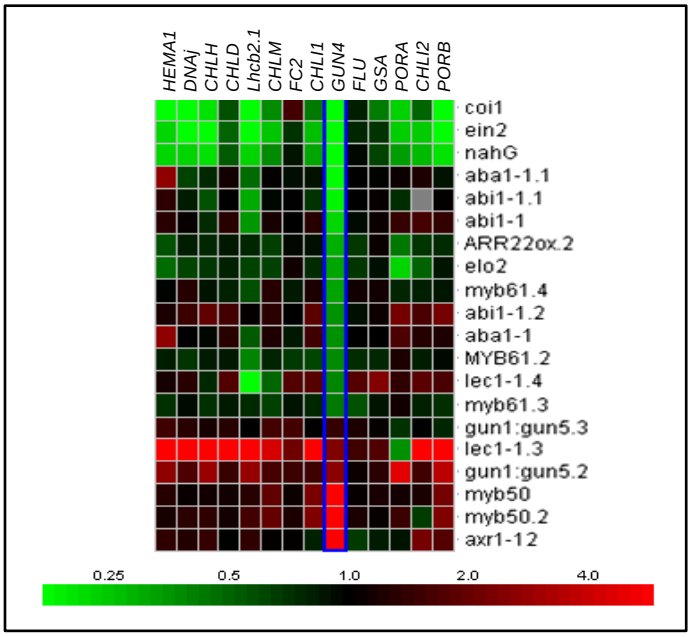

b)

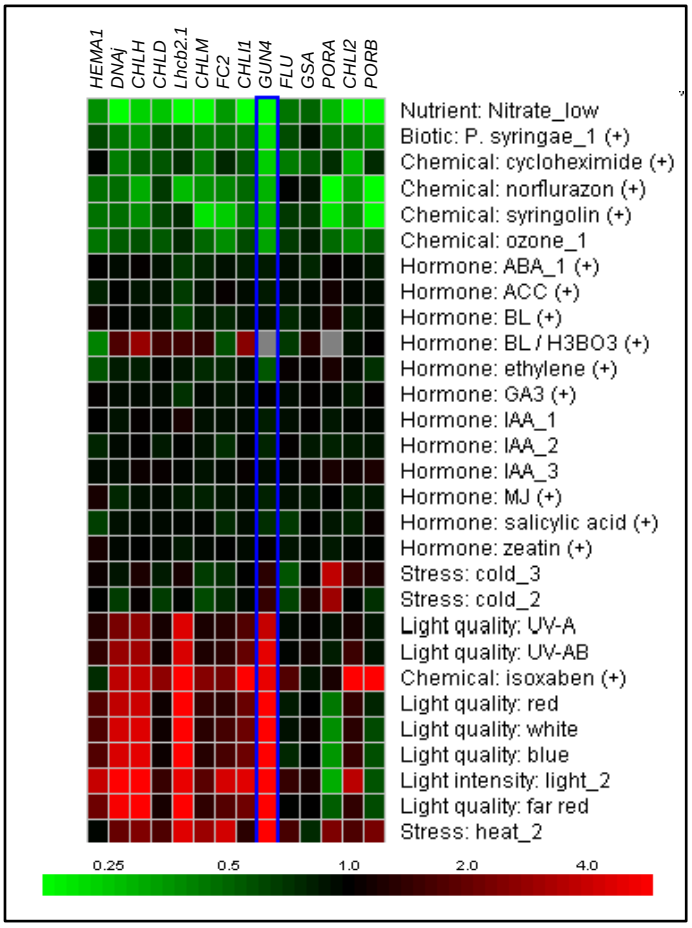

Figure 3.18 Bioinformatics analysis of *GUN4* expression. a) Analysis of expression of tetrapyrrole-related genes in response to different stimuli, b) analysis of expression of tetrapyrrole-related genes in different *Arabidopsis* mutant backgrounds. Data taken from the Genevestigator™ program (Zimmerman *et al*., 2005) and each expression point is based on n = ≥2 from different microarray experiments.

Figure 3.18a indicates that the majority of genes studied (excluding *FC2*, *FLU* and *GSA*) are down-regulated in *coi1*, *ein2* and *nahG* mutants. These genes are all involved in hormone signalling (jasmonic acid, ethylene and salicylic acid, respectively) in response to stress (Delaney *et al*., 1994; Xie *et al*., 1998; Alonso *et al*., 1999), however, when assessing the impact of hormone feeding (figure 3.18b), other than brassinolide, none of the genes are affected. Additionally, the same set of genes are upregulated (excluding *PORA*, which is downregulated) in the *lec1* mutant. *LEC1* has transcription factor activity and is responsible for embryogenesis (Lee *et al*., 2003a), which suggests it has a role in preventing chlorophyll synthesis in the seed.

It is clear, however, that while many of the genes under study present a similar pattern of expression, *GUN4* is affected by many more mutations. Firstly, *GUN4* expression is considerably reduced in all of the *aba1* and *abi1* lines, and this is mirrored only partially in the *Lhcb* genes which will likely relate to the lower chlorophyll levels in some lines of these mutants (Pogson *et al*., 1998). This again, however, does not relate to an increase in transcript abundance during ABA feeding experiments (figure 3.18b). This is particularly interesting in light of the recent publication (Shen *et al*., 2006) highlighting *CHLH* as an ABA receptor. Although *CHLH* shows no change of expression in either the *aba1* or *abi1* mutant, or with feeding of ABA, this does not rule out the possibility of altered protein levels under these conditions.

GUN4 is strongly up-regulated in the *axr1* mutant. *AXR1* encodes a subunit of the RUB1 activating enzyme that regulates the protein degradation activity of Skp1-Cullin-Fbox complexes, primarily, but not exclusively, affecting auxin responses.

Finally, *GUN4* is upregulated in the *myb50* mutant and downregulated in the *myb61* mutant. *MYB50* and *MYB61* are part of a super-family of transcription factors required for the regulation of almost all processes within organisms from every kingdom. In plants, MYBs have been particularly associated with hormone signalling (Chen *et al*., 2006), and recently with control of *CAB* expression (Churin *et al*., 2003). All members share the conserved MYB DNA-binding domain which generally comprises up to three imperfect repeats, each forming a helix-turn-helix structure of about 53 amino acids (reviewed in Stracke *et al*., 2001). However, despite the

divergent nature of this family, on a phylogenetic tree of 140 MYB genes, including 133 from *Arabidopsis* (Stracke *et al*., 2001), *MYB50* and *MYB61* group together, which might suggest that these genes are responsible for the regulation of similar targets.

3.2.8.3. GUN4 co-regulated factors

Using the Genevesigator™ program it is also possible to discover genes with a similar pattern of regulation to your gene-of-interest. In this case stimuli known to down- or up-regulate the *GUN4* gene (low nitrate, *P.syringae*, norflurazon, cyclohexamide, syringolin, all light treatments and heat stress) were used to find similarly regulated genes. Using a ratio threshold of 1.0 (default setting), three genes were returned: At1g75690, At1g22630 and At5g20935. At1g75690 and At1g22630 both show Cysteine-rich domains characteristic of the chaperone protein DnaJ, and At1g75690 shows a 45.1% similarity to Bundle Sheath Defective Protein 2 from *Zea mays*, and is targeted to the chloroplast. While At5g20935 has an unknown molecular function but shows similarity to Os07g0164200 from *Oryza sativa* and to the hypothetical protein Tery_2896 from *Trichodesmium erythraeum*.

However, these similarly regulated genes were pulled out based only on 13 treatments. In order to establish the limit of co-regulation across a wider range of treatments it is possible to study the correlation of two genes over 2507 microarray experiments. Despite At1g22630 and At5g20935 showing a good positive correlation over the limited number of experiments originally tested, in a more thorough test they fail to show a significant positive correlation (Pearson's coefficient of 0.378 and 0.284 based on a linear scale, respectively). On the other hand, At1g75690 shows a very significant positive correlation (Pearson's coefficient of 0.679 based on a linear scale).

Interestingly, the *BSD2* (*BUNDLE SHEATH DEFECTIVE 2*) gene from *Zea mays*, which is required for formation of the RUBISCO enzyme (Brutnell *et al*., 1996), is also a member of the Dnaj-like family. Mutations in the *BSD2* gene result in altered chloroplast formation and a disruption in chlorophyll accumulation (Brutnell *et al*., 1996). Additionally, mutations in the recently identified Dnaj-type family member

from *Arabidopsis*, *SCO2* (*SNOWY COTYLEDONS 2*), result in a severely reduced chlorophyll content, which is made more severe by application of an extended dark pre-treatment (Albrecht *et al*., 2008).

3.2.8.3.1. The DNAj-like family

To understand how well the sequence of At1g75690 aligns with other members of the DNAj family in *Arabidopsis*, a BLASTP search was submitted for the DNAj-like region of the *At1g75690* protein sequence. All proteins that were returned in this search, as well as the *E.coli* Dnaj protein and the Bsd2 protein from *zea mays*, are presented in a phylogenetic tree in figure 3.19. Although the *SCO2* protein sequence was also included in the construction of this tree, the sequence did not contain enough similarity with the other proteins to align correctly and was therefore omitted from the final tree.

At1g75690 aligns well with other members of the DNAj family, and most strongly with the At2g38000 and At2g34860 genes. While At2g38000 has not been annotated with any function or structure other than DNAj-like, At2g34860 has been named *EMBRYO SAC DEVELOPMENT ARREST 3* (*EDA3*) due to its involvement in female gametophyte development (Pagnussat *et al*., 2005). Both genes are expressed and the protein products are targeted to the chloroplast.

Although At1g75690 aligns with the sequence of Bsd2 of *Zea mays*, At3g47650 groups more closely, and is indeed annotated as Bsd2-like in the The *Arabidopsis* Information Resource (TAIR; Swarbreck *et al*., 2008); therefore At1g75690 is likely to have a different function to Bsd2. Additionally, when the protein sequence of *SCO2*, a DNAj-like gene which affects tetrapyrrole synthesis, was included in the alignment, a tree was unable to be constructed due to the dissimilarity of this sequence. This suggests that, although *SCO2* may contain a DNAj-like sequence, it is a more peripheral member of this family, and again, At1g75690 is likely to have a different function.

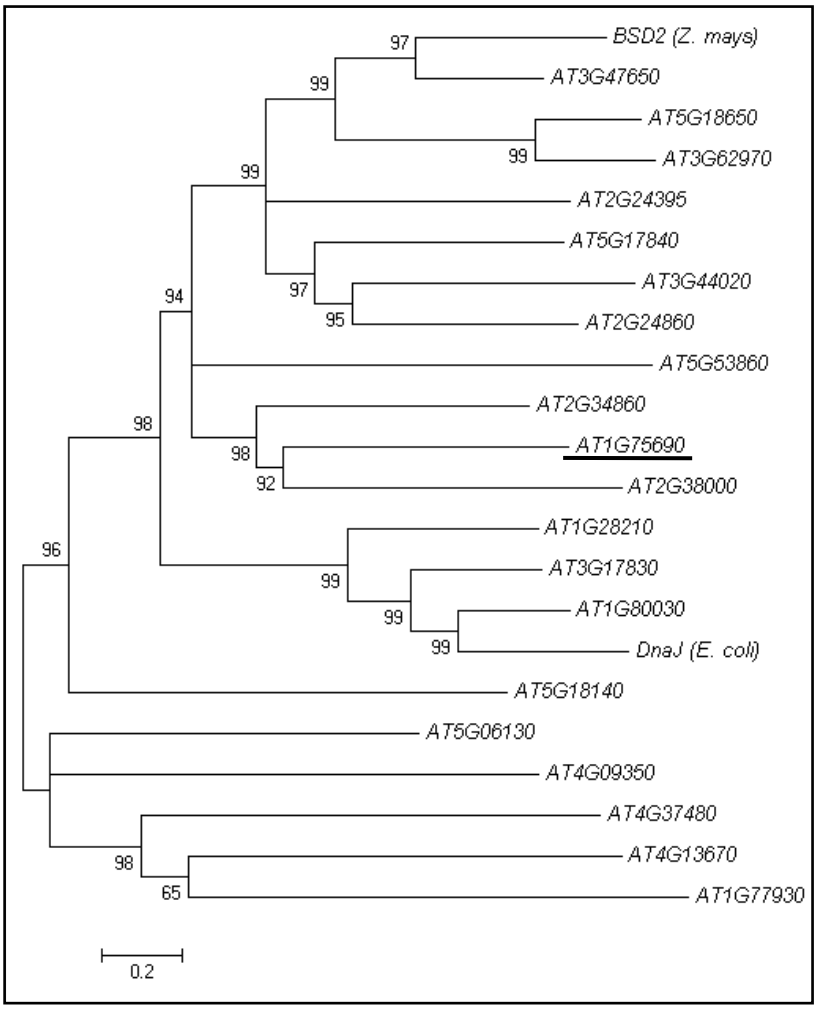

Figure 3.19 Phylogeny of the DNAj-Type protein family from *Arabidopsis thaliana*, the Dnaj protein from *E.coli*, and the *Bsd2* gene from *Zea mays* defined from the full length protein sequence (Tamura *et al*., 2007). Numbers indicate the percent Bootstrap value. The At1g75690 gene is underlined.

Further study into the 16.3 kDa protein sequence of At1g75690 revealed a chloroplast targeting sequence (TargetP: Emanuelsson *et al*., 2007), and the presence of a single helix region (ConPred: Arai *et al*., 2004) (data not shown).

3.2.7.3.2. Regulation of At1g75690

As At1g75690 was initially identified as having a similar regulatory pattern to *GUN4*, a study was conducted to assess the light regulation of At1g75690 under different wavelength treatments, compared to dark treatment, using RT-PCR (figure 3.20). At1g75690 is strongly induced under all wavelengths tested, and most strongly under far-red and blue light treatment. As At1g75690 contains a chloroplast targeting sequence this is not entirely surprising, as the chloroplast may only be formed and begin to function upon exposure to light. However, this data supports that gained from Genevestigator™, in terms of light regulation of At1g75690.

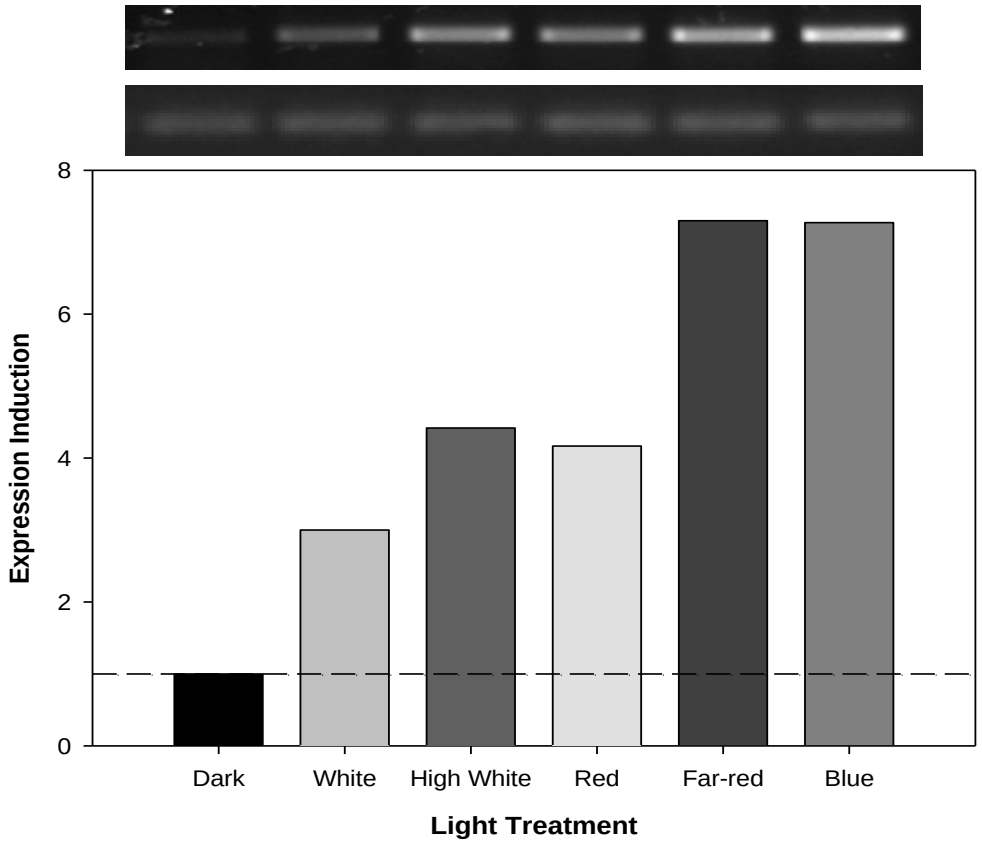

Figure 3.20 Light induced expression of the *At1g75690* gene from *Arabidopsis* analysed by semi-quantitative PCR, and compared to the standard gene *YLS8*, following 2d dark and 24h of dark, Wc (110 µmol m^{-2} s^{-1}), high Wc (550 µmol m^{-2} s^{-1}), red (80 µmol m^{-2} s^{-1}), far-red (10 µmol m^{-2} s^{-1}) or blue (20 µmol m^{-2} s^{-1}) light treatment. One of three repeat experiments, with similar results, is shown.

3.3. Discussion

3.3.1. *CHLH* and *GUN4* are major targets for light regulation during de-etiolation

In this study the light regulation of transcript abundance for eight genes related to chelatase activity at the major branchpoint of the tetrapyrrole pathway was studied. Of the four genes encoding the three subunits of Mg-chelatase only *CHLH* showed significant light regulation during the earliest phase of de-etiolation, although *CHLI1* did show some induction by 24h. These results are consistent with those reported in previous studies. Analysis of tetrapyrrole gene expression using an *Arabidopsis* miniarray identified *CHLH* as one of four key regulatory genes in the pathway together with *HEMA1*, *CAO* and *CRD1* encoding glutamyl-tRNA reductase, chlorophyll *a* oxygenase and Mg-protoporphyrin IX monomethylester cyclase respectively (termed cluster 1) (Matsumoto *et al*., 2004). In this earlier study *CHLI1*, *CHLI2*, *CHLD* and *FC2* were in second cluster of moderately light-regulated genes with *FC1* in a third cluster. The data presented here is generally in agreement with these results although more evidence for moderate light regulation of *CHLI1* and *FC2* than for the other three genes in that cluster was seen in the current study. Evidence that *CHLH* is the most highly regulated of the Mg-chelatase subunits at the level of transcript abundance has been consistently obtained. In greening barley *CHLH* transcript and protein was light-regulated while *CHLI* and *CHLD* showed little response (Jenson *et al*., 1996; Peterson *et al*., 1999) and this pattern was repeated when diurnal regulation of Mg-chelatase genes was examined in mature tobacco plants (Papenbrock *et al*., 1999). For the two ferrochelatase genes this study found a moderate light response for *FC2*, particularly in Bc, with little change at all for *FC1*. This difference in response to white light has also been seen previously (Matsumoto *et al*., 2004) and is consistent with the proposed role of *FC2* in synthesizing heam predominantly for photosynthesis (Singh *et al*., 2002).

One of the most notable results from the current study is that the *GUN4* gene was highly responsive to light treatments and showed a remarkably similar expression pattern to that seen for *CHLH*. A response profile that is consistent with a cluster 1 gene as defined by Matsumoto *et al.* (2004). *GUN4* is a regulator of Mg-chelatase activity and co-purifies with *CHLH* in a complex isolated from *Arabidopsis*

chloroplasts (Larkin *et al*., 2003). The *GUN4* protein binds to both protoporphyrin IX and Mg-protoporphyrin and stimulates Mg-chelatase activity in a recombinant *Synechocystis* enzyme system (Larkin *et al*., 2003) by reducing the Mg^{2+} concentration required for activity (Davison *et al*., 2005). Given the close association between *CHLH* and *GUN4* it is perhaps not surprising that they share such a similar regulatory profile. The results from this study indicate that the regulation of *GUN4* expression is a key early step in photoreceptor regulation of chlorophyll biosynthesis during de-etiolation.

The observation that *CHLM* was highly responsive to light signals was quite surprising. In a previous study Matsumoto *et al.* (2004) did not observe significant regulation of *CHLM* under white light (designated a cluster 3 gene). Similarly, only a moderate increase in *CHLM* expression was seen in greening tobacco and barley seedlings (Alawady *et al*., 2005), although enzyme activity in barley seedlings was increased more than 10-fold in response to light. Additionally, the light-induced expression profile of *CHLM* was markedly different to that observed for *CHLH* and *GUN4*. In general, *CHLM* was induced more slowly than *CHLH* and *GUN4* perhaps simply reflecting the fact that this gene encodes a later enzyme in the pathway. However, a 4h time difference in the first peak of expression is quite considerable and might have an important regulatory role during this crucial early phase of de-etiolation (Alawady and Grimm, 2005). Alternatively, if the CHLM protein accumulates significantly in darkness then the later induction of *CHLM* may simply reflect an increased long-term demand for chlorophyll.

As transcriptional changes are only one indicator of gene expression, protein levels for CHLH and CHLI were also studied during de-etiolation. In general this correlated well with the transcript data and are broadly consistent with what we know about changes in tetrapyrrole metabolism during de-etiolation. However, it would also be interesting to measure tetrapyrrole intermediate levels in order to assess total flux through the pathway.

3.3.2. Multiple photoreceptors regulate chlorophyll biosynthesis during de-etiolation

The light response profile for *CHLH* and *GUN4* of a rapid induction of expression followed by a second broad peak is similar to that observed for *Arabidopsis CAB2*, which classically shows an acute photoreceptor-mediated response followed by high amplitude circadian oscillations (Millar and Kay, 1996). From this response pattern it might be predicted that both genes are circadian regulated and for *CHLH* there is good evidence that this is the case (Papenbrock *et al*., 1999; Matsumoto *et al*., 2004). Analysis of the photoreceptors regulating this response demonstrated that phyA mediated responses to FRc and Bc while phyB played a major role under Rc. A role for cry2 was also observed after 24h Bc treatments with some evidence for a small contribution by cry1 in the induction of *CHLH* at 24h. These results are similar to those observed previously for *HEMA1* (McCormac and Terry, 2002a).

There has been extensive analysis of gene expression changes during the first phase of a Rc treatment with 206 genes induced ≥2-fold within 1h Rc, most of which are under the control of phyA (Tepperman *et al*., 2006). In this gene set transcription factors are 3-fold overrepresented with 50% of the 22 most strongly Rc-induced genes falling into this functional category. This has led to a model whereby the primary function of phytochrome is to initiate a cascade of transcriptional regulation *via* a limited number of initial targets (Quail, 2002). Interestingly, only three tetrapyrrole-related genes were identified as induced by 1h Rc: *CHLH*, *GUN4* and *CAO*. In the current study the first time point analysed was 2h Rc, but both *CHLH* and *GUN4* were significantly induced by this timepoint (4- and 2.5-fold respectively) and it is likely that at 1h Rc expression was already approaching the 2.5–3-fold response seen by Tepperman *et al.* (2006). Given the rapidity of the response of these genes to Rc it is likely that they are primary targets of phytochrome signalling.

Previously it has shown that the *fhy1* and *fhy3* mutants had a strong effect on *HEMA1* expression under both FRc and Rc (McCormac and Terry, 2002a). FHY1 is required for nuclear import of phyA (Rosler *et al*., 2007) while FHY3 is transcription factor that mediates phyA-dependent changes in gene expression under FRc (Wang and Deng, 2002b; Lin *et al*., 2007). In this study, FRc induction of both *CHLH* and

GUN4 was completely abolished in *fhy1* and *fhy3* entirely consistent with their proposed roles in phyA signalling. The results under Rc are more difficult to explain. The *fhy1* mutant had a strong effect on expression of both genes at 24h, but did not prevent induction completely as seen previously for *HEMA1* (McCormac and Terry, 2002a). *FHY1* is one of a pair of genes required for nuclear import of phyA and this may account for the residual activity. However, the Rc-induction of *CHLH* and *GUN4* was dependent in our assay on phyB, not phyA. This would suggest that *FHY1* also has a role to play in phyB responses although such an observation has not been reported. Indeed, it has been shown that Rc results in degradation of FHY1 (Shen *et al*., 2005). FHY1 has been shown to affect *CHS* expression under Rc, but in this case the response was under the control of phyA (Barnes *et al*., 1996). In that study *Lhcb* expression under Rc was unaffected in *fhy1*, a result that was also observed here (McCormac and Terry, 2002a). A similar situation appears to exist for FHY3, which also functions redundantly with a second, related protein, FAR1 (Lin *et al*., 2007). Moreover, the *fhy3* mutant has been reported to be hyper-responsive Rc (Whitelam *et al*., 1993). In the current study the *fhy3* mutant only affected expression at 24h and not 8h even though both responses were primarily under the control of phyB. An explanation for this result may come from the recent demonstration that FHY3 functions in response to Rc *via* direct input to the circadian clock (Allen *et al*., 2006). Such a role for FHY3 could account for both the time-dependent effect of the *fhy3* mutant on *CHLH* and *GUN4* expression seen here and the previous observation by McCormac and Terry (2002) for *HEMA1*.

In addition to phyA and phyB we also observed an input by the cryptochrome photoreceptors to *CHLH* and *GUN4* regulation. This was predominantly cry2 as the *cry1* mutant had little effect on *CHLH* and *GUN4* expression except for a minor, redundant role in regulating *CHLH* at 24h. The input of cry2 in the regulation of *CHLH* and *GUN4* was mostly confined to the 24h timepoint with the peak of expression after 4h Bc being predominantly under the control of phyA. The importance of phyA in this response is perhaps not surprising given that a role for phyA in mediating Bc responses is well established (Duek and Fankhauser, 2003) and that phyA is a critical photoreceptor during the very early stages of de-etiolation (Tepperman *et al*., 2006).

3.3.3. The input of green light does not account for the downregulation in *CHLD* under white light

The discovery that *CHLD* expression is down-regulated under Wc light, but not under Rc or Bc, led to the hypothesis that another wavelength may be affecting gene expression. Recently Folta (2004) and Dhingra *et al*. (2006) have published work concerning the regulation of morphological and transcriptional changes in *Arabidopsis* following exposure to green light. Interestingly, Dhingra *et al*. (2006), using a micro-array approach, showed that *CHLD* is not affected by green light treatment, and this was confirmed in this study. However, this now leads to the hypothesis that a wavelength other than green light, which is present in fluorescent white light, is controlling *CHLD* gene expression.

3.3.4. *GUN4* may be the primary target in the tetrapyrrole pathway for multiple hormone signals

Data presented here, compiled from a range of searches using the Genevestigator ™ package, show that *GUN4* expression is highly responsive to an impairment in the signalling of many plant hormones. The first of these, and perhaps the most significant, is the identification that *GUN4* transcript levels are reduced in the *aba1* and *abi1* mutants.

ABA1 encodes a single copy zeaxanthin epoxidase gene that functions in the first step of the biosynthesis of the ABA hormone. This mutant was originally identified in 1982 (Koorneef *et al*.) and has reduced levels of ABA and brown/yellow leaves. Given the fact that none of the genes studied in the tetrapyrrole pathway show a down-regulation in transcript abundance, other than *GUN4*, this clearly leads to the hypothesis that *GUN4* is able to sense the reduction in ABA, and is the primary cause of the brown/yellow leaf phenotype.

What is also striking about the transcription profile of this mutant is the up-regulation of the *HEMA1* gene. One possible explanation of this alteration in the transcriptome could be placed on the plastid retrograde signal, where a change in the levels of *GUN4* expression in this mutant would cause an adjustment in the signal

from the chloroplast. The plastid signal has been shown to down-regulate the levels of many genes, including *HEMA1* (McCormac *et al*., 2001), meaning that a lack of this signal would allow transcription to continue.

ABI1 encodes a calcium ion binding/protein phosphatase type 2C and acts negatively in facilitating ABA signalling (Koorneef *et al*., 1984; Gosti *et al*., 1999). The *GUN4* gene is down-regulated in both *abi1* alleles (*abi1-1.1* and *abi1-1.2*) while there is no reduction in transcription of the other tetrapyrrole synthesis genes in the *abi1-1.1* background, with many of them in fact up-regulated, including *CHLH* and *CHLI1*. This correlates well with the phenotype of the *abi1* mutant, which is described as having dark green rosette leaves and bright green stems i.e. an increase in chlorophyll levels (Parcy and Giraudat, 1997).

Concurrently, *GUN4* transcript levels are reduced in the *lec1-1.4* mutant. Although this gene has been implicated primarily in embryo maturation, the *lec1* mutant also has a reduced abundance of *ABI3* transcripts. *ABI1* and *ABI3* have been shown to interact to control ABA responses in vegetative tissues (Parcy and Giraudat, 1997), adding further support to the theory that *GUN4* is regulated by ABA.

GUN4 transcription is also increased in the *axr1* mutant. *AXR1* (*AUXIN RESISTANT 1*) encodes a subunit of the RUB1 activating enzyme that regulates the protein degradation activity of Skp1-Cullin-Fbox complexes, primarily affecting auxin responses (Leyser *et al*., 1993), although jasmonic acid signalling has also been implicated (Tiryaki and Staswick, 2002). However, AXR1 also acts with AS1 (ASSYMETRIC LEAVES 1) to exclude BP (BREVIPEDICELLUS) from leaves, and thus promote leaf fate (Hay *et al*., 2006). Interestingly, the AS1 signalling pathway has been shown to include hormonal inputs such as auxin, gibberellin, jasmonic acid and salicylic acid stimuli, and AS1 shows considerable similarity to the MYB family (Chen *et al*., 2006). Additionally, although there is no change in chlorophyll content in the *axr1* mutant, the *as1-15* mutant is described as having bright green rosette leaves. Therefore, the increased transcription rate of *GUN4* in the *axr1* mutant may be tied in with a now redundant function of *AS1*.

3.3.5. *MYB50* and *MYB61* control *GUN4* expression and are antagonistically regulated by light

In a screen for mutations that affect tetrapyrrole synthesis-related gene expression, using the Genevestigator™ microarray database, *myb50* and *myb61* were identified as up- and down-regulating *GUN4* expression, respectively. These genes are members of a super family of transcription factors which are primarily associated with responses to homones (Yanhui *et al*., 2006), but have also been implicated a variety of other responses, including regulation of *CAB* gene expression in wheat and barley (Churin *et al*., 2003).

MYB61 has previously been shown to be required for mucilage deposition and extrusion in the seed coat, in a TTG-independent pathway (Penfield *et al*., 2001), and stomatal closure (Liang *et al*., 2005). The latter has close links with ABA signalling, which has also been reported to also control the tetrapyrrole pathway (Pogson *et al*., 1998; Barrero *et al*., 2008; section 5.2.3). A study by Yanhui *et al*. (2006) showed that *MYB61* is also responsive to auxin stimulus, and *MYB50* is upregulated by GA, auxin JA and SA treatment. Previously cytokinin was shown to regulate *HEMA1* expression (Masuda *et al*., 1995; McCormac and Terry, 2002a), thereby regulating total flux through the pathway, and mutations in the ABA synthesis and signalling pathways are known to affect tetrapyrrole synthesis (see section 5.2.3 for further discussion). As the effect of *myb50* and *myb61* mutation on gene expression was limited to *GUN4*, and did not affect either *HEMA1* or *CHLH*, this suggests that *GUN4* might be the site for hormonal input into the chlorophyll branch of the tetrapyrrole pathway.

3.3.6. *At1g75690*, a member of the DNAj-like family, is co-regulated with *GUN4*

In a screen for genes with a similar pattern of expression to *GUN4*, using the Genevestigator™ program, the most highly correlating candidate was At1g75690, which encodes a Dnaj-like protein. The *Escherichia coli* DnaJ proteins are involved in protein folding, protein transport or in the degradation of misfolded proteins (Cheetham and Caplan, 1998). The Dnaj family is recognised as containing four domains: a N-terminal α-helical J domain, a flexible linker glycine/phenylalanine

(G/F) rich domain, a cystein rich domain and a variable C-terminal domain (Cheetham and Caplan, 1998). However, the proteins in this family are highly divergent and it is not uncommon for one or two of the latter domains to be missing. It is therefore not surprising that the At1g75690 protein from *Arabidopsis* shares only 24% identity with the Dnaj protein of *E.coli*.

Interestingly, the *BSD2* (*BUNDLE SHEATH DEFECTIVE 2*) gene from *zea mays*, which is required for formation of the RUBISCO enzyme (Brutnell *et al*., 1996), is also a member of the DNAj-like family. Mutations in the *BSD2* gene result in altered chloroplast formation and a disruption in chlorophyll accumulation (Brutnell *et al*., 1996). Additionally, mutations in the recently identified Dnaj-type family member from *Arabidopsis*, *SCO2* (*SNOWY COTYLEDONS 2*), result in a severely reduced chlorophyll and Pchlide content, which is positively correlated with length of dark pre-treatment (Albrecht *et al*., 2008).

Analysis of the expression pattern of the At1g75690 gene revealed that it is highly light regulated under all on the wavelengths tested, which may be related to the fact that this protein is chloroplast targeted. Taken together this data suggests that, like *SCO2*, the At1g75690 DNAj-like protein might have a role in regulating tetrapyrrole synthesis, such as Mg-chelatase enzyme formation, in a similar manner to BSD2 from *Zea mays*.

Chapter 4: Regulation of the tetrapyrrole pathway by PIF1 and PIF3

4.1 Introduction

Light is a key environmental factor that regulates plant growth and development, and perception of light by plants is therefore vital for adaptation and survival. A number of photoreceptors have evolved for this function, and much is known about the specificity of each class for different wavelengths of light in the model plant species *Arabidopsis thaliana* (see section 1.3.1 for a more detailed overview). The main photoreceptors for blue and UV light detection are the cryptochromes and phototropins, while red and far-red light is exclusively perceived by the phytochrome family. Five members, phyA-E, are present as homodimers and heterodimers *in vivo* (Sharrock and Clack, 2004), and each subunit consists of a ~125 kDa polypeptide covalently linked to an open-chain tetrapyrrole chromophore, phytochromobilin (Lagarias and Lagarias, 1989; Rockwell *et al*., 2006). Irradiation by red light results in a conformational change in the phytochrome molecule from the biologically inactive Pr form to the active Pfr form, and subsequent translocation to the nucleus (Yamaguchi *et al*., 1999; Chen *et al*., 2005). However, the signalling mechanism of phyA is slightly different where neither phyA in the Pr form, synthesized in the dark, nor the photoconverted Pfr form is active in inducing the signal. Instead the short-lived signal is produced during phototransformation from Pfr to Pr (Shinomura *et al*., 2000). In *Arabidopsis*, under prolonged light exposure, ~2500 genes (10% of the genome) are regulated by phytochromes (Tepperman *et al*., 2006; Quail, 2007); however, it is not yet fully understood how this signal is initiated once the phytochome molecule has entered the nucleus.

PHYTOCHROME INTERACTING FACTOR 3 (PIF3) was identified in a screen for phytochrome binding proteins (Ni *et al*., 1998), and was shown to interact with the Pfr form of both phyA and phyB (Ni *et al*., 1999; Zhu *et al*., 2000). Since then PIF1, PIF4, PIF5 and PIF6 have been identified (Huq and Quail, 2002; Huq *et al*., 2004; Khanna *et al*., 2004), and, along with PIF3, are all members of the *Arabidopsis* bHLH subfamily 15 (Toledo-Ortiz *et al*., 2003; Deuk and Fankhauser, 2005). However, only PIF1 and PIF3 have been shown to interact with the Pfr form of phyA,

and PIF4 and PIF5 show a weaker affinity for phyB. Additionally, the HLH region of the PIF molecule allows the formation of homodimers and heterodimers (Toledo-Ortiz *et al*., 2003), adding a further level of complexity to the signalling mediated by these factors.

bHLH factors are known to bind to a cis-element called the E-box, through an approximately 15 basic amino acid region, although there are different types of E-boxes depending on the central two nucleotides. Concordantly the PIF proteins bind to a cis-acting regulatory element found in the promoter region of target genes. PIF1, PIF3 and PIF4 bind specifically to a subtype of the E-box called the G-box (5'-CACGTG-3') (Martinez-Garcia *et al*., 2000; Huq and Quail, 2002; Huq *et al*., 2004). Finally, binding of the PIFs to phytochrome has been mapped to a conserved sequence motif at their N-terminal region, designated as the active phytochrome-binding (APB) motif (Khanna *et al*., 2004). Site-directed mutagenesis showed that four invariant amino acid residues (ELxxxxGQ) common in all PIFs are critical determinants of the APB motif. Additionally, PIF1 and PIF3 can bind the active form of phyA through the APA domain (Al-Sady *et al*., 2006).

Mutational studies of the *PIF* genes have allowed many of their functions to be elucidated; however, it is not always clear if they are exhibiting a positive or negative effect, or a combination of the two. At the centre of this argument is the original phytochrome interacting factor, PIF3. The initial characterization of *PIF3* antisense lines showed a hyposensitive phenotype under continuous red light, suggesting that PIF3 functions positively in controlling photomorphogenesis (Ni *et al*., 1998). Additionally, PIF3 has been shown to function positively in chloroplast development and greening processes during the initial hours of de-etiolation, as *pif3* seedlings have chlorophyll levels lower than those of wild type (Kim *et al*., 2003; Monte *et al*., 2004), and PIF3 also acts positively in the light-induced accumulation of anthocyanin (Kim *et al*., 2003; Shin *et al*., 2007). However, several more recently discovered alleles have shorter hypocotyls and more expanded cotyledons than wild-type seedlings under continuous red light, suggesting that PIF3 functions as a negative regulator of morphological phenotypes under red light (Kim *et al*., 2003; Monte *et al*., 2004). Thus the mechanism of PIF3 action is less than clear.

PIF1, on the other hand, has been consistently labelled as a negative regulator, which is required for repression of light-induced seed germination and inhibition of hypocotyl elongation (Oh *et al*., 2004), and hypocotyl negative gravitropism and repression of protochlorophyllide accumulation in the dark (Huq *et al*., 2004; Oh *et al*., 2004). However, Oh *et al*. (2004) also showed that the *pil5pif3* (*pif1pif3*) double mutant has an additive effect to either the *pif1* or *pif3* single mutants, in terms of hypocotyl extension, negative gravitropism and germination (Oh *et al*., 2004).

Intriguingly, a number of studies have also linked the function of *PIF3* with the circadian clock, not least the identification that PIF3 is able to bind one member or the central regulator, TOC1 (Yamashino *et al*., 2003). However, the *pif3* mutant has since been shown to exhibit normal rhythms of *TOC1*, and the other members of the central oscillator, CCA1 and LHY (Oda *et al*., 2004; Viczian *et al*., 2005), indicating that PIF3 is not required for phytochrome input to the clock.

Previously, PIF1 and PIF3-mediated regulation of tetrapyrrole-synthesis genes has indicated that they were required for light induction of *CHLH* and *GUN4* (see section 3.2.4.). However, as PIF1 has been shown to act negatively in the regulation of chlorophyll accumulation, and PIF3 acts positively, this result is particularly interesting. The current study was undertaken to understand how PIF1 and PIF3 act on the tetrapyrrole pathway through further study of the *pif1*, *pif3* and *pif1pif3* mutants, with the hypothesis that both proteins act negatively in regulating chlorophyll biosynthesis.

4.2 Results

4.2.1 Expression of tetrapyrrole synthesis genes in the *pif* mutants

Previously, *CHLH* and *GUN4* expression was studied in the *pif1-2* and *pif3-3* mutant alleles, and showed no light induction under red and far-red light compared to WT (figure 3.7, 3.9 and 3.10). However, *pif1* mutant seedlings have previously been shown to accumulate protochlorophyllide in the dark (Huq *et al*., 2004), suggesting an upregulation of tetrapyrrole genes in the dark. Expression of *GUN4* was therefore examined in the dark in the *pif1-2* and *pif3-3* mutant alleles, compared to WT and the *phy*A mutant (figure 4.1).

This data confirms that in the *pif1-2* and *pif3-3* mutants there is an increase in *GUN4* expression following 3d dark treatment, while expression is comparable to WT in the *phyA* mutant, suggesting that PIF1 and PIF3 act as repressors of gene expression in the dark. However, by 4d dark treatment this increase is no longer apparent as *GUN4* expression returns to WT levels in the *pif1-2* and *pif3-3* mutants. Interestingly, expression of *CHLH* has been studied previously at this 4d timepoint, with similar results, to argue against PIF3 functioning as a negative regulator of gene expression (Monte *et al*., 2004). The apparent switch between negative and positive mechanisms of regulation that the PIF proteins exhibit over *GUN4* expression, was studied using new *pif1*, *pif3* and *pif1pif3* double mutant alleles (Stephenson *et al*., 2009). The *pif1pif3* double mutant was constructed using an independently isolated *pif3* T-DNA insertion allele that is identical to *pif3-1* (Kim *et al*., 2003) and a new *pif1* allele designated *pif1-101*. Using these mutants, *HEMA1* expression was studied over 5d of dark treatment following germination (figure 4.2).

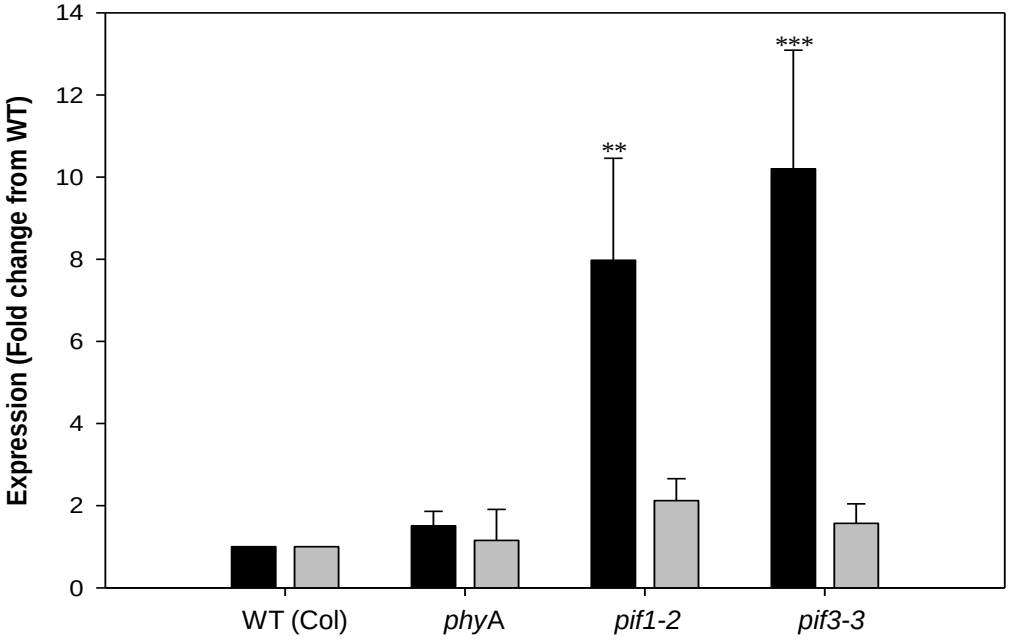

Figure 4.1 Expression of *GUN4* in the *pif1-2* and *pif3-3* mutants, compared to WT and *phyA* mutant, following growth for 3 (black bar) or 4d dark (grey bar). ** = P = <0.01, *** = P = <0.005. Values are mean ± SE of 3 independent experiments.

a)

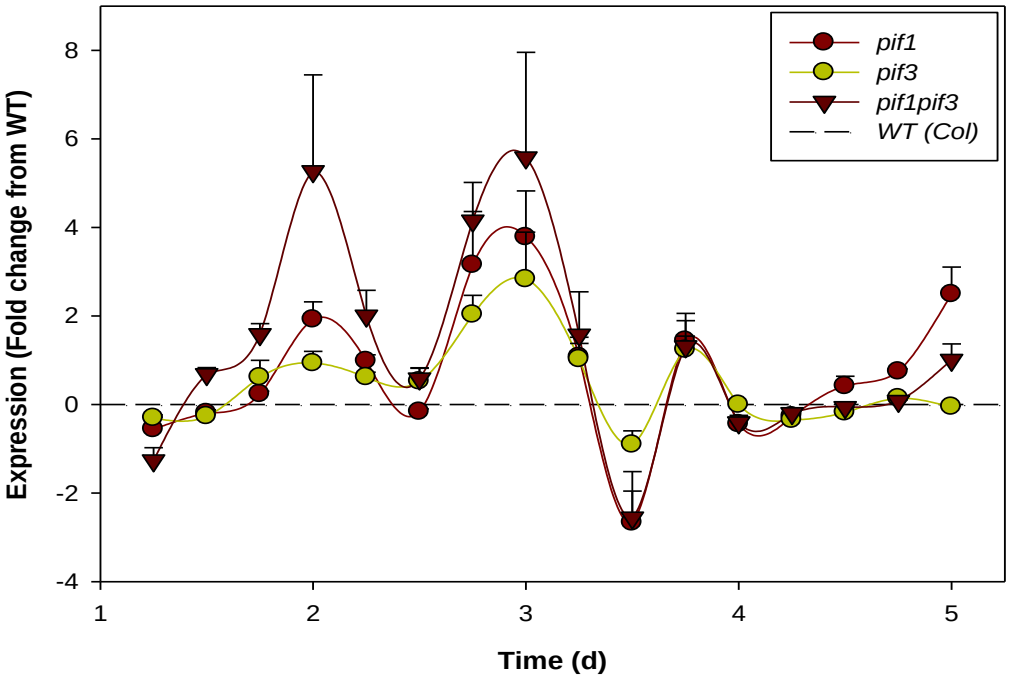

b)

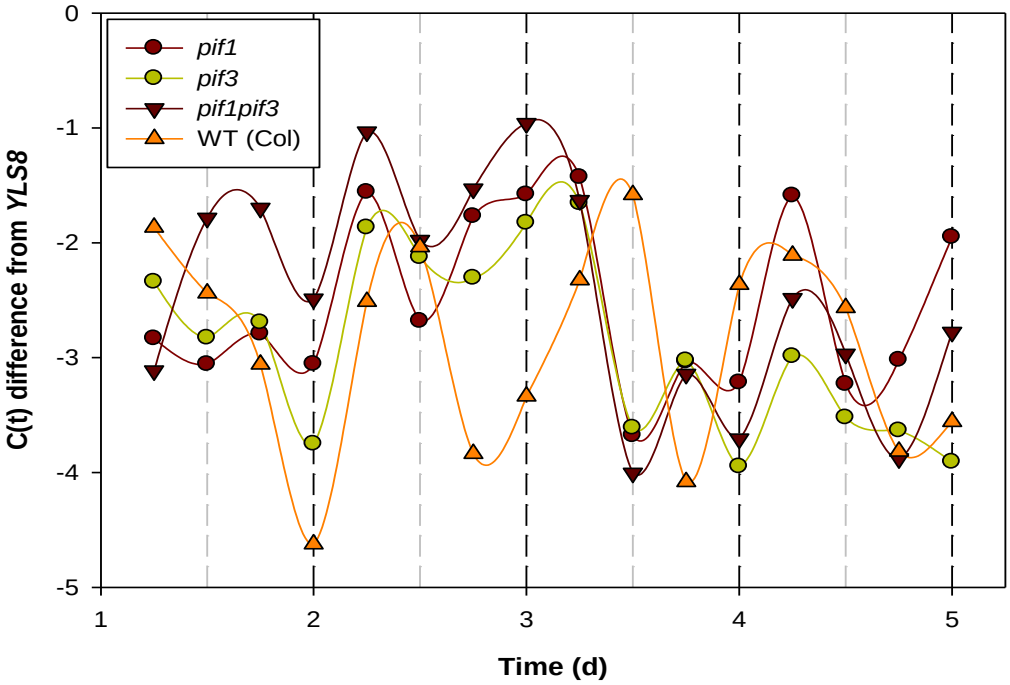

Figure 4.2 Expression of *HEMA1* in the *pif* mutants following up 5d of dark treatment. a) Expression of *HEMA1*, presented as fold change from WT, b) expression of *HEMA1*, presented as C(t) difference from *YLS8*. Red circles = *pif1*, green circles = *pif3*, inverted red triangles = *pif1pif3*, orange triangles = WT. Values in a) are mean ± SE of ≥3 independent experiments, values in b) are mean of ≥3 independent experiments.

Over this 5d dark timecourse *HEMA1* expression fluctuates considerably in the *pif* mutants compared to WT (figure 4.2a), although they generally show an induction of gene expression. The pattern of expression is strongly indicative of a circadian rhythm, and also shows a stronger response in the *pif1pif3* double mutant compared to either of the single mutants. As this data is presented as fold expression difference from WT, it is presumed that *HEMA1* expression is constant in the WT over this period. To find if this was the case data is also presented as *HEMA1* C(t) difference from *YLS8* (figure 4.2b), as the C(t) value for *YLS8* is known to be remain constant (data not shown). It is now possible to see that in the WT *HEMA1* expression is following a circadian rhythm-like pattern, with a period of ~23h and an amplitude of ~1.25 C(t); which was confirmed using the Chi-squared periodogram statistic ($p = 0.031$; Sokolove and Bushell, 1978). Although the *pif* mutants show a similar pattern to each other, and expression also fluctuates, the wavelength is much more varied, the amplitude is only ~0.75 C(t), and they do not show a statistically significant rhythm. Previously, PIF3 has been shown to bind to the promoter of *CCA1* and *LHY* (Ni *et al*., 1999; Martinez-Garcia *et al*., 2000), and to the TOC1 protein (Yamashino *et al*., 2003), yet does not affect input into the circadian clock (Oda *et al*., 2004; Viczian *et al*., 2005). To test whether the input to the clock has been compromised under these conditions, expression of the central oscillator genes *CCA1*, *LHY* and *TOC1* was studied alongside the known circadian-regulated gene *CAX1* (Harmer *et al*., 2000; figure 4.3), but the *pif* mutations do not affect the expression of these genes. Additionally, the expression of *PIF1* and *PIF3* was studied to assess whether they are themselves regulated by the circadian clock, which indicated a strong rhythmic pattern in the transcription of these genes (figure 4.3). Unfortunately the aforementioned genes could not be assessed for the significance of their rhythm due to too few timepoints.

Compared to WT, the *pif* mutants also positively affect the expression of *CHLH*, *GUN4*, *GSA* and *PORA* (figure 4.4), and transcript levels of *HEMA1* and *PORA* correlate well with protein content of Glu-TR and POR (figure 4.5). However, when the expression of *HEMA1*, *CHLH* and *GUN4* was studied after 24h Wc treatment, following 2d dark pre-treatment there is only a small increase in transcript in the *pif* mutants compared to WT, and no difference following 4d dark pre-treatment (figure 4.6).

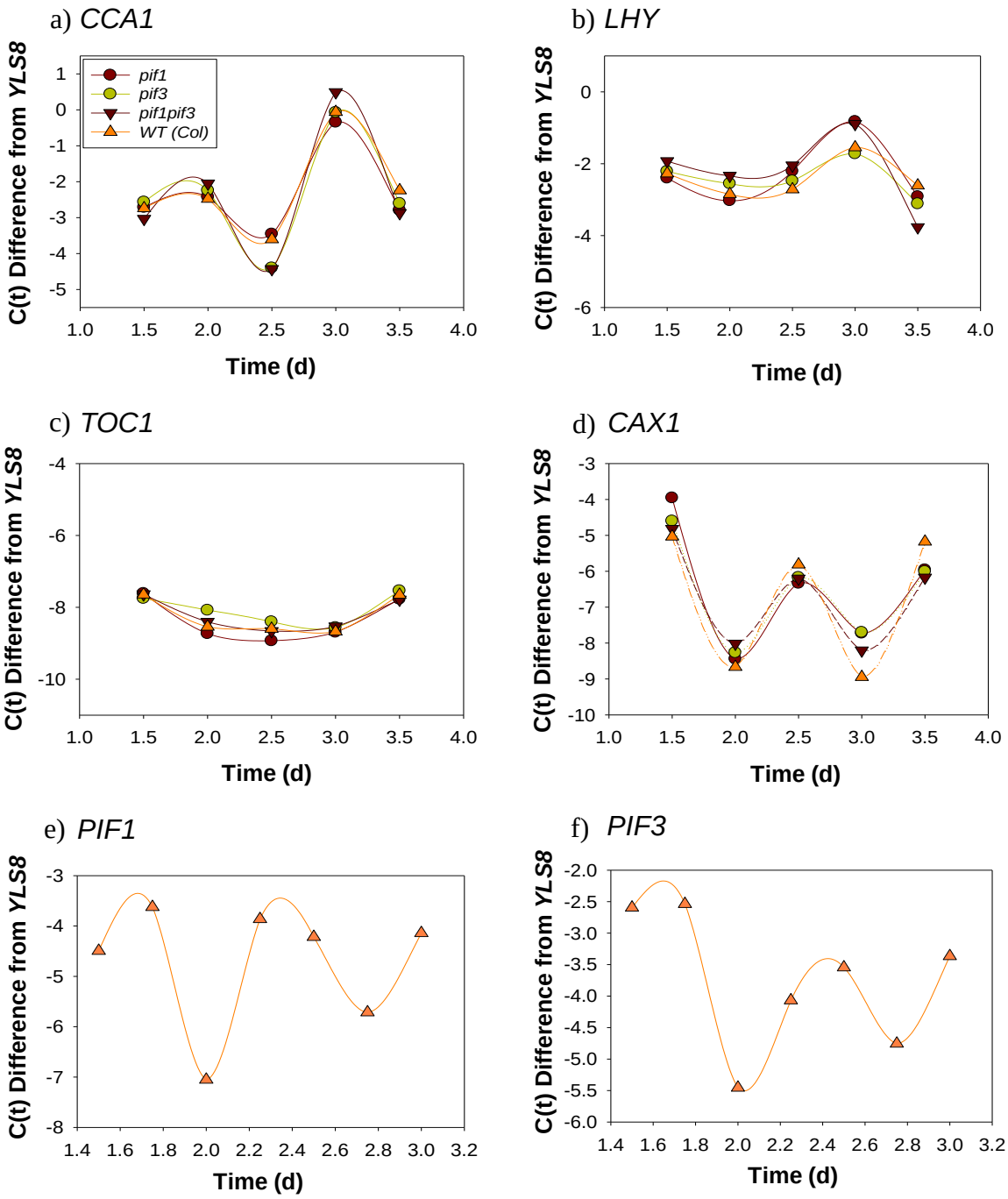

Figure 4.3 Expression of circadian clock/rhythm-associated genes following up to 3.5d of dark treatment, presented as C(t) difference from *YLS8*. a) *CCA1*, b) *LHY*, c) *TOC1*, d) *CAX1*, e) *PIF1*, f) *PIF3*. Values are mean ≥3 independent experiments.

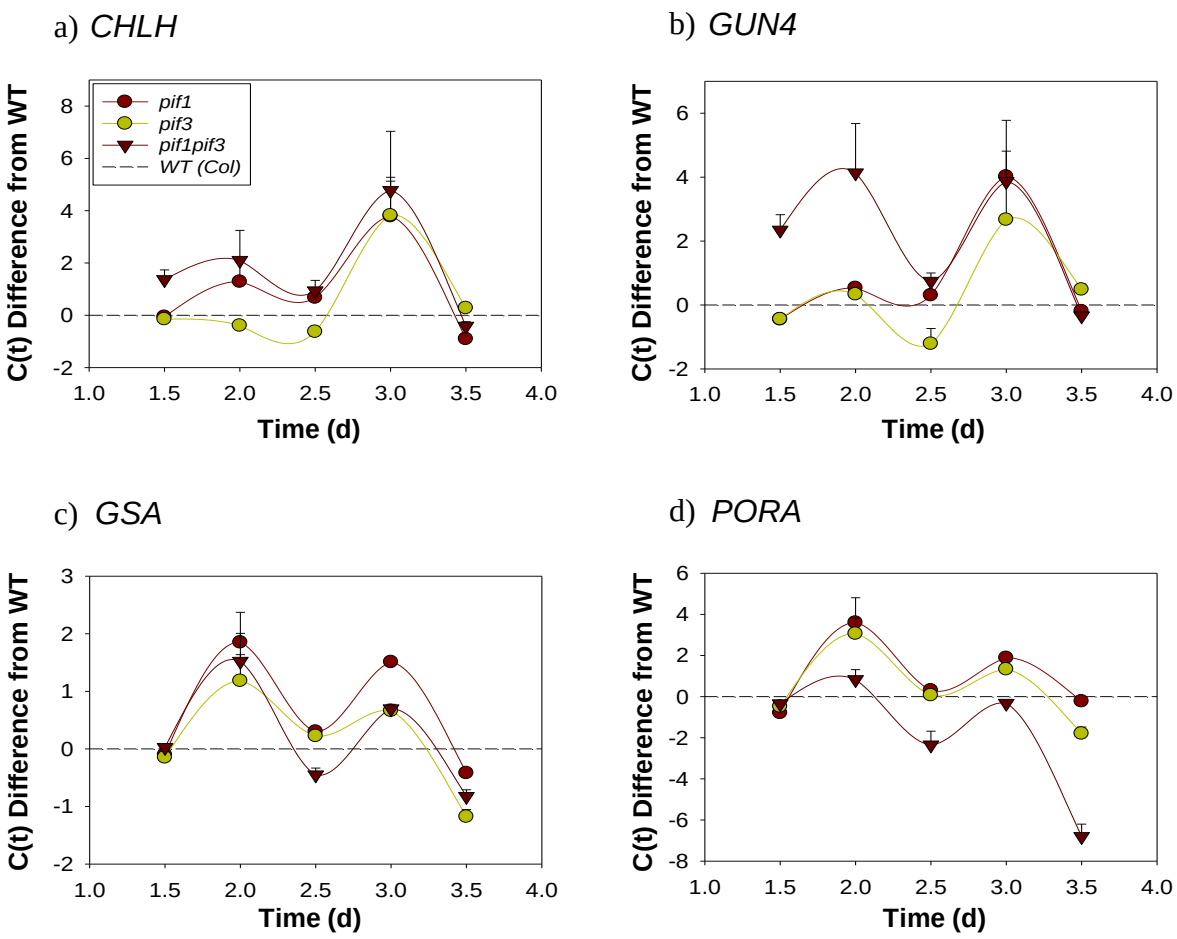

Figure 4.4. Expression of tetrapyrrole synthesis genes in the *pif* mutants following up to 3.5d of dark treatment. a) *CHLH*, b) *GUN4*, c) *GSA*, d) *PORA*. All data is presented as fold difference from WT. Values are mean ± SE of ≥3 independent experiments.

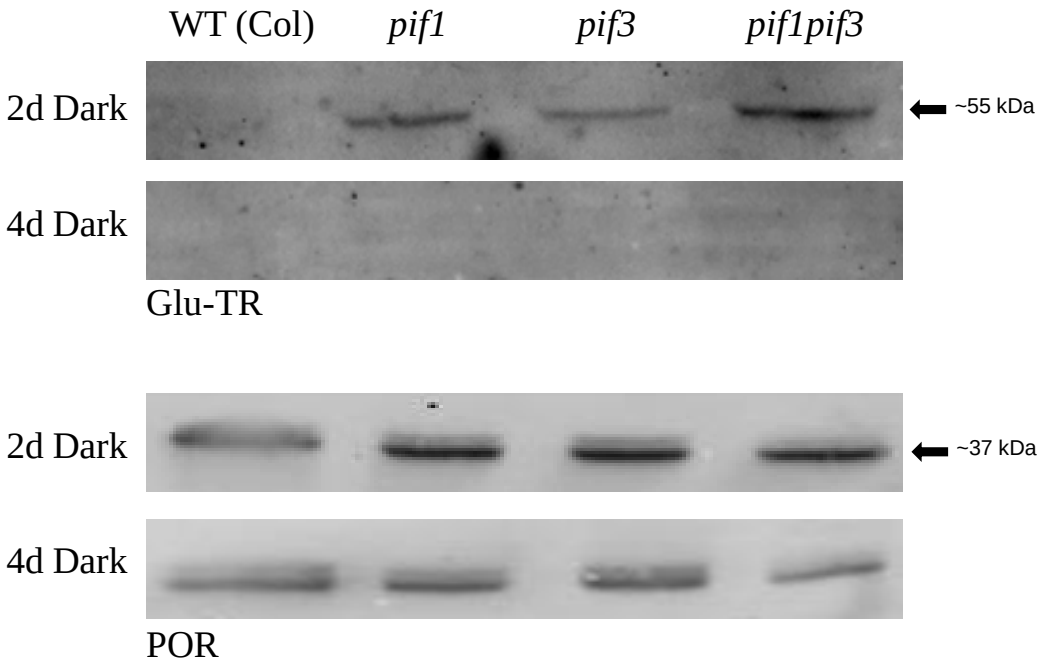

Figure 4.5. Expression of tetrapyrrole the synthesis proteins Glu-TR and POR in the *pif* mutants, compared to WT, following 2 or 4d dark treatment. One of two repeat experiments, with similar results, is shown.

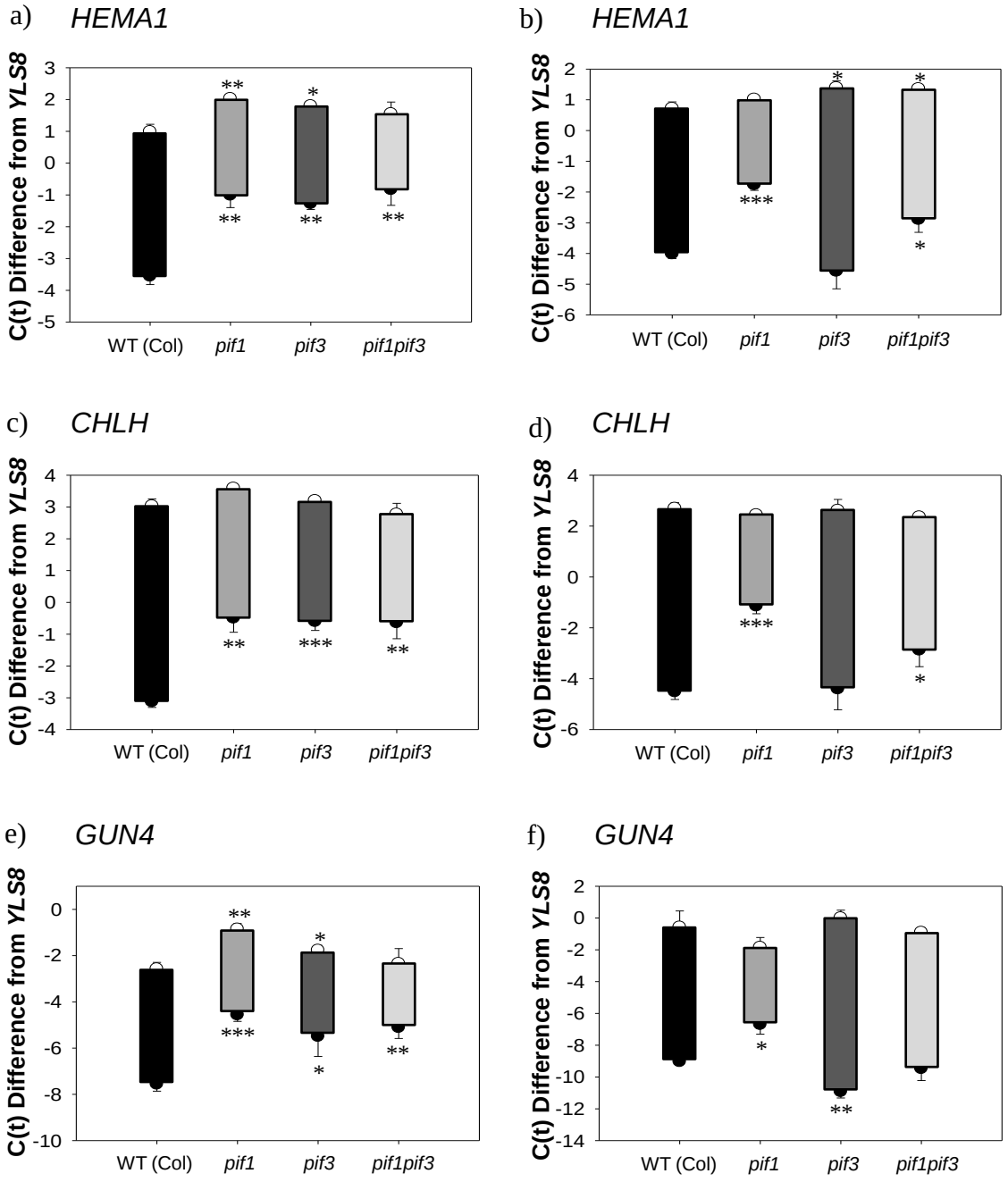

Figure 4.6. Light induction of *HEMA1* (a and b), *CHLH* (c and d) or *GUN4* (e and f) in the *pif* mutants, compared to WT; data presented as C(t) difference from *YLS8*. a), c) and e) 3d dark compared to 2d dark and 24h Wc light (110 µmol m^{-2} s^{-1}). b), d) and f) 5d dark compared to 4d dark and 24h Wc light (110 µmol m^{-2} s^{-1}). Black circles = dark treatments, white circles = light treatments. * = P = <0.05, ** = P = <0.01, *** = P = <0.005. Values are mean ± SE of ≥3 independent experiments.

4.2.2 The impact of the *pif* mutants on the chlorophyll branch of the tetrapyrrole pathway

HEMA1 is a key regulator of the tetrapyrrole pathway and changes in the expression of the *HEMA1* gene, and more importantly the Glu-TR enzyme, are known to closely correlate with tetrapyrrole synthesis (see section 1.2 for more detailed discussion). As mutations in the *pif* genes result in an upregulation of *HEMA1* and Glu-TR, protochlorophyllide (Pchlide) accumulation was studied in both the *pif1-2* and *pif3-3* mutants (figure 4.7a) and the new *pif* mutants (figure 4.7b), over the initial 5d of dark growth following germination.

In both alleles of *pif* mutants there is an increase in Pchlide accumulation compared to WT during dark treatment, and this response is additive in the *pif1pif3* double mutant, which shows the strongest accumulation of any lines.. Also, while the WT does not show a significant rise in Pchlide content between 3 and 5d, the *pif* mutants continue to accumulate pigment through the treatment, although the rate is fastest between 2 and 3 days. Concordantly, this partially correlates with Glu-TR levels, which are higher in the *pif* mutants following 2d dark treatment, but are not detectable after 4d (figure 4.5a). However, POR protein levels, which have been shown previously to increase in parallel with Pchlide (Griffiths, 1978; Apel *et al*., 1980; Ryberg and Sundqvist, 1982; Sundqvist and Dahlin, 1997), are lower in the *pif1pif3* mutant than WT after 4d dark treatment (figure 4.5b), although this does relate to *PORA* expression (figure 4.4d). Interestingly though, POR protein expression has been shown to be uncoupled from Pchlide accumulation during the far-red block of greening response (McCormac and Terry, 2002b).

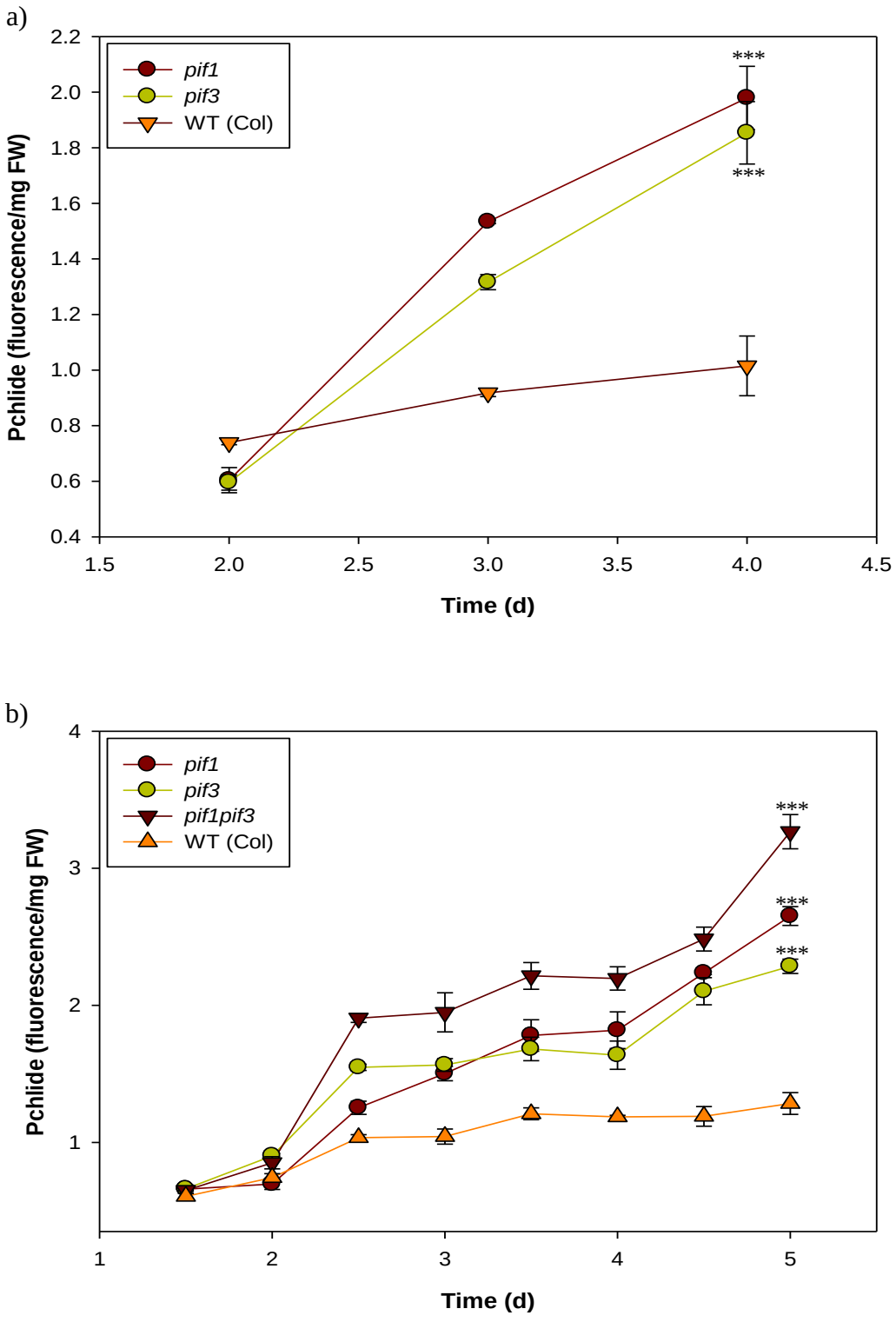

Figure 4.7. Protochlorophyllide accumulation in the *pif* mutants. a) Protochlorophyllide content of the *pif1-2* and *pif3-3* mutants, compared to WT, following up to 4d dark treatment, b) protochlorophyllide content of the *pif1-101*, *pif3-1* and *pif1pif3* double mutants, compared to WT, following up to 5 days dark treatment. Red circles = *pif1*, green circles = *pif3*, inverted red triangles = *pif1pif3*, orange triangles = WT. *** = P = <0.005. Values are mean ± SE of 4 independent experiments.

Upon transfer to light the POR enzyme becomes activated and allows the formation of Chlide (chlorophyllide) and essentially chlorophyll. Therefore, an increase in Pchlide content in the dark might be expected to relate to an increase in chlorophyll synthesis in the light. However, exposure of Pchlide to light also results in the formation of damaging reactive oxygen species, too many of which leads to a cell death signal, demonstrated well by the far-red block of greening response and the *flu* mutant (see sections 1.3.4 and 1.5.1 for a more detailed discussion). Concordantly, chlorophyll accumulation was measured in the *pif* mutants following different periods of dark pre-treatment (figures 4.8a-e) and different intensities of light (figure 4.8f), to asses their greening potential.

Following 2d dark pre-treatment and subsequent light treatment, the *pif* mutants are more able to accumulate chlorophyll than WT, and this response is strongest in the *pif1pif3* double mutant. However, following 3 or 4d dark pre-treatment the *pif* mutants (excluding *pif1* after 3d) accumulate less chlorophyll than WT, consistent with previous data for *pif1* (Huq *et al*., 2004). Additionally, the reduction in chlorophyll content in partially relieved if the light intensity is reduced, and enhanced if the light intensity is increased. Under all treatments, the effect of the *pif1pif3* double mutation is more dramatic than either of the single mutants. Taken together, this data strongly suggests that the PIF1 and PIF3 proteins act together to negatively regulate chlorophyll synthesis.

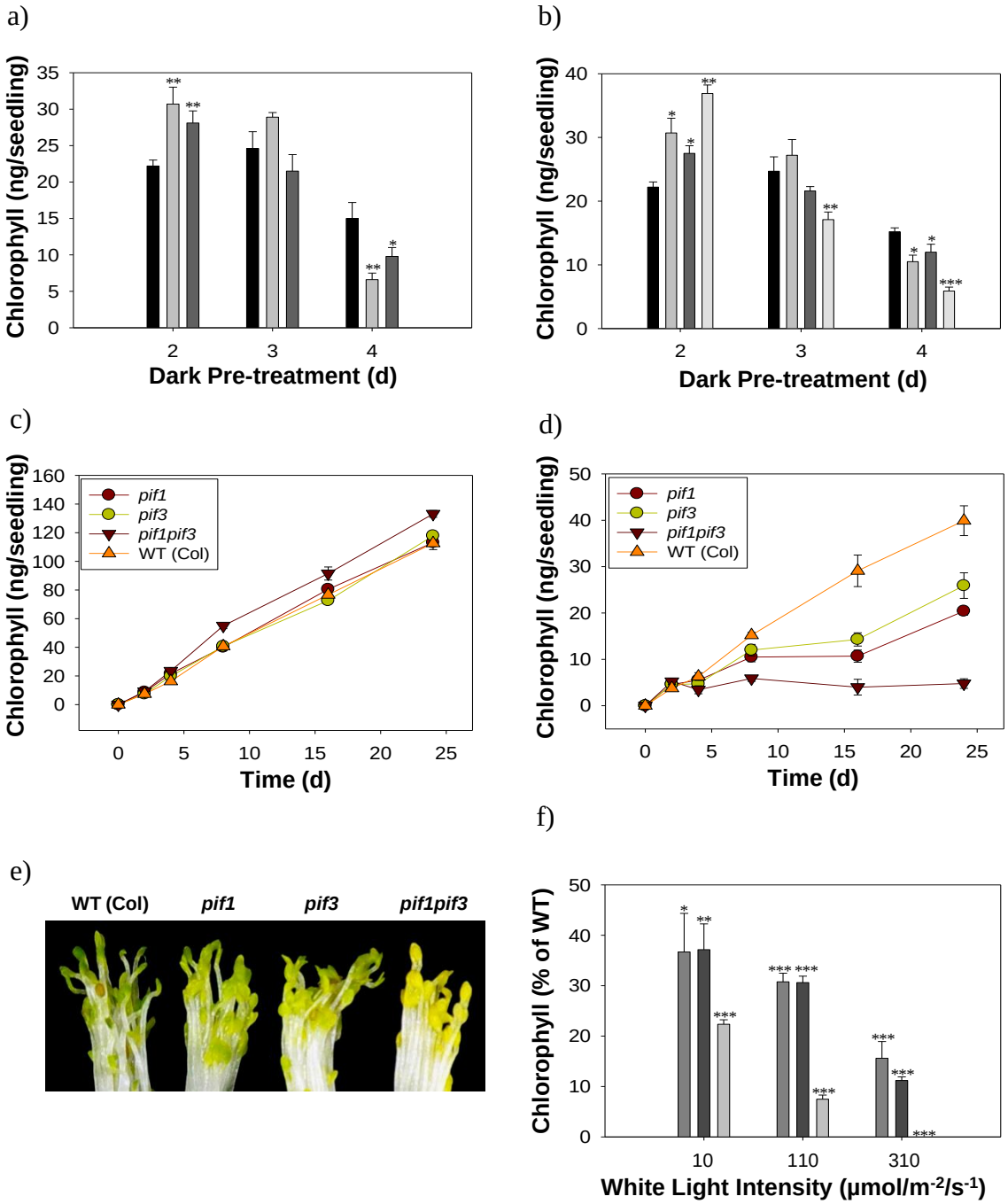

Figure 4.8. Chlorophyll accumulation in the *pif* mutants. a) Chlorophyll content of the *pif1-2* and *pif-3* mutants, compared to WT, following different periods of dark pre-treatment and 8h Wc, b) chlorophyll content of the *pif1-101*, *pif3-1* and *pif1pif3* double mutants, compared to WT, following different periods of dark pre-treatment and 8h Wc, c) chlorophyll content of the *pif1-101*, *pif3-1* and *pif1pif3* double mutants, compared to WT, following 2d dark pre-treatment and up to 24h Wc, d) chlorophyll content of the *pif1-101*, *pif3-1* and *pif1pif3* double mutants, compared to WT, following 4d dark and up to 24h Wc, e) phenotype of the *pif1-101*, *pif3-1* and *pif1pif3* double mutants, compared to WT, following 4d dark pre-treatment and 24h Wc, f) chlorophyll content of the *pif1-101*, *pif3-1* and *pif1pif3* double mutants following 4d dark pre-treatment and 24h Wc at different intensities; data is presented as percent of WT. All data is presented as ng chlorophyll per seedling unless otherwise stated. All Wc treatments were at 110 µmol m^{-2} s^{-1} unless otherwise stated. * = P = <0.05, ** = P = <0.01, *** = P = <0.005. Values are mean ± SE of 4 independent experiments.

4.2.3 The role of *PIF1* and *PIF3* in regulating de-etiolation

In the dark COP1 is required for the degradation of positive regulators of photomorphogenesis via ubiquitylation and subsequent targeting by the 26S proteasome. Upon light exposure COP1 is excluded from the nucleus, thereby allowing photomorphogenesis to proceed (von Arnim and Deng, 1994; Seo *et al*., 2003; Yi and Deng, 2005). Previously, PIF1 and PIF3 have been shown to be rapidly degraded following light exposure (Bauer *et al*., 2004; Al-Sady *et al*., 2006; Shen *et al*., 2005; Shen *et al*., 2008), and this is controlled by COP1 (Bauer *et al*., 2004; Shen *et al*., 2005). Together with the fact that PIF1 and PIF3 act to negatively regulate chlorophyll synthesis in the dark, this could suggest that these genes function as general positive regulators of seedling etiolation in the dark. To test this hypothesis the *pif* mutant phenotype was studied in the dark.

In the dark the *pif* mutants have a consistently shorter hypocotyl length compared to WT (figure 4.9a) and this response is stronger in the *pif1pif3* double mutant than either of the single mutants, yet they are shown here to germinate at similar times to the WT (figure 4.10). To test whether this response might be due to residual Pfr resulting from the 2h W treatment normally used to induce germination, *pif* mutant hypocotyls were also measured in the absence of this treatment (4.9b). The *pif* mutants again displayed a shorter hypocotyl, which therefore suggests a partial constitutive photomorphogenic phenotype. This hypothesis is also supported by the open cotyledon phenotype of dark grown *pif* mutants (figure 4.11), which is similar to that seen in the *cop1* mutant phenotype in the dark (Deng and Quail, 1992).

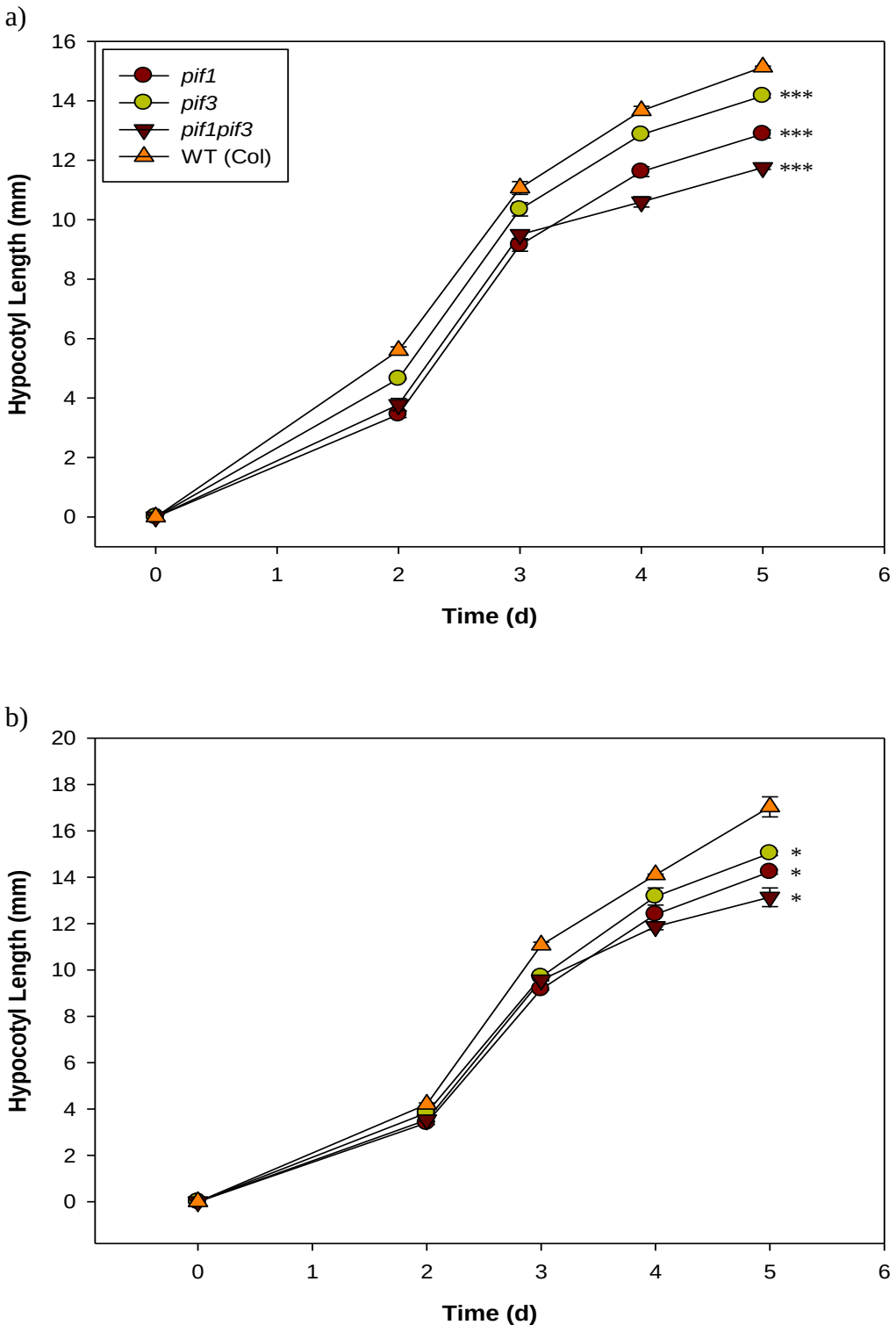

Figure 4.9. Hypocotyl lengths of the *pif* mutants, compared to WT, following up to 5 days dark treatment with light pre-treatment (a), or up to 5d dark treatment without light pre-treatment (b). * = P = <0.05, *** = P = <0.005. Values are mean ± SE of 3 independent experiments.

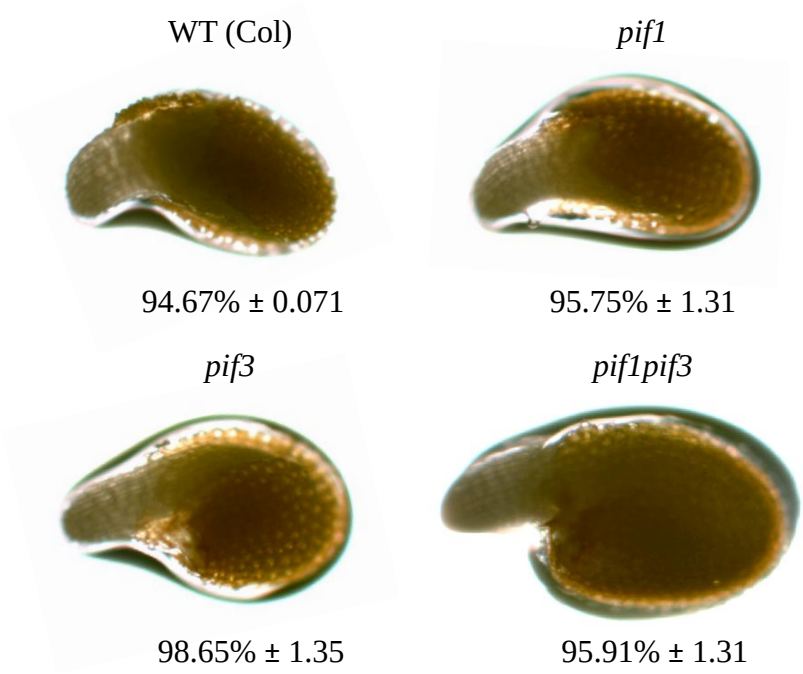

Figure 4.10. Seedling phenotype of the *pif* mutants, compared to WT, following 1 day dark treatment. Percentage of germinated seeds is indicated below each genotype. All photos are to scale and representative of the population.

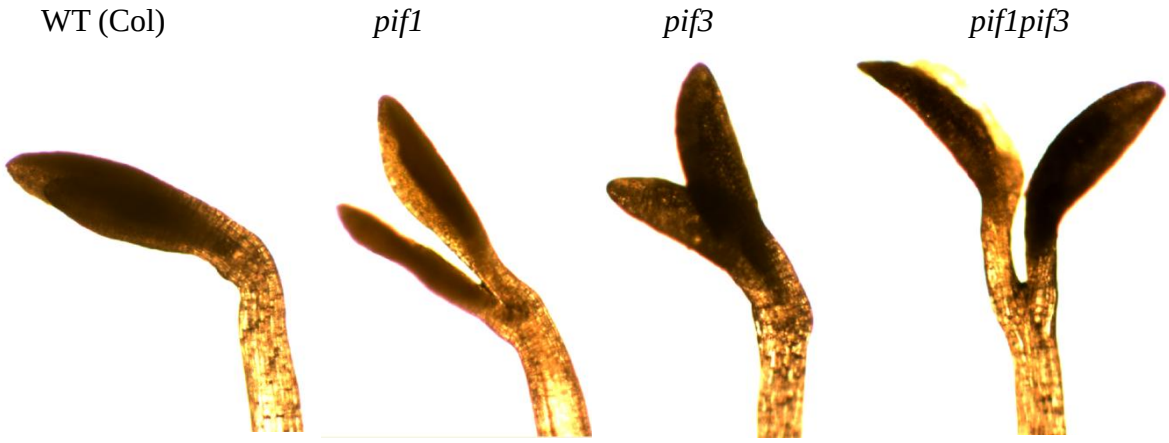

Figure 4.11. Cotyledon opening in the *pif* mutants, compared to WT, following 4 days dark treatment. All photos are to scale and representative of the population.

In the dark the *cop1* mutant has also been shown to produce chloroplast-like structures in place of etioplasts, as a further sign of constitutive photomorphogenesis. In the current study, etioplasts of the *pif* mutants were studied following 4d dark treatment to see if a similar phenotype was present (figure 4.12). In the WT seedlings (figure 4.12a) there is a clear formation of a prolamellar body (PLB) and a small accumulation of prothylakoid membrane, which is typical of seedlings at this age. In the *pif1* and *pif3* single mutants (figures 4.12b and 4.12c, respectively), on the other hand, membrane formation is considerably more advanced, suggesting a semi-constitutive photomorphogenic phenotype. In the *pif1pif3* double mutant, although there was a range of developmental stages (figures 4.12d and 4.12e), approximately 1/3 of etioplasts contained no PLB and membranes had begun to form more chloroplast-like structures.

Previously in this study, the *pif* mutants have been shown to bleach following prolonged dark treatment followed by Wc exposure (figure 4.8), and this was attributed to an increase in protochlorophyllide accumulation in the dark (figure 4.7). To help confirm this hypothesis, chloroplast structure was examined in the *pif* mutants following 2 or 4d dark pre-treatment and 24h Wc (figure 4.13 and figure 4.14, respectively).

When seedlings received only 2d dark pre-treatment, chloroplast formation in the *pif* mutants was similar to the WT control. However, there is some evidence to suggest more advanced development in the *pif* mutants. Firstly, approximately 25% of WT plastids contained a less defined region which resembles the etioplastic PLB (figure 4.13a), while the remaining 75% appeared relatively mature (figure 4.13b). Secondly, thylakoid stacking appeared marginally more developed in the *pif* mutants, and particularly *pif1* and the *pif1pif3* double mutants (figures 4.13c and 4.13e, respectively). However, importantly, the *pif3* mutant is clearly no less developed than the WT control (figure 4.13d), suggesting that PIF3 is not required to positively control chloroplast development.

a) WT (Col)

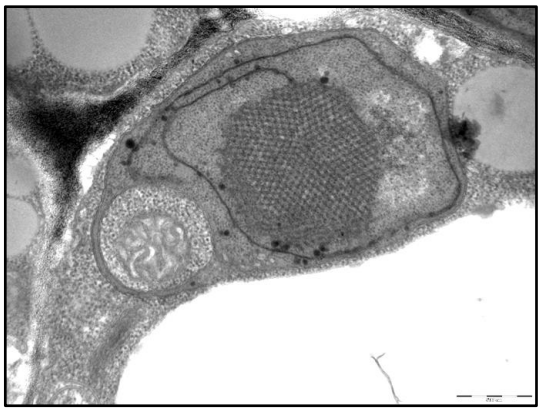

b) *pif1*

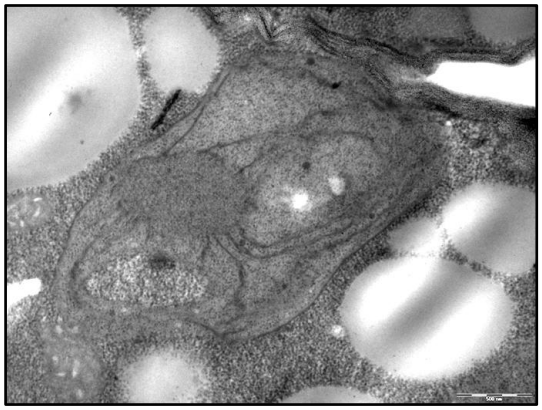

c) *pif3*

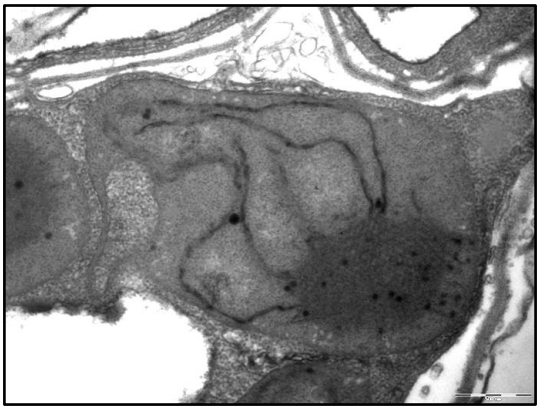

d) *pif1pif3*

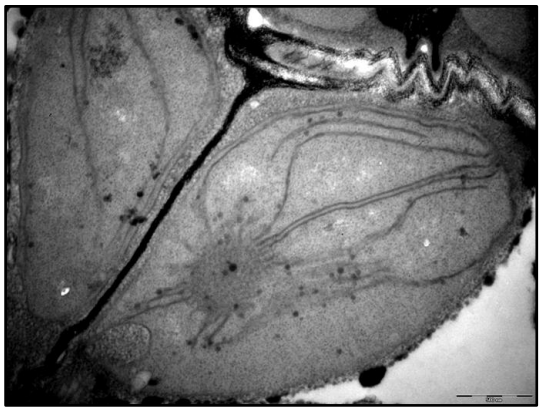

e) *pif1pif3*

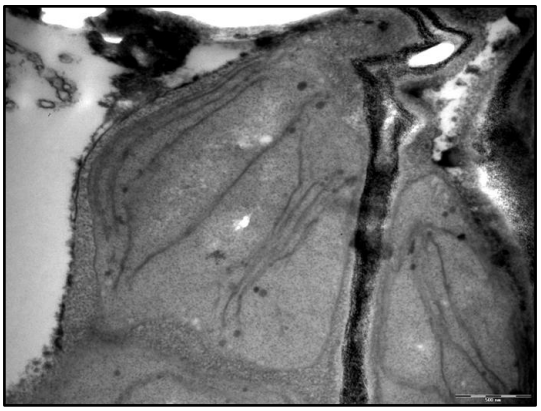

Figure 4.12. Etioplast development in the *pif* mutants following 4d dark treatment. a) WT, b) *pif1*, c) *pif3*, d) and e) *pif1pif3*. Photographs are representative of the total plastid population determined through study of 4 sections from 2 independent biological replicates.

a) WT (Col)

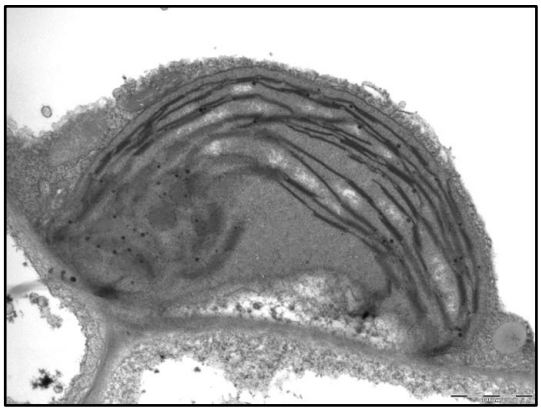

b) WT (Col)

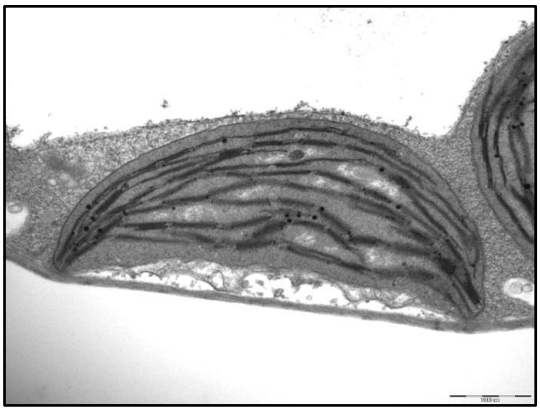

c) *pif1*

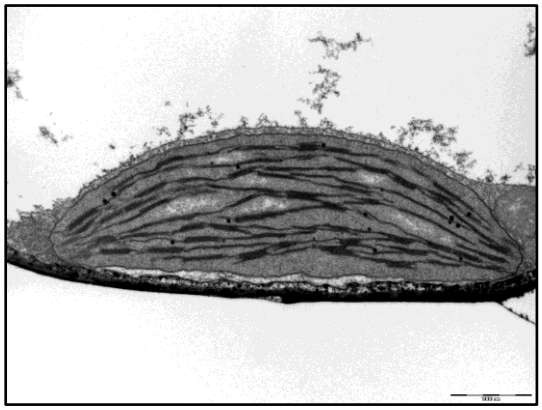

d) *pif3*

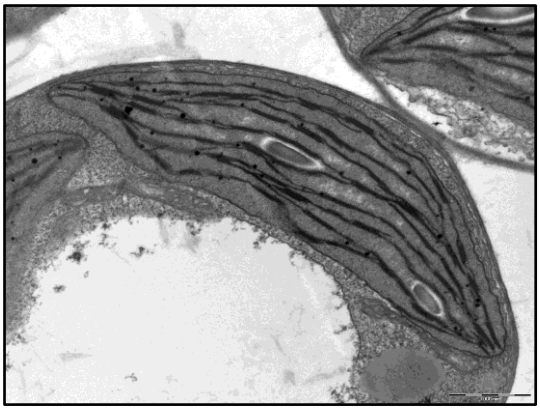

e) *pif1pif3*

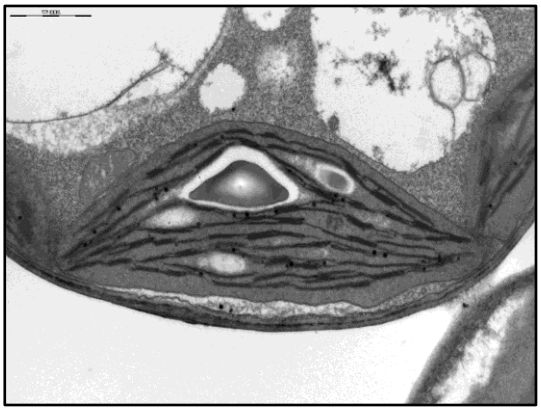

Figure 4.13. Chloroplast development in the *pif* mutants following 2d dark pretreatment and 24h Wc. a) and b) WT, c) *pif1*, d) *pif3*, e) *pif1pif3*. Photographs are representative of the total plastid population determined through study of 4 sections from 2 independent biological replicates.

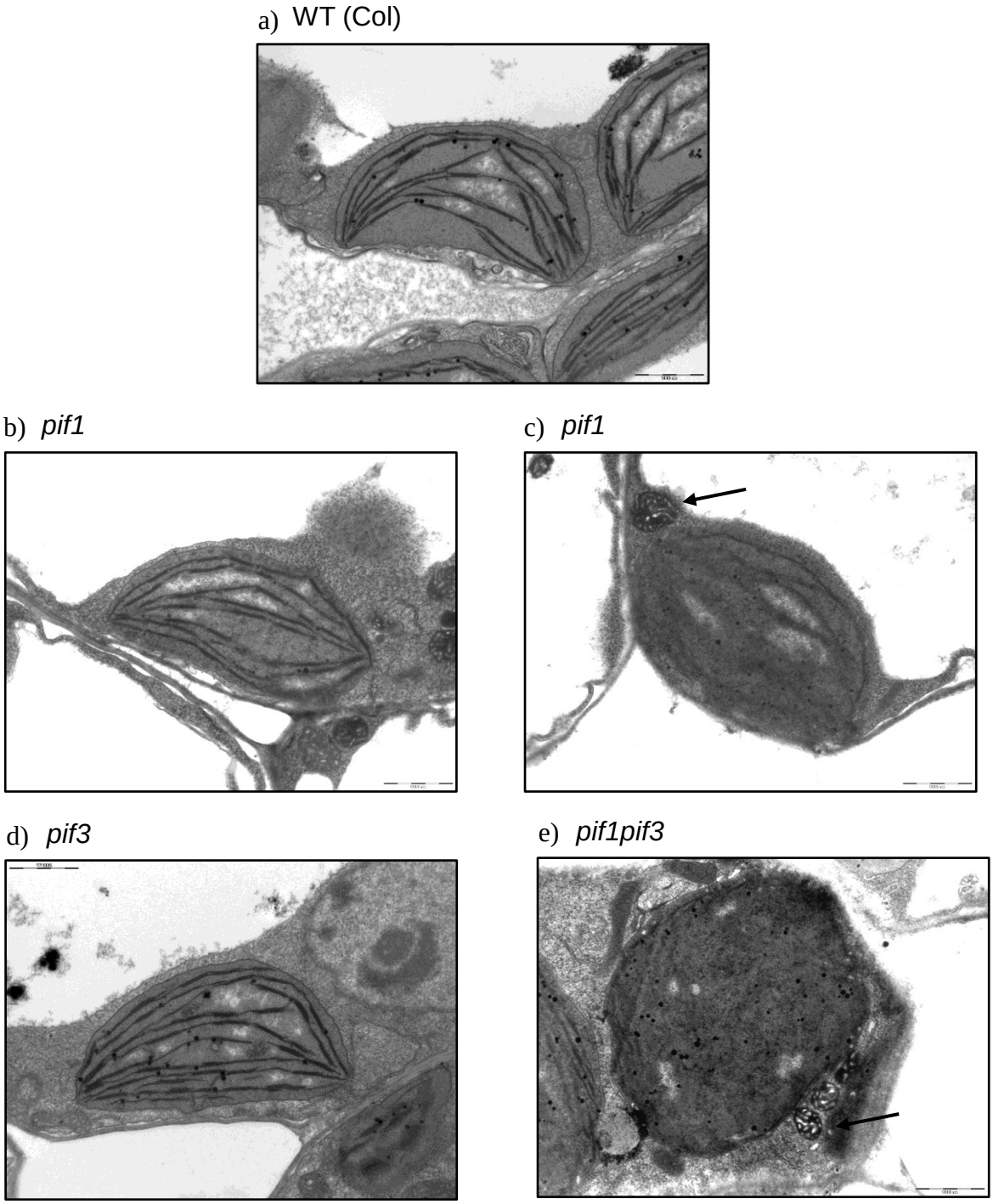

Figure 4.14. Chloroplast development in the *pif* mutants following 4d dark pretreatment and 24h Wc. a) WT, b) and c) *pif1*, d) *pif3*, e) *pif1pif3*. Arrow = mitochondria. Photographs are representative of the total plastid population determined through study of 4 sections from 2 independent biological replicates.

Following 4d dark pre-treatment, the WT control presented relatively well developed chloroplasts (figure 4.14a), although the membranes were less uniform than 2d dark pre-treated plastids. In the *pif1* mutant, on the other hand, only approximately 50% of plastids displayed a similar phenotype to the WT (figure 4.14b). The remaining 50% displayed undefined thylakoid membranes and a general fuzzy appearance (figure 4.14c), which is attributed here to photo-damage of the plastid. Interestingly, other organelles within the cell still display clear structure, such as the mitochondrion indicated with an arrow. The *pif1pif3* double mutant also presents these undefined plastids (figure 4.14e), although they account for >75% of the total within the samples studied. Finally, the *pif3* mutants did not display a high percentage of photo-damaged plastids, although they were still sparsely present. Instead the plastids appeared better developed than the WT, indicating that *PIF3* is not required as a positive regulator of chloroplast development.

Finally, the *pif1pif3* double mutant is shown to enhance the previously reported hypocotyl hypersensitive response of both the *pif1* and *pif3* single mutants to R and FR light (figure 4.15; Kim *et al*., 2003; Oh *et al*., 2004). This suggests that the *PIF* genes also act as negative regulators of photomorphogenesis in the light.

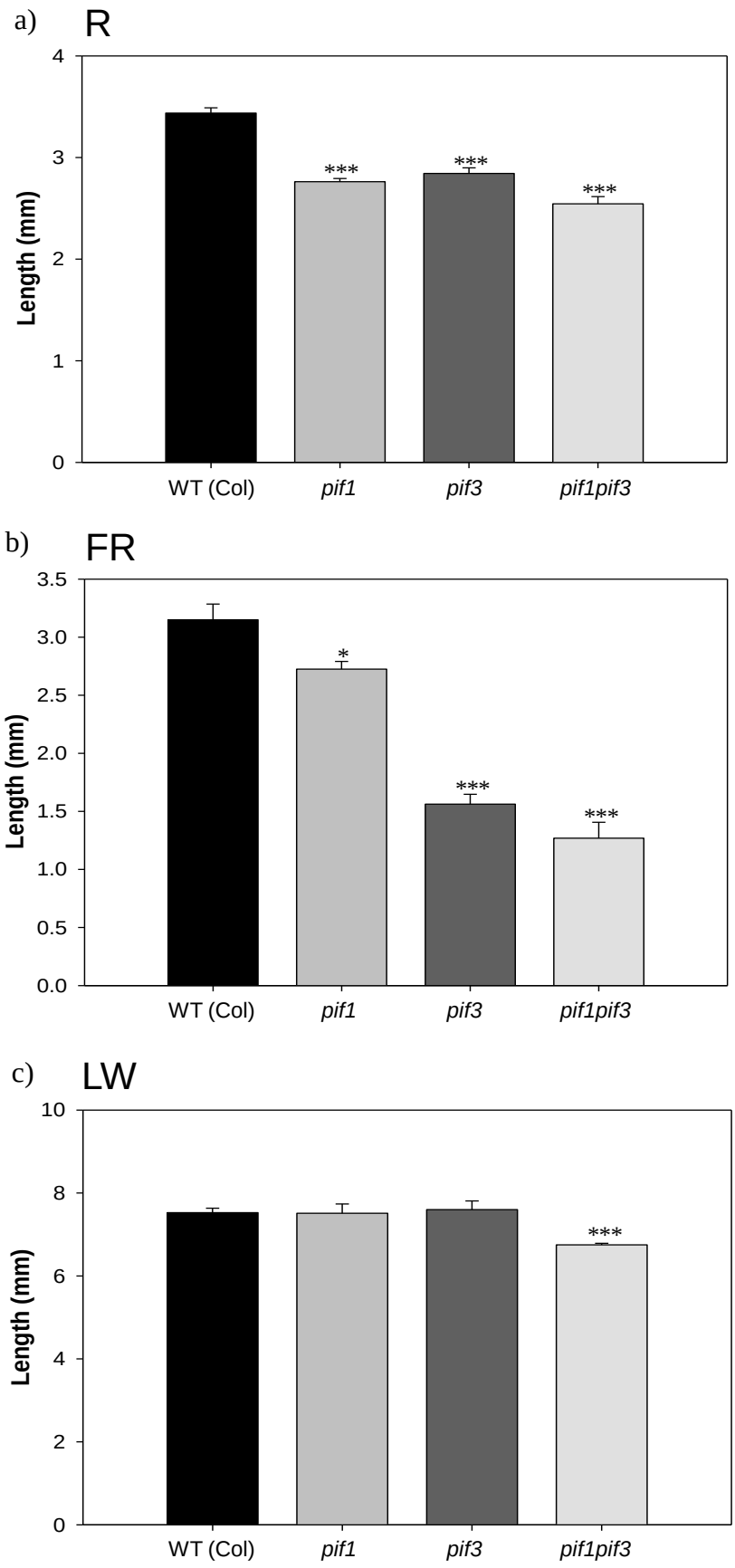

Figure 4.15. Hypocotyl lengths of the *pif* mutants, compared to WT, following 1 day dark pre-treatment and 5 days red (80 µmol m^{-2} s^{-1}), (a), far-red (10 µmol m^{-2} s^{-1}) (b) or low Wc (15 µmol m^{-2} s^{-1}) (c). * = P = <0.05, *** = P = <0.005. Values are mean ± SE of 3 independent experiments.

4.3 Discussion

4.3.1 PIF3 is a negative regulator of chloroplast development

Previously the *pif3* mutant had been described as showing inhibition of chloroplast development (Monte *et al*., 2004) and the hypothesis that PIF3 acts positively early in signal transduction (and negatively in the longer term) is still current (Monte *et al*., 2007; Al-sady *et al*., 2008). However, the data presented here are consistent with PIF3 functioning as a repressor of chloroplast development in the dark. Pchlide synthesis was higher in *pif3* than WT seedlings (figure 4.7) and initial rates of chlorophyll synthesis were also greater (figure 4.8). *pif3* seedlings also showed more advanced development of etioplasts and chloroplasts (figure 4.12, 4.13 and 4.14). In these respects the *pif3* mutant behaved identically to the *pif1* mutant, which has previously been identified as a negative regulator of chloroplast development (Huq *et al*., 2004), and the *pif1pif3* double mutant showed an additive phenotype. Many of the conclusions from the previously reported loss of induction of chloroplast genes in *pif3* (Monte *et al*., 2004; Al-Sady *et al*., 2008) may be explained using the data presented here, and the observations that overexpression of PIF3 is not sufficient for induction of phytochrome-regulated genes and that DNA-binding of PIF3 in the dark is required for chloroplast development (Al-Sady *et al*., 2008) are also consistent with a role for PIF3 as a repressor. Additionally, the phytochrome-interacting PIF proteins have generally been shown to be acting as repressors not activators of photomorphogenic responses (Bae and Choi, 2008; Duek and Fankhauser, 2005; Leivar *et al*., 2008) and the current results are therefore consistent with a common molecular mechanism for this class of signalling protein. The reason for the previous misinterpretation of the *pif3* mutant phenotype is that seedlings transferred to WL after 4d dark showed a reduced level of chlorophyll compared to WT (figure 4.8). This response, which is identical for *pif1* and exaggerated in a *pif1pif3* double mutant, is most likely due to photo-oxidative destruction of chlorophyll. The results presented here are consistent with this explanation as the loss of chlorophyll is dependent on the length of the dark period prior to transfer (and therefore the degree of excess Pchlide production), the fluence rate of WL and the time of WL exposure (figure 4.8). Misregulation of the tetrapyrrole synthesis pathway commonly leads to a photobleaching phenotype (e.g. Meskauskiene *et al*., 2001) and over accumulation of

Pchlide is well established as leading to photo-oxidative damage (Meskauskiene *et al*., 2001), for example in the FR block of greening response (McCormac and Terry, 2002b).

4.3.3 PIF1 and PIF3 repress the expression of key chlorophyll synthesis genes

The rate limiting step for Pchlide (and chlorophyll) synthesis is the enzyme glutamyl tRNA reductase (Tanaka and Tanaka, 2007). Light regulation of this step is mediated through changes in expression of the *HEMA1* gene (McCormac and Terry, 2002a) and *HEMA1* is one of a small group of highly regulated tetrapyrrole genes including *CHLH* and *GUN4* (see chapter 3 for a more detailed discussion). The increase in *HEMA1* expression and consequent increase in glutamyl tRNA reductase protein can fully account for the observed increase in Pchlide levels in the *pif1* and *pif3* mutants. It was previously suggested that the increase in tetrapyrrole synthesis in *pif1* was due to a subtle downregulation of the ferrochelatase gene (*FC2*) and an upregulation of the haem oxgenase *HO3* resulting in less free haem and less inhibition of glutamyl tRNA reductase activity (Moon *et al*., 2008). These genes were not directly studied here, however, as *HO3* has exceptionally low expression in seedlings, and its loss has no impact on chromophore synthesis in the presence of HO1 (Emborg *et al*., 2006), it is unlikely that changes in *HO3* and *FC2* make more than a minor contribution to tetrapyrrole synthesis compared to the substantial increase in levels of the rate-limiting enzyme of the pathway. One reason that previous studies did not observe the changes seen here is that microarrays using dark-gown *pif1* (Moon *et al*., 2008) and *pif3* (Monte *et al*., 2004) and their follow-up analyses were all performed using seedlings that had been grown for 4d in the dark. As is clear from our current studies (figure 4.1 and 4.2) differences between WT and the *pif* mutants are minor at this time.

4.3.4 PIF1 and PIF3 may function in the output from the circadian clock

The data presented here shows that the *pif1* and *pif3* mutations affect circadian regulation of *HEMA1*, *CHLH* and *GUN4. HEMA1* and *CHLH* have previously been shown to be circadian regulated in the light (Matsumoto *et al*., 2004), but this is the first demonstration of circadian regulation for *GUN4.* The altered clock regulation of

HEMA1 was not due to a major defect in the circadian clock as the *pif* mutants did not have a strong effect on the expression of the core clock components *CCA1*, *LHY* and *TOC1* (figure 4.3). Interestingly, CAX1, a H^+/Ca^{2+} antiporter unrelated to chloroplast function (Hirschi *et al*., 1996) which has previously been shown to be circadian regulated (Harmer *et al*., 2000), was also unaffected, suggesting that PIF1 and PIF3 function specifically in circadian control of genes involved in chloroplast development. A circadian clock has previously been shown to be functional in dark-grown *Arabidopsis* seedlings, with entrainment initiated through changes in temperature or imbibition (Salomé *et al*., 2008), and can be observed just 2d after imbibition (Salomé *et al*., 2008) or even earlier (Kato *et al*., 2007). Analysis of multiple circadian microarray experiments suggests that *PIF1*, but not *PIF3*, expression is under circadian control (Covington *et al*., 2008). However, a low amplitude circadian rhythm has also been observed previously for *PIF3* using a *PIF3:LUC+* reporter construct (Viczián *et al*., 2005). In the data presented here *PIF1* and *PIF3* showed a robust circadian regulation in dark-grown seedlings suggesting that clock regulation of PIF function is via circadian control of expression. Although phytochrome has a major role in the entrainment of the circadian clock by light (Fankhauser and Staiger, 2002) it has previously been shown PIF3 does not play a significant role in controlling light input or function of the clock (Monte *et al*., 2004; Oda *et al*., 2004; Viczián *et al*., 2005). Although we cannot completely rule out a role in entrainment, the apparent specificity of the response for chloroplast development genes suggests otherwise.

It is therefore suggested that the PIF proteins might fuction as part of the output from the clock. In the current study the *PIF* genes appear to cycle in the same circadian phase as *HEMA1* (figure 4.2 and 4.3), which is evidence against a simple mechanism of circadian regulated *PIF* repression of *HEMA1* expression. However, the resolution of the qPCR data presented here might not permit the detection of a subtle difference in circadian phase, and does not show protein synthesis and half-life differences between PIF and tetrapyrrole-synthesis proteins, and thus this model might still be possible. Alternatively, phenotypes of the clock mutants and overexpressing lines are very similar to those displayed in plants with aberrant *PIF* expression. It is therefore also feasible that the interaction between TOC1 and the PIF proteins is key in regulating de-etiolation (figure 4.16). As the phenotype of the *toc1* mutant is

consistently opposite to that displayed for either the *pif1* or *pif3* mutants, it is possible that *TOC1* is required to sequester the PIF proteins in the dark. This is also supported through the observation of the same phenotype in *CCA1* overexpressing seedlings, and the opposing phenotype in *toc1* mutant seedlings. The reason for this mechanism of *PIF* regulation is not immediately clear, as *TOC1* expression is highest in the dark which is the time when the *PIF* proteins are required for activity. However, during the dark period *PIF3* expression and activity is at its highest, and the *TOC1* method of regulation is proposed to limit activity to a) allow haem synthesis for energy production, and b) prevent excessive hypocotyl elongation and energy expenditure. Then, following light transfer, when *TOC1* expression is inhibited by *CCA1/LHY*, phytochrome has been shown to cause a mobility shift in PIF3, which results in phosphorylation-mediated degradation (Al-sady *et al*., 2006). Similarly, PIF1 degradation in the light was shown to be mediated by direct interaction with phytochrome (Shen *et al*., 2008). Therefore, the light regulation of *PIF* gene expression, circadian regulated TOC1 control of PIF protein activity, and *COP1* degradation of PIF proteins could give a precise system for controlling de-etiolation.

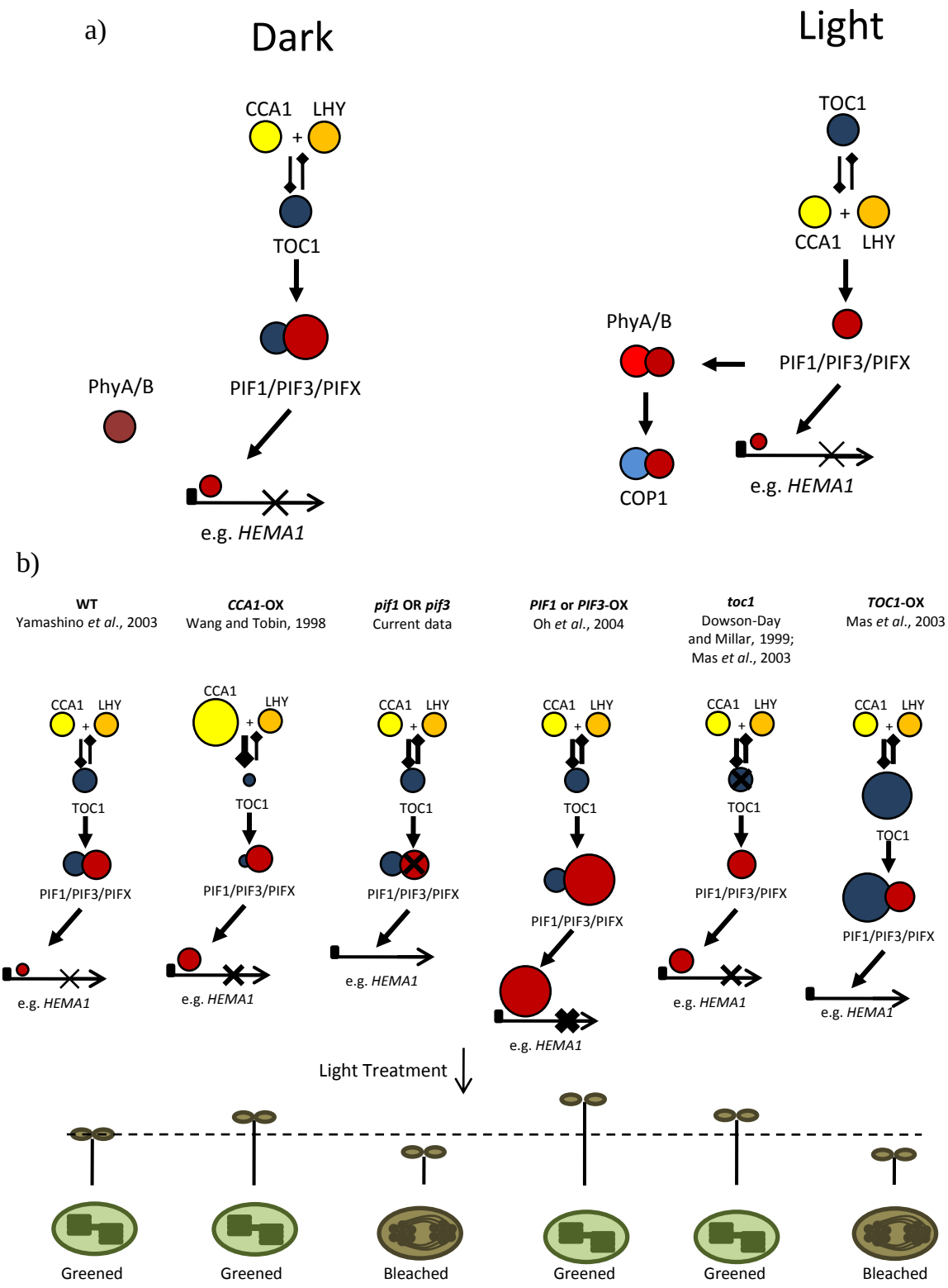

Figure 4.16. Model for *TOC1* control of *PIF* activity. a) *TOC1* acts in the dark to suppress the activity of the PIFs, which are highly expressed. In the light, *TOC1* expression is suppressed by CCA1 and LHY, which allows PIF activity. However, the light induced degradation of PIF is now mediated by the phytochrome family. b) Alterations in expression of *CCA1*, *PIF1/3* and *TOC1*, and the resulting phenotypes, may be explained through the model outlined in a). Hypocotyl data is based upon extended periods of red or far-red light treatment, and chloroplast formation is based upon transfer into white light following >3d dark treatment. Size of protein symbols indicates relative abundance.

4.3.2 The *pif1pif3* double shows a constitutively photomorphogenic phenotype

One interesting phenotype observed here for the *pif1pif3* double mutant was that it showed a moderate constitutive photomorphogenic response in dark-grown seedlings (figure 4.11 and 4.12). Both *pif1* and *pif3* single mutants showed a similar, but less pronounced response (figure 4.11) and this response was seen even when seeds were kept in complete darkness post imbibition (data not shown). A shorter hypocotyl in the dark has been seen previously for *pif3* (Kim *et al*., 2003; Oh *et al*., 2004) and *pif1* (Shen *et al*., 2005) and a similar phenotype with expanded cotyledons, hook opening and hypocotyl inhibition was recently observed for *pif1*, *pif3* and a *pif1pif3* double mutant (Leivar *et al*., 2008). In this case the authors reported a synergistic interaction between PIF1 and PIF3 in contrast to the additive phenotype reported here. A constitutive photomorphogenic phenotype of the *pif1pif3* double mutant is expected based on the stronger, dominant negative phenotype of overexpressed truncated PIF1 (Shen *et al*., 2008). Presumably, in this case the PIF1 protein is interfering with the function of additional PIFs including PIF4 and PIF5 (Leivar *et al*., 2008). Interestingly, constitutive activation of phytochromes in the dark also results in this phenotype, which could result from Pfr-mediated degradation of multiple PIFs (Su and Lagarius, 2007). However, it remains to be seen whether the *pif1pif3* double mutant still requires the presence of seed Pfr (produced during seed set) to reveal the response.

In conclusion, the data presented here clearly show that PIF1 and PIF3 both function as negative regulators of chloroplast development. This appears to be part of the circadian regulation of this response, although further study is required to understand the exact mechanism.

Chapter 5: Identifying Regulators of Tetrapyrrole Biosynthesis

5.1. Introduction

The tetrapyrrole pathway, which is responsible for the synthesis of at least four essential compounds in higher plants, is under intense regulatory pressure. Additionally, many of the intermediates in the pathway are potentially phototoxic. Therefore regulation is required for three main reasons: to control unnecessary synthesis of output compounds, thereby reducing energy consumption; to manage intermediate synthesis and prevent photo-damage; and to ensure that tetrapyrrole synthesis is not the rate limiting step in later essential processes.

Previously the pathway has been shown to be regulated by photoreceptors, such as the phytochromes and cryptochromes (McCormac *et al*., 2001; chapter 3), transcription factors, such as the phytochrome-interacting factors (Oh *et al*., 2004; chapter 4), direct regulation of enzymes through energy requirements (summarised in Cornah *et al*., 2002), and through direct interaction with external proteins, such as FLU and GUN4 (Meskauskiene *et al*., 2001; Mochuzuki *et al*., 2001; Meskauskiene and Apel, 2002; Larkin *et al*., 2003; chapter 3).

The aim of the current study is firstly to increase the understanding of known mechanisms of regulation of the pathway. This will be achieved through mutant and over-expression studies of the *GUN4* and *FLU* genes, where analysis will focus on accumulation of intermediate and terminal compounds, and study into the role of ABA in regulating the pathway. Secondly, this study aims to identify novel regulators of the pathway, including investigation into the possible role of the MYB50 and MYB61 transcription factors (discussed in chapter 3) in regulating chlorophyll synthesis. Additionally, the *Arabidopsis OHP1* and *OHP2* genes, homologs of which were shown to positively affect chlorophyll biosynthesis in *Synechocystis* (Xu *et al*., 2002), will be assessed in their ability to regulate the tetrapyrrole pathway.

5.1.1 GUN4

The *HEMA1* gene, which acts at the start of the tetrapyrrole pathway in the first commited step, was shown to be induced by phytochrome and cryptochrome signalling in response to light perception (McCormac *et al*., 2001). Since then it has been demonstrated that *HEMA1*, and the Glu-TR protein, are also controlled by the plastid signal, haem feedback, the FLU protein, and sugar and hormone signals (see section 1.2. for a more detailed discussion), consequently this has been highlighted as a key regulatory site in the pathway (McCormac and Terry, 2002a; McCormac and Terry, 2004).

As the *HEMA1* gene is located early in the pathway and is required for regulation of the whole pathway, it is likely that at least one other key regulatory gene is present at the chelatase branchpoint in the pathway. Previously (see chapter 3), it has been demonstrated that both *GUN4* and *CHLH*, in a similar manner to *HEMA1* (McCormac *et al*., 2001; McCormac and Terry, 2002a), are highly light regulated, while the *CHLD*, *CHLI1*, *CHLI2*, *FC1* and *FC2* genes are relatively not regulated by light. Additionally, using published microarray data it was also shown that, while the genes encoding the Mg-chelatase subunits are similarly regulated by a range of stimuli and mutations, *GUN4* is uniquely regulated under many conditions (Zimmerman *et al*., 2005). This suggests that *GUN4* might be a key site for regulation at the branchpoint in the tetrapyrrole pathway.

In this study plants overexpressing the *GUN4* gene were produced and studied alongside the *gun4-1* mutant to determine their ability to de-etiolate effectively to further understand how this gene is required for regulation of the tetrapyrrole pathway.

5.1.2 FLU

In a mutant screen, conducted by Meskauskiene *et al*. (2001), plants were selected for their inability to restrict the accumulation of Pchlide in the dark and consequently died when grown under light/dark cycles as a result of ROS over-production. This phenotype was linked to a mutation in the *FLU* (*FLUORESCENT UNDER BLUE LIGHT*) gene (figure 5.9) which results in increased activity of Glu-

TR, to which the *FLU* protein binds (Meskauskiene and Apel, 2002). This input into the regulation of *HEMA1*/Glu-TR was shown to be independent to that of either light or haem regulation following further studies. Firstly, although *FLU* mRNA is shown to fluctuate between etiolated and light-grown seedlings (Goslings *et al*., 2004), *FLU* protein levels remain constant; and secondly, the *flu* mutant can partially rescue the inhibition of ALA synthesis found in the *hy1* mutant (Goslings *et al*., 2004). However, it is unknown why or when the *FLU* gene is required to regulate Glu-TR, and what impact an over-production of FLU may have. In an aim to answer this question *FLU* over-expressing plants were produced and analysed for their ability to accumulate Pchlide and chlorophyll, and regulate hypocotyl extension.

5.1.3 ABA

Originally named abscissin or dormin for its role in abscission and dormancy, ABA has since been highlighted has having a major role in drought tolerance, as well as sex determination (Mohan Ram and Juiswal, 1972), pollination (Kovaleva and Zakharova, 2003), senescence (Hunter *et al*., 2004), inhibition of ethylene synthesis (Sharp and LeNoble, 2002) and interplay with JA signalling (Andersson *et al*., 2004). Additionally, recently a number of links between the ABA signalling and the tetrapyrrole pathway have been reported, however, the exact mechanisms of control have yet to be elucidated. Firstly (and as discussed in section 1.2.8.), CHLH was identified as an ABA receptor (Shen *et al*., 2006) capable of signalling distinct ABA responses from those of FCA, the other known ABA receptor (Razem *et al*., 2004; Razem *et al*., 2006). However, as CHLH binds ABA independently of Proto IX, it is possible that its role ABA signal perception might be distinct from that of chlorophyll synthesis (Shen *et al*., 2006).

Secondly, ABI4 has been shown to be involved in the GUN1 and GUN2-5 chloroplast-to-nucleus signalling pathways, and is able to bind the CACC motif in the *Lhcb* promoter, which is considerably over-represented in the GUN1 and GUN2-5 signalling targets (Koussevitzky *et al*., 2007). Again, however, this function appears to be independent of the role of ABI4 in ABA signalling, as the *aba1* mutant, which is mutated in the gene encoding zeaxanthin epoxidase, shows a WT signalling response

when grown on lincomycin.

Two cases of disrupted tetrapyrrole synthesis, as a result of aberrations in the carotenoid/ABA synthesis pathway, have also been reported. The *aba1* mutant has been shown to be affected its ability to accumulate chlorophyll (Pogson *et al*., 1998), and shows a partially de-etiolated phenotype when grown in the dark (Barrero *et al*., 2008). Additionally, *SPC1*/*ZDS*, the gene encoding a *z-CAROTENE DESATURASE*, which is essential for carotenoid biosynthesis, is reported to be involved in chloroplast development, photoprotection and retrograde signalling (Dong *et al*., 2007). In all cases, however, the authors concluded that the deleterious effects on the tetrapyrrole pathway caused by these mutations is a result of the lack of carotenoids and/or disruption of the plastid signal, rather than the lack of ABA.

Using the Genevestigator™ program (Zimmerman *et al*., 2005), it was demonstrated here that mutations in the *aba1* and *abi1* genes result in a down-regulation in *GUN4* expression (section 3.18a). This finding was particularly interesting as, according to the microarray data, these mutations had little or no effect on the expression of other tetrapyrrole synthesis genes. The *ABA1* gene is known to code for the zeaxanthin epoxidase enzyme, which is required for the epoxidation of zeaxanthin to violaxanthin via antheraxanthin (Rock and Zeevaart, 1991). The *aba1* mutant is therefore deficient in xanthophylls that appear later in the synthesis pathway, as well as ABA. *ABI1* and *ABI2* encode members of the 2C class of protein serine/threonine phosphatases (PP2C), and are negative regulators of ABA signalling (Gosti *et al*., 1999). Consequently, the *abi1* and *abi2* mutations markedly reduce ABA responsiveness in both seeds and vegetative tissues, although they control both distinct and overlapping responses (Yoshida *et al*., 2006). *ABI3* encodes a B3 domain transcription factor (Giraudat *et al*., 1992) and is expressed mainly in seeds and meristematic tissue with a low level of expression in vegetative tissue (Finkelstein *et al*., 2002). *ABI4* encodes an APETALA2 domain transcription factor (Finkelstein *et al*., 1998) and *ABI5* encodes a bZIP domain transcription factor (Finkelstein and Lynch, 2000). *ABI4* and *ABI5* are expressed most abundantly in developing seeds, but both also have low levels of vegetative expression (Finkelstein *et al*., 1998; Finkelstein and Lynch, 2000). Although *ABI3*, *ABI4* and *ABI5* were all identified as negative regulators of seed germination in the ABA signalling pathway, they are infact positive

regulators of ABA signalling, and mutants therefore exhibit a hyposensitive ABA response.

5.1.4 MYB50 and MYB61

Using the Genevestigator™ program (Zimmerman *et al*., 2005) to identify mutations that affected *GUN4* expression, the *MYB50* and *MYB61* genes were identified as potential regulators of the tetrapyrrole pathway (section 3.2.2.). *MYB50* and *MYB61* are members of a super-family of transcription factors required for the regulation of almost all processes within organisms from every kingdom. In plants, MYBs have been particularly associated with hormone signalling (Chen *et al*., 2006), and recently with control of *CAB* expression (Churin *et al*., 2003). All members share the conserved MYB DNA-binding domain which generally comprises up to three imperfect repeats, each forming a helix-turn-helix structure of about 53 amino acids (reviewed in Stracke *et al*., 2001).

Interestingly, *MYB50* and *MYB61*, which are the only MYB mutants present in the Genevestigator™ database, group together in a phylogenetic tree of 138 other MYBs (figure 3.19). However, according to Genevestigator™, mutations in *MYB50* cause an up-regulation of *GUN4* expression and mutations in *MYB61* cause a down-regulation of *GUN4* expression (figure 3.18a).

5.1.5 OHP1 and OHP2

In green algae and higher plants light capture is achieved, in part, by antenna complexes consisting of three-helix light harvesting chlorophyll *a*/*b* binding proteins (LHC), chlorophylls *a* and *b*, and carotenoids. In cyanobacteria and red algae, however, a water-soluble light-harvesting complex, known as the phycobilisome, is present, where phycobilins are covelently bound to the antenna polypeptides (Grossman *et al*., 1995). Although no direct LHC homologues were detected in cyanobacteria, Dolganov *et al*. (1995) discovered a single helix, high light inducible protein (hliA), which later was identified as being part of a five-member family of single helix, small CAB-like proteins (ScpA-E), and the prime candidates for LHC

homologues (Funk and Vermaas, 1999). Interestingly, however, these Scps show a higher similarity to relatives of LHCs in *Arabidopsis*, including the family of *EARLY LIGHT-INDUCED PROTEINS* (*ELIP*s; Adamska, 1997, 2001; Montane and Kloppstech, 2000), the *PsbS* protein of PSII (Funk, 2001), stress-enhanced proteins (*SEP*s) (Heddad and Adamska, 2000), *LIL3* and *LIL3-like* genes of unknown function, and the *ONE HELIX PROTEIN* (*OHP1*; Jansson *et al*., 2000). These genes (excluding *PsbS*) are now collectively known as *LIL* (Light-Inducible-Like).

In the cyanobacterium *Synechosystis* the five Scps have been studied in some detail and their roles have been somewhat elucidated. Firstly, ScpA was shown to associate with the tetrapyrrole synthesis enzyme ferrochelatase (Jansson, 1999), and is required for its function. As yet, no similar partnership has been discovered in *Arabidopsis*, although a one helix domain is present at the C-terminal end of ferrochelatase II (Chow *et al*., 1998). ScpB and ScpE have both been shown to positively affect chlorophyll biosynthesis through alterations in Glu-TR activity (Xu *et al*., 2002), where it was hypothesised that when chlorophyll was lacking a build up of Scps would occur and result in a feedback to Glu-TR. Finally, ScpC and ScpD have been shown to associate with photosystem II (PSII) when damage occurs, and are thought to act as a temporary pigment resevoir (Promnares *et al*., 2006; Yao *et al*., 2007).

Interestingly, the *ELIP2* protein in *Arabidopsis* was recently shown to regulate the tetrapyrrole biosynthesis pathway through regulation of the activity of both Glu-TR and Mg-Chelatase (Tzvetkova-Chevolleau *et al*., 2007), suggesting that ELIP2 could be orthologous to ScpB and/or ScpE, and Tzvetkova-Chevolleau *et al.* (2007) concluded that this was due to sensing of free chlorophyll. This mechanism would therefore have a twofold benefit: 1) prevent a buildup of free chlorophyll and the resulting oxidative stress, 2) prevent a lack of free chlorophyll, thereby maximising energy capture.

Conversely, very little has been done to investigate the role of *OHP1*, and whether it too may have a role in regulating tetrapyrrole biosynthesis. Current understanding places *OHP1*, and the more recently discovered *OHP2* (Andersson *et al*., 2003), as high light inducible, and expression occurs in a light intensity-dependent

manner (Jansson *et al*., 2000; Andersson *et al*., 2003). Both proteins contain a single helix with most similarity to the first of the three LHC helices (Jansson *et al*., 2000; Andersson *et al*., 2003), and OHP1 contains both chloropyll and helix-helix binding sites (Jansson *et al*., 2000). OHP2 has been shown to localise with photosystem I (PSI) (Andersson *et al*., 2003), suggesting that it has a role in PSI protection in a similar manner to the proposed function of ScpC and ScpD in regards to PSII. The localisation and function of OHP1, on the other hand, has yet to be elucidated.

This study was undertaken to determine whether OHP1 and OHP2 have a role in regulating tetrapyrrole biosynthesis, in a similar manner to ScpB and ScpE, to which they have considerable homology. This was achieved through three means: 1) phylogenetic analysis of the LIL and Scp families to establish the probability that OHP1 and/or OHP2 are orthologous to ScpB or ScpE, 2) analysis of the *ohp1* and *ohp2* mutants to establish whether they have an effect on tetrapyrrole synthesis, and 3) the production of *OHP1* and *OHP2* overexpression lines for the same purpose.

5.2. Results

5.2.1. GUN4 regulation of the tetrapyrrole pathway

5.2.1.1. Chlorophyll accumulation in the *gun4* mutant

Chlorophyll *a*, chlorophyll *b* and total chlorophyll levels were measured in de-etiolating WT and *gun4-1* mutant (figure 5.1) *Arabidopsis thaliana* seedlings following 2d dark and up to 5d (120h) Rc, Bc or Wc (figure 5.2).

Under all light conditions studied there was a reduced rate of chlorophyll synthesis in the *gun4* mutant compared to wild type. Under both Rc and Bc the profiles of chlorophyll accumulation were similar, with *gun4* unable to synthesise any significant levels of chlorophyll in the first 8h. Under Wc chlorophyll hardly accumulated in the first 16h in *gun4*, while it was already present after 4h in wild-type seedlings. After 24h the *gun4* mutant was able to accumulate only 41, 46 and 26% of wild-type chlorophyll levels under Rc, Bc and Wc, respectively. After 120h *gun4* accumulated 58% of WT levels under Rc and Bc, and only 24.5% under Wc.

Following both 24h and 120h of all light treatments the ratio of chlorophyll *a*:chlorophyll *b* was increased in the *gun4* mutant. This increase was most dramatic following 120h Wc with a ratio of 3.22 and 7.65 for WT and *gun4*, respectively.

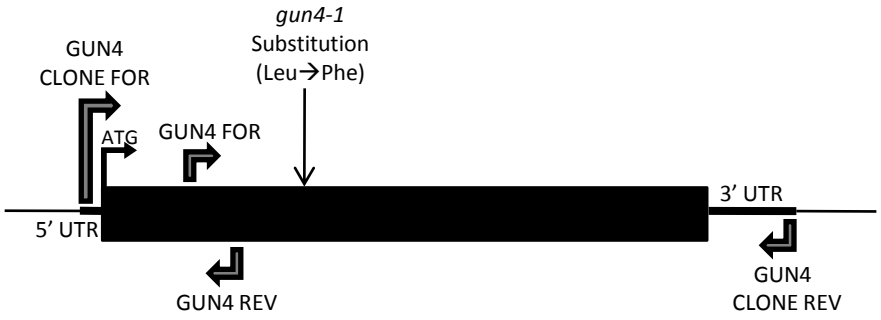

Figure 5.1 Schematic representation of the *GUN4* gene, indicating the polymorphism site resulting in the *gun4-1* mutant and primer positions used for expression and over-expression studies. 1cm = 100bp.

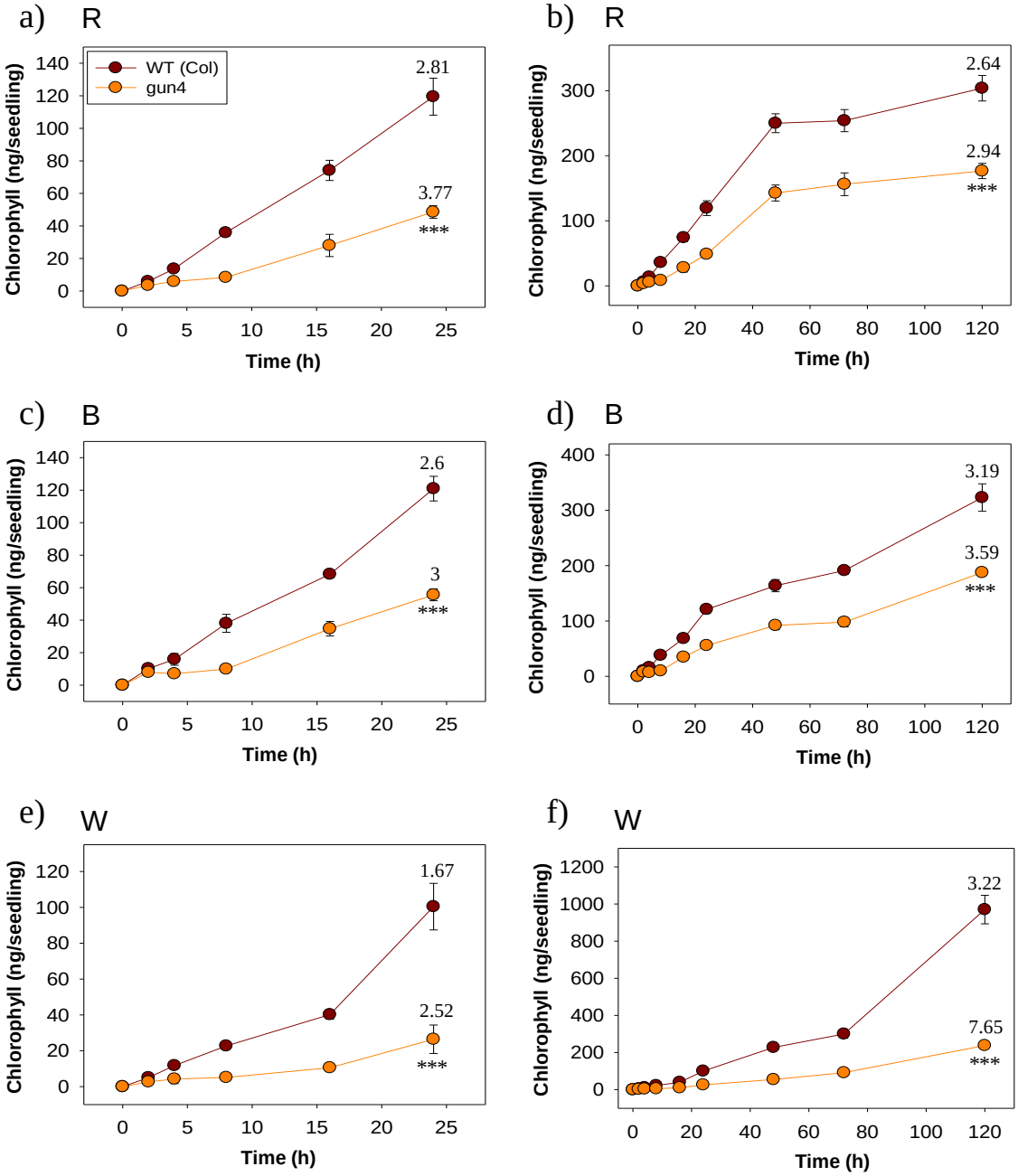

Figure 5.2 Chlorophyll accumulation in *gun4-1* mutant seedlings following red (a and b; 80 µmol m^{-2} s^{-1}), blue (c and d; 20 µmol m^{-2} s^{-1}) or white (e and f; 110 µmol m^{-2} s^{-1}) light treatment. Chlorophyll accumulation was measured over both the initial 24 hours of light treatment (a, c and e), and over an extended 120 hour period (b, d and f). Chlorophyll *a*/*b* ratios are indicated for the final time point in both cases. *** = P = <0.005. Values are mean ± SE of 3 independent experiments.

5.2.1.2. Expression of tetrapyrrole-synthesis genes in the *gun4* mutant

Previously it was shown that low *CHLM* expression resulted in both low MgPMT synthesis and low chlorophyll content (Alawady and Grimm, 2004). However, interestingly, reduced MgPMT activity also correlated with reduced Mg chelatase activity and a low synthesis rate of 5-aminolevulinate, but with enhanced ferrochelatase activity. In contrast, high MgPMT activity led to inverse activity profiles, indicating a direct influence of MgPMT, in combination with Mg chelatase, on the metabolic flux of ALA and the distribution of protoporphyrin into the branched pathway (Alawady and Grimm, 2004). They also showed that the modified enzyme activities in tetrapyrrole biosynthesis in the transgenic plants could be explained by changes of certain corresponding mRNA contents, where increased 5-aminolevulinate synthesis and Mg chelatase activity correlate with enhanced transcript levels of the *HemA*, *Gsa*, and *CHLH* (Alawady and Grimm, 2004).

As *GUN4* acts to enhance Mg-chelatase efficiency, and mutations also result in reduced chlorophyll accumulation, the light-inductive expression of tetrapyrrole synthesis genes was examined in the *gun4* mutant compared to WT using real-time PCR (figure 5.3). Unlike the antisense lines of *CHLM*, the *gun4* mutant has the same expression pattern of *HEMA1, CHLH* and *FC2* as the WT, although this does not rule out the possibility of altered Mg- or Fe-chelatase activity. The expression of *FC1* and *HO1*, on the other hand, was reduced in the *gun4* mutant.

As the *gun4-1* mutation is a result of a base change, *GUN4* is still expressed and retains some activity. However, interestingly, in the *gun4* mutant *GUN4* is no longer induced following 24h Wc treatment, which will further reduce chlorophyll synthesis capacity. Additionally, the expression of *PORA* is more downregulated in the *gun4* mutant, and *CAO* is less upregulated, compared to WT following light treatment, which may account for the differences in chlorophyll *a*/*b* ratios.

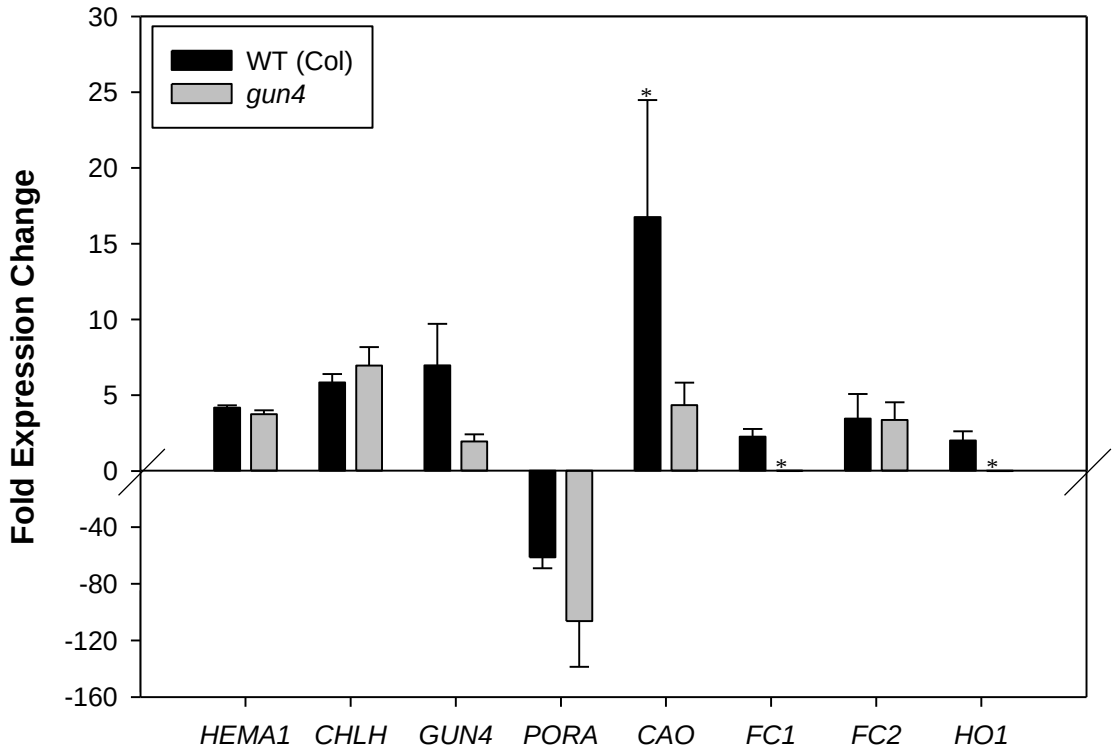

Figure 5.3 Expression change of tetrapyrrole genes in WT and *gun4* mutant seedlings following 3d dark compared to 2d dark and 1d Wc (110 µmol m^{-2} s^{-1}), normalised to *YLS8* using real-time PCR. * = P = <0.05. Values are mean ± SE of 3 independent experiments.

5.2.1.3. *GUN4* overexpression lines

5.2.1.3.1. Production of the *GUN4* overexpression lines

GUN4 overexpression lines were produced using a *GUN4* clone containing the CACCAAAAAAA 5' sequence, required for the Gateway™ (Invitrogen, CA, USA) system, synthesised by reverse transcription from mRNA isololated from *Arabidopsis thaliana* seedlings. This was recombined into a pMDC32 vector containing a double CaMV 35S constitutive promoter for enhanced overexpression and hygromycin resistance gene, which was later sequenced to confirm successful recombination (figure 5.4). These constructs were transformed into 6 WT (denoted WT G4 1-6) and 6 *gun4-1* mutant (denoted *gun4* G4 1-6) mature *Arabidopsis* plants (T0) using the floral dip method, and the resulting offspring screened for successful transformation on selective media containing hygromycin antibiotic. From the surviving stock of seedlings (T1), two transformants for WT seedlings (denoted 1 or 2) and one transformant for *gun4* mutant seedlings (donoted 1) were chosen at random and transferred to soil and self-fertilised. The T2 offspring were then screened on selective media containing hygromycin, and the survival of T2 lines is shown in Table 5.1.

Table 5.1 Survival of T2 *GUN4* overexpressing lines on selective media containing hygromycin antibiotic.

Plant Line	**Died**	**Survived**	**% Survived**	**Predicted Insert Number**
WT G4 1.1	47	206	81.4	1
WT G4 1.2	47	200	81	1
WT G4 2.1	34	172	83.5	1/2
WT G4 2.2	47	210	81.7	1
WT G4 3.1	52	197	79.1	1
WT G4 3.2	44	149	77.2	1
***gun4* G4 2.1**	13	68	84	1/2
***gun4* G4 5.1**	14	86	86	1/2
***gun4* G4 6.1**	26	86	76.8	1
WT	130	0	0	0

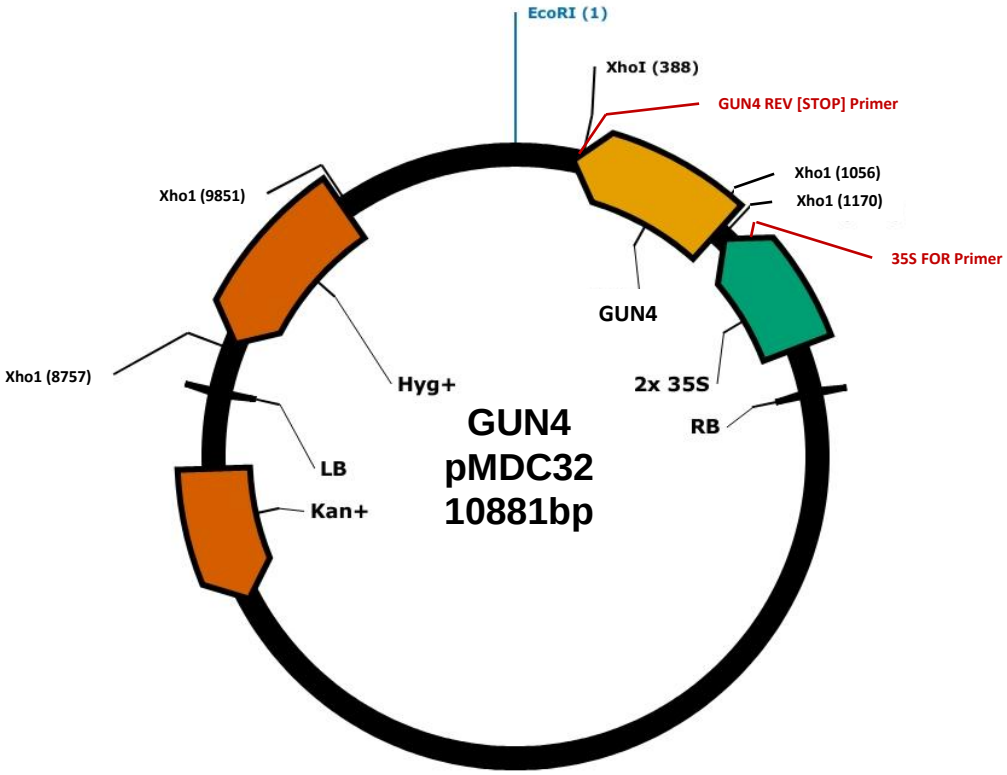

Figure 5.4 GUN4 pMDC32 construct used to produce *GUN4* overexpression lines. Genetic material between the left border (LB) and right border (RB) was transformed into *Arabidopsis* using *Agrobacteria*, where the hygromycin (Hyg+) resistance gene allowed selection of successfully transformed plants and the 2x 35S CaMV promoter inferred overexpression of the *GUN4* gene. The Kanamycin (Kan+) resistance gene, which is not transferred to the plant, allowed selection of successful transformation in *E.coli* and *A.tumefaciens*. Primer and restriction sites, used to confirm successful plasmid recombination during production, are indicated.

Three survivors (denoted 1, 2 or 3) from each selection were transferred to soil and self fertilised. Homozygote plants were determined by selecting for 100% survival of offspring on hygromycin selective media (Table 5.2).

5.2.1.3.2. Confirmation of insert presence and level of overexpression

Seedlings from each of the homozygote lines, along with WT, were grown under Wc for 5d. Insert presence was confirmed by DNA extraction and PCR (figure 5.5a). The overexpressing capacity of the homozygote transformants was then tested initially through RNA extraction and RT-real time PCR using *GUN4* qPCR primers (figure 5.5b). This shows that while the WT G4 2.1.2, WT G4 2.2.3, *gun4* G4 2.1.1 and *gun4* 5.1.2 lines show a clear and substantial increase in expression (49, 66, 21 and 14 fold increase, respectively), the WT G4 1.2.2 and *gun4* G4 6.1.1 lines have only a WT level of expression. Interestingly, however, the mature phenotype of the overexpressing lines (figure 5.6) indicates that the WT G4 1.2.2 and *gun4* G4 6.1.1 lines present a *gun4* mutant phenotype, while the other lines are more similar to WT.

Table 5.2 Survival of T3 *GUN4* overexpressing lines on selective media containing hygromycin antibiotic.

Plant Line	Died	Survived	% Survived	Result
WT G4 1.1.1	7	34	82.9	Het
WT G4 1.1.2	8	36	81.8	Het
WT G4 1.1.3	8	26	76.5	Het
WT G4 1.2.1	9	23	71.9	Het
WT G4 1.2.2	0	33	100	**Hom**
WT G4 1.2.3	8	15	65.2	Het
WT G4 2.1.1	4	24	85.7	Het
WT G4 2.1.2	0	34	100	**Hom**
WT G4 2.1.3	DNG	DNG	-	-
WT G4 2.2.1	9	19	67.9	Het
WT G4 2.2.2	7	22	75.9	Het
WT G4 2.2.3	0	38	100	**Hom**
WT G4 3.2.1	8	31	79.5	Het
WT G4 3.2.2	6	19	76	Het
WT G4 3.2.3	3	13	81.3	Het
***gun4* G4 2.1.1**	0	30	100	**Hom**
***gun4* G4 2.1.2**	5	20	80	Het
***gun4* G4 2.1.3**	5	33	86.8	Het
***gun4* G4 5.1.1**	7	19	73.1	Het
***gun4* G4 5.1.2**	0	38	100	**Hom**
***gun4* G4 5.1.3**	5	24	82.8	Het
***gun4* G4 6.1.1**	0	26	100	**Hom**
***gun4* G4 6.1.2**	7	17	70.8	Het
***gun4* G4 6.1.3**	7	22	75.9	Het
WT	31	0	0	WT

DNG = did not germinate, Het = heterozygous, Hom = homozygous, WT = wild type.

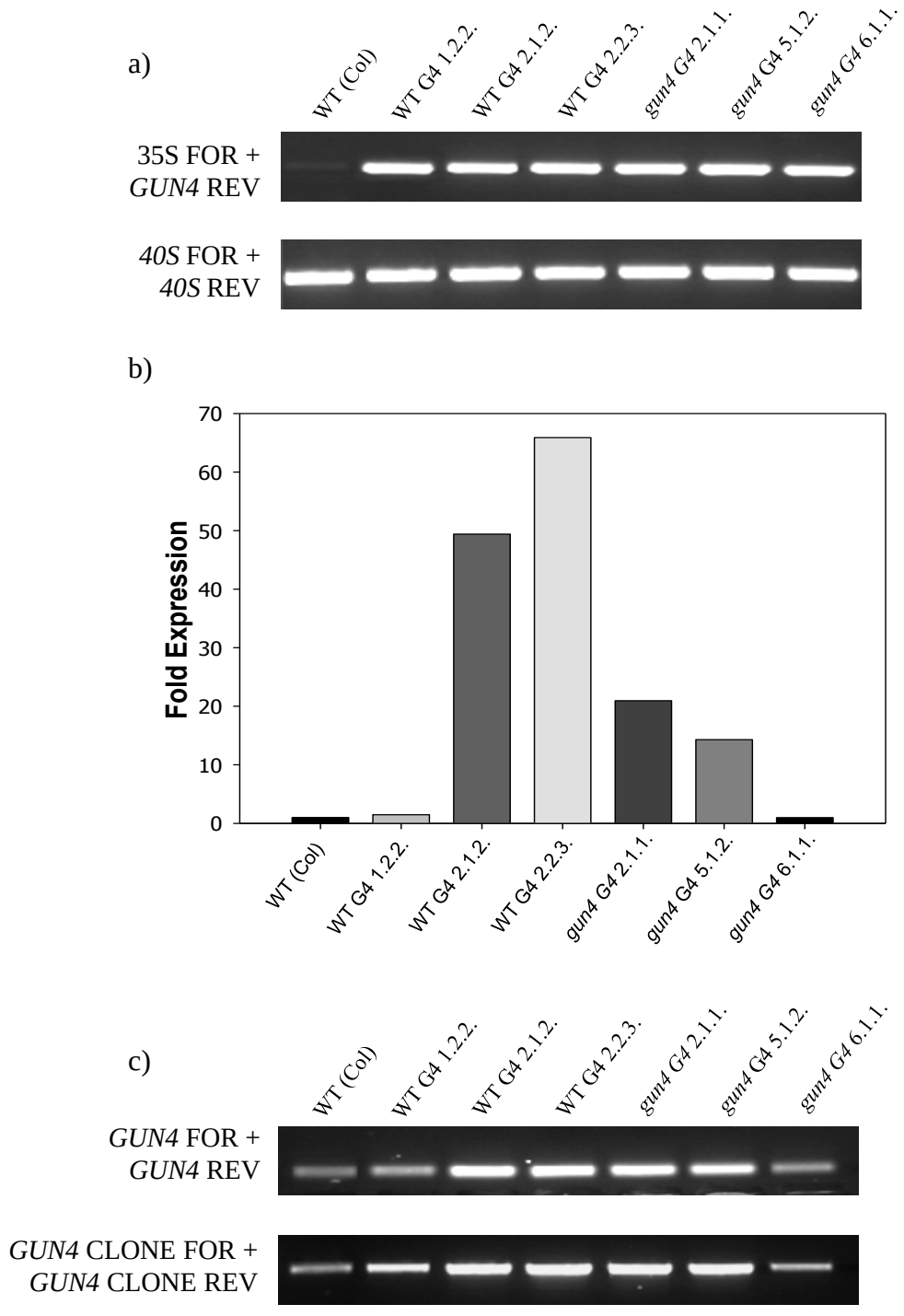

Figure 5.5 Confirmation of the presence of the 35S:*GUN4* constuct in transgenic *Arabidopsis thaliana* plants. a) gPCR reaction confirming the presense of the *GUN4* over expressing construct in 6 transgenic lines, and the absence of the construct in a WT plant. b) Expression of *GUN4* in transgenic plants compared to WT determined using real-time PCR , following 2d dark and 24h Wc (110 µmol m^{-2} s^{-1}). c) Expression of a small region of the *GUN4* gene (upper gel) and the full length *GUN4* gene (lower gel) in transgenic plants compared to WT using traditional RT-PCR, following 2d dark and 24h Wc (110 µmol m^{-2} s^{-1}). n = 1.

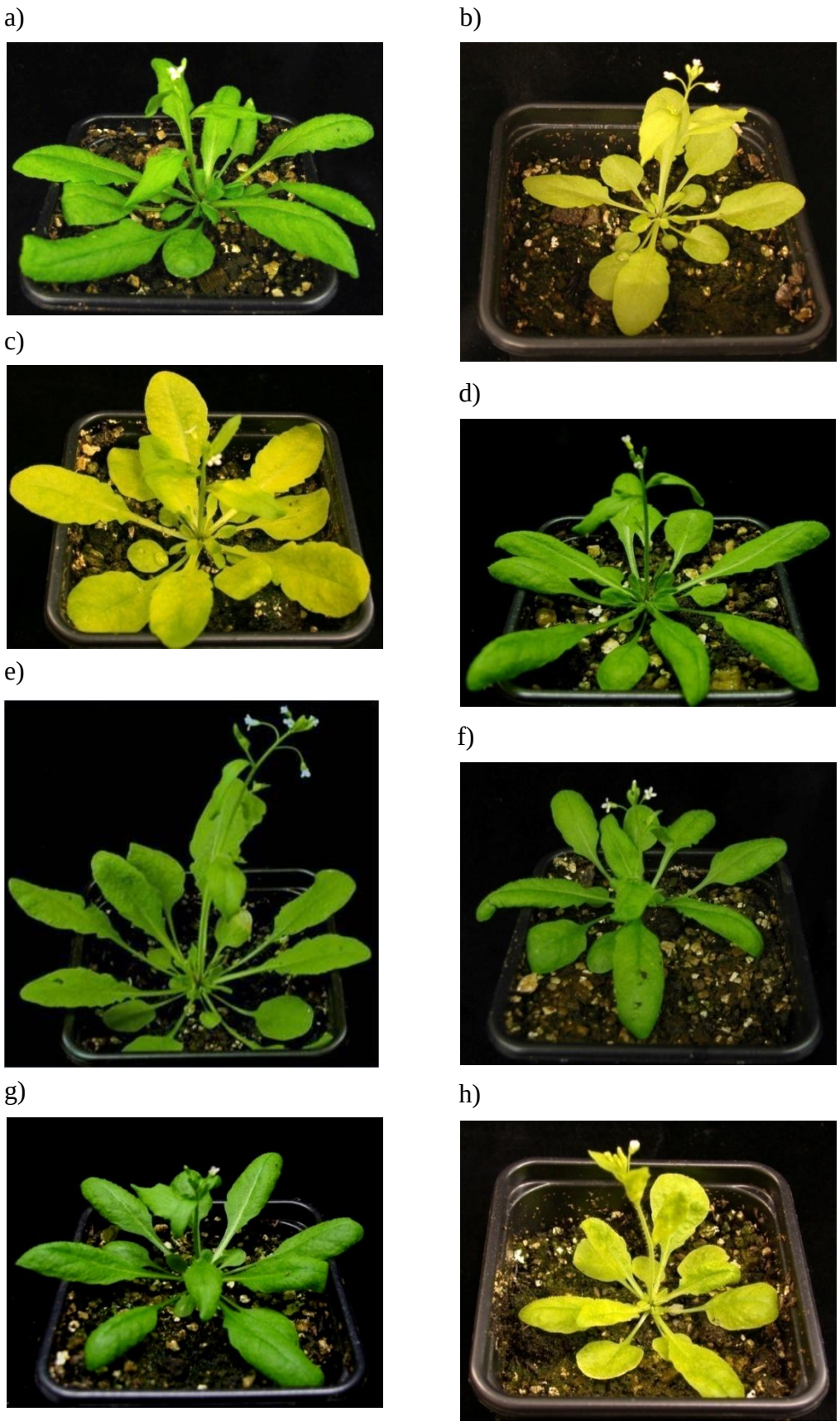

Figure 5.6 Mature phenotype of *GUN4* over expressing plants compared to WT and the *gun4-1* mutant. a) WT (Col-0), b) *gun4-1*, c) WT G4 1.2.2., d) WT G4 2.1.2., e) WT G4 2.2.3., f) *gun4* G4 2.1.1., g) *gun4 G4* 5.1.2., h) *gun4* G4 6.1.1. Plants were grown under 16h/8h light (80 µmol m^{-2} s^{-1})/dark cycles and photographs taken within one week of first flower opening.

The lack of overexpression in WT G4 1.2.2 and *gun4* G4 6.1.1, coupled with the *gun4* mutant phenotype, strongly suggest that silencing is occurring. However, in order for the WT G4 1.2.2 line to appear chlorophyll deficient, expression should be considerably reduced. One possibility is that the primers used for qPCR expression are detecting one of the products of RNA breakdown from silencing. To test this, the expression pattern was checked by traditional RT-PCR using both the qPCR small product primers and primers for the complete *GUN4* CDS (figure 5.5b and 5.5c). This confirms similar expression levels using both qRT- and traditional RT-PCR in all lines, suggesting that silencing is infact not occurring. However, it may still be possible that the products detected in these PCR reactions are a result of the RNA extraction which effectively results in a snapshot of the transcriptome i.e. if *GUN4* expression is massively increased in these lines then the silencing machinery may not be able to process all transcripts immediately, yet they remain present for too short a period for translation to occur. This would mean that although transcript expression is detectable in these lines, protein expression will be reduced. One further explaination could be that the T-DNA has been inserted into another gene that disrupts chlorophyll synthesis, although this is unlikely as more than one independent like produced this phenotype.

5.2.1.3.3. Protochlorophyllide and chlorophyll accumulation in the *GUN4* overexpression lines

Protochlorophyllide accumulation in the *GUN4* overexpressing plants, compared to WT and the *gun4* mutant, was measured following 5d dark treatment (figure 5.7a), and chlorophyll content was measured following 2d dark and 24h Wc (figure 5.7b). These values correlate well with each other (figure 5.7c) and with the level of *GUN4* expression (figure 5.7d) in the different lines. Interestingly, this data shows that increasing the expression of *GUN4* can subsequently increase the chlorophyll synthesis capacity of the plant.

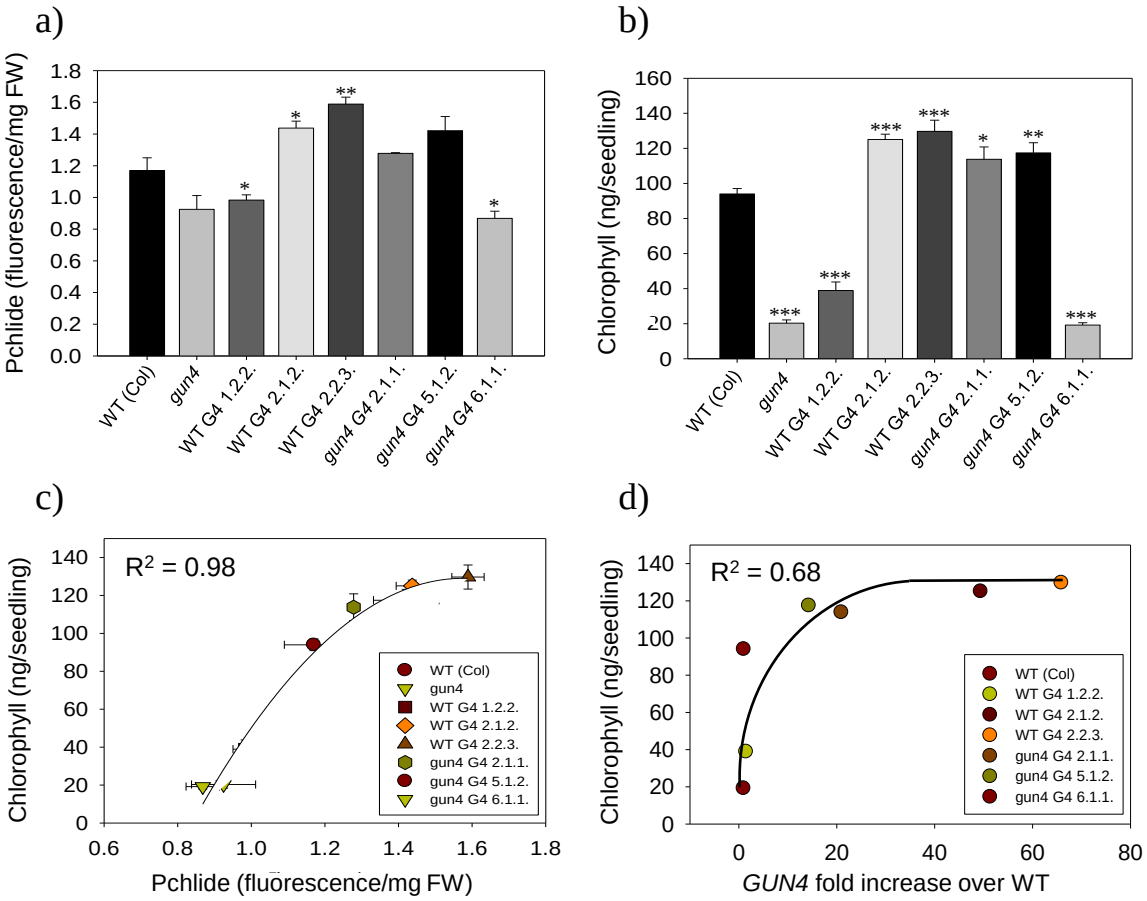

Figure 5.7 Protochlorophyllide and chlorophyll accumulation in the *GUN4* over expressing plants, compared to WT and the *gun4-1* mutant. a) Pchlide accumulation following 5d dark treatment (n = 4), b) chlorophyll accumulation following 2d dark and 24h Wc (110 µmol m^{-2} s^{-1}) (n = 4), c) correlation between protochlorophyllide accumulation in the dark and chlorophyll accumulation in the light, d) correlation between *GUN4* fold expression and chlorophyll accumulation in the light. * = P = <0.05 ** = P = <0.01, *** = P = <0.005. Values are mean ± SE of 4 independent experiments.

5.2.1.3.4. Control of hypocotyl extension in the *GUN4* overexpression lines

It has been postulated previously that *GUN4* may be responsible for distributing protoporphyrin IX to both branches of the tetrapyrrole pathway (Davison *et al*., 2005). One assay to test intermediate flow into the haem branch is through hypocotyl measurements under Rc and FRc light, which relates to the levels of phytochromobilin produced for phytochrome synthesis. Hypocotyl length of the *GUN4* overexpressing plants, compared to WT and the *gun4* mutant, was measured following 1d dark and 5d Rc, FRc or dark treatment (figure 5.8).

All lines show no significant difference in the dark hypocotyl length, however, the *gun4* mutant and *gun4* G4 6.1.1 line both show an increase under Rc (133 and 125% of WT, respectively) and FRc (116 and 108% of WT, respectively). As the *gun4* G4 6.1.1 lines has a *gun4* mutant mature phenotype (figure 5.8) this might suggest that the lack of GUN4 protein in these lines is indeed causing a reduction in phytochromobilin synthesis. However, the WT G4 1.2.2 line, which also displayed a chlorophyll deficient phenotype and was therefore predicted to be silenced, does not show an increase in hypocotyl length (figure 5.8).

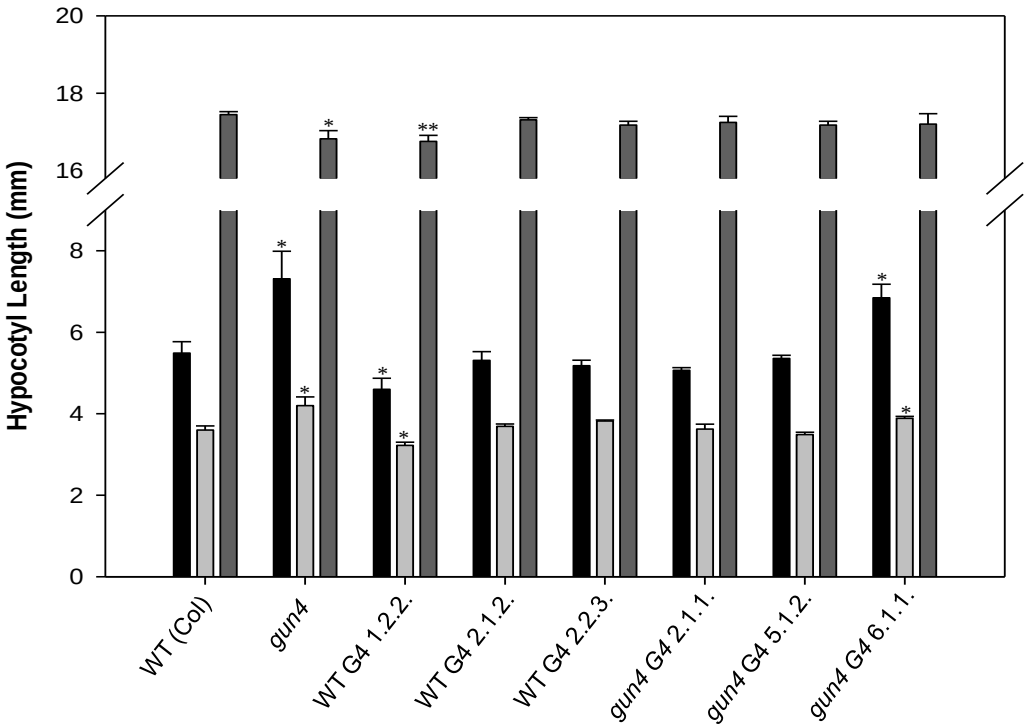

Figure 5.8 Hypocotyl length of the *GUN4* over expressing plants, compared to WT and *gun4* mutant, following 1d dark and 5d red light (black bar), far-red light (light grey bar) or dark (dark grey bar). * = P = <0.05, ** = P = <0.01. Values are mean ± SE of 3 independent experiments.

5.2.2. *FLU* regulation of the tetrapyrrole pathway

5.2.2.1. *FLU* overexpression lines

5.2.2.1.1. Production of *FLU* overexpression lines

FLU overexpression lines were produced in WT and *flu* mutant (figure 5.9) lines using the same protocol as for *GUN4* (see section 5.2.1.3.1.). The survival of T2 and T3 seedlings, from growth on hygromycin selective media, are shown in Table 5.3 and Table 5.4, respectively, and the FLU pMDC32 construct is shown in figure 5.10.

Table 5.3 Survival of T2 *FLU* overexpressing lines on selective media containing hygromycin antibiotic.

Plant Line	Died	Survived	% Survived	Predicted Insert Number
WT FLU 3.2	7	26	78.8	1
WT FLU 3.3	2	36	94.7	2
WT FLU 3.4	2	33	94.3	2
WT FLU 3.5	12	31	72.1	1
WT FLU 4.1	10	24	70.6	1
WT FLU 4.2	33	10	23.3	?
WT FLU 4.3	34	0	0	0
WT FLU 4.4	4	33	89.2	2
WT FLU 4.5	8	25	75.8	1
WT FLU 6.1	13	26	66.7	1
WT FLU 6.2	28	0	0	0
WT FLU 6.4	8	34	81	1
***flu* FLU 4.1**	34	1	2.9	0
***flu* FLU 4.2**	5	32	86.5	2
***flu* FLU 4.6**	5	34	87.2	2
***flu* FLU 5.2**	6	21	77.8	1
WT	42	0	0	0

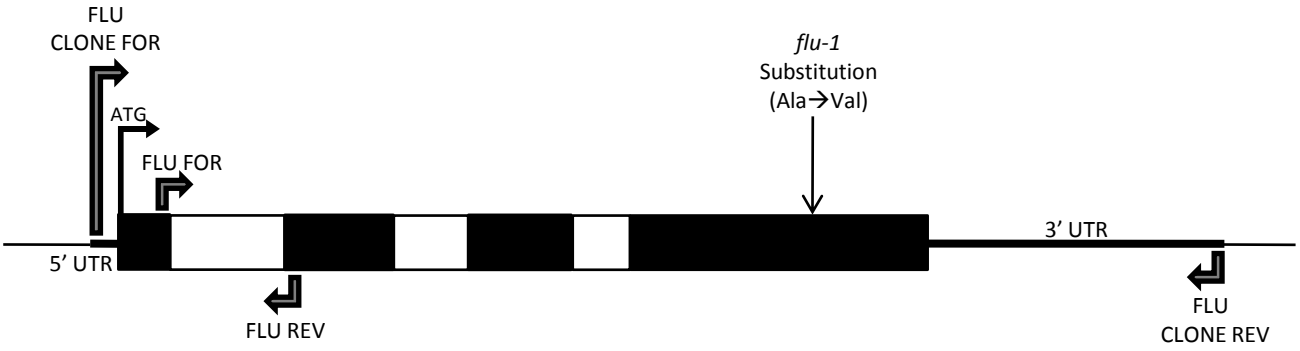

Figure 5.9 Scematic representation of the *FLU* gene, indicating the polymorphism site resulting in the *flu-1* mutant, and primer positions used in expression and over-expression studies (1cm = 150bp).

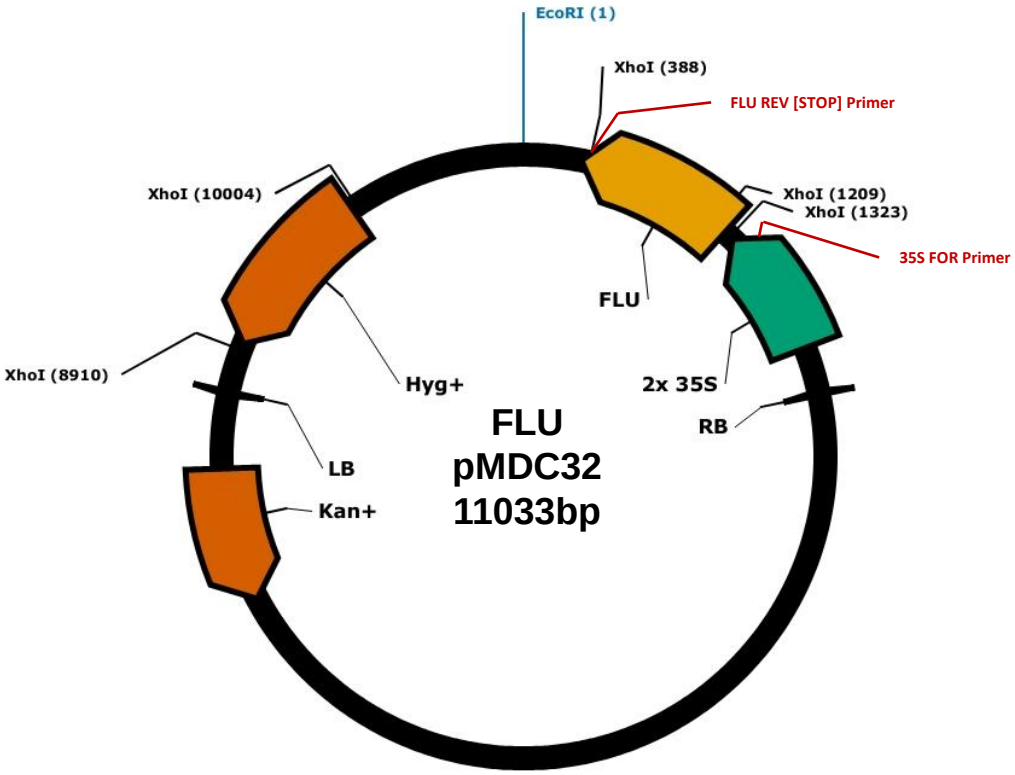

Figure 5.10 FLU pMDC32 construct used to produce *FLU* overexpression lines. Genetic material between the left border (LB) and right border (RB) was transformed into *Arabidopsis* using *Agrobacteria*, where the hygromycin (Hyg+) resistance gene allowed selection of successfully transformed plants and the 2x 35S CaMV promoter inferred overexpression of the *FLU* gene. The Kanamycin (Kan+) resistance gene, which is not transferred to the plant, allowed selection of successful transformation in *E.coli* and *A.tumefaciens*. Primer and restriction sites, used to confirm successful plasmid recombination during production, are indicated.

Table 5.4 Survival of T3 *FLU* overexpressing lines on selective media containing hygromycin antibiotic.

Plant Line	Died	Survived	% Survived	Result
WT FLU 3.2.2	8	30	78.9	Het
WT FLU 4.1.1	0	50	100	**Hom**
WT FLU 4.1.4	46	0	0	WT
WT FLU 4.4.1	8	27	77.1	Het
WT FLU 4.5.3	0	46	100	**Hom**
WT FLU 6.1.1	9	19	67.9	Het
WT FLU 6.1.2	10	29	74.4	Het
WT FLU 6.1.3	10	37	78.7	Het
WT FLU 6.1.4	0	35	100	**Hom**
***flu* FLU 4.6.1**	10	33	76.7	Het
***flu* FLU 4.6.2**	1	49	98	**Hom**
***flu* FLU 4.6.3**	11	40	78.4	Het
***flu* FLU 4.6.4**	8	25	75.8	Het
***flu* FLU 5.2.1**	9	21	70	Het
***flu* FLU 5.2.4**	10	24	70.6	Het
WT	35	0	0	WT

Het = heterozygous, Hom = homozygous, WT = wild type.

5.2.2.3.2. Confirmation of insert presence and level of overexpression

Seedlings from each of the homozygote lines, along with WT, were grown under Wc for 5d. Insert presence was confirmed by DNA extraction and PCR (figure 5.11a). The transcript levels of the homozygote transformants was then tested through RNA extraction and RT-real time PCR (figure 5.11b). This indicates that all homozygous lines are overexpressing *FLU*, and that WT FLU 4.5.3 has the highest expression (34 fold increase over WT).

5.2.2.3.3. Protochlorophyllide and chlorophyll accumulation in the *FLU* overexpression lines

As the *flu* mutant has previously been shown to accumulate protochlorophyllide in the dark, due to a lack of repression of Glu-TR (Meskauskiene and Apel, 2002), the protochlorophyllide content of the *FLU* overexpression lines was

determined following 5d dark treatment (figure 5.12a).

Compared to WT, and particularly the *flu* mutant, the *FLU* overexpression lines show a reduction in protochlorophyllide content, and the strongest response is in the WT FLU 4.5.3 line which contains only 78% of WT Pchlide. Additionally, the Pchlide content of the overexpression lines negatively correlates with *FLU* expression (figure 5.12c), which is consistant with its proposed role. Consequently, chlorophyll content of the *FLU* overexpression lines was measured following 2d dark and 24h Wc treatment (5.12b). This figure shows, however, that there is no difference in chlorophyll content, although it is worth noting that the *flu* FLU 4.6.2 line was able to survive that dark to light transition indicating a rescue of the *flu* mutant phenotype.

5.2.2.3.4. Control of hypocotyl extension in the *FLU* overexpression lines

As *FLU* is known to regulate Glu-TR, a key regulatory site for intermediate flow into both chelatase branches, the ability of the *FLU* overexpression lines to control hypocotyl extension was determined, which might indicate misregulation of phytochromobilin synthesis (figure 5.13).

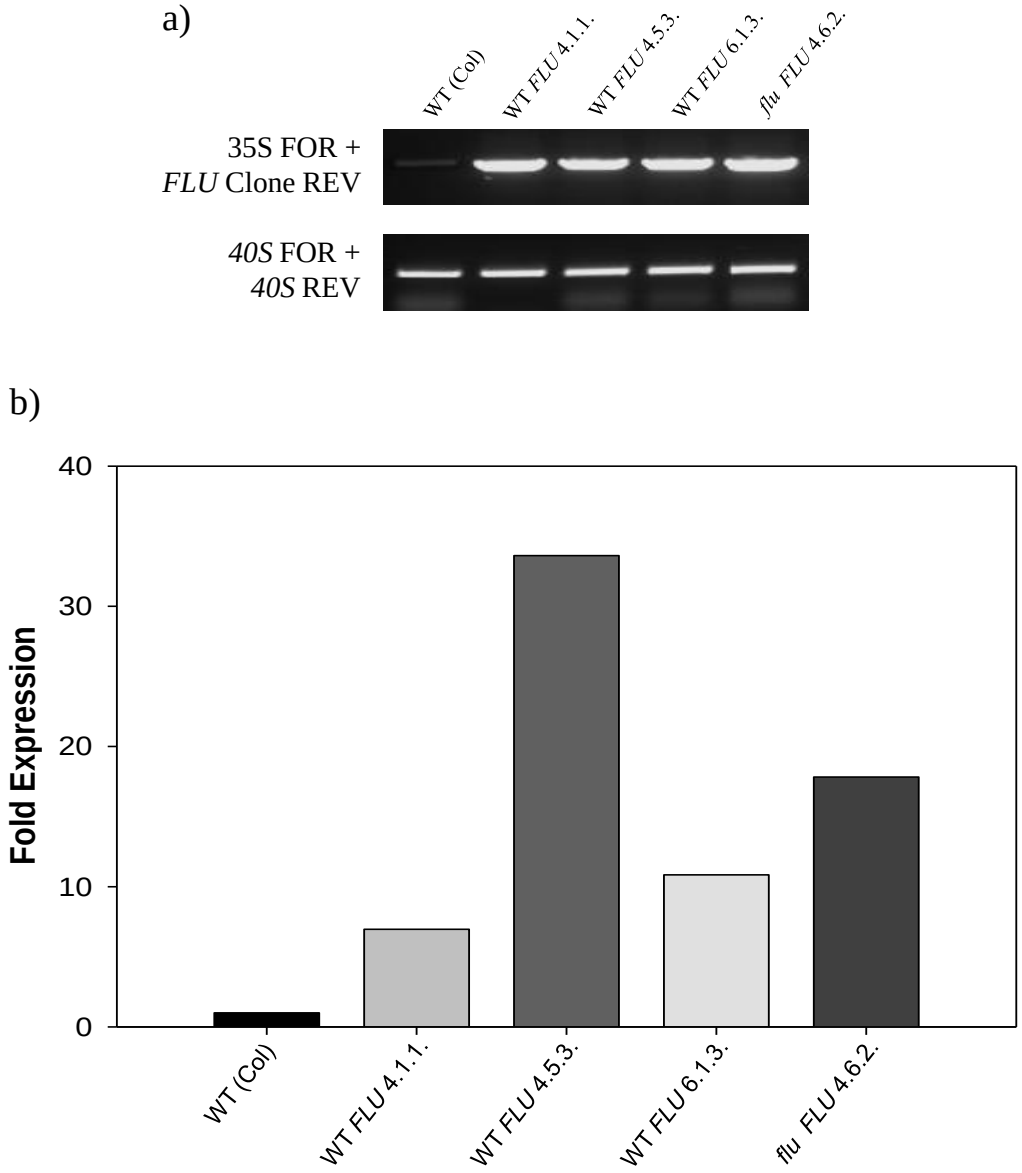

Figure 5.11 Confirmation of the presence of the 35S:*FLU* constuct in transgenic *Arabidopsis thaliana* plants. a) gPCR reaction confirming the presense of the *FLU* over expressing construct in 4 transgenic lines, and the absence of the construct in a WT plant. b) Expression of *FLU* in transgenic plants compared to WT calculated using real-time PCR, following 7d white light (110 µmol m^{-2} s^{-1}) growth. n = 1.

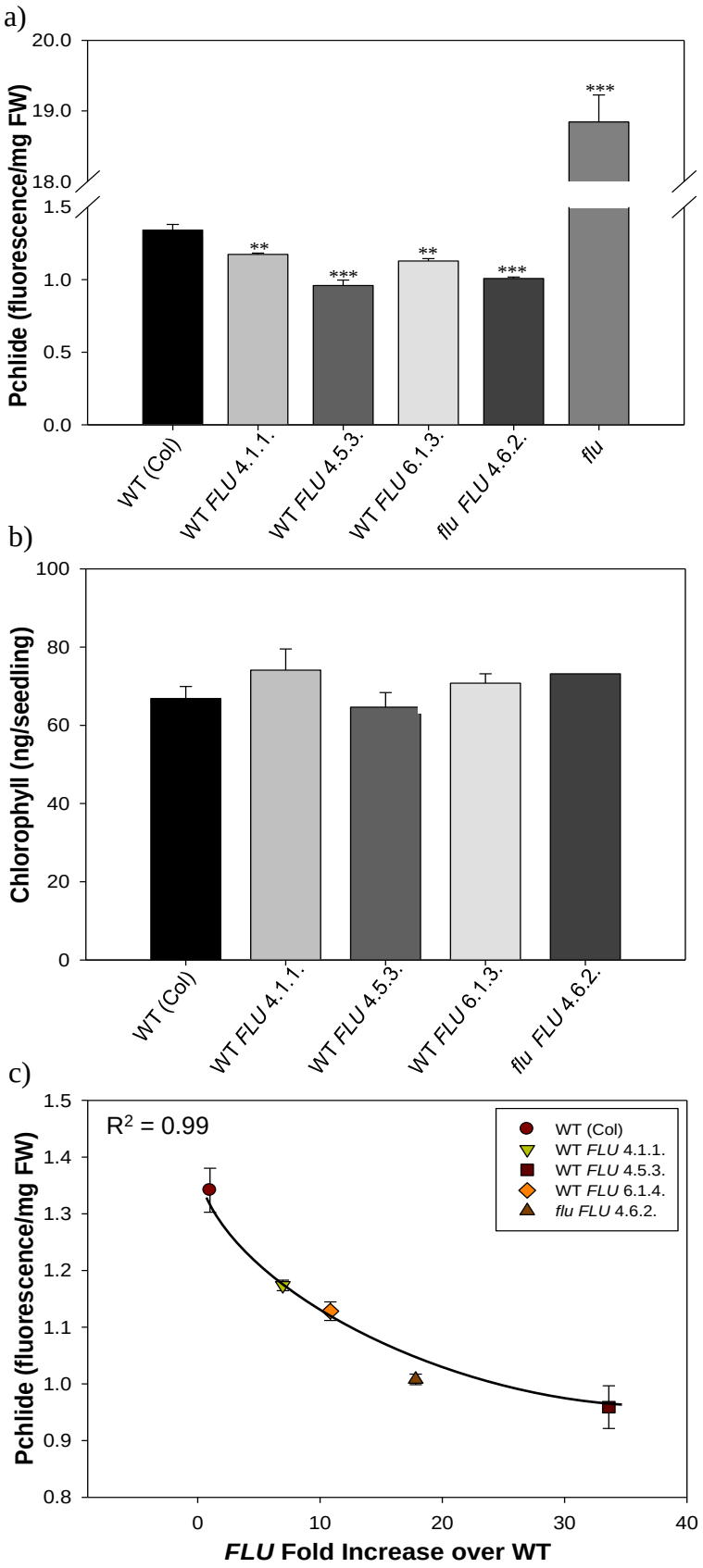

Figure 5.12 Protochlorophyllide and chlorophyll accumulation in the *FLU* over expressing plants, compared to WT and the *flu* mutant. a) Protochlorophyllide accumulation following 5d dark treatment (n = 4). b) Chlorophyll accumulation following 2d dark and 24h Wc (110 µmol m^{-2} s^{-1}) (n = 4). c) Correlation between *FLU* fold expression and chlorophyll accumulation in the light. ** = P = <0.01, *** = P = <0.005. Values are mean ± SE of 3 independent experiments.

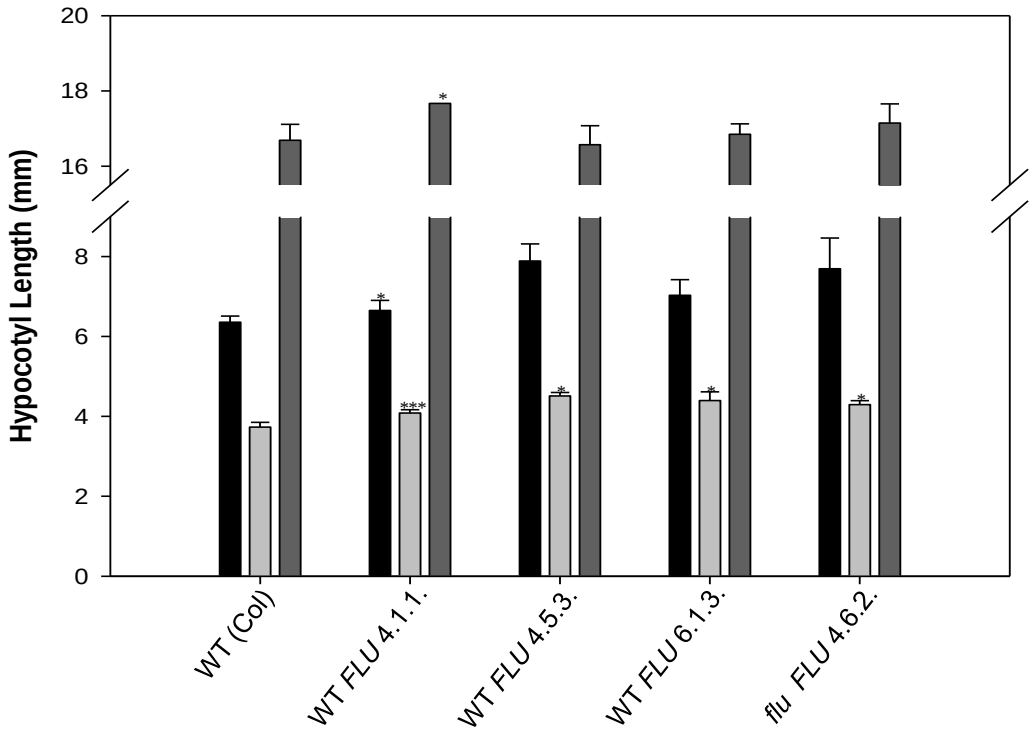

Figure 5.13 Hypocotyl length of the *FLU* over expressing plants, compared to WT and *flu* mutant, following 1d dark and 5d red light (80 µmol m^{-2} s^{-1}) (black bar), far-red light (10 µmol m^{-2} s^{-1}) (light grey bar) or dark (dark grey bar). * = P = <0.05, *** = P = <0.005. Values are mean ± SE of 3 independent experiments.

Despite the maintainace of chlorophyll synthesis in these lines, the strongest overexpressors, WT FLU 4.5.3 and *flu* FLU 4.6.2, do show a marginal increase in hypocotyl length under red and far-red light. It has previously been hypothesised that different pools of protoporphyrin IX are made available to the chlorophyll and haem branches of the tetrapyrrole pathway (Cornah *et al*., 2003), therefore if the overexpression of FLU results in maintainance of the chlorophyll pool but a reduction in the haem pool then this might provide an explanation for the lack of phytochromobilin.

5.2.3. ABA as a regulator of the tetrapyrrole pathway

5.2.3.1. Mutants in the ABA synthesis and signalling pathways

Using bioinformatics to understand the regulation of the *GUN4*, the *aba1* (L*er*) and *abi1* (L*er*) mutations were highlighted as strongly down-regulating *GUN4* expression (figure 3.19). These mutants were therefore selected for further study into the effect of ABA on tetrapyrrole synthesis. Additionally, the *abi2* (L*er*). *abi3* (L*er*), *abi4* (Col) and *abi5* (WS) mutants, which also have aberrant ABA signalling, were selected for further study. They were assessed in their ability to de-etiolate effectively, in terms of chlorophyll accumulation, hypocotyl elongation and tetrapyrrole gene expression changes under different light conditions.

5.2.3.2. Expression of tetrapyrrole-synthesis genes in ABA mutants

Previously, *HEMA1*, *CHLH*, *GUN4* and *PORA* have been shown to be key regulators of the tetrapyrrole pathway, therefore these genes were specifically chosen for this study. Figure 5.14 shows the light induction of these genes in the ABA mutant backgrounds compared to their respective WT.

As the Genevestigator™ program indicated specific regulation of *GUN4* by *aba1* and *abi1* it is surprising to see that this is the only gene, of the four chosen, to be unaffected in any of the mutants studied. On the other hand, *HEMA1* and *CHLH* are regulated similarly in almost all of the mutants. In both cases *aba1* and *abi2* cause an

increase in light induction, *abi1* results in a minor increase, and the *abi3*, *abi4* and *abi5* mutations result in reduced light induction. The effect on *PORA* expression is also quite dramatic. Here *aba1*, *abi4* and *abi5* result is less down regulation of *PORA* expression, and this is particularly strong in the *abi4* mutant. Conversely, *abi2* and *abi3*, and to a lesser extent *abi1*, cause an increase in *PORA* downregulation.

5.2.3.3. Chlorophyll synthesis in the ABA mutants

As the ABA mutants were shown to affect the expression of *HEMA1*, *CHLH* and *PORA*, this suggested that the potential to accumulate chlorophyll might also be affected. Chlorophyll content was measured following 2d dark and 24h Wc in the mutants and their respective wild type controls (figure 5.15a). This data shows that while the *aba1*, *abi4* and *abi5* mutants are deficient in chlorophyll, compared to WT, the *abi1*, *abi2* and *abi3* mutants are able to accumulate more chlorophyll. Interestingly, the ability to accumulate chlorophyll is closely linked to *PORA* expression in these mutants (figure 5.15b), where an increase in the downregulation of *PORA* is positively correlated with an increase in chlorophyll accumulation, but not with *HEMA1* or *CHLH* expression.

5.2.3.4. Regulation of hypocotyl extension in the ABA mutants

Hypocotyl length was measured in the ABA synthesis and signalling mutants following Rc, FRc and dark treatment (figure 5.16) to determine any affect on phytochromobilin synthesis.

Under all treatments the *abi2*, *abi3* and *abi5* mutants have a WT hypocotyl length. On the other hand, following all treatments, and particularly in the dark, the *aba1* and *abi1* mutants are shorter than the Ler WT, suggesting either 1) a partial constitutive photomorphogenic phenotype, or 2) a lack of energy preventing growth. Finally, the *abi4* mutant has a significantly longer hypocotyl than the WT under Rc, suggesting that it is less able to perceive the light, although it is still shorter than the *phy*B mutant. However, under both FRc and dark treatment the *abi4* mutant is shorter than WT, indicating a possible role in phyB-specific light signalling.

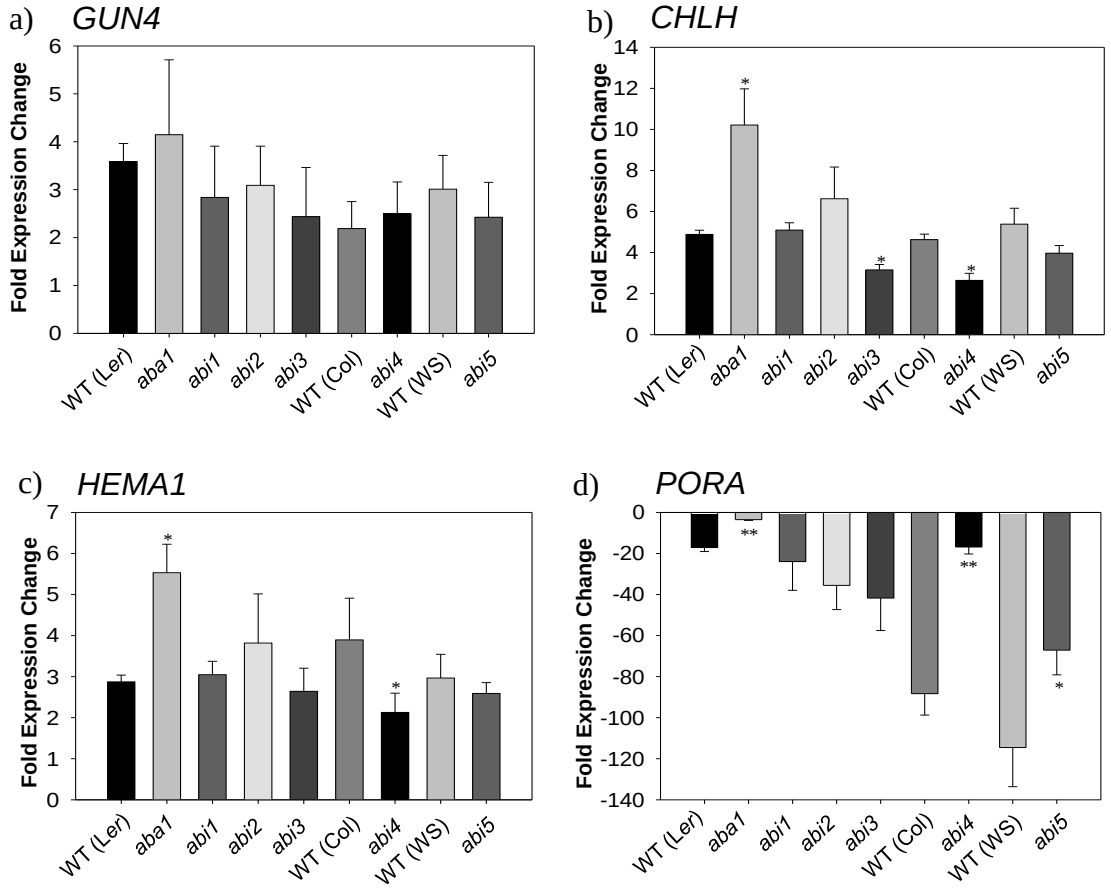

Figure 5.14 Induction of tetrapyrrole synthesis genes in ABA synthesis and signalling mutants following 2d dark and 24h Wc (110 µmol m^{-2} s^{-1}) compared to 3d dark, normalized to *YLS8* using real-time PCR. a) *GUN4*, b) *CHLH*, c) *HEMA1*, d) *PORA*. * = P = <0.05, ** = P = <0.01. Values are mean ± SE of 3 independent experiments.

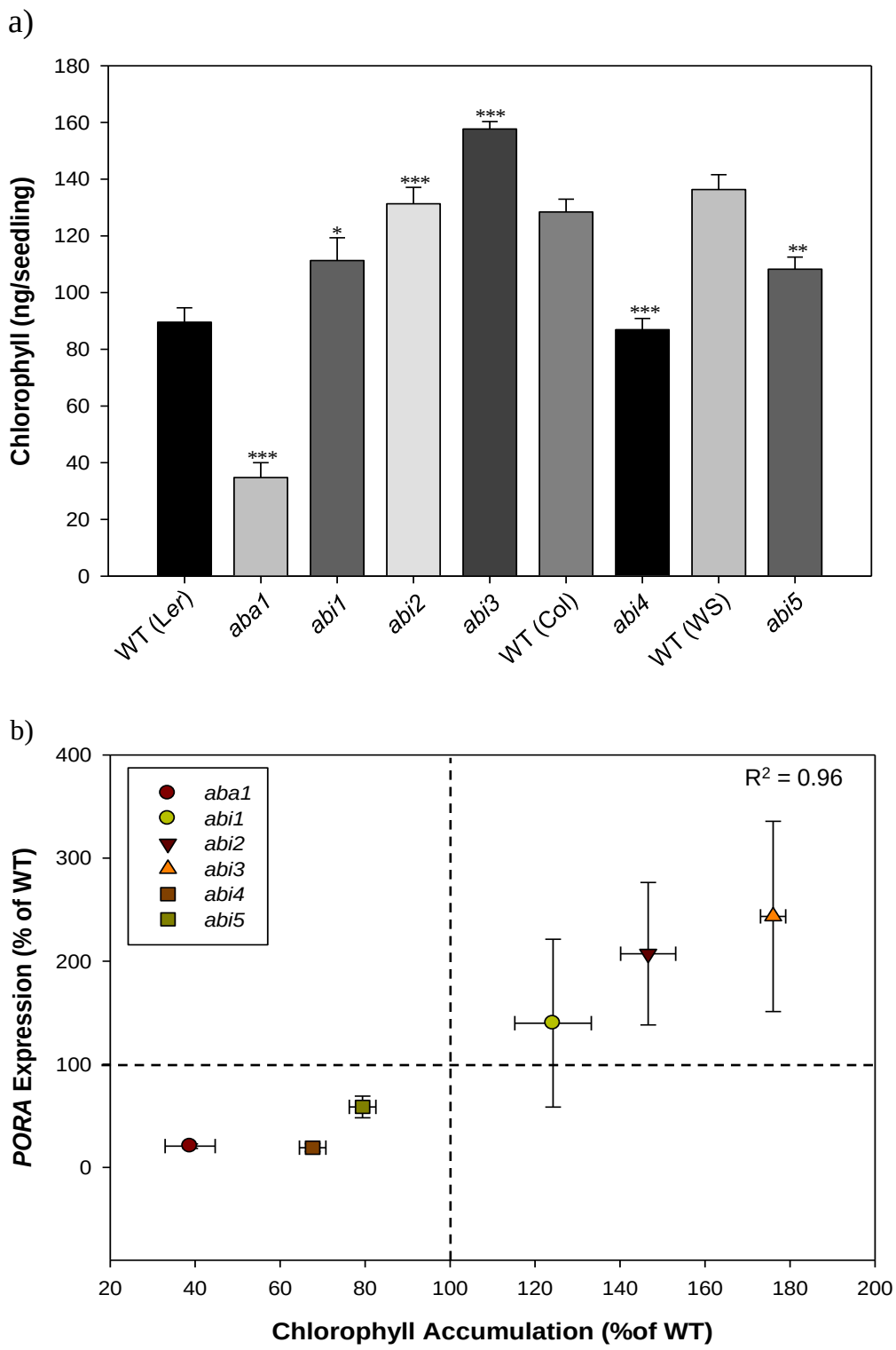

Figure 5.15 Chlorophyll accumulation in ABA synthesis and signalling mutants following 2d dark and 24h Wc (110 µmol m^{-2} s^{-1}). a) Chlorophyll accumulation in the ABA mutants, shown as ng/seedling, compared to the corresponding WT (L*er* = *aba1*, *abi1*, *abi2*, *abi3*; Col = *abi4*; WS = *abi5*) (n = 4), b) correlation between chlorophyll accumulation, shown as percent of WT, and *PORA* expression. * = P = <0.05, ** = P = <0.01, *** = P = <0.005. Values are mean ± SE of ≥3 independent experiments.

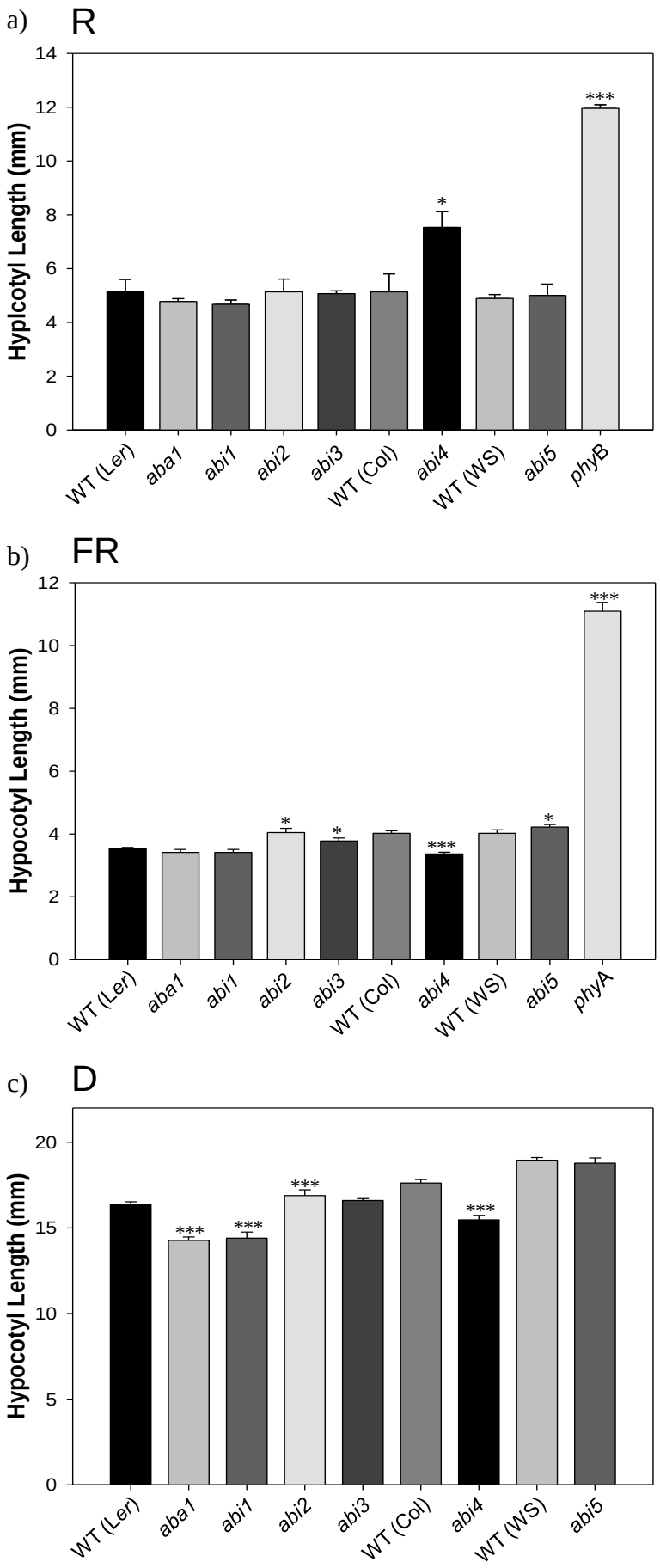

Figure 5.16 Hypocotyl length of ABA synthesis and signalling mutants following 1d dark and 5d Red (80 µmol m^{-2} s^{-1}) (a), Far-red (10 µmol m^{-2} s^{-1}) (b), or dark (c) treatment. * = P = <0.05, *** = P = <0.005. Values are mean ± SE of 3 independent experiments.

5.2.4. *MYB50* and *MYB61* regulation of the tetrapyrrole pathway

5.2.4.1 Light regulation of *MYB50* and *MYB61*

To further understand how these genes might impact *GUN4* expression, the regulation of *MYB50* and *MYB61* was studied under different wavelengths of light (figure 5.17).

Under all light treatments MYB50 is similarly upregulated to ca. 2.5-3 fold, although less so under blue light. On the other hand, MYB61 is downregulated under all light treatments, most strongly under blue light. As MYB proteins are known to have transcription factor activity this result, coupled with the opposing effects on GUN4 expression, might indicated a role for MYB50 and MYB61 in antagonistic regulation of the tetrapyrrole pathway in response to light and hormonal stimulus.

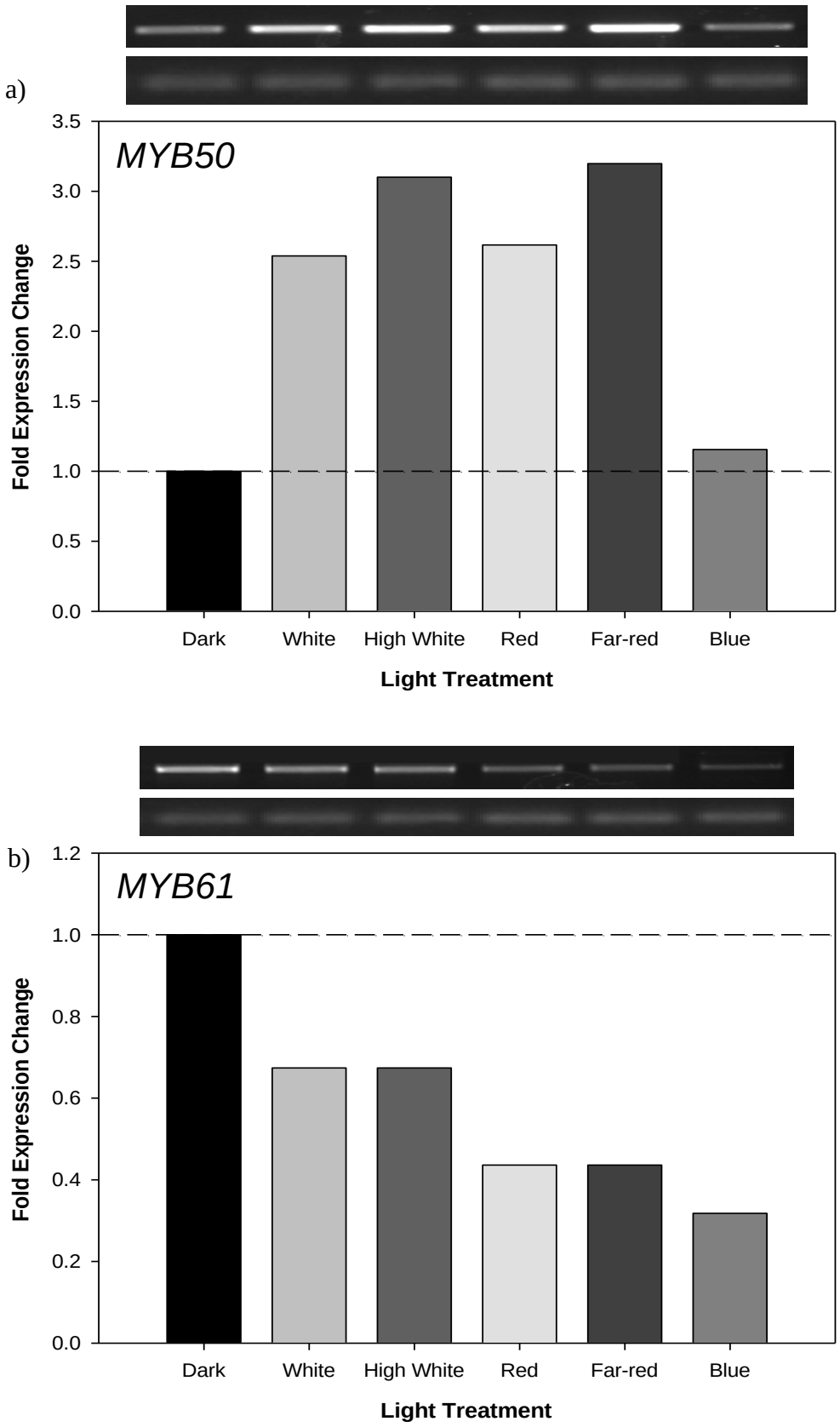

Figure 5.17 Light induction of *MYB50* and *MYB61*. Expression of *MYB50* (a) and *MYB61* (b) following 3d dark or 2d dark and 1d white (110 µmol m^{-2} s^{-1}), high white (550 µmol m^{-2} s^{-1}), red (80 µmol m^{-2} s^{-1}), far-red (10 µmol m^{-2} s^{-1}) or blue (20 µmol m^{-2} s^{-1}) light, normalized to *YLS8* using pixel densitometry following traditional RT-PCR. One of three repeat experiments, with similar results, is shown.

5.2.4.2. The *myb50* and *myb61* mutants

The aim of this study was to establish whether *MYB50* and *MYB61* could have antagonistic roles in the light-mediated control of *GUN4* expression. To achieve this a *myb50* SALK mutant and a *myb61* SM mutant were identified and assessed in their ability to de-etiolate effectively, in terms of chlorophyll accumulation, hypocotyl elongation and tetrapyrrole gene expression changes under different light conditions.

5.2.4.2.1. Production of the *myb50* and *myb61* mutants

A heterozygous T-DNA insertion SALK line (SALK_035416: Alonso *et al*., 2003) was obtained for *MYB50*, and was used to produce a homozygous line through self fertilisation and selection on kanamycin antibiotic; and a homozygous T-DNA insertion SM line (SM_3_30853; Tissier *et al*., 1999) was obtained for *MYB61*. A schematic of the genes, insertion sites, and primers used to confirm zygosity, and the confirmation of homozygous insert and knockdown (*myb50*) and knockout (*myb61*) of gene expression is shown in figure 5.18.

5.2.4.2.2. Regulation of the tetrapyrrole pathway in the *myb50* and *myb61* mutants

As the *myb50* and *myb61* mutants were previously shown, using the Genevestigator™ program (figure 3.20), to specifically regulate the *GUN4* gene, regulation of the tetrapyrrole-synthesis genes were studied in these mutants directly using real-time PCR (figure 5.19). Expression of *HEMA1*, *CHLH*, *GUN4*, *FC2* and *PORA* were specifically studied, following 2d dark and 24h Wc treatment, as these genes are known to be key sites for regulation.

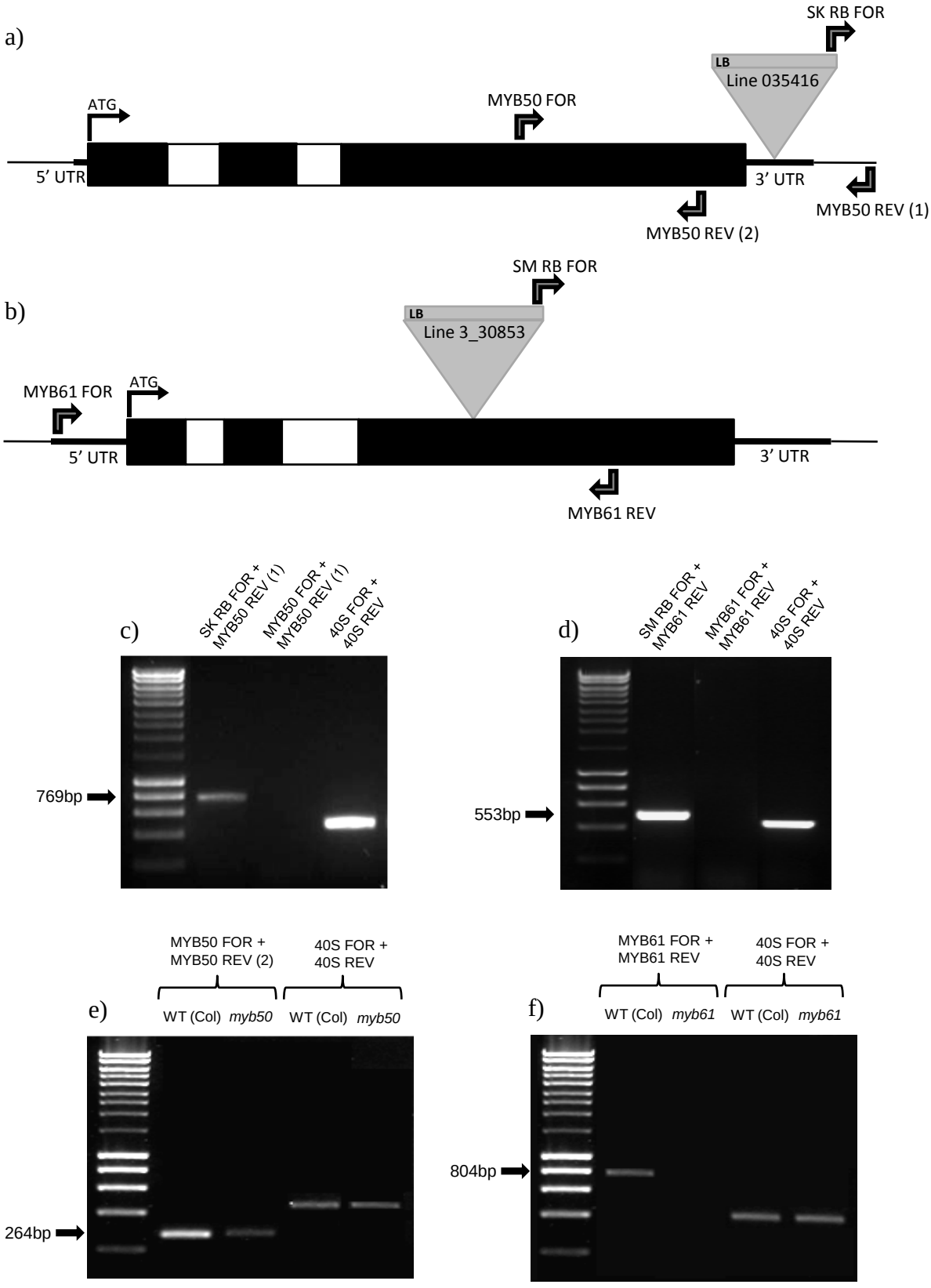

Figure 5.18 Insertional mutagenesis of the *MYB50* and *MYB61* genes of *Arabidopsis thaliana*. a) SALK insert position in the *MYB50* gene (1cm = 100bp), b) SM insert position in the *MYB61* gene (1cm = 100bp), c) and d) homozygous insert confirmation by PCR, e) expression of *MYB50* and *40S* rRNA in the *myb50* mutant compared to WT, f) expression of *MYB61* and *40S* rRNA in the *myb61* mutant compared to WT.

HEMA1, *CHLH* and *FC2* are all marginally more upregulated in the *myb* mutants following Wc light treatment, compared to WT, and this is consistently stronger in the *myb61* mutant. *GUN4* is also more upregulated in both mutants but to a much more significant degree, where expression reaches 22 and 18 fold induction in the *myb50* and *myb61* mutants, respectively, compared to only 7 fold in the WT. This does not fit entirely with the results from Genevestigator™ which suggested that although *GUN4* was upregulated in the *myb50* mutant, it was infact downregulated in *myb61*.

PORA expression is also affected in the *myb50* mutant, where it is downregulated more strongly than the WT (81 and 61 fold, respectively), while expression in *myb61* (60 fold) is comparable to WT.

5.2.4.2.3. Regulation of *MYB50* and *MYB61* by each other

As *MYB50* and *MYB61* are antagonistically regulated by light (figure 3.20) but show similar patterns of regulation of the tetrapyrrole pathway (figure 5.19) it is possible that these genes are required for the same function at different diurnal periods. It may also be possible, therefore, that these genes are required to regulate each other in cycles similar to those for *LHY*/*CCA1* and *TOC1* in the circadian clock (see section 1.3.5 for further information), to perform this function. Regulation of *MYB50* and *MYB61* was consequently studied in the *myb61* and *myb50* mutants, respectively, to further help elucidate function (figure 5.20).

In *myb61* and WT seedlings *MYB50* is strongly upregulated following 2d dark and 24h Wc, suggesting that *MYB61* is not required for *MYB50* regulation. However, in the *myb50* mutant *MYB61* is more weakly expressed in the dark and is no longer downregulated following light treatment, suggesting that *MYB50* is also a suppressor of *MYB61* expression following light transfer.

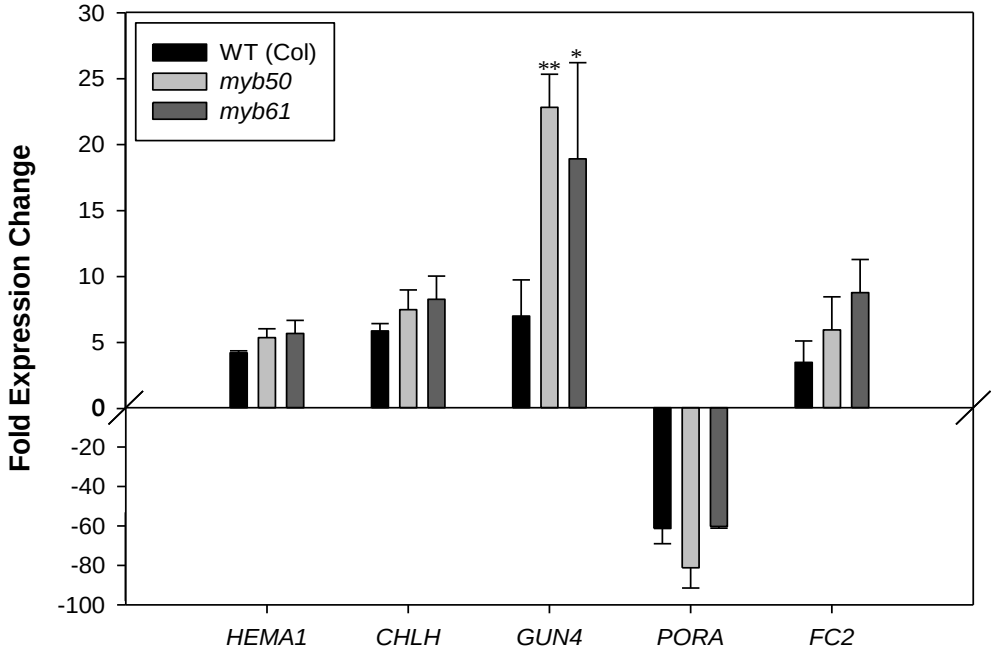

Figure 5.19 Expression change of tetrapyrrole genes in the *myb50* and *myb61* mutants compared to WT following 2d dark and 24h Wc (110 µmol m^{-2} s^{-1}) or 3d dark, normalised to *YLS8* using real-time PCR. a) *HEMA1*, b) *CHLH*, c) *GUN4*, d) *FC2*, e) *PORA*. * = P = <0.05, ** = P = <0.01. Values are mean ± SE of 3 independent experiments.

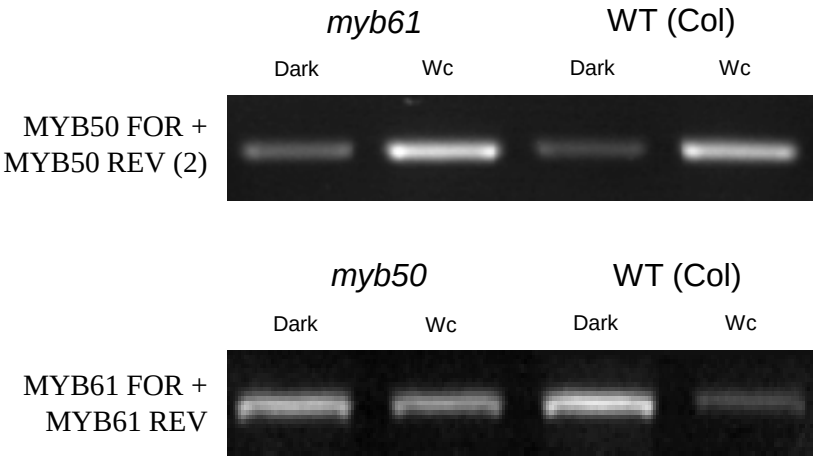

Figure 5.20 Expression change of the *MYB50* and *MYB61* genes in the *myb50* and *myb61* mutants compared to WT following 2d dark and 24h Wc (110 µmol m^{-2} s^{-1}) or 3d dark. One of three repeat experiments, with similar results, is shown.

5.2.4.2.4. Chlorophyll accumulation in the *myb50* and *myb61* mutants

As the *MYB50* and *MYB61* genes have been shown by both microarray and RT-PCR to regulate *GUN4*, and given the requirement for *GUN4* expression for chlorophyll accumulation (e.g. figure 5.2), the protochlorophyllide and chlorophyll content in these mutants was determined (figure 5.21).

Figure 5.21a indicates that there is a significant increase in protochlorophyllide content in both the *myb50* and *myb61* mutants, compared to WT. Interestingly, these increases are also similar to the levels accumulated in the *GUN4* overexpression lines (figure 5.7a), and therefore might relate directly to the increases in *GUN4* expression. This hypothesis is supported by the finding that two MYB transcription factors from barley, *HvMCB1* and *HvMCB2*, bind to, and control the plastid-developmental regulation of *CAB1*, a chlorophyll binding protein (Churin *et al*., 2003). These genes are not homologous to *MYB50* and *MYB61*, but it suggests that MYB-regulated input into the chlorophyll synthesis pathway is entirely plausible. However, while there is an increase in chlorophyll content in the *myb50* mutant, following 2 or 4d dark pretreatment (138 and 109% of WT, respectively), the *myb61* mutant contains only 83% of WT levels following both treatments.

5.2.4.2.5. Regulation of hypocotyl extension in the *myb50* and *myb61* mutants

The hypocotyl lengths of the *myb* mutants was measured in the dark and under red and far-red light (figure 5.22) to help determine if these genes are required for the regulation of phytochromobilin synthesis.

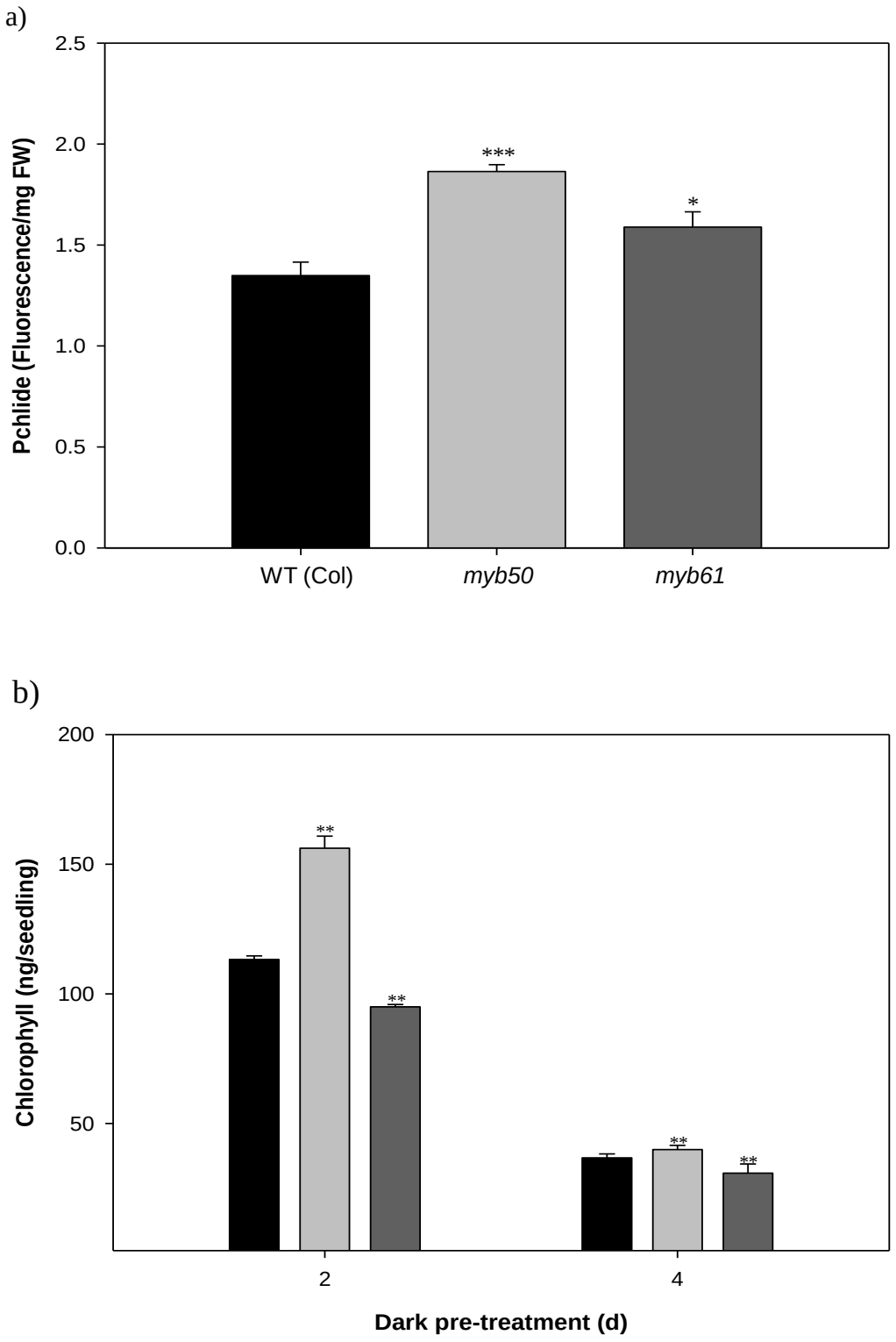

Figure 5.21 Protochlorophyllide and chlorophyll accumulation in the *myb50* and *myb61* mutants, compared to WT. a) Protochlorophyllide content following 6d dark treatment, b) chlorophyll content following 2d dark and 24h Wc (110 µmol m^{-2} s^{-1}). Black bar = WT, light grey bar = *myb50*, dark grey bar = *myb61*. * = P = <0.05, ** = P = <0.01, *** = P = <0.005. Values are mean ± SE of 4 independent experiments.

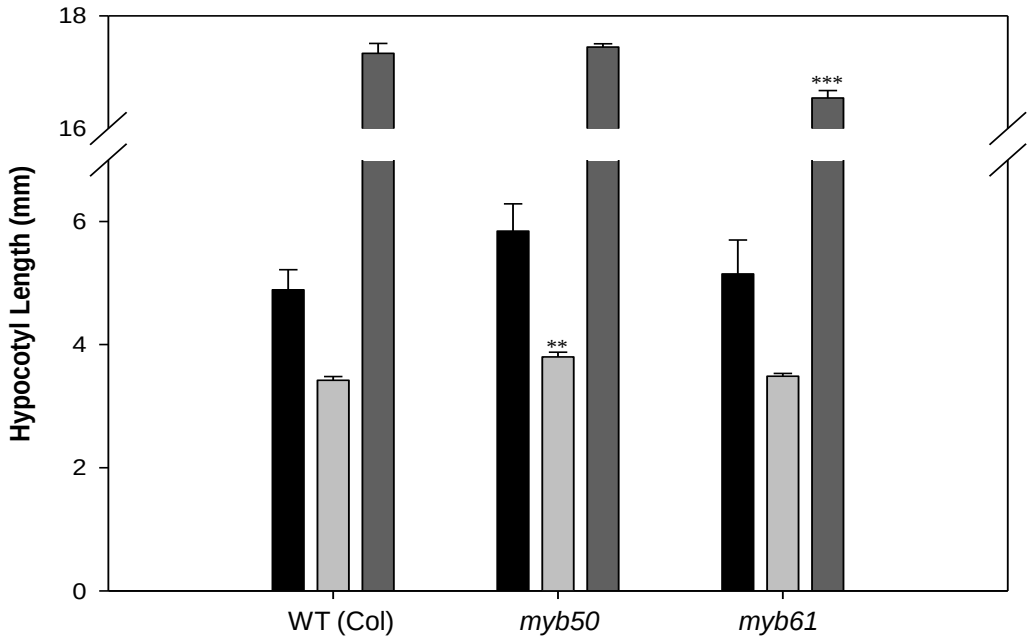

Figure 5.22 Hypocotyl length of the *myb50* and *myb61* mutants compared to WT following 1d dark and 5d red light (80 µmol m^{-2} s^{-1}) (black bar), far-red light (10 µmol m^{-2} s^{-1}) (light grey bar) or dark (dark grey bar). ** = P = <0.01, *** = P = <0.005. Values are mean ± SE of 3 independent experiments.

In the dark there is no difference in length of the *myb50* mutant compared to WT (17.4 and 17.3 mm, respectively), however, the *myb61* mutant is significantly shorter (16.5 mm). This phenotype has previously been associated with an increase in phytochrome content in the seed (Boylan and Quail, 1991), activation of phytochrome responses in the dark (Deng and Quail, 1992), disruption of the circadian rhythm (Dowson-Day and Millar, 1999), and reduction of energy reserves in the seed (Penfield *et al*., 2004). Although *MYB61* may be playing a role in any of these responses, in this case the down-regulation in gene expression in the chlorophyll branch of the tetrapyrrole pathway in the *myb61* mutant may be resulting in a larger pool of protoporphyrin IX being channelled into the haem branch, and consequently in a higher phytochromobilin content.

Under red and far-red light there is no difference in the hypocotyl length of *myb61* compared to WT, but the *myb50* mutant is marginally longer under both conditions. The expression data and chlorophyll content of the *myb50* mutant suggest that this gene is normally required for the negative regulation of genes in the chlorophyll branch of the tetrapyrrole pathway. Therefore, in the mutant background fewer intermediates will be available for the haem branch, which could result in a reduction in phytochromobilin and consequently a reduction in light perception.

5.2.5. *OHP1* and *OHP2* regulation of the tetrapyrrole pathway

5.2.5.1. LIL-family sequence analysis

Previously *OHP1* was identified as a potential homolog of the ScpE protein from *Synechosystis* (Jansson *et al*., 2000), which has been shown to regulate the tetrapyrrole pathway through the Glu-TR enzyme, along with ScpB (Xu *et al*., 2002). Using the nucleotide sequences for ScpB and ScpE from *Synechosystis sp. PCC 6803*, obtained from the Cyanobase online resource (Nakamura, 2000), a BLASTx search was run here against the *Arabidopsis* genome.

Both ScpB and ScpE yielded OHP1 in the top three results for *Arabidopsis*, giving a 40.0 and 36.2 score, respectively, suggesting that a similar role for OHP1 may

exist in *Arabidopsis*. Interestingly, the ScpB and ScpE sequences are also more similar to OHP1 than the OHP2, ELIP, SEP or LIL3 proteins. However, it seems that ScpB is more homologous to the C-terminal region of ferrochelatase II than OHP1, and ferrochelatase II also appears in the results for ScpE.

5.2.5.2. Helix analysis

Based upon the confirmation of OHP1 homology with ScpB and/or ScpE, a BLASTp search covering *Arabidopsis thaliana* was conducted on the membrane spanning helix (MSH) of OHP1 and an alignment (figure 5.23a) and phylogenetic tree (figure 5.23b) were constructed from this information.

This search yielded all of the *LIL* genes (*ELIP*, *SEP*, *LIL3* and *OHP2*) previously identified, but also a number of other interesting results. The C-terminal region of ferrochelase II, which was identified previously as having high homology with ScpB, was also shown here to have a high level of similarity with the second helix of ELIP1 and ELIP2. This helix region on FC2 is likely filling the role of ScpA, which was previously shown to associate with the ferrochelatase from *Synechosystis* (Jansson, 1999). Secondly, two previously unidentified proteins, RDCP (Rieske (2Fe-2S) Domain Containing Protein; encoded by At1g17500) and FKBP-type (FK506 Binding Protein-type peptidyl-prolyl cis-trans isomerise; encoded by At3g12340), and the PsbS protein all align well with the MSH from OHP1. While the FKBP-type helix is most similar to the first helix from ELIP1 and ELIP2, RDCP and PsbS are most similar to each other. Finally, it is interesting that, while OHP2 groups most closely with the SEP1 and SEP2 proteins, OHP1 and ScpE are found together on a separate branch. This strongly suggests that OHP1 may be an ortholog of ScpE, and therefore regulate the Glu-TR enzyme in the tetrapyrrole pathway.

Additionally, the ConPred online program (Arai *et al*., 2004) was used to generated a protein structure model for OHP1 and OHP2 (figure 5.24). This indicates that while the length of the internal C-terminus of the proteins are similar, the sequence of the MSH and the size of the external N-terminus are different, which might suggest different functions within the plant.

a)

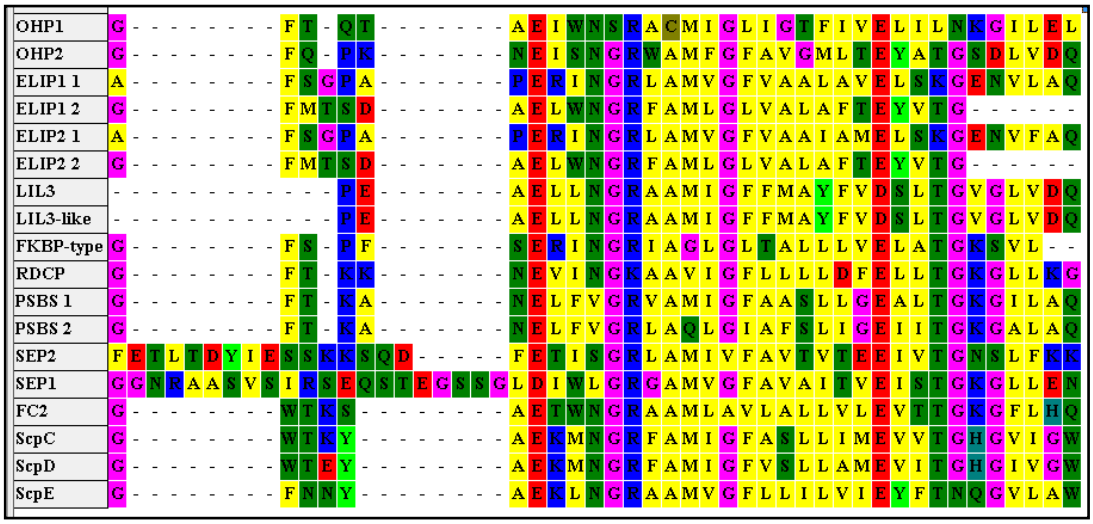

b)

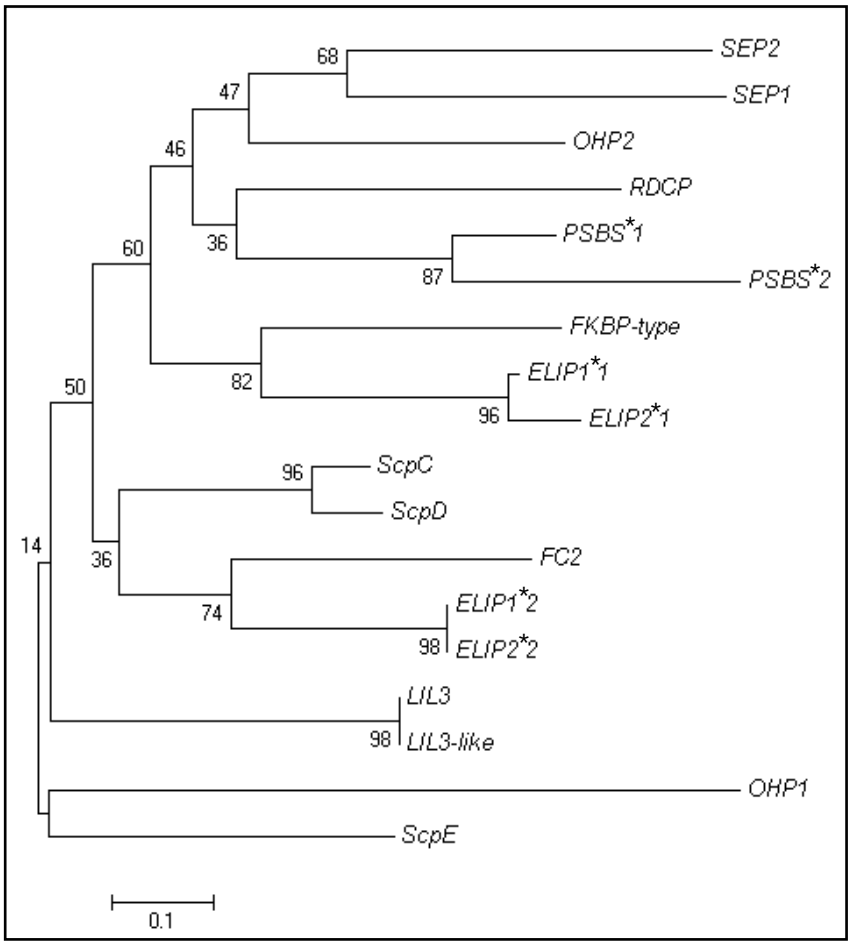

Figure 5.23 Phylogenetic analysis of *LIGHT HARVESTING CHLOROPHYLL* a/b *BINDING PROTEIN-like* (*LHC*-like) genes with significant similarity to the Membrane Spanning Helix (MSH) from *OHP1*. a) Alignment of the MSH from *Arabidopsis* LHC-like genes and the *Small CAB-Like Protein* (*Scp*) genes from *Synechosystis sp. PCC 6803.* b) Phylogenetic tree generated from the alignment in (a). Starred (*) numbers following gene names relate to helix number. NB: the MSH from ScpA and ScpB would not align to the LHC-like genes from *Arabidopsis thaliana* and are therefore omitted. Numbers indicate the percent Bootstrap value.

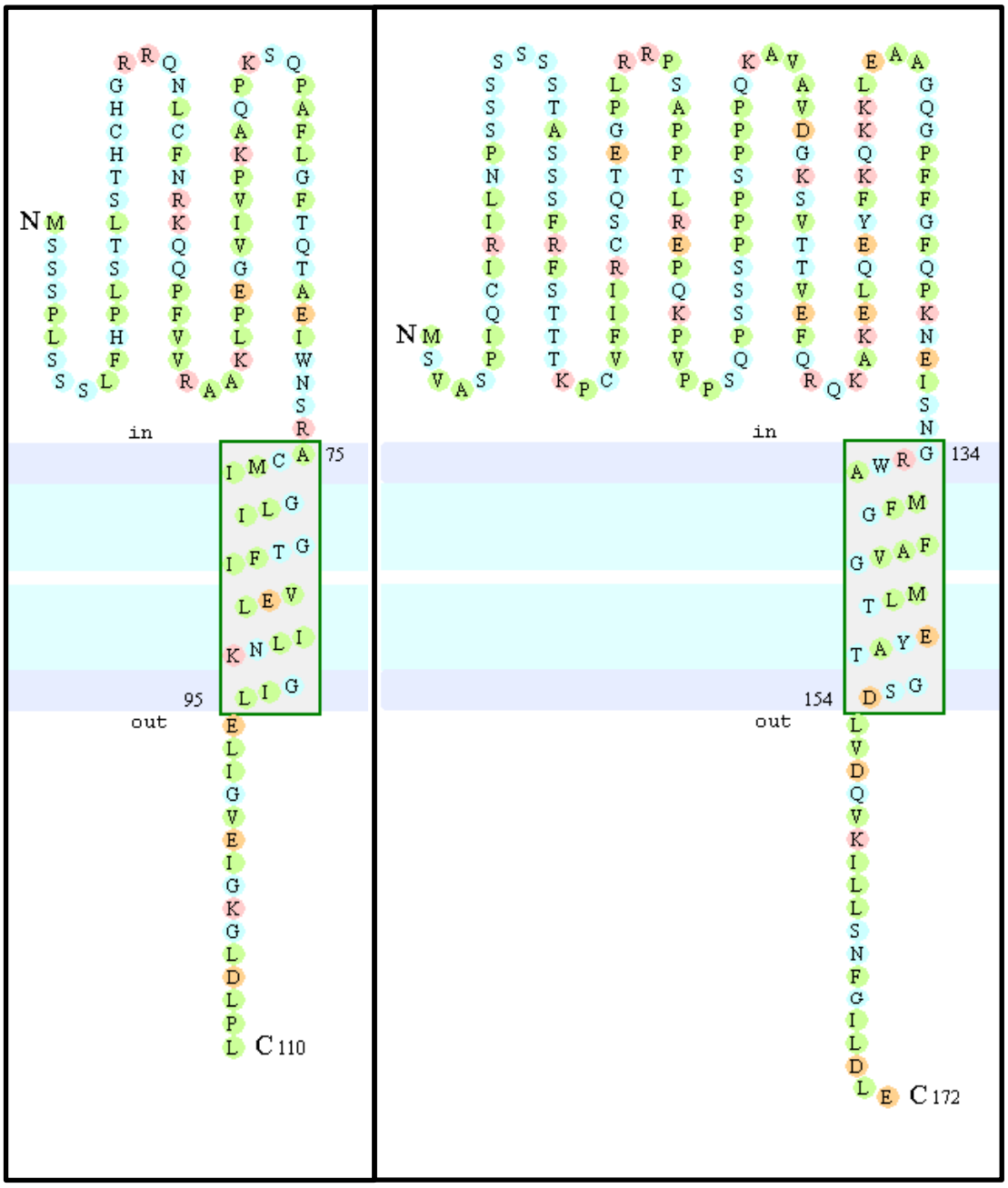

Figure 5.24 Analysis of the predicted protein structure of OHP1 (a) and OHP2 (b), generated using the ConPred online program (Arai *et al*., 2004).

5.2.5.2. Expression of the LIL genes

5.2.5.2.1. Bioinformatics approach

To further understand the role of the *LIL* genes within *Arabidopsis*, and their potential role in regulating the tetrapyrrole pathway, their expression was studied. Initially, the Genevestigator™ online program was used to highlight the light-inducible nature of the *OHP*, *ELIP* and *LIL3* genes in comparison to *GUN4* (figure 5.25). This indicates that the both *OHP* genes and *LIL3* follow a very similar pattern of expression to *GUN4*, and are induced under most light treatments, other than high white light, UV irradiation and a low R-FR ratio. Alternatively, the *ELIP* genes are induced under almost all treatments, but are downregulated by some UV treatments and an 8h photoperiod. The *LIL3-like* gene, on the other hand, is relatively unregulated by any light treatments.

5.2.5.2.2. RT-PCR approach

To follow up on the data gained from Genevestigator™, RT-PCR was conducted to establish the light-induction of the *LIL* genes: *OHP1*, *OHP2*, *ELIP1*, *ELIP2*, *LIL3* and *LIL3-like* following 24h of different wavelengths of light (figure 5.26a). This data confirms that, of the 6 genes studied, only *LIL3-like* shows no light-inductive properties. The 5 remaining genes are upregulated by all wavelengths although this is strongest under Wc and HWc. Additionally, there is only marginal upregulation of *LIL3* by Bc, and *ELIP1* and *ELIP2* by Rc.

As the *ELIP* genes are designated as early light inducible, the expression of these genes was also studied over the initial 2h of Wc and HWc treatment (figure 5.26b). Interestingly the *ELIP* genes show a strong induction of expression under both treatments, while the *OHP* genes are marginally upregulated and the *LIL3* genes are unregulated.

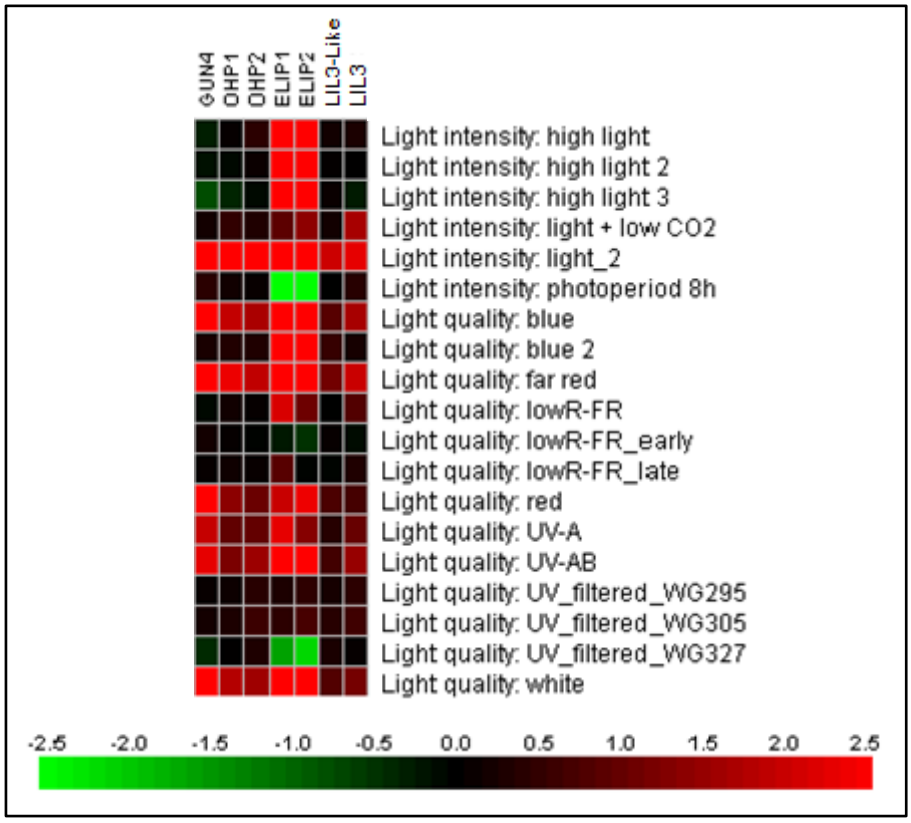

Figure 5.25 Bioinformatics analysis of *LHC*-like gene expression in response to light, using the Genevestigator™ online program (Zimmerman *et al*., 2005).

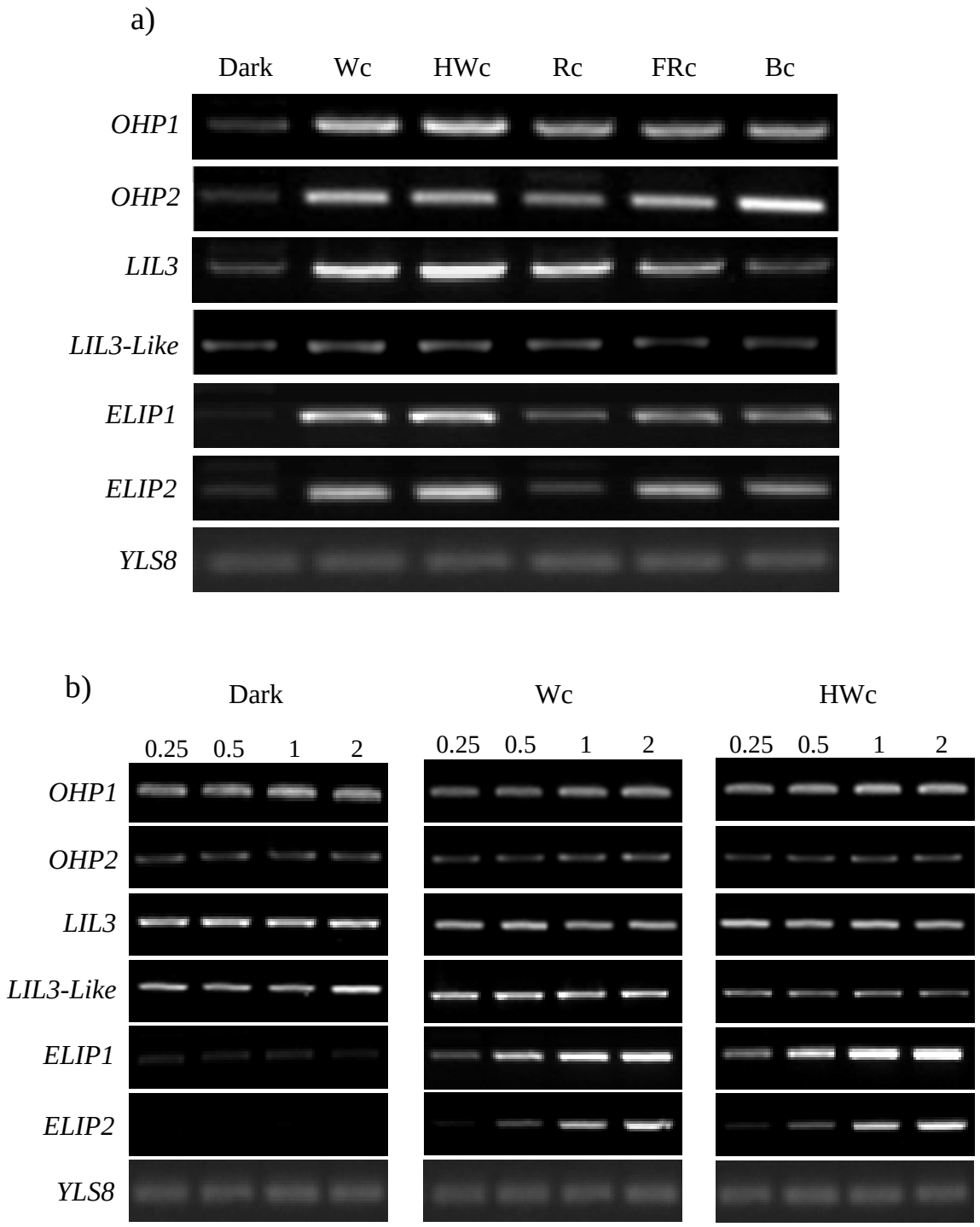

Figure 5.26 Light induced regulation of the *OHP*, *LIL3* and *ELIP* genes analysed by semi-quantitative RT-PCR and compared to the control gene *YLS8*. a) Expression following 2d dark and 24h of dark, white light (Wc; 110 µmol m^{-2} s^{-1}), high white light (HWc; 550 µmol m^{-2} s^{-1}), red (Rc; 80 µmol m^{-2} s^{-1}), far-red (FRc; 10 µmol m^{-2} s^{-1}) or blue (Bc; 80 µmol m^{-2} s^{-1}) light treatment. b) Expression following 2d dark and up to 2h dark, Wc or HWc. One of three repeat experiments, with similar results, is shown.

5.2.5.3. The *ohp1* and *ohp2* mutants

To further understand the role of *OHP1* and *OHP2* within the plant, and elucidate whether they might be functioning as regulators of the tetrapyrrole pathway, analysis of *ohp1* and *ohp2* mutants was undertaken.

5.2.5.3.1. Production of the *ohp1* and *ohp2* mutants

Segregating populations of three independent *ohp1* T-DNA insertion lines (designated 272, 362 and 631) and one *ohp2* insertion line (designated 071) were obtained from the GABI-KAT population (Li *et al*., 2007; figure 5.27). Ten seeds were initially planted on soil, with no selection, and plants (designated 1-10) were tested after ~4 weeks for homozygosity via gPCR. As no homozygote lines were identified a random selection of heterozygote plants were self fertilised and 5 offspring from each (designated 1-5) were planted and tested for homozygocity. As the second round of screening also produced no homozygote plants, seeds were individually plated on ½ MS media, containing no supplementary sucrose, to test for seed/seedling viability. All lines achieved >95% germinated, however, for all lines tested ~25% of seedlings produced completely white cotyledons, and consequently died within 10 days of germination (Table 5.5 and figure 5.28). These lethal seedlings are presumed to be the homozygote mutants from each line. The only exception was seedlings from *ohp1* line 631 which produced faintly green cotyledons but grew at a considerably reduced rate compared to WT. This initial survival of *ohp1* 631 might relate to the insert being present in the promoter of this line, which might allow some expression of *OHP1*.

Previously, mutants which have been shown to present a similar phenotype to *ohp1* and *ohp2*, such as *sco1* (*snowy cotyledons 1*; Albrecht *et al*., 2006), were able to be rescued through growth on media supplemented with sucrose. *ohp1* and *ohp2* segregating mutant lines were therefore grown on ½ MS media supplemented with 1.5% sucrose (Table 5.6 and figure 5.28).

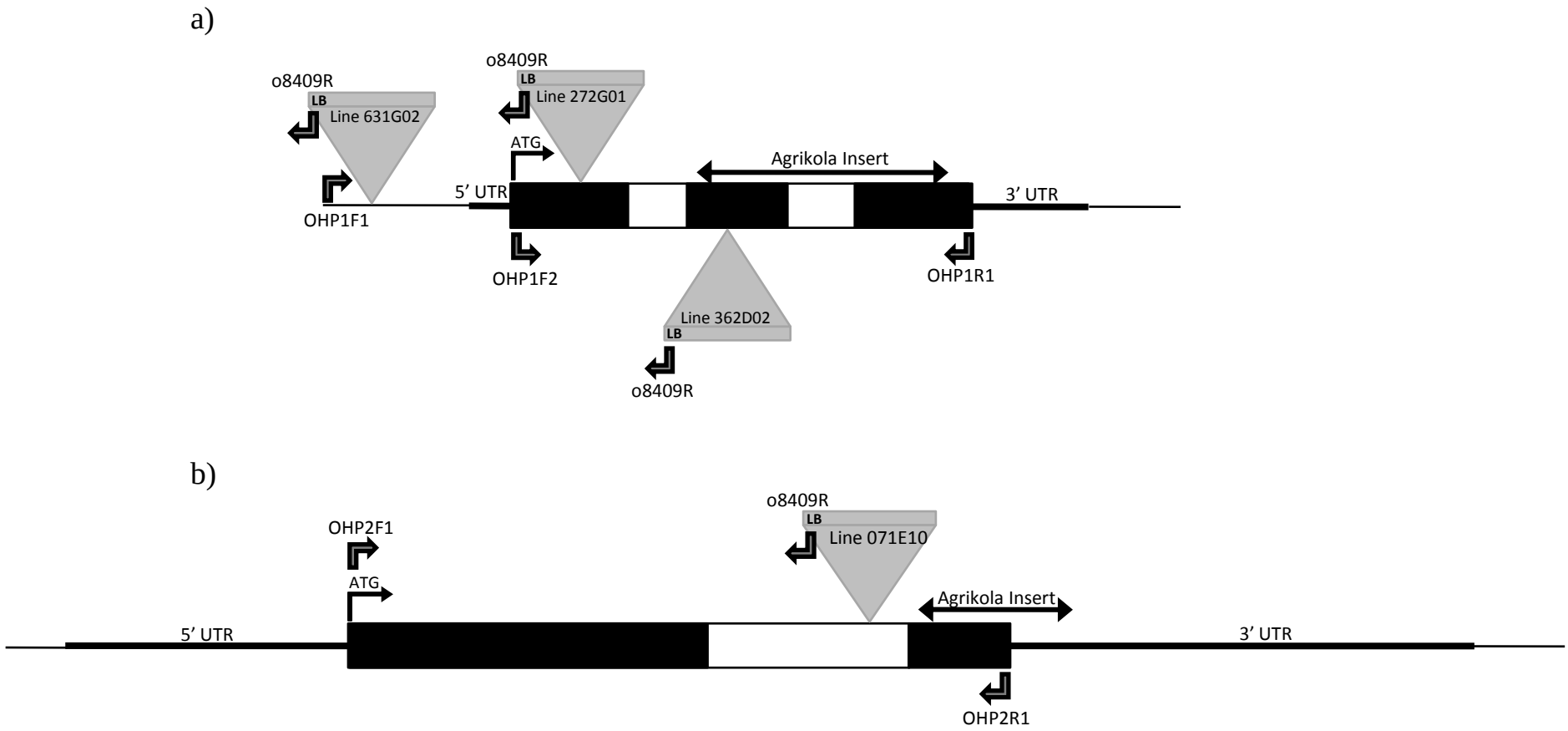

Figure 5.27 Insertional mutagenesis of the *OHP1* (a) and *OHP2* (b) genes from *Arabidopsis thaliana*. Figures are drawn to scale and indicate the position of three inserts (272, 362 and 631) in the OHP1 gene, and single insert (071) in the OHP2 gene. Primers used for insert confirmation are shown. 1cm = 100bp.

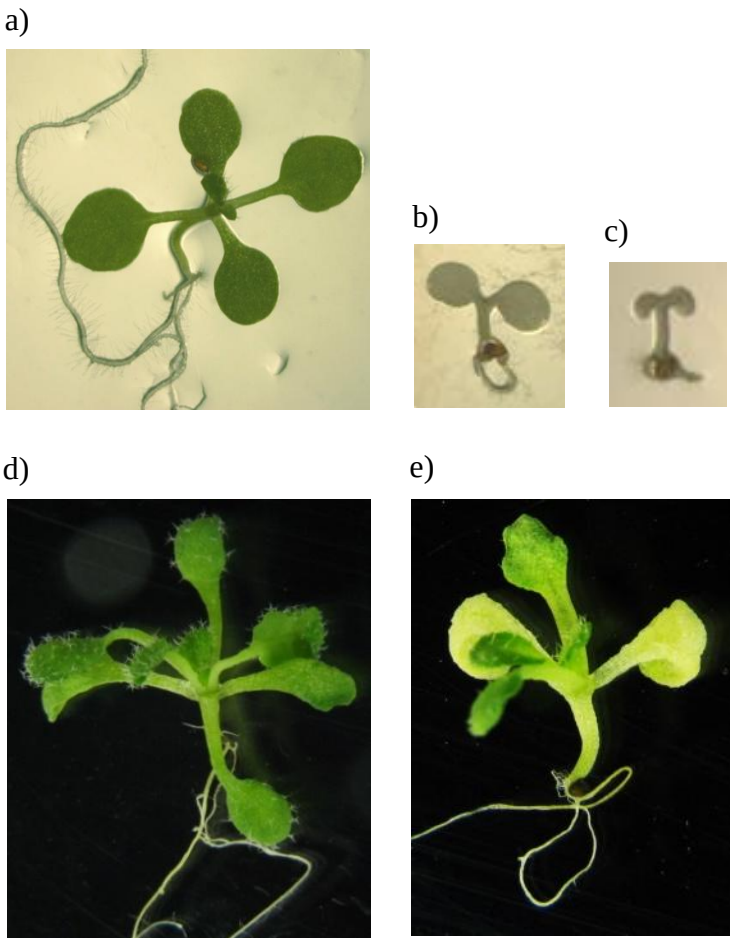

Figure 5.28 Seedling phenotype of the *ohp1* and *ohp2* mutants from *Arabidopsis thaliana*. a) WT, b) *ohp1* (362) and c) *ohp2* (071), following 14d Wc (110 µmol m^{-2} s^{-1}) on ½ MS media without supplementary sucrose. d) WT and e) *ohp1* (362) following 14d Wc (110 µmol m^{-2} s^{-1}) on ½ MS media containing 1.5% supplementary sucrose . All photographs are representative of the population and are to scale.

Table 5.5 Segregating *ohp* mutant seedling survival on media containing ½ MS salts, and no supplementary sucrose.

Plant Line	Bleached	Greened	% Bleached
***ohp1* 272 2.1**	15	39	27.78
***ohp1* 272 3.1**	16	41	28.1
***ohp1* 272 7.1**	14	35	28.6
***ohp1* 362 1.2**	13	30	30.2
***ohp1* 362 2.2**	11	35	23.9
***ohp1* 362 3.2**	9	39	18.8
***ohp1* 631 1.1**	13*	30	30.3
***ohp1* 631 2.1**	8*	29	21.6
***ohp1* 631 3.1**	14*	34	29.2
***ohp2* 071 5.1**	10	32	23.8
***ohp2* 071 8.1**	9	23	28.1
***ohp2* 071 10.1**	2	40	4.7

* = seedlings produced faintly green cotyledons but failed to mature.

Table 5.6 Segregating *ohp* mutant seedling survival on media containing ½ MS salts, and 1.5% supplementary sucrose.

Plant Line	Bleached	Greened	% Bleached
***ohp1* 272 2.1**	0	42	0
***ohp1* 272 3.1**	0	43	0
***ohp1* 272 7.1**	0	39	0
***ohp1* 362 1.2**	1	38	2.54
***ohp1* 362 2.2**	1	45	2.17
***ohp1* 362 3.2**	1	43	2.33
***ohp1* 631 1.1**	0	50	0
***ohp1* 631 2.1**	0	39	0
***ohp1* 631 3.1**	0	44	0
***ohp2* 071 5.1**	1	45	2.17
***ohp2* 071 8.1**	2	56	3.45
***ohp2* 071 10.1**	1	44	2.32

Following growth on media containing sucrose, although the cotyledons of homozygote seedlings were still colourless, true leaves were able to form, presumably because energy provided by the sucrose was compensating for the non-photosynthetic cotyledons. In an attempt to produce a population of homozygote seed, following 2 weeks growth on media containing supplementary sucrose, seedlings were transplanted to soil. However, despite the green true leaves homozygote plants were still unable to survive on soil, while WT and heterozygote plants transferred

successfully. *ohp1* line 631 were the only exception and transferred to soil successfully, although these mutants again showed a reduced growth rate and did not reach a reproductive phase.

5.2.5.3.2. The phenotype of *ohp* mutants grown in the dark

To assess whether the lethality of the *ohp* mutants is related, and limited to, photomorphogenic growth, segregating populations were grown in the dark to assess their skotomorphogenic phenotype. Figure 5.29 indicates that hypocotyl length in the segregating populations follows a normal gaussian distribution, and as >95% of seedlings germinated (data not shown), this indicates that the *ohp* mutations do not impact on dark growth. Consequently the role of the *OHP* genes in regulating the tetrapyrrole pathway was determined through the ability of these mutants to accumulate protochlorophyllide (figure 5.30).

While Pchlide accumulation is unaffected in the *ohp2* 071 mutant line compared to WT, in all of the *ohp1* lines, and particularly the stronger 272 and 362 lines, there is a reduction in Pchlide accumulation. Additionally, as the reduction in Pchlide has presumably come entirely from the homozygote seed (~25%), this is a significant reduction. This result correlates well with the hypothesis that *OHP1* is a homolog of the ScpE gene from *Synechosystis*, which was shown to positively affect chlorophyll biosynthesis through alterations in Glu-TR activity (Xu *et al*., 2002).

5.2.5.4. *OHP1* and *OHP2* overexpression lines

5.2.5.4.1. Production of the *OHP1* and *OHP2* overexpression lines

OHP1 and *OHP2* overexpressing lines were produced using the same protocol as for *GUN4* (see section 5.2.1.3.1.), although only WT plants were used for transformation. The survival of T2 and T3 seedlings, from growth on hygromycin selective media, is shown in Table 5.7 and Table 5.8, respectively, and the OHP1 and OHP2 pMDC32 constructs are shown in figure 5.31.

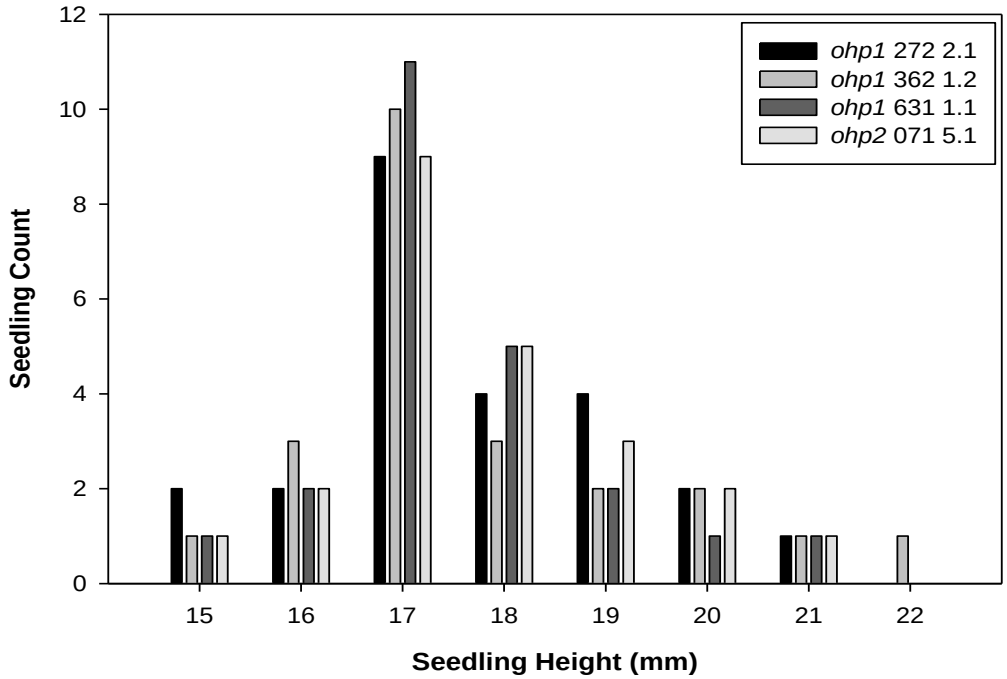

Figure 5.29 Hypocotyl length of the *ohp1* and *ohp2* mutants following 5d dark treatment. Numbers are generated from a single plate from which >95% germination was achieved, and is representative of all replicates.

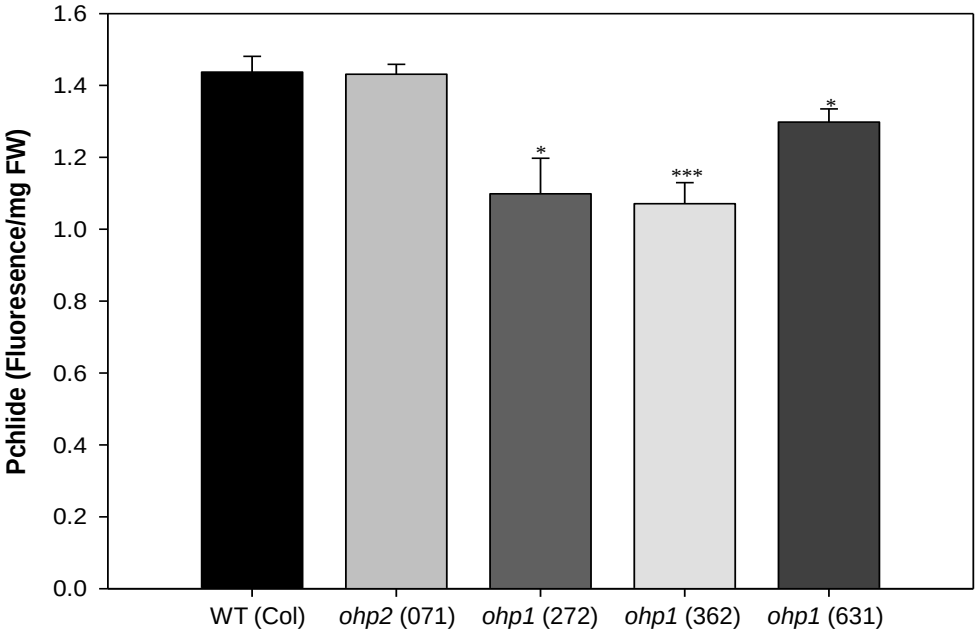

Figure 5.30 Protochlorophyllide accumulation in the *ohp1* and *ohp2* mutants using segregating populations, compared to WT, following 5d dark treatment. * = P = <0.05, *** = P = <0.005. Values are mean ± SE of 4 independent experiments.

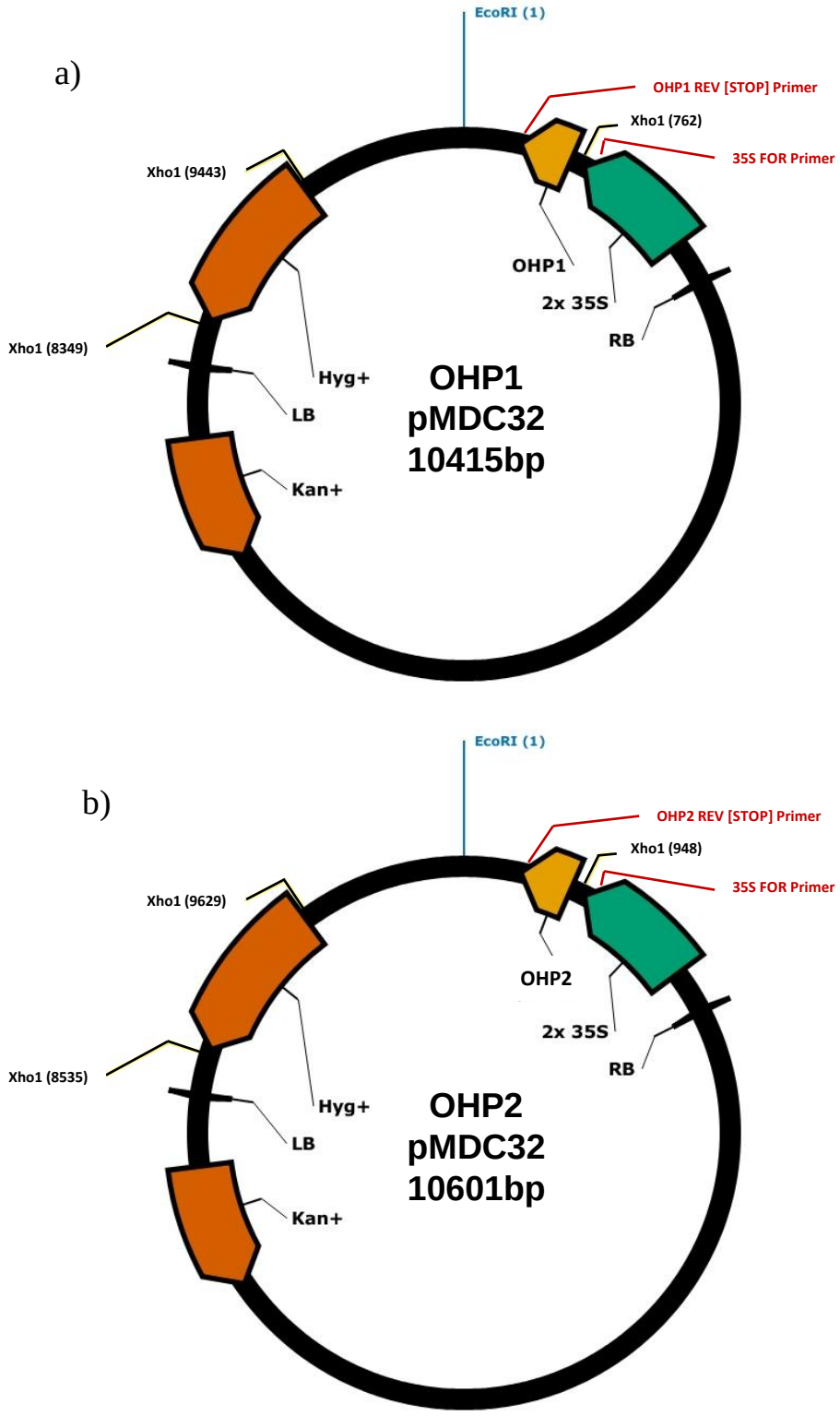

Figure 5.31 OHP1 pMDC32 and OHP2 pMDC32 constructs used to produce *OHP1* (a) and *OHP2* (b) overexpression lines. Genetic material between the left border (LB) and right border (RB) was transformed into *Arabidopsis* using *Agrobacteria*, where the hygromycin (Hyg+) resistance gene allowed selection of successfully transformed plants and the 2x 35S CaMV promoter inferred overexpression of the *OHP1* or *OHP2* gene. The Kanamycin (Kan+) resistance gene, which is not transferred to the plant, allowed selection of successful transformation in *E.coli* and *A.tumefaciens*. Primer and restriction sites, used to confirm successful plasmid recombination during production, are indicated.

Table 5.7 Survival of T2 *OHP1 and OHP2* overexpressing lines on selective media containing hygromycin antibiotic.

Plant Line	Died	Survived	% Survived	Predicted Insert Number
OHP1 1.1	8	40	83.3	1
OHP1 1.2	9	28	75.7	1
OHP1 3.1	4	12	75	1
OHP1 3.2	6	16	72.7	1
OHP1 6.1	7	29	80.6	1
OHP1 6.2	7	32	82.1	1
OHP1 6.3	8	27	77.1	1
OHP2 2.3	7	31	81.6	1
OHP2 2.4	8	29	78.4	1
OHP2 4.1	0	45	100	2+
OHP2 4.2	0	42	100	2+
OHP2 5.1	9	34	79.1	1
OHP2 5.2	6	22	78.6	1
OHP2 5.4	7	33	82.5	1
WT	54	0	0	0

5.2.5.4.2. Confirmation of insert presence and level of overexpression

Seedlings from each of the homozygote lines, along with WT, were grown under Wc for 5d. Insert presence was confirmed by DNA extraction and PCR (figure 5.32a). The overexpressing capacity of the homozygote transformants was then tested through RNA extraction and RT-real time PCR (figure 5.32b). This indicates that all homozygous lines are overexpressing *OHP1* or *OHP2*, although the level of expression is much weaker than was seen previously for either the *GUN4* or *FLU* constructs (figure 5.5 and figure 5.11, respectively).

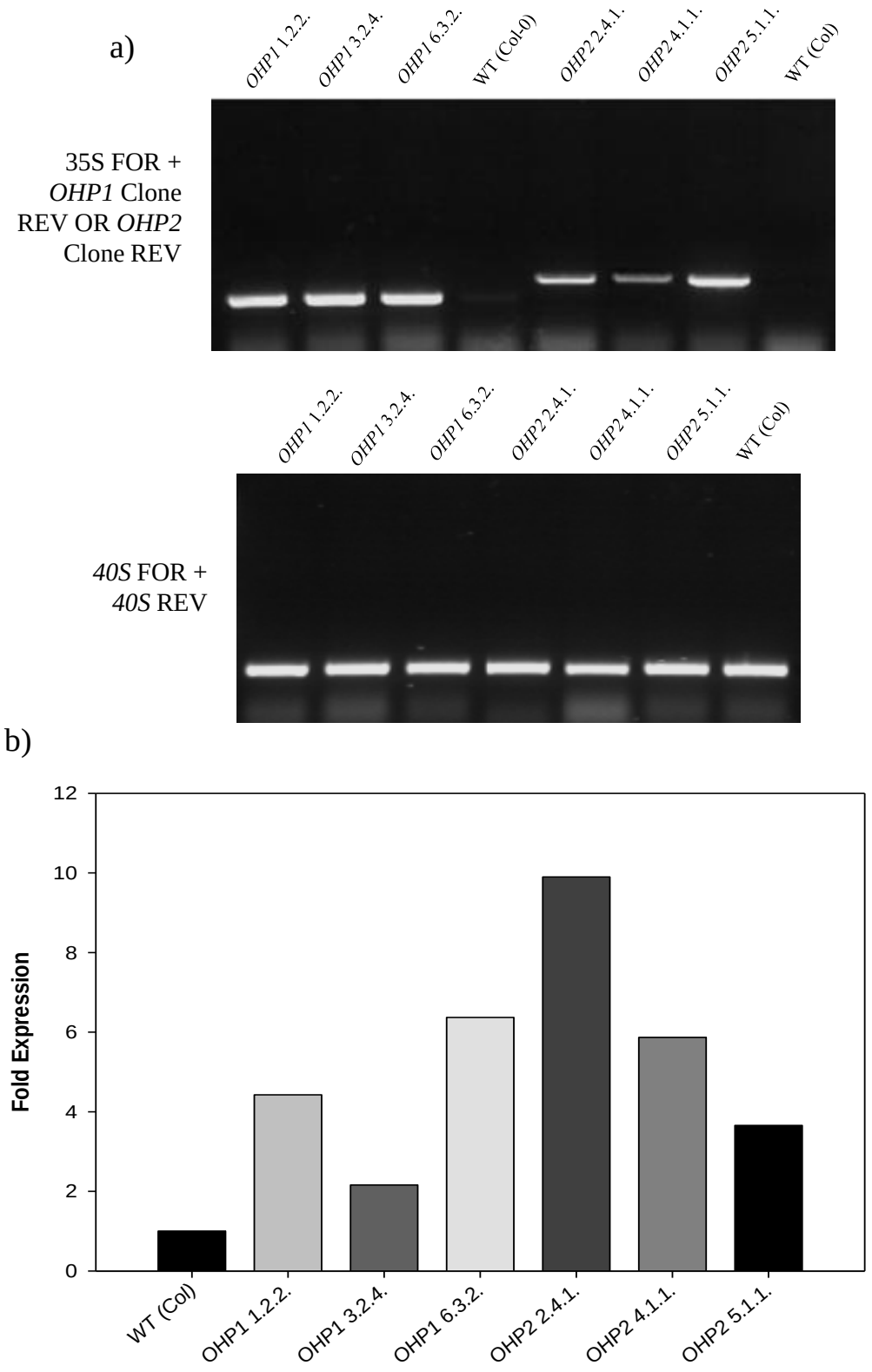

Figure 5.32 Confirmation of the presence of the 35S:*OHP1* and 35S:*OHP2* constucts in transgenic *Arabidopsis thaliana* plants. a) gPCR reaction confirming the presense of the over expressing construct in 3 35S:*OHP1* and 3 35S:*OHP2* transgenic lines, and the absence of the construct in a WT plant, b) expression of *OHP1* and *OHP2* in transgenic plants compared to WT calculated using real-time PCR, following 7d white light (110 µmol m^{-2} s^{-1}) growth (n = 1).

Table 5.8 Survival of T3 *OHP1 and OHP2* overexpressing lines on selective media containing hygromycin antibiotic.

Plant Line	Died	Survived	% Survived	Result
OHP1 1.2.1	9	20	69	Het
OHP1 1.2.2.	0	40	100	**Hom**
OHP1 1.2.3.	9	35	79.56	Het
OHP1 1.2.4.	9	31	77.5	Het
OHP1 3.2.4.	0	27	100	**Hom**
OHP1 6.1.1.	35	0	0	WT
OHP1 6.1.4.	31	0	0	WT
OHP1 6.2.1.	35	1	2.8	WT
OHP1 6.2.2.	36	0	0	WT
OHP1 6.3.1.	9	29	76.3	Het
OHP1 6.3.2.	0	42	100	**Hom**
OHP2 2.3.4.	40	0	0	WT
OHP2 2.4.1.	0	45	100	**Hom**
OHP2 2.4.4.	6	46	88.5	Het
OHP2 4.1.1.	0	50	100	**Hom**
OHP2 4.1.2.	0	48	100	**Hom**
OHP2 4.1.4.	0	44	100	**Hom**
OHP2 4.2.3.	0	45	100	**Hom**
OHP2 4.2.4.	0	48	100	**Hom**
OHP2 5.1.1.	0	47	100	**Hom**
OHP2 5.1.2.	2	35	94.6	Het
OHP2 5.1.3.	0	46	100	**Hom**
OHP2 5.1.4.	0	45	100	**Hom**
OHP2 5.2.1.	5	35	87.5	Het
OHP2 5.2.4.	9	38	80.9	Het
OHP2 5.4.3.	0	46	100	**Hom**
OHP2 5.4.4.	7	33	82.5	Het

Het = heterozygous, Hom = homozygous, WT = wild type.

5.2.5.4.3. Pchlide and chlorophyll accumulation in the OHP overexpression lines

Previously, the ScpB and ScpE genes from *Synechosystis* have both been shown to positively affect chlorophyll biosynthesis through alterations in Glu-TR activity (Xu *et al*., 2002). Additionally, the segregating *ohp1* mutant was shown to be deficient in protochlorophyllide accumulation, although the segregating *ohp2* mutant contained WT levels (figure 5.30). Protochlorophyllide and chlorophyll accumulation was therefore determined in the *OHP1* and *OHP2* overexpressing seedlings (figure

5.33).

In the *OHP1* overexpressing lines both protochlorophyllide and chlorophyll levels are comparable to WT. However, the overexpression of *OHP2* has reduced the ability of the seedling to accumulate either Pchlide or chlorophyll. For both pigments the OHP2 4.1.1 line has the largest reduction, despite these seedlings not showing the highest expression.

5.2.5.4.4. Control of hypocotyl extension in the OHP overexpression lines

To further characterise the ability of the *OHP* genes to regulate the tetrapyrrole pathway, the hypocotyls of the *OHP1* and *OHP2* overexpression lines were measured following red, far-red and dark treatment (figure 5.34). Under all conditions the *OHP2* lines show a WT hypocotyl length, indicating that phytochromobilin synthesis is not affected. However, all of the *OHP1* overexpressors show a hypersensitive response to red light but not far-red or dark, suggesting a possible role in phyB synthesis or signalling.

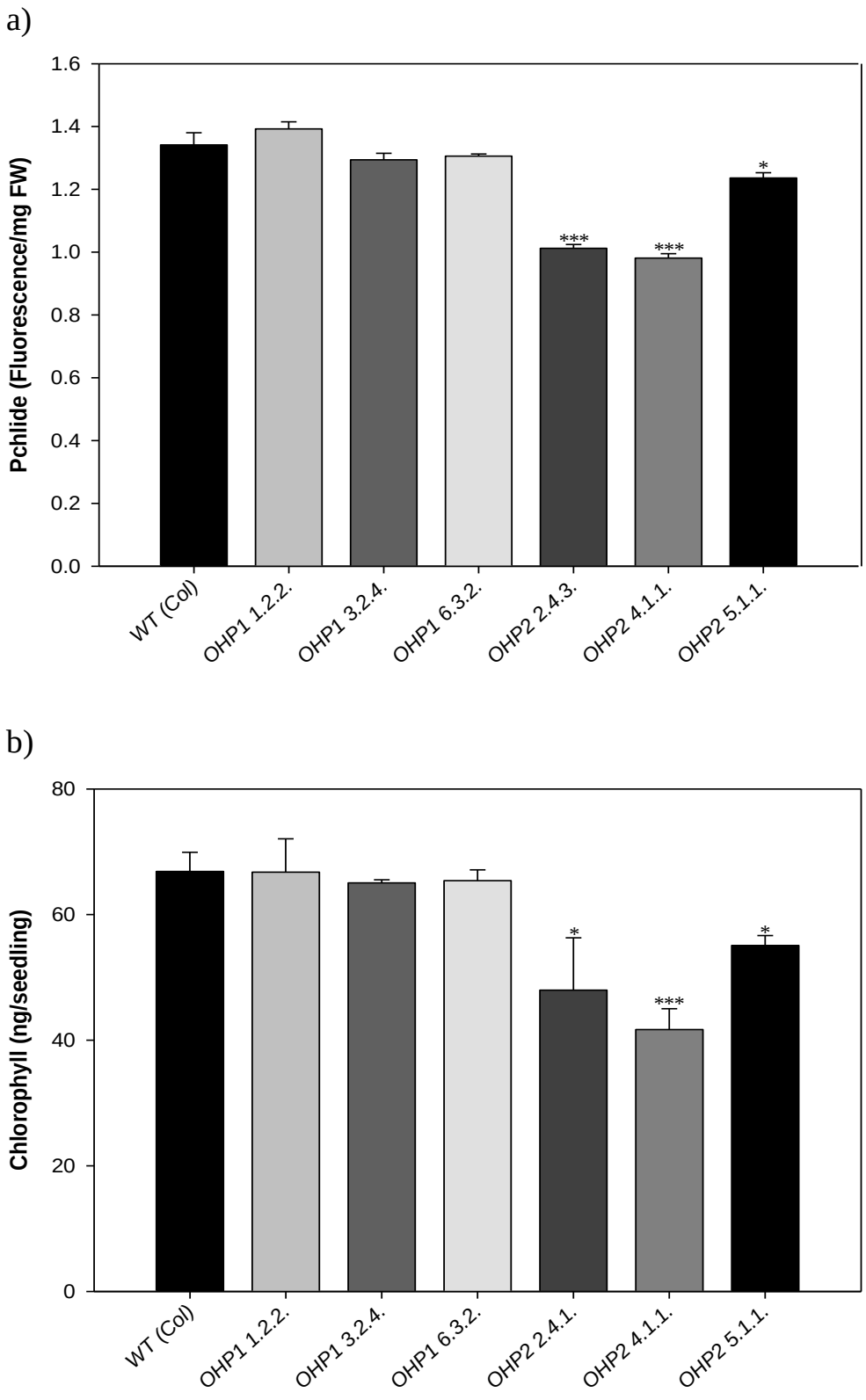

Figure 5.33 Protochlorophyllide and chlorophyll accumulation in the *OHP1* and *OHP2* over expressing plants, compared to WT. a) Protochlorophyllide accumulation following 5d dark treatment, b) chlorophyll accumulation following 2d dark and 24h Wc (110 µmol m^{-2} s^{-1}). * = P = <0.05, *** = P = <0.005. Values are mean ± SE of 4 independent experiments.

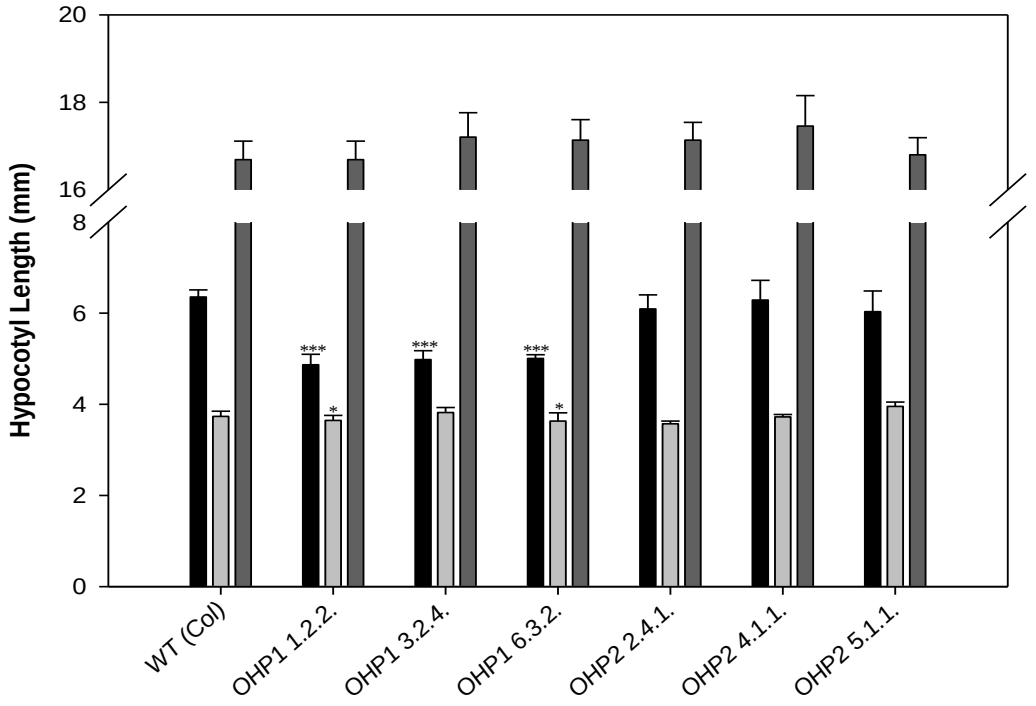

Figure 5.34 Hypocotyl length of the *OHP1 and OHP2* over expressing plants, compared to WT, following 1d dark and 5d red light (80 µmol m^{-2} s^{-1}) (black bar), far-red light (10 µmol m^{-2} s^{-1}) (light grey bar) or dark (dark grey bar). * = P = <0.05, *** = P = <0.005. Values are mean ± SE of 3 independent experiments.

5.3. Discussion

5.3.1. *GUN4* regulates multiple aspects of the tetrapyrrole pathway

Manipulation of the *GUN4* gene, to cause both an increase and a reduction in expression, demonstrates that it is a critical regulator of the tetrapyrrole pathway on multiple levels. Previously it has been shown that mutations in *GUN4* result in a decrease in chlorophyll accumulation (Larkin *et al*., 2003), and this was confirmed in the current study which shows a marked reduction in chlorophyll synthesis under Rc, Bc and Wc during de-etiolation. Additionally, overexpression of *GUN4* results in an increase in the synthesis of both Pchlide in the dark and chlorophyll following light transfer.

Earlier studies have suggested that *GUN4* acts as a chaperone of protoporphyrin IX to the Mg-chelatase enzyme (Larkin *et al*., 2003; Davison *et al*., 2005; Verdacia *et al*., 2005), and thus loss of GUN4 results in a reduction of Mg-chelatase activity and consequently less chlorophyll. However, it was also shown here that the *gun4* mutant is also less able to regulate hypocotyl extension under Rc and FRc, but not in the dark, suggesting a reduction in light detection, which may not be explained by the current hypothesis.

Previously it has been shown that alterations in *CHLM* transcript level, through overexpression and silencing, led to changes in Glu-TR and Mg-chelatase expression and activity (Alawady and Grimm, 2004). Similarly, in the current study the light inductive expression of tetrapyrrole synthesis genes were analysed in the *gun4* mutant. Although this data did not suggest any impact on the expression of *HEMA1* or *CHLH*, two of the major sites of regulation of the pathway, loss of *GUN4* activity did result in a reduction in *FC1*, *HO1*, *PORA* and *CAO* expression. These changes in expression, which do not necessarily relate to protein content or enzyme activity, may explain both the chlorophyll and hypocotyl data. Firstly, a reduction in *CAO* activity results in a higher chlorophyll *a*/*b* ratio (Oster *et al*., 2000), and a reduction in *HO1* or *HY1* activity causes a reduced rate of phytochromobilin synthesis, and therefore a reduction in phytochrome content (Weller *et al*., 1996; Terry and Kendrick, 1996; Lagarias *et al*., 1997; Davis *et al*., 1999). Interestingly, a reduction in *HO1* activity has also been

shown to increase chlorophyll *a*/*b* ratios (Weller *et al*., 1996). Additionally, as *HEMA1* is well established as being regulated through the plastid signal (McCormac *et al*., 2001) but is unaffected in this study, this suggests a more direct mode of regulation. Alternatively, but not entirely exclusively, Davison *et al*. (2005) suggested that *GUN4* may also be required to channel protoporphyrin IX towards Fe-chelatase, which could account for both a direct reduction in phytochromobilin synthesis, and an indirect reduction in chlorophyll synthesis through negative feedback inhibition due to increased haem levels, in the *gun4* mutant.

It is also interesting to note that increasing *GUN4* transcript can increase the capacity for chlorophyll accumulation, indicating that ambient GUN4 levels, under normal conditions, are limiting to chlorophyll synthesis.

5.3.2. Overexpression of *FLU* reduces flow through the tetrapyrrole pathway

Previously it has been shown that the FLU protein is a critical regulator of the tetrapyrrole pathway through repression of the Glu-TR enzyme (Meskauskiene and Apel, 2002), as such the *flu* mutant fluoresces under blue light due to vast increases in protochlorophyllide accumulation (Mesauskiene *et al*., 2001). Additionally, this regulation was shown to be independent of haem negative feedback and light signalling (Goslings *et al*., 2004). However, although *FLU* orthologs have been found in other species (e.g. barley, Lee *et al*., 2003b), the exact requirement for *FLU* as a regulator of the pathway is as yet unknown.

In the present study *FLU* overexpressing lines were analysed in their ability to regulate the tetrapyrrole pathway. In assays used to establish control of the chlorophyll and haem branch (Pchlide/chlorophyll accumulation (figure 5.12) and hypocotyl length under red and far-red light (figure 5.13), respectively) there is evidence to suggest that these seedlings have a reduced flow through the pathway. However, one might have expected a lethal effect as a result of a marked reduction in haem synthesis, due to the dramatic phenotype of the *flu* mutant (figure 5.12; Meskauskiene *et al*., 2001). Collectively, this data suggests that the FLU protein is required to constitutively reduce, but not inhibit, Glu-TR activity under most conditions. As a

result increasing the FLU content of the seedling can only reduce flow through the pathway through binding the limited amount of free Glu-TR. To add support to this hypothesis it would be interesting to study FLU protein levels in the *FLU* overexpression lines, and attempt to identify conditions under which the FLU protein is regulated in the WT.

5.3.3. ABA signals regulate the tetrapyrrole pathway

In a search of the Genevestigator™ microarray database (Zimmerman *et al*., 2005) for factors that regulate tetrapyrrole genes, the *aba1* and *abi1* mutants were highlighted as specifically negatively regulating the *GUN4* gene (figure 3.19). In this study tetrapyrrole-synthesis gene expression was assayed in the ABA synthesis and signalling mutants *aba1, abi1, abi2, abi3, abi4* and *abi5,* and consequently assessed in their ability to de-etiolate effectively.

Interestingly, these mutations had little or no effect on *GUN4* expression, as none of them displayed a significantly different response to WT (figure 5.14a). On the other hand the light induction of *HEMA1* and *CHLH* was strongly and similarly affected in many of these mutants. In general, mutations in the negative regulators of ABA signalling, *ABI1* and *ABI2*, resulted in a marginal upregulation, while the positive regulators, *ABI3*, *ABI4* and *ABI5*, resulted in a downregulation (figure 5.14b and 5.14c). Collectively this would suggest that ABA is normally responsible for an increase in activity of the pathway. This has been suggested previously as the *aba1* mutant, which is required for ABA synthesis, is chlorophyll deficient (Pogson *et al*., 1998). However, in the current study the *aba1* mutant was shown to significantly upregulate *HEMA1* and *CHLH* expression. This might therefore suggest that ABA is involved in the degradation of chlorophyll rather than the synthesis, which could be related to a lack of the photo-protective compounds xanthophylls, thereby resulting in a feedback to upregulate chlorophyll synthesis.

PORA expression is also, in general, closely linked with *HEMA1* and *CHLH*, where *PORA* is marginally more downregulated in the *abi1* and *abi2* mutants, and less downregulated in the *abi4* and *abi5* mutants (figure 5.14d). However, expression of

PORA is downregulated in the *aba1* mutant and upregulated in the *abi3* mutant, which is not consistant with *HEMA1* and *CHLH* expression. On the other hand, *PORA* expression very closely correlates with chlorophyll accumulation in these mutants (figure 5.13b), which indicates that the downregulation of POR, which is controlled by the phytochromes (Runge *et al*., 1996), is also a determinant of chlorophyll levels. When the hypocotyl lengths of these mutants was measured in the dark and following red and far-red light treatment there was little change in any of the mutants compared to WT. Only the *abi4* mutant showed any significant increase in hypocotyl length, and this was specific to red light suggesting an involvement in phyB signalling rather than a lack of phytochromobilin synthesis. However, the downregulation of *HEMA1* expression in the *abi4* mutant, coupled with the lack of chlorophyll, suggests that there may be less flow through the pathway. This might implicate ABI4 as a candidate for ABA regulatory input into the the tetrapyrrole pathway, through which all other signals pass. It has also previously been suggested that ABI4 is required for the chloroplast-to-nucleaus signal via the *GUN1* and *GUN2-5* pathways, and is able to bind the *Lhcb1*2* promotor (Koussevitzky *et al*., 2007), which indicates a link to light signalling networks.

On the other hand, the *aba1* mutant has a shorter hypocotyl under all treatments, and this is consistant with a previous study which showed that *aba1* is partially de-etiolated in the dark (Barrero *et al*., 2008). One interesting point to note is that *abi5* had a WT hypocotyl length under all conditions, however, Chen *et al*. (2008) demonstrated that *ABI5* overexpressing plants had a shorter hypocotyl length due to hypersensitivity to light. The mode of action was shown to be *HY5* interaction with the *ABI5* promotor, and therefore highlighted a key mechanism for the integration of light and ABA signals. However, similar to the current study, the authors also noted that *abi5* mutants did not show any change in hypocotyl length, which could mean that ABI5 is not directly required in light signalling.

In conclusion, it is shown here that many aspects of the ABA signal are able to regulate the tetrapyrrole pathway. The *ABA1* gene, which has been shown previously to regulate de-etiolation in the dark (Barrero *et al*., 2008) and chlorophyll accumulation in the light (Pogson *et al*., 1998), shows a particularly strong response. Of the ABA signalling mutants, *abi4* is the only one to show a consistent

downregulation of genes in the pathway and output from the pathway. It is therefore suggested that ABI4 may be the direct input into the tetrapyrrole pathway through which other aspects of the ABA signal are directed.

5.3.4. *MYB50* and *MYB61* regulate the tetrapyrrole pathway through *GUN4*

MYB50 and *MYB61* are closely related in a family of nearly 200 R2R3-type transcriptional regulators (Stracke *et al*., 2001). Previously MYB transcription factors have been shown to regulate a wide array of target genes, including major synthesis pathways such as the flavonoid pathway (Davies and Schwinn, 2003), and more specifically for *CAB* gene expression (Churin *et al*., 2003). In turn, *MYB* gene expression has been demonstrated to be controlled by a number of cues, such as hormones and light (Chen *et al*., 2006; Takos *et al*., 2006).

In this study the expression of *MYB50* and *MYB61* was studied under different wavelengths of light. Interestingly, while *MYB50* was upregulated under all of the light treatments, *MYB61* was downregulated under similar conditions (figure 5.17). This result allows the hypothesis that *MYB50* and *MYB61* normally antagonistically regulate *GUN4* expression and that this may be subtly controlled by light treatment. Interestingly, *MYB50* was most strongly affected by red and far-red light, and least affected by blue light, and conversely for *MYB61*. This might suggest that *MYB50* is controlled by the phytochome family of photoreceptors, and is more important under red and far-red light, and *MYB61* is controlled by the cryptochromes, and is required under blue light.

Using T-DNA insertion mutants for *MYB50* and *MYB61*, it was demonstrated here that these transcription factors are required for the suppression of *GUN4* expression, but do not regulate the other major targets for chlorophyll regulation, *HEMA1* and *CHLH*. Additionally, as *MYB50* and *MYB61* are regulated antagonistically by light, and *MYB50* is required for suppression of *MYB61* in the light; these genes may be required for precise regulation of the tetrapyrrole pathway during diurnal cycles. Interestingly, Chen *et al*. (2006) showed that *MYB50* and *MYB61* are regulated by both similar and distinct hormone signals; therefore *GUN4*

also provides a site for hormonal control over the tetrapyrrole pathway.

It has been shown previously that the repression of gene transcription by many regulators is often achieved through the presence of a specific motif in the protein sequence of the transcription factor (Hiratsu *et al*., 2003; Ohta *et al*., 2001). This sequence, known as the EAR (ERF-associated Amphiphillic Repression) motif, has been shown to be a present in the class II ETHYLENE-RESPONSIVE ELEMENT-BINDING FACTOR (ERF), TFIIIA-type zinc finger repressors of transcription, that include SUPERMAN (SUP) (Ohta *et al*., 2001), and can cause members of MYB family, such as PAP1, to act as suppressors when bound chimerically to these proteins (Hiratsu *et al*., 2003). Indeed, Hiratsu *et al*. (2003) failed to identify any transcription factors which were not converted to transcriptional repressors when bound to the EAR motif, suggesting that this domain may be used to identify repressive transcription factors. As MYB50 and MYB61 were both shown here to function as repressors of *GUN4* expression they should be key candidates to test this theory, however, the EAR motif was not identified in the protein sequence of either regulator. As a result this might advocate that MYB50 and MYB61 are not required to directly suppress *GUN4* expression, and instead activate another suppressor of this gene, or could simply suggest that the EAR motif is not a general signal for gene repression. It would consequently be interesting to find the exact binding sites of MYB50 and MYB61.

5.3.5. *OHP1* and *OHP2* are regulators of the tetrapyrrole pathway

This study was initially undertaken to establish whether *OHP1*, which is shown to be homologous to the *ScpE* gene from *Synechosystis* (figure 5.23; Jansson *et al*., 2000), and *OHP2*, another member of the *LIL* (Light-Induced-Like) family (Andersson *et al*., 2003), are regulators of the tetrapyrrole pathway. Previously, ScpB and ScpE were shown to regulate chlorophyll synthesis in *Synechosystis* through the Glu-TR enzyme (Xu *et al*., 2002). Additionally, overexpression of *ELIP2*, a close relative of the *OHP* genes, results in a dramatic reduction in chlorophyll content in *Arabidopsis* (Tzvetkova-Chevolleau *et al*., 2007), although mutation of both *elip1* and *elip2* also resulted in a subtle reduction in chlorophyll accumulation (Rossini *et al*.,

2006). In the current study, mutant and overexpression lines of *OHP1* and *OHP2* indicated that they may also have a role in tetrapyrrole-synthesis regulation.

Although there was difficulty in establishing homozygous *ohp* mutant lines it was possible to use the segregating mutant populations, and doing so the *ohp1* 362 line was shown to contain only 74% of the WT protochlorophyllide levels following 5d dark treatment (figure 5.30). This strongly suggests a major role for the *OHP1* gene in regulating Pchlide accumulation in the dark, as a homozygous population would be expected to contain an even lower level. This hypothesis is further supported by the fact that the *ohp1* 631 line, which contains an insert in the promoter region of the gene and is able to survive growth on soil, shows a smaller reduction in Pchlide levels. On the other hand, the *ohp2* mutant segregating population contained WT levels of Pchlide but *OHP2* overexpressors displayed a reduction in both chlorophyll and Pchlide (figure 5.33). As previously discussed, a very similar phenotype was seen in *ELIP2* overexpressing plants (Tzvetkova-Chevolleau *et al*., 2007) and the authors demonstrated that this was due to a general reduction in the activity of the major regulatory enzymes Glu-TR and Mg-chelatase. In contrast the *OHP1* overexpressing seedings contained WT levels of both Pchlide and chlorophyll.

Interestingly, however, the *OHP1* overexpressors did show a reduction in hypocotyl length under red light (figure 5.34), which might suggest an increase in phytochromobilin synthesis, although they did not show any change in hypocotyl length under far-red light. Conversely, the *OHP2* overexpressing lines had a WT hypocotyl length under all treatments, suggesting that the haem branch is unaffected in these seedlings. In conclusion it seems that *OHP1* is indeed acting in a similar manner to ScpE from *Synechosystis*, and certainly suggests that it has control over Pchlide accumulation. However, more work will need to be done to establish whether this control is mediated by changes in Glu-TR activity. On the other hand, *OHP2* appears to be functioning in a more similar manner to *ELIP2* as, although the *ohp2* mutant does not show any phenotype with regards to regulating the tetrapyrrole pathway, the *OHP2* overexpressing line is shown to be deficient in both protochlorophyllide and chlorophyll accumulation.

5.3.6. *OHP1* and *OHP2* are essential for seedling survival during de-etiolation

When the *ohp1* and *ohp2* homozygous mutants were grown on soil or MS media without supplementary sucrose they presented a lethal phenotype. However, growth on media containing supplementary sucrose allowed seedling survival, although the coteledons were still bleached and transfer to soil again resulted in death. It seems apparent that the regulation of the tetrapyrrole pathway by these genes is unlinked to the snowy cotyledon phenotype for a number or reasons: 1) *OHP1* and *OHP2* do not regulate the pathway in the same way, and in fact they appear to oppose each other, 2) there is no increase in protochlorophyllide accumulation in either mutant, which might have resulted in a *flu* phenotype, 3) the possible decrease in haem content in the *ohp1* mutant, due to general reduction in flow through the pathway, should not be rescued on sucrose-containing media.

Previously Budziszewski *et al.* (2001) conducted a T-DNA insert screen for genes that were essential for seedling viability, which resulted in the identification of 131 genes with a similar albino lethal phenotype to those presented here for *ohp1* and *ohp2*. However, neither *OHP1* or *OHP2*, or any of the other *LIL* genes, appeared in the annotated selection of 14 genes they chose to study further.

More recently, Albrecht *et al*. (2006 and 2008) have identified two *snowy cotyledon* mutants (*sco1* and *sco2*), and Mudd *et al*. (2008) characterised the *rne* mutant, all of which have a similar phenotype. Although these genes are all targeted to the chloroplast, they are each shown to have very different functions. *SCO1*, for example, encodes a chloroplast elongation factor G, while *SCO2* encodes a DNAj-like protein, and *RNE* encodes an RNase E/G-like protein. Although this does not point to a possible role for *OHP1* and *OHP2* it does suggest that that they are essential for chloroplast development and/or maintenance during de-etiolation.

It is therefore hypothesised that *OHP1* and *OHP2*, in a similar manner to the Scp genes from *Synechosystis* (Xu et al., 2002; Promnares *et al*., 2006; Yao *et al*., 2007), are essential chlorophyll binding proteins during de-etiolation, as part of the early photosystem complexes. Consequently, they are required to report to the

tetrapyrrole pathway on the availability of chlorophyll, based on the ratio of free to bound OHP protein.

Chapter 6: The Far-Red Block of Greening Response and *saf* Mutants

6.1 Introduction

The chloroplast, which is thought to have derived from an endosymbiotic cyanobacteria, holds a genome containing approximately 60-100 genes (Martin *et al*., 2002; Lopez-Juez and Pyke, 2005). However, the photosynthetic processes that take place within the plastid require a great many more genes, which have are now encoded in the nuclear genome of the host. Indeed, the transfer of nuclear information from the chloroplast to the nucleus has been estimated at one gene for every 16000 pollen grains in tobacco (Huang *et al*., 2003). Consequently the nucleus must communicate with the chloroplast to ensure that synthesis of both groups of proteins is coordinated. Additionally, the chloroplast must communicate with the nucleus for the same reason. These signals, known as 'plastid retrograde signals', are now understood to take at least three forms (discussed in detail in section 1.5), one of which is chloroplast-derived reactive oxygen species (ROS).

The redox state of cells is constantly changing, and this is further enhanced in a photosynthesising cell by the presence of photosynthetic apparatus, which uses light-coupled electron flow to generate energy. Additionally, under high irradiances redox signals are conveyed via the glutathione redox cycle which also results in the production of ROS. Finally, tetrapyrrole intermediates, such as protochlorophyllide (Pchlide), are known to create ROS when exposed to light (reviewed in Pfannschmidt *et al*., 2003). Consequently, determining how the chloroplast is able to direct a precise ROS signal to the nucleus is of great interest and could potentially be of agricultural significance.

Interestingly, although the early stages in the tetrapyrrole pathway are active under far-red light due to the activity of phyA (Dubell and Mullet, 1995), the POR enzyme, which requires activation by light, is not stimulated by this wavelength (Griffiths, 1991). The halt in the pathway at this stage results in an accumulation of protochlorophyllide, a highly phototoxic compound, when *Arabidopsis* is exposed to far-red light. Therefore, following a transfer from an extended period of far-red light

treatment (i.e. more than 2 days) to white light, results death of the seedling in a process known as the far-red block of greening (Barnes *et al*., 1996).

Despite early claims that this response is a direct result of the toxic levels of compounds accumulating within the plant, it has since been discovered that the far-red block of greening infact triggers a programmed cell death response (Barnes *et al*., 1996; McCormac and Terry, 2002b). Programmed cell death requires the stimulation and repression of a number of nuclear genes, which is achieved through the function of a plastid signal. Unlike the proposed Mg-protoporphyrin signal, which was elucidated through the *gun* mutations, the far-red block of greening appears to be caused by a reactive oxygen species (ROS) signal which has yet to be fully elucidated. However, it has also been found, through microarray studies, that these plastid signals are able to affect both similar and distinct sets of genes (McCormac and Terry, unpublished data).

The *gun* mutants, produced in the early 90s (Susek *et al*., 1993), were generated in a screen for plants that retain expression of nuclear-encoded, chloroplast-located genes in the presence of Norflurazon, a herbicide capable of destroying the developing chloroplast. In a similar manner, a screen was conducted in the Terry lab where transgenic seedlings containing the *HEMA1* promoter linked to the *BAR* gene (for PPT herbicide resistance; figure 1.1) were exposed to a 2d far-red followed by 24h white light treatment on PPT-containing media following EMS treatment. Consequently only seedlings that retained HEMA1 expression following a far-red treatment were able to survive; these mutants were then called *saf* (survived after far-red). The maintenance of a plastid signal following this response was presumed to be due to one of three reasons: 1) a disruption of the phyA signalling mechanism resulting in less far-red light perception, 2) mutations in chloroplast biology causing less damage and/or ROS signal, or 3) mutations in the ROS signalling pathway itself. The aim of this study was to characterise the set of *saf* mutants phenotypically, and subsequently start to elucidate the possible function of the disrupted genes.

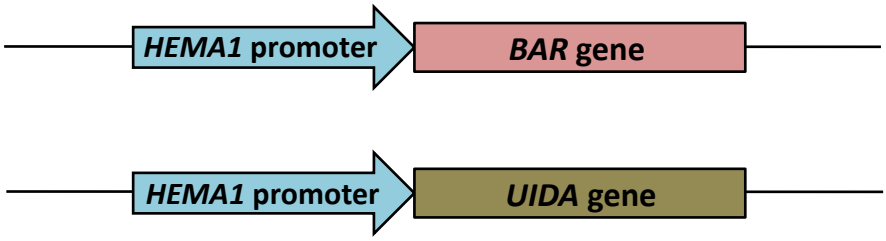

Figure 6.1 Constructs used to produce PT1-1d parental line for the identification of successful *saf* mutation and recovery. The *BAR* gene infers phosphenothricin (PPT) resistance, and *UIDA* allows the use of β-glucuronidase (GUS) for expression studies.

6.2 Results

6.2.1 Phenotypic analysis of the *saf* mutants

A set of 35 *saf* mutants was discovered from the original screen for survivors after far-red light treatment, which exhibited both similar and distinct mature phenotypes. The most commonly observed phenotypes are summarised in Table 6.1.

Table 6.1 Recurring phenotypic observations amongst the *saf* mutants

Phenotypic Observation	saf Mutant Line	Nature of Phenotype
Spiky/Crinkly Leaves	*a13*	Very Spiky Leaves
	a14	Crinkly Leaves
	a26	Spiky Leaves
	a32	Slightly Spiky Leaves
	a34	Crinkly Leaves
	a35	Serrated Leaves
Trichome Mutation	*a14*	Trichome-less
	gun1 saf82[1]	Trichome-less
Chlorophyll Colouration	*a5*	Green Surface, Yellow Veins
	a7	Yellow Surface, Green Veins
	a18	Some Very Chlorotic
	a24	Dark Green Leaves
	a35	Variegated Colouration
Anthocyanin Colouration	*a14*	Lack Anthocyanin
	a18	Lack Anthocyanin
	a34	Lack Anthocyanin
Dwarf	*a5*	Dwarf
	a13	Dwarf
Accumulation of Rosette Leaves	*a7*	Reduced leaf number
	a10	Increased leaf number
	a14	Increased leaf number
	a21	Reduced leaf number
	a26	Reduced leaf number
	a31	Reduced leaf number
WT Phenotype	*a4*	-
	a6	-
	a8	-

[1] = *gun1 saf* mutants were produced in a second, similar screen, in which the parental line also contained a mutation in the *gun1* gene.

Due to the random nature of the EMS mutagenesis process, backcrossing is required to elucidate the mutation site which has resulted in the *saf* phenotype,

therefore 12 lines (*a4*, *a5*, *a6*, *a7*, *a8*, *a10*, *a14*, *a21*, *a24*, *a26*, *a31*, *a34*) were selected from the original pool of 35 and the backcrossing process was started. Prior to selection, in an attempt to eliminate *phyA* and phyA-signalling mutants, an initial hypocotyl screen was conducted under far-red light and any mutants showing a long (>10mm) or intermediate (6-10mm) hypocotyl length were immediately eliminated. The final selection, however, contained mutant lines which displayed both new and interesting phenotypes and wild type phenotypes and, during the backcross process, these were studied in more detail. By the commencement of this project at least three individuals from each of the 12 selected mutants had received one complete round of backcrossing (backcross and selfing).

6.2.1.1 Seedling phenotypes of the saf mutants

Firstly, although the *saf* mutants are known to be able to retain *HEMA1* expression following a 2 day far-red to 24 hour white light treatment, it was interesting to see the greening potential of these seedlings. As the *phyA* mutant, and mutants in members of the phyA signalling pathway, are known to be able to survive the far-red block of greening, it was important to establish whether any of the chosen lines showed any similarity to the *phyA* mutant. The *saf* mutants in this case received 24h dark prior to 3d far-red light and finally 1d white light (figure 6.2). It is clear that a number of these lines show a significant increase in there greening potential, and this is particularly true for *a14* (56.8% green seedlings) and *a26* (55.8% green seedlings), compared to WT (8.6% green seedlings).

Although the survival of these lines is strongly increased, some seedlings still bleached, which was in contrast to the near 100% survival of the *phy*A mutant, suggesting that they are still able to perceive the far-red light. However, to test the possibility that some of these lines may be mutants in *phyA* or the phyA signalling pathway, the hypocotyl length of these mutants was measured following 5 days far-red light, as the *phyA* mutant does not halt hypocotyl extension under far-red light (figure 6.3).

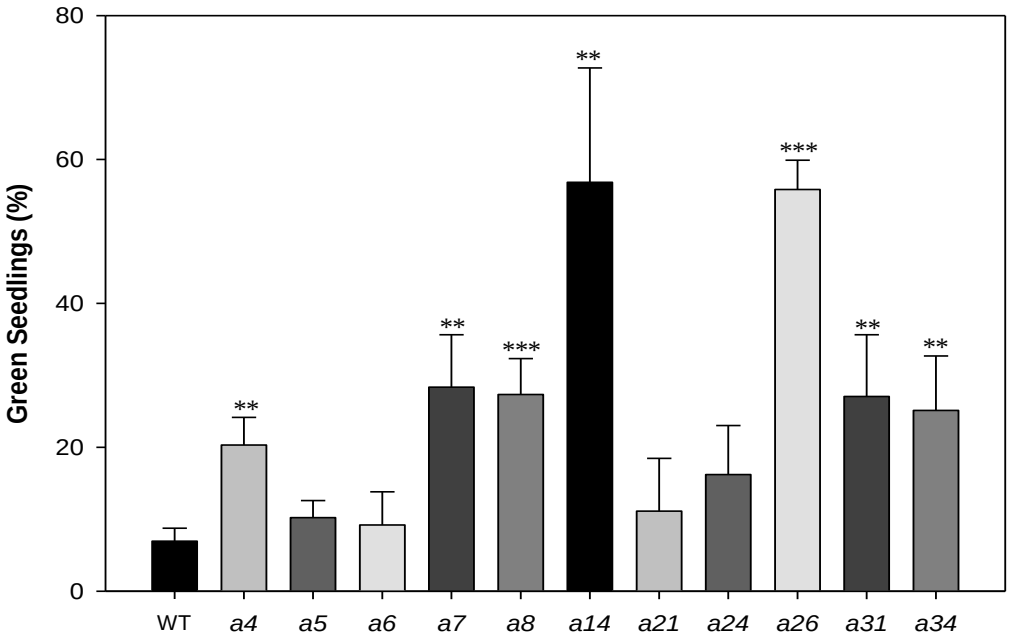

Figure 6.2 Greening response of *saf* mutant seedlings following 3 days FRc light (10 µmol m^{-2} s^{-1}) treatment followed by 1 day Wc light (110 µmol m^{-2} s^{-1}). Following the same treatment 100% of *phy*A mutant seedlings greened effectively. Values are mean ± SE of 3 independent experiments. ** = P = <0.05, *** = P = <0.01.

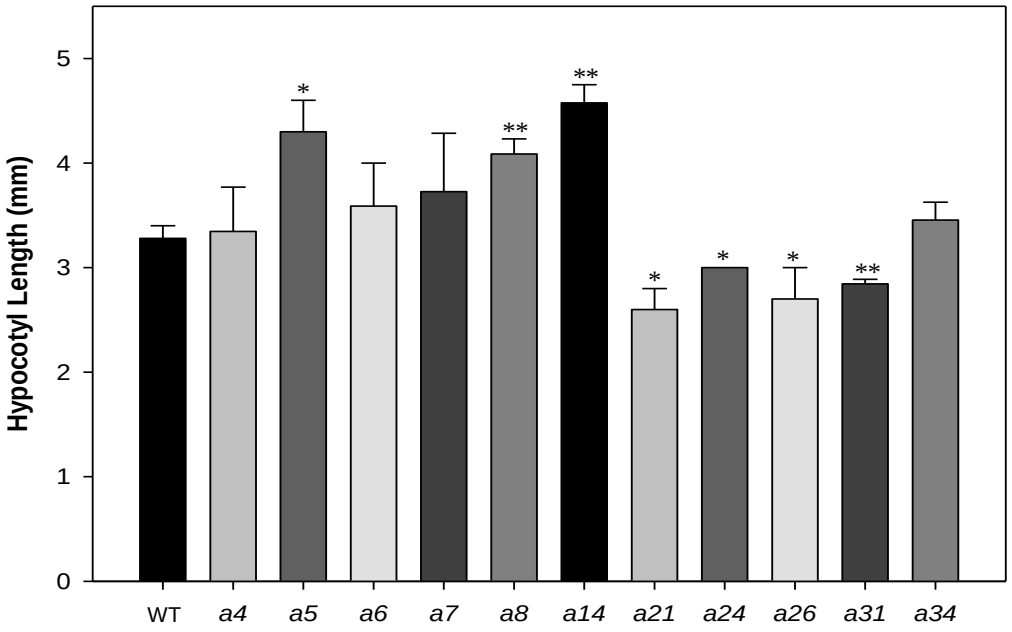

Figure 6.3 Hypocotyl lengths of the *saf* mutants following 1d dark and 5d FRc light (10 µmol m^{-2} s^{-1}) treatment. Following the same treatment *phy*A mutant seedling hypocotyls were 12.8mm. Values are mean ± SE of 3 independent experiments. * = P = <0.1, ** = P = <0.05.

It is clear from this study that none of the chosen lines show a hypocotyl length close to that of *phyA* (12.8mm), although they also do not all show a length similar to WT. Particularly interesting is the fact that *a14* and *a26,* which showed the strongest far-red block of greening survival, do not show a similar hypocotyl length, where *a14* (4.6mm) is marginally longer than WT (3.3mm), along with *a5* (4.3mm) and *a8* (4.1mm), and *a26* (2.7mm) is slightly shorter than WT, along with *a21* (2.6mm), *a24* (3mm) and *a31* (2.8mm).

6.2.1.2 Mature phenotypes of the saf mutants

As already discussed, and outlined in Table 6.1, many of the *saf* mutants displayed interesting phenotypes in the mature plant. For the 12 selected lines these were documented in more detail. The flowering time and leaf number of these mutants is particularly interesting as *phyB*, *phyBphyD* and *phyBphyE* mutants are known to be affected in these phenotypes to differing degrees, due to the shade avoidance response (discussed in more detail in section 1.2.1.1.) (Aukerman *et al*., 1997; Smith and Whitelam, 1997; Devlin *et al*., 1999). The flowering time of the *saf* mutants and the rosette leaf number at flowering are shown in figure 6.4 and figure 6.5, and the appearance of the *saf* mutants upon emergence of the first flower is shown in figure 6.6 and figure 6.7.

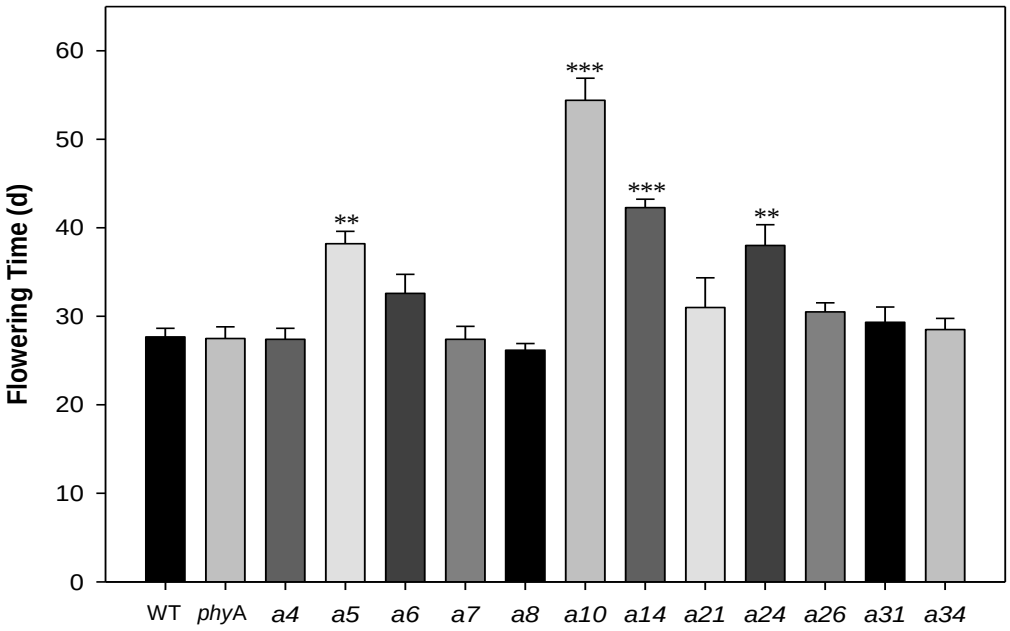

Figure 6.4 Flowering time of the *saf* mutants in long day growth room conditions (16h/8h light (80 µmol m^{-2} s^{-1})/dark). Values are mean ± SE of ≥10 independent experiments. ** = P = <0.01, *** = P = <0.005.

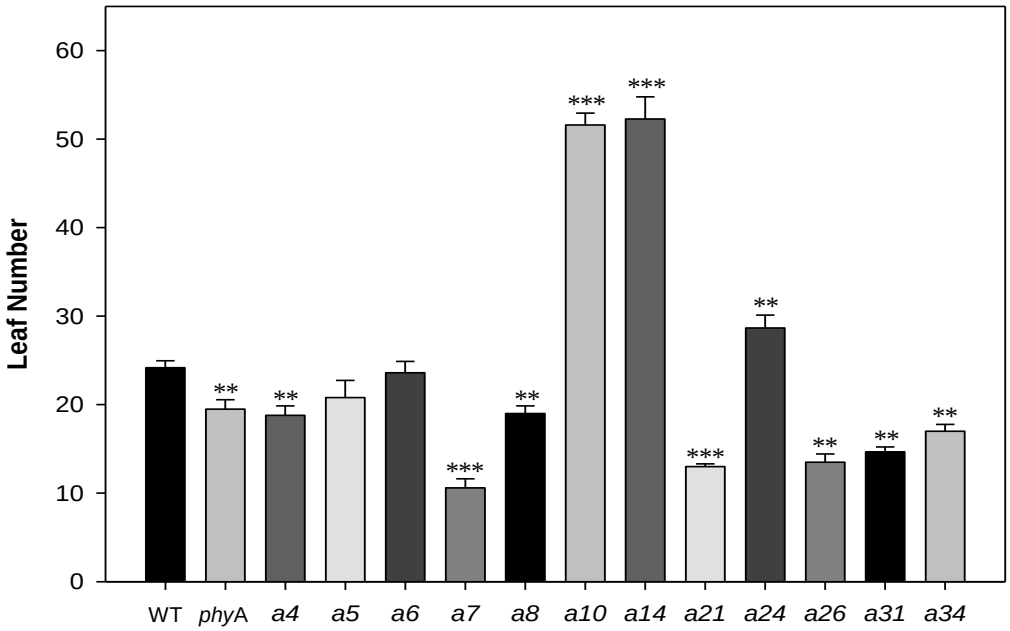

Figure 6.5 Leaf number at the time of flowering in the *saf* mutants in growth room conditions (16h/8h light (80 µmol m^{-2} s^{-1})/dark). Values are mean ± SE of ≥10 independent experiments. * = P = <0.05, ** = P = <0.01, *** = P = <0.005.

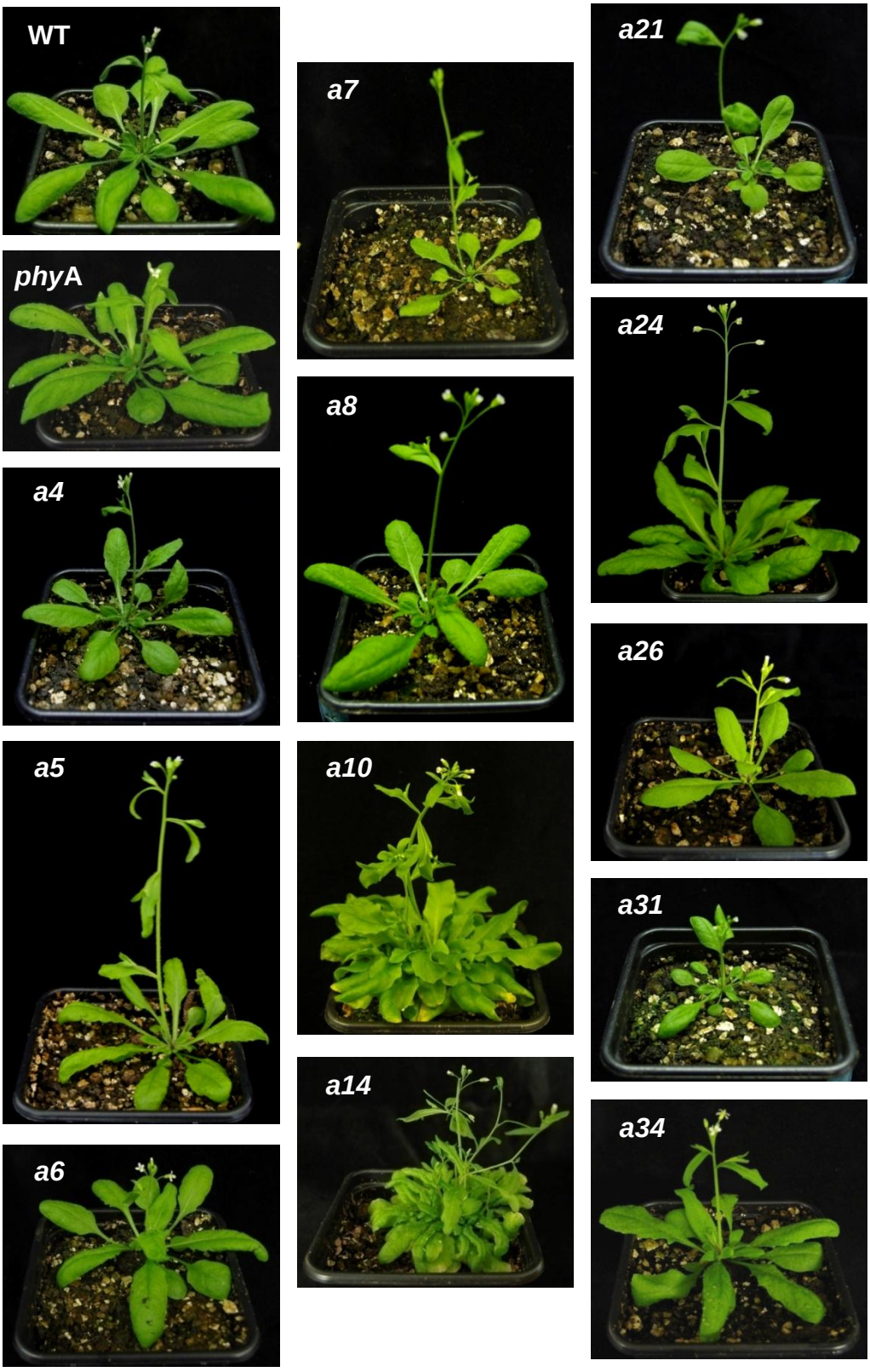

Figure 6.6 Phenotypic analysis of mature *saf* mutants. All of the twelve selected *saf* mutant lines, along with the PT1-1d parental line and *phy*A mutant, were grown on soil under long day growth room conditions (16h/8h light (80 µmol m^{-2} s^{-1})/dark) and photographs taken upon opening of the first flower.

Figure 6.4 shows that none of the *saf* mutants are early flowering, which would suggest that phyB, phyD and phyE are all functioning, as mutations in these photoreceptors results in a constitutive shade avoidance phenotype (Aukerman *et al*., 1997; Devlin *et al*., 1998; Devlin *et al*., 1999). However, *a5, a6, a10, a14* and *a24* all flower significantly later than WT. Although the *phyA* mutant shows a normal flowering time compared to WT, it does have a small, but significant, reduction in leaf number at flowering time (figure 6.5), which is in contrast to Devlin *et al*. (1996) and Johnson *et al*. (1994) who showed that *phy*A mutants have a WT number of rosette leaves. In this experiment, many of the *saf* mutants have a reduced number of rosette leaves, which might suggest a *phyB* mutation, although many other factors have been linked to rosette leaf number and this result may simply indicate a general stress response resulting from EMS disruption of the genome. Three of the *saf* mutants, *a10, a14* and *a24*, showed an increase in rosette leaf number, and for *a10* and *a14* in particular this was quite dramatic (figure 6.5). As *a10, a14* and *a24* also flowered at a later time point, figure 6.8 was constructed to highlight the positive correlation between flowering time and leaf number.

Figure 6.7 Leaf phenotypes of the *saf* mutants compared to WT leaves of a similar age and developmental stage. a) *a7* mutant leaf displaying a smaller, chlorophyll-deficient phenotype. b) *a21* leaf displaying smaller morphology and chlorotic spots. c) *a14* leaf displaying crinkled morphology and trichome-less surface. d) *a24* leaf displaying larger size and dark green colouration. e) Raised rosette leaves of the *a8* plant compared to flattened WT rosette leaves. WT and *saf* mutant lines were grown on soil under long day growth room conditions (16h/8h light (80 µmol m^{-2} s^{-1})/dark). For each panel, the mutant leaf is shown on the right and the equivalent WT on the left.

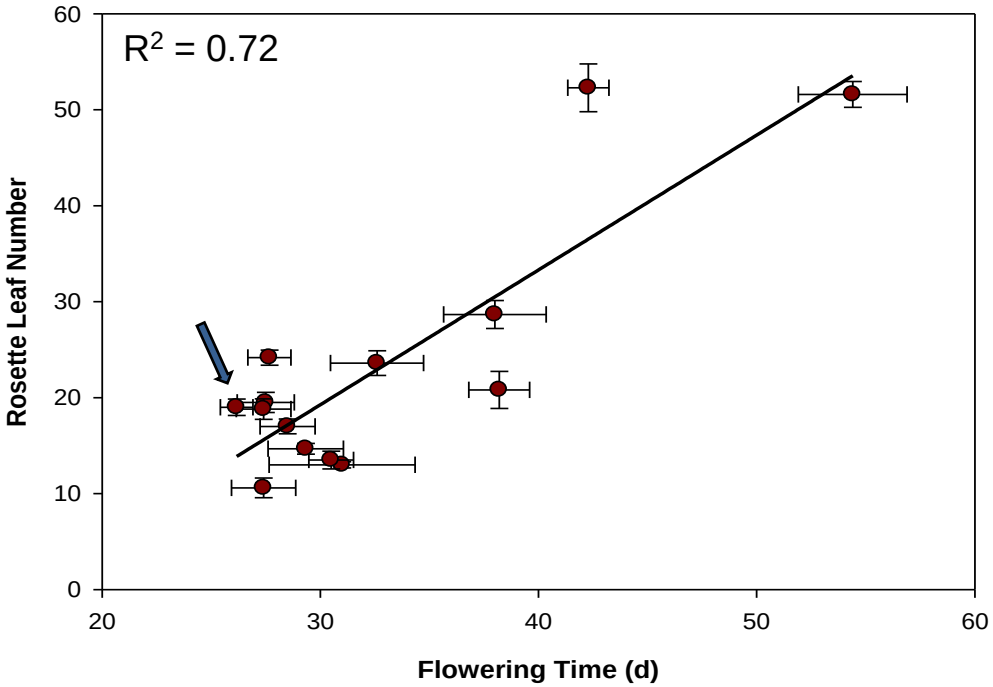

Figure 6.8 Correlation between flowering time and rosette leaf number in the *saf* mutants. Arrow indicates WT (PT1-1d). Data shown is from figures 6.5 and 6.6.

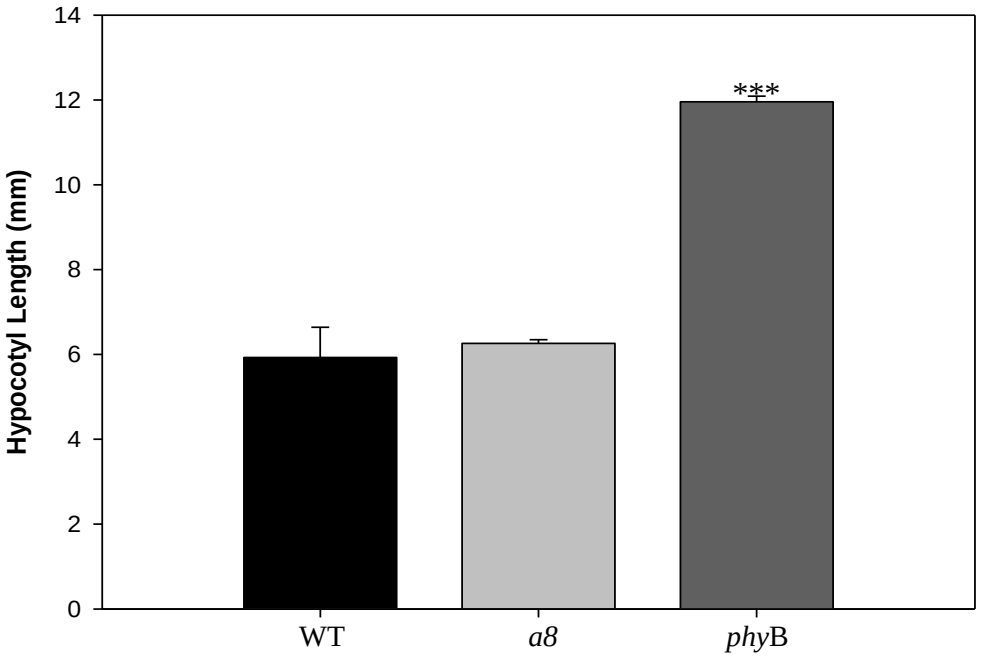

Figure 6.9 Hypocotyl length of the *a8 saf* mutant, compared to WT (PT1-1d) and *phy*B mutant, following 1d dark and 5d red light (80 µmol m^{-2} s^{-1}) treatment. , *** = P = <0.005. Values are mean ± SE of 3 independent experiments.

Some of the *saf* mutants displayed interesting mature leaf phenotypes and these are shown in figure 6.7. Leaves of the *a7* mutant were considerably smaller than WT, and were much lighter green, suggesting chlorophyll deficiency (figure 6.7a). In contrast, the *a24* mutant leaves were larger than WT and appeared much darker (figure 6.7d). Leaves on the *a21* mutant are also considerably smaller than WT, but also shows speckled chlorotic regions (figure 6.7b). Interestingly, this phenotype was also seen in the *laf6* (*Long After Far-red 6*) mutant of *Arabidopsis* (data not shown), which has previously been implicated in chloroplast-to-nucleus signalling due to an increase in levels of protoporphyrin IX (Moller *et al*., 2001). One of the most interesting phenotypes demonstrated by the *saf* mutants is the raised leaves of the *a8* plant (figure 6.7e). The inclination of leaves, which has been attributed to the actions of phyA, B and E, is normally associated with shading by neighbouring leaves (low red:far-red ratio), exposure to low light levels or exposure to dark conditions (Mullen *et al*., 2006). Therefore, this phenotype might suggest a disruption in the *PHYB* or *PHYE* genes, which would result in a constitutive raised leaf phenotype, associated with the shade avoidance response. To test the possibility that phyB activity was compromised in the *a8* line the hypocotyl length under red light was compared to that of WT and *phyB* mutant *Arabidopsis* (figure 6.9). This clearly shows that *a8* does not show an elongated hypocotyl, so it is therefore unlikely to be a *phyB* mutation that is causing the raised leaf phenotype. Additionally, as the phenotypes of the *phyE* mutant are only manifested in a *phyA* and/or *phyB* mutant background, it is also unlikely to be disruption of phyE (Devlin *et al*., 1998).

The *a14* mutant leaf was also smaller, and lighter in colour than WT, but was also lacking trichomes (figure 6.7c). As this trichome-less phenotype was also found in another *saf* mutant, *gun1 saf82*, the relevance of the phenotype was investigated further. The *a14* line was individually crossed with *Arabidopsis* plants mutated in the well established trichome-regulating glabra genes *gl1, gl2, gl3* and *ttg1* (reviewed in detail in by Ishida *et al*., 2008), and the offspring were scored for their ability to form trichomes. The *a14* line crossed with *gl2, gl3* and *ttg1* all produced plants with trichomes, but the *a14/gl1* cross only produced trichome-less plants. This indicates that the *GL1* gene has been disrupted in the *a14* line, however, the lack of survival of *gl1* seedlings following a far-red block of greening treatment (data not shown)

suggests that the *gl1* mutation is not responsible for the *saf* phenotype in the *a14* lines.

6.3 Discussion

6.3.1 *saf* mutant phenotypes suggest a possible role in ROS signalling

As shown in Table 6.1 and figures 6.6 and 6.7, the *saf* mutants exhibit a range of phenotypes. Due to the nature of EMS as a random chemical mutagen, many of these may be due to mutations other than those that create the *saf* phenotype. However, in many cases the mutant phenotypes can be explained by the *saf* phenotype. For example, a high number of the *saf* mutants were late flowering; this could be explained by defects in photoreceptor control. As the far-red block of greening response requires the correct functioning of phyA, any disruption in phyA signalling could result in seedling survival following the screen. Concordantly, impairment in phyB, phyD or phyE signalling would also result in a disturbance in the control of flowering time and would subsequently result in early flowering plants (Goto *et al*., 1991; Johnson *et al*., 1994; Devlin *et al*., 1996). However, the four experiments used here to elucidate the functionality of the phytochromes in the *saf* mutants (greening following far-red block of greening, hypocotyl length under far-red light, flowering time and rosette leaf number) do not consistently highlight any of the mutants as being deficient in phytochrome. However, one mutant which was flagged in all of the studies was *a14*. This line produced the highest percentage of seedlings greening following a 3d far-red block of greening treatment, and also showed the longest hypocotyl under far-red light. This might normally suggest a defect in the phyA signalling pathway; however, *a14* also flowered considerably later than either WT or the *phyA* mutant, and accumulated more than double the number of rosette leaves. One possible explanation is that a defect is indeed present in the phyA signalling pathway in *a14*, but another unrelated mutation, manifested from the EMS treatment, is causing the developmental (leaf and flowering) phenotypes. This will only be elucidated upon study of further back-crossed generations. *a14* was also one of two lines exhibiting a trichome-less phenotype, and it was shown that the *a14* mutant is allelic to *GLABRA1* (*GL1*), which poses some rather interesting questions. It is well known that trichome formation is regulated, in part, by ROS signalling, due to the requirement for endoreduplication (Hulskamp *et al*., 1994). However, the *GL1* protein has yet to be implicated in this signalling mechanism, although it does act as both a transcriptional activator and gibberellic acid-mediated signal (Larkin *et al*., 1994;

Perazza *et al*., 1998). This evidence, combined with the fact that *gl1* does not survive a far-red block of greening, suggests that the *gl1* mutation is not responsible for the *saf* phenotype, rather it is a secondary mutation caused by EMS mutagenesis.

Secondly, anthocyanins are well known for their role in attracting pollinators, but it has also been suggested that they act as visible light screens to protect plants from photoinhibition (Smillie and Hetherington, 1999). Any change in anthocyanin levels, therefore, would suggest that the ROS levels within the chloroplast would be significantly different to those in a WT plant. It is these changes in ROS that could lead to the disruption of the hypothesised ROS retrograde plastid signal.

Defects in chlorophyll formation may be explained in two ways. Firstly the mechanism of *saf* discovery may be at fault. *saf* mutants became apparent when *HEMA1* expression was partially rescued following a 2d far-red block of greening response, however this does not mean that other genes, expression of which are also normally affected, are also restored. Genes such as *GUN4* and *CHLH*, whose expression is normally reduced, may not be fully restored and therefore chlorophyll synthesis would be compromised. Secondly, some of the *saf* mutations may contain defective tetrapyrrole biosynthetic genes, such as the *gun* mutations. This would again result in a lack of chlorophyll production and lead to a semi-chlorotic/chlorotic phenotype. These explanations, however, do not explain the phenotypes visible on *saf* mutants *a5* and *a7*, as their chlorosis is limited to, and does not occur in the veins, respectively.

Finally, a particularly interesting phenotype which developed in the mature *a21* leaf was the appearance of chlorotic spots. Lesions such as these are associated with the 'systemic acquired resistance' response to pathogen infection, resulting from a cell death signalling pathway (Dangl *et al*., 1996). However, mutants have also been identified which produce these lesions in response to environmental conditions, rather than pathogen attack, and have been designated disease lesion mimics. Three of these are mutants in *UROD*, *CPO* and *PPO* (Kruse *et al*., 1995; Mock and Grimm, 1997; Molina *et al*., 1999; Ishikawa *et al*., 2001), all of which encode tetrapyrrole synthesis enzymes. Additionally, it was noted during this project that the *laf6* mutant of *Arabidopsis*, which has altered levels of Mg-proto, also develops necrotic lesions in

mature rosette leaves. The formation of lesions in these plants has been directly related to the formation of ROS, resulting from the increase in phototoxic compounds, (Kruse *et al*., 1995; Mock and Grimm, 1997), however, it seems more likely that, similar to the far-red block of greening response, the cell death in this instance is a result of an apoptotic ROS signal. It is therefore also possible that it is this signal which is causing the survival of the *a21* line following a far-red block of greening treatment.

6.3.2 Future perspectives

Based on the results presented here many of the *saf* mutants may later be implicated as having a role in ROS signalling. However, clearly a lot of work is still required before this will become clear. Firstly it would be interesting to analyse *HEMA1* expression in these mutants following a far-red block of greening treatment, either through GUS expression or conventional PCR, to determine the extent of the block of the plastid signal. On the other hand it is essential that the backcross program is continued, as at the end of this project only one full round (backcross and selfing) was completed for 12 mutant lines. At least three more rounds are required before any results can be fully trusted, although the preliminary results shown here are invaluable in allowing interesting mutants to be selected. Finally, once backcrossing is completed then mapping the mutations to specific genes will allow phenotype to be linked to genotype, at which point the ROS signalling pathway may begin to be elucidated.

Chapter 7: Final Discussion

7.1 Regulation at the first committed step of the tetrapyrrole pathway

The tetrapyrrole pathway is responsible for the production of at least four critically important compounds required during a plants lifecycle: chlorophyll, haem, phytochromobilin and sirohaem. The high energy demands for synthesis of these products, coupled with the fact that many of the intermediate compounds are potentially phototoxic, has resulted in the need for at least one site early in the pathway that is tightly regulated for precise control over flux through the pathway. Previous studies have identified that the *HEMA* gene, and specifically *HEMA1* in *Arabidopsis*, which encodes the Glu-TR protein, is under such control. Hormones, the phytochrome and cryptochrome families of photoreceptors, plastid signals, sucrose and the circadian rhythm have all previously been shown to regulate the *HEMA1* gene, while haem negative feedback and the FLU protein are capable of regulating Glu-TR activity (see section 1.3 for a more detailed discussion). However, despite such comprehensive analysis of this site of regulation the exact mechanism of some of these inputs is still not fully understood. This includes the precise signalling pathway through which phytochrome is able to regulate gene expression, why FLU is required for the regulation of Glu-TR, and the nature of the plastid signalling pathway.

Phytochrome-interacting factor 3 (PIF3) was identified in a screen for phyB binding proteins (Ni *et al*., 1998), and was shown to interact with the Pfr form of both phyA and phyB (Ni *et al*., 1999; Zhu *et al*., 2000). Since then PIF1, PIF4, PIF5 and PIF6 have been identified (Huq and Quail, 2002; Huq *et al*., 2004; Khanna *et al*., 2004), and, along with PIF3, are all members of the *Arabidopsis* bHLH subfamily 15 (Toledo-Ortiz *et al*., 2003; Deuk and Fankhauser, 2005). The initial characterization of *PIF3* antisense lines showed a hyposensitive phenotype under continuous red light, suggesting that PIF3 functions positively in controlling photomorphogenesis (Ni *et al*., 1998). Additionally, PIF3 has been shown to function positively in chloroplast development and greening processes during the initial hours of de-etiolation, as *pif3* seedlings have chlorophyll levels lower than those of wild type (Kim *et al*., 2003; Monte *et al*., 2004), and PIF3 also acts positively in the light-induced accumulation of

anthocyanin (Kim *et al*., 2003; Shin *et al*., 2007). PIF1, on the other hand, has been consistently described as a negative regulator, which is required for repression of light-induced seed germination and inhibition of hypocotyl elongation (Oh *et al*., 2004), as well as hypocotyl negative gravitropism and repression of protochlorophyllide accumulation in the dark (Huq *et al*., 2004; Oh *et al*., 2004).

In the current project it was clearly demonstrated that both PIF1 and PIF3 are required for the negative regulation of the chloroplast development and are alleviated by red/far-red light cues and subsequent phytochrome activation (Chapter 4). Loss of function *pif1* and *pif3* mutants, and the *pif1pif3* double, were all shown to accumulate higher levels of Pchlide in the dark and, following extended dark pre-treatment, resulted in phototoxic bleaching of seedlings when transferred into the light. Interestingly, the loss of both PIF1 and PIF3 in the double mutant produced a more severe response and also resulted in a semi-constitutive photomorphogenic phenotype in the dark, which presented in the early expansion of cotyledons, the inhibition of hypocotyl growth and the production of chloroplast-like etioplasts. Very recent work by Leivar *et al*. (2008) also demonstrated that mutations in the *PIF4* and *PIF5* bHLH-type phytochrome interacting factor genes, as well as *PIF1* and *PIF3*, show a semi-constitutive photomorphogenic phenotype. Additionally, microarray studies on a dark grown quadrupole *pif1pif3pif4pif5* mutant, which displayed near-complete constitutive photomorphogenic phenotypes including short hypocotyls, open cotyledons and disrupted hypocotyl gravitropism, indicated that it had a gene expression pattern similar to that of red light-grown wild type (Shin *et al*., 2009). However, neither of these studies demonstrated exactly how these phytochrome-interacting factors are able to negatively regulate photomorphogenesis. It has been suggested previously that the increase in tetrapyrrole synthesis in *pif1* was due to a subtle downregulation of the ferrochelatase gene *FC2* and an upregulation of the haem oxgenase *HO3* resulting in less free haem and less inhibition of glutamyl tRNA reductase activity (Moon *et al*., 2008). However, the *HO3* gene is only expressed to very low levels and antisense *FC2* lines show no reduction in phytochromobilin synthesis (A. Smith, personal communication), suggesting that changes in expression of these genes would make no more than a minor contribution to tetrapyrrole synthesis.

In the current study, analysis of the expression of *HEMA1* in the different *pif*

mutants indicated that these proteins were likely acting to negatively regulate the expression of this gene. Additionally, the altered expression pattern, compared to WT, was indicative of a disruption in the rhythmic expression through the circadian clock, which is particularly interesting in light of the role that PIFs have previously been suggested to play in this mechanism. Firstly, PIF3 has been shown to bind the promoters of *CCA1* and *LHY* (Martinez-Garcia *et al*., 2000; Huq and Quail, 2002) and directly bind TOC1 (Yamashino *et al*., 2003), three of the central circadian oscillator genes. However, the *pif3* mutant does not disrupt the expression of these genes in light/dark cycles (Oda *et al*., 2004; Viczian *et al*., 2005) or in constant darkness (chapter 4), and does not control resetting of the clock (Viczian *et al*., 2005). Secondly, expression of CAX1, a H^+/Ca^{2+} antiporter unrelated to chloroplast function (Hirschi *et al*., 1996) which has previously been shown to be circadian regulated (Harmer *et al*., 2000), was unaffected in any of the *pif* mutants in the work presented here, indicating that the circadian rhythm is still active in the control of some genes. Finally, analysis of multiple circadian microarray experiments suggests that *PIF1* is under circadian control (Covington *et al*., 2008), and a low amplitude circadian rhythm has also been observed previously for *PIF3* using a *PIF3:LUC+* reporter construct (Viczián *et al*., 2005). In the data presented here *PIF1* and *PIF3* showed a robust circadian regulation in dark-grown seedlings suggesting that clock regulation of PIF function is via circadian control of expression.

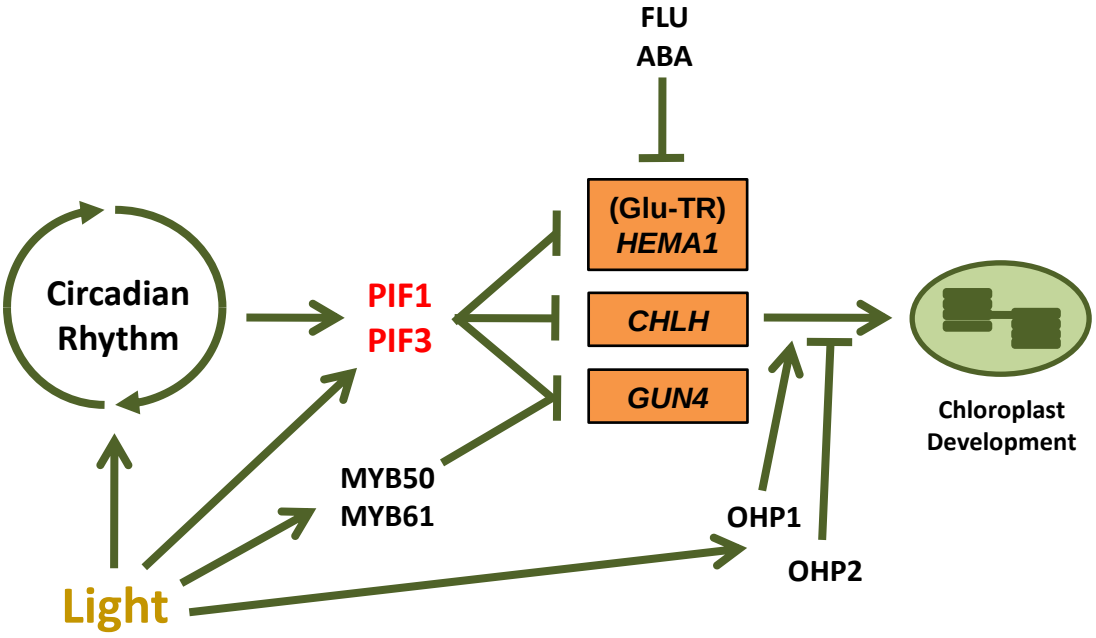

Figure 7.1 Summary of the understanding of regulators of the tetrapyrrole pathway discussed throughout this report. Light signalling, through the phytochrome and cryptochrome families of photoreceptors, directly and indirectly regulates *PIF1*, *PIF3*, *MYB50* and *MYB61* expression, which are responsible for repressing the expression of the key regulatory sites in the tetrapyrrole pathway: *HEMA1*, *CHLH* and *GUN4*. Light also regulates the expression of *OHP1* and *OHP2*, which are required to control total flux through the tetrapyrrole pathway and promote chloroplast development. The ABA hormone and FLU protein are light-independent regulators of *HEMA1* expression and Glu-TR activity, respectively, and are required to maintain total flux through the tetrapyrrole pathway.

It is also interesting to note that a number of other studies have shown that chloroplast development is under the control of the circadian rhythm. The GLK proteins, for example, have been shown to regulate chloroplast development in a cell-autonomous manner (Fitter *et al*., 2002; Waters *et al*., 2008) and these genes are under the control of an endogenous rhythm, most likely circadian. Additionally, Dodd *et al*. (2005) showed that chlorophyll accumulation could be increased by correctly aligning the plants circadian phase with the diurnal phase, and that this was altered in a *toc1* mutant. Consequently, it is suggested here that PIF1 and PIF3 form part of the output from the clock and are required to specifically regulate chloroplast-related genes (figure 7.1). The exact mechanism for this control is not yet fully understood; however, as the phenotype of the *toc1* mutant is consistently opposite to that displayed for either the *pif1* or *pif3* mutants, it is possible that *TOC1* is required to sequester the *PIF* proteins in the dark.

At the same time, the FLU protein has received at lot of attention yet its function in regulating the tetrapyrrole pathway is also not fully understood. FLU was discovered in a mutant screen, conducted by Meskauskiene *et al*. (2001), for the inability of seedlings to restrict the accumulation of Pchlide in the dark (see section 1.5.1 for a more detailed discussion). These plants were described as resembling dark-grown seedlings that had been fed exogenous ALA (Meskauskiene *et al*., 2001), and they rapidly bleached and died following exposure to W light. Subsequently, the FLU protein was shown to interact with Glu-TR, and is an essential negative regulator of flux through the pathway (Meskauskiene and Apel, 2002; figure 7.1). Since then the FLU transcript has been shown to modestly fluctuate, however, FLU protein levels do not change (Goslings *et al*., 2004). Indeed, evidence has yet to be shown to implicate FLU in any understandable mechanism of regulation and consequently a study was undertaken in the current project to help further our knowledge of this protein.

FLU overexpressing seedlings were studied alongside WT and *flu* mutants and assesed in their ability to de-etiolate effectively, through hypocotyl extension and chlorophyll synthesis assays (Chapter 5). As the FLU protein has been shown to bind and inhibit Glu-TR it might be expected that a dramatic reduction in chlorophyll and

haem synthesis would be observed, however, although there was a reduction in Pchlide synthesis in the dark, in plants overexpressing *FLU* up to 30 fold, there was no reduction in chlorophyll synthesis in light grown seedlings. Concordantly, there was also only a modest increase in hypocotyl length of overexpressing plants, compared to WT, when grown under red or far-red light, indicating only a small reduction in phytochromobilin synthesis. One possible explanation for this limited decrease in flow through the pathway could be that if the levels of haem are reduced too dramatically then seedlings would fail to grow, and therefore only those which maintain a set level of flux are able to survive. Alternatively, it might be that that the FLU protein is required to constitutively reduce, but not inhibit, Glu-TR activity under most conditions (figure 7.1). As a result increasing the FLU content of the seedling can only reduce flow through the pathway through binding the limited amount of free Glu-TR. To add support to this hypothesis it would be necessary to study the FLU protein levels in the *FLU* overexpression lines, and attempt to identify conditions under which the FLU protein is regulated in the WT.

The potential for the plastid signal to regulate the expression of genes encoding chloroplast-targeted genes has become a topic for intense discussion over recent years. However, the exact signalling pathway is far from understood, and it now seems apparent that one of the previously identified signalling molecules, Mg-Proto (Strand *et al*., 2003), in fact plays no role in this response (Mochizuki *et al*., 2008; Moulin *et al*., 2008). One possible regulatory mechanism, which has subsequently become the most likely candidate, is a directed ROS signal (Pfannschmidt *et al*., 2003). In the current study 12 EMS mutants were studied which were able to retain *HEMA1* expression following a far-red block of greening treatment and as a result potentially form part of the ROS plastid signalling pathway (Chapter 6). These mutants were shown to display a number of interesting phenotypes, including the ability for many of them to green following a potential lethal far-red treatment. Additionally, many of these phenotypes, such as the accumulation of anthocyanin or defects in leaf morphology, may be explained through a disruption in ROS accumulation/signalling. However, a great deal more work is required to fully understand the role of these mutants in controlling the expression of *HEMA1* during a far-red block of greening treatment.

Finally, during this project a number of novel regulators of the tetrapyrrole pathway were identified including a number of ABA signalling factors and the recently identified OHP proteins (Chapter 5). The *aba1* mutant, which is defective in the early stages of ABA synthesis, was shown to result in an increase in *HEMA1* expression, compared to WT, following white light treatment. The *aba1* mutant is also shown to have reduced chlorophyll content (Pogson *et al*., 1998), and this might suggest that the increase in *HEMA1* expression occurs in an attempt to boost flux through the pathway to increase chlorophyll synthesis (figure 7.1). Further study is required on this subject to understand the exact mechanisms at work. The OHP proteins were also shown in this project to control flux through the pathway (figure 7.1). Mutations in the cyanobacterial homolog of *OHP1, ScpE,* has previously been shown to result in a reduction in Pchlide and protohaem (Xu *et al*., 2002), and similarly here the *ohp1* mutant contained a marked reduction in Pchlide synthesis. *OHP1* overexpressing plants, on the other hand, did not show any change in chlorophyll content, although they did present a reduced hypocotyl length under red light which might suggest an increase in phytochromobilin synthesis. Interestingly, while the *ohp2* mutant did not display any change in Pchlide content, the *OHP2* overexpressing plant was deficient in both Pchlide in the dark and chlorophyll in the light. This phenotype is similar to that presented by plants overexpressing the *ELIP2* gene (Tzvetkova-Chevolleau *et al*., 2007), which is a member of the same *LIL* family as the *OHP* genes. In this case ELIP2 was shown to regulate both Glu-TR and Mg-chelatase, and it is suggested here that OHP2 might have a similar function. However, perhaps the most interesting result from study of these genes was the 'snowy cotyledons' produced by the homozygous mutants. This phenotype has been seen a number of times previously in different mutants including a chloroplast elongation factor (*SCO1*) and a disulphide isomerase (*SCO2*) (Albrecht *et al*., 2006, 2008). Interestingly, both of these proteins were targeted to the chloroplast, as the OHP proteins are expected to do, and *sco1* was able to be rescued by growth on sucrose-containing media. Previously, mutants isolated with cotyledon-specific defects in chloroplast biogenesis were shown to be impaired in plastid gene transcription (Privat *et al*., 2003, for example), and the SCO1 and SCO2 proteins are also suggested to be involved in plastid transcription and protein folding, respectively. Therefore the current work might also imply a role for the OHP proteins in the plastid transcriptional or translational machinery.

7.2 Regulation at the branchpoint of the tetrapyrrole pathway

As discussed, control over the first committed precursor into a pathway is key in regulating total flux. However, the tetrapyrrole pathway also contains a chelatase branchpoint which is responsible for separating the synthesis of chlorophyll from that of haem and phytochromobilin. As the requirements for chlorophyll synthesis differ over the course of the year, during certain times of the day and in different tissues, while the requirement for haem remains relatively constant, this branchpoint provides a second site for intense regulation. The magnesium chelatase enzyme, which produces the early chlorophyll precursor Mg-proto, has been shown to be more highly regulated that ferrochelatase, which produces protohaem. Additionally, one of the subunits of Mg-chelatase, CHLH, appears to be the key site for regulation (Tanaka and Tanaka, 2007). However, many of the exact mechanisms for regulation are yet to be fully understood, not least the role of the regulatory protein GUN4. Throughout this project the regulation of Mg-chelatase has been studied in relation to light input and the role of the PIF proteins, the function of GUN4, and the identification of novel regulators of this branchpoint.

Chapter 3 clearly indicates that the *CHLH* gene is the most highly regulated of Mg-chelatase subunits under red, far-red, blue and white light. However, it is also shown that *GUN4* follows the same pattern of regulation and is almost as highly regulated, suggesting that GUN4 might also be a key site of regulation in the pathway. Subsequently it was shown that the regulation of *GUN4* and *CHLH* was a result of the phytochrome and cryptochome photoreceptors, as mutations in the *PHY* and *CRY* genes resulted in a reduction in expression. Additionally, PIF1 and PIF3 were shown to be one of the key phytochrome-mediated mechanisms in regulating the expression of *CHLH* and *GUN4*, in a similar manner to *HEMA1* (Chapter 4; figure 7.1). Interestingly, *CHLM*, the next gene in the chlorophyll branch, was also shown to be light-regulated, however, the pattern of expression was different where the peak in expression occurred consistently later than *CHLH* or *GUN4* (Chapter 3). This might simply indicate a later requirement for CHLM synthesis, although such a long delay in expression could indicate a more critical role for this enzyme during de-etiolation.

The role of GUN4 in acting both as a regulator of Mg-chelatase and as a key regulated site itself was of particular interest. The *GUN4* gene was originally identified in a screen for mutants that maintained expression of *Lhcb* following exposure to the herbicide Norflurazon, which blocks plastid development, and therefore the plastid-to-nucleus signal. Five mutants were originally identified and became known as *genomes uncoupled 1-5 (gun1-5)* (Susek *et al*., 1993; Mochizuki *et al*., 2001). The discovery that a *gun4/gun5* double mutant produced a more severe chlorophyll-deficient mutant than either a *gun4* or *gun5* mutant, and the copurification of GUN4 and CHLH, provided the first clues as to the role of GUN4 in tetrapyrrole regulation. Modeling of the GUN4 protein has since revealed that a cleft in its structure is capable of accommodating approximately half of a protoporphyrin IX molecule (Davison *et al*., 2005; Verdacia *et al*., 2005). Further studies suggested that *GUN4* might become essential for Mg-protoporphyrin IX when Mg^{2+} is at low concentrations, where at 2 mM Mg^{2+} Mg-chelatase is virtually inactive in the absence of *GUN4*, but becomes almost fully active in its presence (Davison *et al*., 2005).

Following a transcriptomics approach, using the Genevestigator™ online program (Zimmerman *et al*., 2005), it seemed clear that *GUN4* was under intense regulation from an array of sources (Chapter 3). Interestingly, analysis of some of these inputs resulted in confirmation of their role in regulating *GUN4*, such as the MYB50 and MYB61 transcription factors which are proposed here to be required for suppression of *GUN4* expression (Chapter 5; figure 7.1). However, at the same time ABA1 and ABI1 were specifically implicated by Genevestigator™ to regulate *GUN4*, yet following further analysis they appeared to play more of a role in regulating *HEMA1*, *CHLH* and *PORA* (Chapter 5; figure 7.1). Nevertheless, this information remains important in our understanding of the role of ABA in regulating the tetrapyrrole pathway and it may still become apparent that ABA1 and ABI1 are required for *GUN4* regulation at a different time.

Analysis of the *gun4* mutant alongside *GUN4* overexpressing plants suggested that GUN4 also functions in regulating the haem branch (Chapter 5), as *gun4* mutant seedlings display an extended hypocotyl under red and far-red light, and *GUN4* overexpressing plants show a marginally shorter hypocotyl under the same conditions. Additionally, it was shown that *FC1*, *HO1* and *CAO* are downregulated in the *gun4*

mutant, suggesting a dual role for GUN4 in regulating both branches of the tetrapyrrole pathway, although more work is required to elucidate its exacted role. It is also interesting to note that *GUN4* overexpressing plants were more able to synthesise Pchlide in the dark and chlorophyll in the light, indicating that the amount of GUN4 is limiting to this process in WT plants. Together this data strongly suggests a major role for GUN4 as a regulator of multiple aspects of the tetrapyrrole pathway, including both the chlorophyll and haem branches, and therefore is itself a key site for regulation.

In summary, the tetrapyrrole pathway is clearly under intense regulatory pressure and the functioning of many of these factors is far from fully understood. The current project has helped in furthering our knowledge on many of these aspects but has also opened up avenues of research on new regulators which will aid in the overall understanding of tetrapyrrole synthesis.

References

Adamska I. (1997) Elips: light-induced stress proteins. *Physiol. Plant*, 100: 794–805.

Adamska I. (2001) The Elip family of stress proteins in the thylakoid membranes of pro-and eukaryote. In E.M. Aro, B. Andersson, eds, Advances in Photosynthesis and Respiration-Regulation of Photosynthesis. Vol. 11, Kluwer Academic Publishers, Dordrecht, The Netherlands, pp 487–505.

Ahmad M. and Cashmore A.R. (1993) *HY4* gene of *A. Thaliana* encodes a protein with characteristics of a blue-light photoreceptor. *Nature*, 366: 162–166.

Ahmad M., Grancher N., Heil M., Black R.C., Giovani B., Galland P. and Lardemer D. (2002) Action spectrum for hypocotyl growth inhibition suggests dosage-dependent synergism among cryptochrome photoreceptors of *Arabidopsis thaliana*. *Plant Physiol.*, 129: 774–785.

Ahmad M., Jarillo J.A., Smirnova O. and Cashmore A.R., (1998) Cryptochrome blue-light photoreceptors of *Arabidopsis* implicated in phototropism. *Nature*, 392: 720-723.

Ahmad M., Lin C. and Cashmore A.R. (1995) Mutations throughout an *Arabidopsis* blue-light photoreceptor impair blue light-responsive anthocyanin accumulation and inhibition of hypocotyl elongation. *Plant J.*, 8: 653–658.

Akthar M. (1994) The modification of acetate and propionate side chains during the biosynthesis of haems and chlorophylls: mechanistic and stereochemical studies. In D.J. Chadwick, K. Ackrill, eds, Biosynthesis of tetrapyrrole pigments. John Wiley and sons, Chichester, UK, pp 131-152.

Alabadí D., Yanovsky M. J., Más P., Harmer S. L. and Kay, S. A. (2002) Critical role for *CCA1* and *LHY* in maintaining circadian rhythmicity in *Arabidopsis*. *Curr. Biol.*, 12: 757–761.

Alabadí, D., Oyama T., Yanovsky M.J., Harmon F.G., Más P. and Kay S.A. (2001) Reciprocal regulation between *TOC1* and *LHY/CCA1* within the *Arabidopsis* circadian clock. *Science*, 293: 880–883.

Alawady A., Reski R., Yaronskaya E. and Grimm B. (2005) Cloning and expression

of the tobacco CHLM sequence encoding Mg protoporphyrin IX methyltransferase and its interaction with Mg chelatase. *Plant Mol. Biol*., 57: 679–691

Albrecht V., Ingenfeld A. and Apel K. (2006) Characterization of the snowy cotyledon 1 mutant of *Arabidopsis thaliana*: the impact of chloroplast elongation factor G on chloroplast development and plant vitality. *Plant Mol. Biol.*, 60: 507–518.

Albrecht V., Ingenfeld A. and Apel K. (2008) *Snowy cotyledon 2* : the identification of a zinc finger domain protein essential for chloroplast development in cotyledons but not in true leaves. *Plant Mol. Biol.*, 66: 599-608.

Allen T., Koustenis A., Theodorou G., Somers D.E., Kay S.A., Whitelam G.C., and Devlin P.F. (2006) *Arabidopsis FHY3* specifically gates phytochrome signaling to the circadian clock. *Plant Cell*, 18: 2506–2516.

Alonso J.M., Hirayama T., Roman G., Nourizadeh S. and Ecker J.R. (1999) *EIN2*, a bifunctional transducer of ethylene and stress responses in *Arabidopsis*. *Science*, 284: 2148–2152.

Alonso J.M., Stepanova A.N., Leisse T.J., Kim C.J., Chen H., Shinn P., Stevenson D.K., Zimmerman J., Barajas P., Cheuk R., Gadrinab C., Heller C., Jeske A., Koesema E., Meyers C.C., Parker H., Prednis L., Ansari Y., Choy N., Deen H., Geralt M., Hazari N., Hom E., Karnes M., Mulholland C., Ndubaku R., Schmidt I., Guzman P., Aguilar-Henonin L., Schmid M., Weigel D., Carter D.E., Marchand T., Risseeuw E., Brogden D., Zeko A., Crosby W.L., Berry C.C. and Ecker J.R. (2003) Genome-Wide insertional mutagenesis of *Arabidopsis thaliana*. *Science*, 301: 653-657.

Al-Sady B., Ni W., Kircher S., Schäfer E. and Quail P.H. (2006) Photoactivated phytochrome induces rapid PIF3 phosphorylation as a prelude to proteosome-mediated degradation. *Molecular Cell*, 23: 439–446.

Al-Sady B., Kikis E.A., Monte E. and Quail P.H. (2008) Mechanistic duality of transcription factor function in phytochrome signaling. *Proc. Natl. Acad. Sci. USA*, 105: 2232–2237.

Anderson J.P., Badruzsaufari E., Schenk P.M., Manners J.M., Desmond O.J., Ehlert C., Maclean D.J., Ebert P.R. and Kazan K. (2004) Antagonistic interaction

between abscisic acid and jasmonate-ethylene signaling pathways modulates defense gene expression and disease resistance in *Arabidopsis*. *Plant Cell*, 16: 3460-3479.

Andersson U., Heddad M. and Adamska I. (2003) Light stress-induced one-helix protein of the chlorophyll a/b-binding family associated with photosystem I. *Plant Physiol.*, 132: 811–820.

Ang L.H., Chattopadhyay S.,Wei N., Oyama T., Okada K., Okada K., Batschauer A. and Deng X.-W. (1998) Molecular interaction between COP1 and HY5 defines a regulatory switch for light control of *Arabidopsis* development. *Mol. Cell.*, 1: 213–222.

Apel K., Santel H.J., Redlinger T.E. and Falk H. (1980) The protochlorophyllide holochrome of barley (*Hordeum vulgare* L.): isolation and characterization of the NADPH-protochlorophyllide oxidoreductase. *Eur. J. Biochem.*, 111: 251–258.

Arai M., Mitsuke H., Ikeda M., Xia J.-X., Kikuchi T., Satake M. and Shimizu T. (2004) ConPred II: a consensus prediction method for obtaining transmembrane topology models with high reliability. *Nucleic Acids Res.*, 32: 390-393.

Aukerman M.J., Hirschfeld M., Wester L., Weaver M., Clack T., Amasino R.M. and Sharrock R.A. (1997) A deletion in the *PHYD* gene of the *Arabidopsis* Wassilewskija ecotype defines a role for phytochrome D in red/far-red light sensing. *Plant Cell*, 9: 1317-1326.

Bae G. and Choi G. (2008) Decoding of light signals by plant phytochromes and their interacting proteins. *Annu. Rev. Plant Biol.*, 59: 281-311.

Bagnall D. J., King R.W. and Hangarter R.P. (1996) Blue-light promotion of flowering is absent in *hy4* mutants of *Arabidopsis*. *Planta*, 200: 278–280.

Ballesteros M. L., Bolle C., Lois L.M., Moore J.M., Vielle-Calzada J.-P., Grossniklaus U. and Chua N.-H. (2001) *LAF1*, a MYB transcription activator for phytochrome A signalling. *Genes Dev.*, 15: 2613–2625.

Balmer Y., Koller A., del Val G., Manieri W., Schürmann P. and Buchanan B.B. (2003) Proteomics gives insight into the regulatory function of chloroplast

thioredoxins. *Proc. Natl. Acad. Sci. USA*, 100: 370–375.

Barnes S.A., Nishizawa N.K., Quaggio R.B., Whitelam G.C. and Chua N-H. (1996) Far-red light blocks greening in *Arabidopsis* seedlings via a phytochrome A-mediated change in plastid development. *Plant Cell*, 8: 601-615.

Barnes S.A., Quaggio R.B. and Chua N-H. (1995) Phytochrome signal transduction: Characterisation of pathways and isolation of mutants. *Philos. Trans. R. Soc. Lond. B Biol. Sci.*, 350: 67-74.

Barrero J.M., Rodriguez P.L., Quesada V., Alabadi D., Blazquez M.A., Boutin J.-P., Marion-Poll A., Ponce M.R. and Luismicol (2008) The *ABA1* gene and carotenoid biosynthesis are required for late skotomorphogenic growth in *Arabidopsis thaliana*. *Plant, Cell and Environ.*, 31: 227–234.

Bauer C.E., Elsen S. and Bird T.H. (1999). Mechanisms for redox control of gene expression. *Annu. Rev. Microbiol.*, 53, 495–523.

B auer D., Viczian A., Kircher S., Nobis T., Nitschke R., Kunkel T., Panigrahi K.C., Adam E., Fejes E., Schafer E. and Nagy F. (2004) Constitutive photomorphogenesis 1 and multiple photoreceptors control degradation of phytochrome interacting factor 3, a transcription factor required for light signaling in *Arabidopsis*. *Plant Cell*, 16: 1433–1445.

Beale S.I. (1999) Enzymes of chlorophyll biosynthesis. Photosynth. Res., 60: 43–73.

Beator J. and Kloppstech K. (1993) The circadian oscillator coordinates the synthesis of apoproteins and their pigments during chloroplast development. *Plant Physiol.*, 103: 191-196.

Botto J.F., Sanchez R.A., Whitelam G.C. and Casal J.J. (1996) Phytochrome A mediates the promotion of seed germination by very low fluences of light and canopy shade light in *Arabidopsis*. *Plant Physiol.*, 110: 439-444.

Bougri O. and Grimm B. (1996) Members of a low-copy number gene family encoding glutamyl-tRNA reductase are differentially expressed in barley. *Plant J.*, 9: 867–78.

Bouly J. P., Giovani B., Djamei A., Mueller M., Zeugner A., Dudkin E.A., Batschauer A. and Ahmad M. (2003) Novel ATP-binding and autophosphorylation activity associated with *Arabidopsis* and human cryptochrome-1. *Eur. J. Biochem.*,

270: 2921–2928.

Boylan M.T. and P.H. Quail (1991) Phytochrome A overexpression inhibits hypocotyl elongation in transgenic *Arabidopsis. Proc. Natl. Acad. Sci. USA*, 88: 10806-10810.

Briggs W.R. and Christie J.M. (2002) Phototropins 1 and 2: versatile plant blue-light receptors. *Trends Plant Sci.*, 7: 204–210.

Briggs W.R., Beck C.F., Cashmore A.R., Christie J.M., Hughes J., Jarillo J.A., Kagawa T., Kanegae H., Liscum E., Nagatani A., Okada K., Salomon M., Rüdiger W., Sakai T., Takano M., Wada M., and Watson J.C. (2001) The phototropin family of photoreceptors. *Plant Cell*, 13: 993–997.

Briggs W.R., Christie J.M. and Salomon M. (2001) Phototropins: a new family of flavinbinding blue light receptors in plants. *Antiox. Redox Signal.*, 3: 775–788.

Brudler, R., Hitomi K., Daiyasu H., Toh H., Kucho K., Ishiura M., Kanehisa M., Roberts V.A., Todo T., Tainer J.A. and Getzoff E.D. (2003) Identification of a new cryptochrome class. Structure, function, and evolution. *Mol. Cell*, 11: 59–67.

Brutnell T.P., Sawers R.J.H., Alexandra Mant A. and Langdale J.A. (1996) *BUNDLE SHEATH DEFECTIVE2*, a Novel Protein Required for Post-Translational Regulation of the rbcL gene of Maize. *Plant Cell*, 11: 849-864.

Butler W.L., Norris K.H., Seigelman H.W. and Hendricks S.B. (1959) Detection, assay, and preliminary purification of the pigment controlling photoresponsive development of plants. *Proc. Natl. Acad. Sci. USA*, 45:1703–1708.

Canamero R. C., Bakrim N., Bouly J.P., Garay A., Dudkin E.E., Habricot Y. and Ahmad M. (2006) Cryptochrome photoreceptors Cry1 and Cry2 antagonistically regulate primary root elongation in *Arabidopsis thaliana*. *Planta*, 224: 995-1003.

Casal J.J. and Mazzella M.A. (1998) Conditional synergism between cryptochrome 1 and phytochrome B is shown by the analysis of *phyA*, *phyB*, and *hy4* simple, double, and triple mutants in *Arabidopsis. Plant Physiol*., 118: 19–25.

Casal J.J., Luccioni L.G., Oliverio K.A. and Boccalandro H.E. (2003) Light, phytochrome signalling and photomorphogenesis in *Arabidopsis. Photochem.*

Photobiol. Sci., 2: 625–636.

Castelfranco P.A. and Jones O.T.G. (1975) Protoheme turnover and chlorophyll synthesis in greening barley tissue. *Plant Physiol.*, 55: 485–490.

Castillon A., Shen H. and Huq E. (2007) Phytochrome Interacting Factors: central players in phytochrome-mediated light signaling networks. *Trends Plant Sci*., 12: 514–52.

Cheetham M.E. and Caplan A.J. (1998) Structure, function and evolution of DnaJ: conservation and adaptation of chaperone function. *Cell Stress and Chaperones*, 3: 28–36.

Chen M., Schwab R. and Chory J. (2003) Characterization of the requirements for localization of phytochrome B to nuclear bodies. *Proc. Natl. Acad. Sci. USA*, 100: 14493–14498.

Chen Y.H., Yang X.Y., He K., Liu M.H., Li J.G., Lin Z.Q., Zhang Y.F., Wang X.X., Qiu X.M., Shen Y.P., Zhang L., Deng X.H., Luo J.C., Deng X.W., Chen Z.L., Gu H.Y. and Qu L.J. (2006) The MYB transcription factor superfamily of *Arabidopsis*: expression analysis and phylogenetic comparison with the rice MYB family. *Plant. Mol. Biol.*, 60:107–124.

Chow K.-S., Singh D.P., Roper J.M. and Smith A.G. (1997) A single precursor protein for ferrochelatase-I from *Arabidopsis* is imported in vitro into both chloroplasts and mithocondria. *J. Biol. Chem*., 272: 27565–27571.

Chow K.S., Singh D.P., Walker A.R. and Smith A.G. (1998) Two different genes encode ferrochelatase in *Arabidopsis*: mapping, expression and subcellular targeting of the precursor proteins. *Plant J.*, 15: 531–541.

Christie J.M., Salomon M., Nozue K., Wada M. and Briggs W.R. (1999) LOV (light, oxygen, or voltage) domains of the blue-light photoreceptor phototropin (nph1): Binding sites for the chromophore flavin mononucleotide. *Proc. Natl. Acad. Sci. USA*, 96: 8779–8783.

Churin Y., Adam E., Kozma-Bognar L., Nagy F. and Börner T. (2003) Characterization of two Myb-like transcription factors binding to *CAB* promoters in wheat and barley. *Plant Mol. Biol.*, 52: 447–462.

Clack T., Mathews S. and Sharrock R.A. (1994) The phytochrome apoprotein family

in *Arabidopsis* is encoded by five genes: the sequences and expression of *PHYD* and *PHYE. Plant. Mol. Biol.*, 25: 413–27.

Cornah J.C., Roper J.M., Singh D.P. and Smith A.G. (2002) Measurement of ferrochelatase activity using a novel assay suggests that plastids are the major site of haem biosynthesis in both photosynthetic and non-photosynthetic cells of pea (*Pisium sativum L.*). *Biochem. J.*, 362: 423-432.

Cornah J.E., Terry M.J. and Smith A.G. (2003) Green or red: what stops the traffic in the tetrapyrrole pathway? *Trends Plant Sci.*, 8: 224-230.

Covington M. F., Panda S., Liu X.L., Strayer C.A., Wagner D.R., and Kay S.A. (2001) *ELF3* modulates resetting of the circadian clock in *Arabidopsis*. *Plant Cell*, 13: 1305–1315.

Covington M.F., Maloof J.N., Straume M., Kay S.A. and Harmer S.L. (2008) Global transcriptome analysis reveals circadian regulation of key pathways in plant growth and development. *Genome Biol.*, 9: R130.

Crosson S., Rajagopal S. and Moffat K. (2003) The LOV domain family: photoresponsive signaling modules coupled to diverse output domains. *Biochem.*, 42: 2–10.

Czechowski T., Stitt M., Altmann T., Udvardi M.K. and Scheible W-R. (2005) Genome-wide identification and testing of superior reference genes for transcript normalization in *Arabidopsis*. *Plant Physiol.*, 139: 5-17.

Dailey HA (1990) Conversion of coproporphyrinogen to protoheme in higher eukaryotes and bacteria: Terminal three enzymes. In Dailey HA, ed, Biosynthesis of Heme and Chlorophylls, pp 123-161. McGraw-Hill, New York, USA

Dale J. E. (1988) The control of leaf expansion. Ann. Rev. Plant *Physiol. Plant* Mol. Biol., 39: 267-295.

Dangl J.L., Dietrich R.A. and Richberg M.H. (1996) Death don't have mercy: cell death programs in plant–microbe interactions. *Plant Cell*, 8: 1793–1807.

Davies K.M. and Schwinn K.E. (2003) Transcriptional regulation of secondary metabolism. Funct. *Plant Biol.*, 30: 913–925.

Davis S.J. (2006) The phytochrome chromophore. In Schafer E. and Nagy F., eds, Photomorphogenesis in plants and bacteris. Springer, Netherlands, pp 41-63.

Davison P.A., Schubert H.L., Reid J.D., Iorg C.D., Heroux A., Hill C.P. and Hunter C.N. (2005) Structural and biochemical characterisation of Gun4 suggests a mechanism for its role in chlorophyll biosynthesis. *Biochemistry*, 44: 7603-7612.

Delaney T.P., Uknes S., Vernooij B., Friedrich L., Weymann K., Negrotto D., Gaffney T., Gut-Rella M., Kessmann H., Ward E. and Ryals J. (1994) A central role of salicylic acid in plant disease resistance. *Science*, 266: 1247–1250.

Deng X. W., Matsui M., Wei N., Wagner D., Chu A.M., Feldmann K.A. and Quail P.H. (1992) *COP1*, an *Arabidopsis* regulatory gene, encodes a protein with both a zinc-binding motif and a G beta homologous domain. *Cell*, 71: 791–801.

Deng X.W. and Quail P.H. (1992) Genetic and phenotypic characterization of *cop1* mutants of *Arabidopsis thaliana*. *Plant J.*, 2: 83–95.

Desnos T., Puente P., Whitelam G.C. and Harberd N.P. (2001) *FHY1*: a phytochrome A-specific signal transducer. *Genes Dev.*, 15: 2980–2990.

Devlin P.F., Halliday K.J., Harberd N.P. and Whitelam G.C. (1996). The rosette habit of *Arabidopsis thaliana* is dependent upon phytochrome action: novel phytochromes control internode elongation and flowering time. *Plant J.*, 10, 1127-1134.

Devlin P,F., Patel S.R. and Whitelam G.C. (1998) Phytochrome E influences internode elongation and flowering time in *Arabidopsis*. *Plant Cell*, 10: 1479-1487.

Devlin P.F., Robson P.R., Patel S.R., Goosey L., Sharrock R.A. and Whitelam G.C. (1999) Phytochrome D acts in the shade-avoidance syndrome in *Arabidopsis* by controlling elongation growth and flowering time. *Plant Physiol.*, 119: 909-915.

Dhingra A., Bies D.H., Lehner K.R. and Folta K.M. (2006) Green Light Adjusts the Plastid Transcriptome during Early Photomorphogenic Development. *Plant Physiol.*, 142: 1256-1266.

Dodd A.N., Salathia N., Hall A., Kevei E., Toth R., Nagy F., Hibberd J.M., Millar A.J.

and Webb A.A. (2005) Plant circadian clocks increase photosynthesis, growth, survival, and competitive advantage. *Science*, 309: 630-633.

Dolganov N.A.M., Bhaya D. and Grossman A.R. (1995) Cyanobacterial protein with similarity to the chlorophyll a/b binding proteins of higher plants: evolution and regulation. *Proc. Natl. Acad. Sci. USA*, 92: 636–640.

Dong H., Deng Y., Mu J., Qingtao L., Wang Y., Xu Y., Chu C., Chong K., Lu C. and Zuo J. (2007) The *Arabidopsis SPONTANEOUS CELL DEATH 1* gene, encoding a z-carotene desaturase essential for carotenoid biosynthesis, is involved in chloroplast development, photoprotection and retrograde signalling. *Cell Res.*, 17: 458-470.

Dowson-Day M.J. and Millar A.J. (1999) Circadian dysfunction causes aberrant hypocotyl elongation patterns in *Arabidopsis*. *Plant J.*, 17: 63–71.

Doyle M. R., Davis S.J., Bastow R.M., McWatters H.G., Kozma-Bognár L., Nagy F., Millar A.J. and Amasino R.M. (2002) The *ELF4* gene controls circadian rhythms and flowering time in *Arabidopsis thaliana*. *Nature*, 419: 74–77.

Drechsler-Thielmann B., Dornemann D. and Senger H. (1993) Synthesis of protoheme via both the C4-pathway and Shemin pathway in the pigment mutant C-2A of Scenedesmus obliquus. *Z. Naturforsch*, 48c: 584-589.

Dubell A.N. and Mullet J.E. (1995) Continuous far-red light activates plastid DNA synthesis in pea leaves but not full cell enlargement or an increase in plastid number per cell. *Plant Physiol.*, 109: 95-103.

Duek P. D. and Fankhauser C. (2003) *HFR1*, a putative bHLH transcription factor, mediates both phytochrome A and cryptochrome signalling. *Plant J.*, 34: 827–836.

Duek P.D. and Fankhauser C. (2005) bHLH class transcription factors take centre stage in phytochrome signalling. *Trends Plant Sci.*, 10: 51-54.

Duggan J. and Gassman M. (1974) Induction of porphyrin synthesis in etiolated bean leaves by chelators of iron. *Plant Physiol.*, 53: 206–215.

Emanuelsson O., Brunak S., von Heijne G. and Nielsen H. (2007) Locating proteins in the cell using TargetP, SignalP, and related tools. *Nature Protocols*, 2: 953-971.

Emborg T.J., Walker J.M., Noh B. and Vierstra R.D. (2006) Multiple heme oxygenase family members contribute to the biosynthesis of the phytochrome chromophore in *Arabidopsis*. *Plant Physiol.*, 140: 856-868.

Fairchild C. D., Schumaker M. A. and Quail P. H. (2000) *HFR1* encodes an atypical bHLH protein that acts in phytochrome A signal transduction. *Genes Dev.*, 14: 2377–2391.

Fankhauser C. (2001) The phytochromes, a family of red/far-red absorbing photoreceptors. *J. Biol. Chem*., 276: 11453-11456.

Fankhauser C. and Staiger D. (2002) Photoreceptors in *Arabidopsis thaliana*: light perception, signal transduction and entrainment of the endogenous clock. *Planta*, 216: 1–16.

Farre E.M., Harmer S.L., Harmon F.G., Yanovsky M.J. and Kay S. A. (2005) Overlapping and distinct roles of *PRR7* and *PRR9* in the *Arabidopsis* circadian clock. *Curr. Biol.*, 15: 47–54.

Feldbrugge M., Sprenger M., Dinkelbach M., Yazaki K., Harter K., and Weisshaar B. (1994) Functional analysis of a light-responsive plant bZIP transcriptional regulator. *Plant Cell*, 6: 1607–1621.

Finkelstein R.R. (1994) Mutations at two new *Arabidopsis* ABA response loci are similar to the *abi3* mutations. *Plant J*., 5: 765–771.

Finkelstein R.R. and Lynch T.J. (2000) The *Arabidopsis* abscisic acid response gene *ABI5* encodes a basic leucine zipper transcription factor. *Plant Cell*, 12: 599–609.

Finkelstein R.R., Gampala S.S.L. and Rock C.D. (2002) Abscisic acid signaling in seeds and seedlings. *Plant Cell Supplement*, 14: S15–S45.

Finkelstein R.R., Wang M.L., Lynch T.J., Rao S. and Goodman H.M. (1998). The *Arabidopsis* abscisic acid response locus *ABI4* encodes an APETALA2 domain protein. *Plant Cell*, 10: 1043–1054.

Fitter D.W., Martin D.J., Copley M.J., Scotland R.W. and Langdale J.A. (2002) *GLK* gene pairs regulate chloroplast development in diverse plant species. *Plant J.*, 31: 713-727.

Fodje M.N., Hansson A., Hansson M., Olsen J.G., Gough S., Willows R.D. and A.l. Karadaghi S. (2001) Interplay between an AAA module and an integrin I domain may regulate the function of magnesium chelatase. *J. Mol. Biol.*, 311: 111–122.

Folta K.M. (2004) Green Light Stimulates Early Stem Elongation, Antagonizing Light-Mediated Growth Inhibition. *Plant Physiol.*, 135: 1407–1416.

Folta K.M. and Spalding E.P. (2001) Unexpected roles for cryptochrome 2 and phototropin revealed by high-resolution analysis of blue light-mediated hypocotyl growth inhibition. *Plant J.*, 26: 471–478.

Fowler S., Lee K., Onouchi H., Samach A., Richardson K., Morris B., Coupland G. and Putterill J. (1999) *GIGANTEA*: a circadian clock-controlled gene that regulates photoperiodic flowering in *Arabidopsis* and encodes a protein with several possible membrane-spanning domains. *Eur. J. Mol. Biol.*, 18: 4679–4688.

Franklin K. A., Davis S. J., Stoddart W.M., Vierstra R.D. and Whitelam G.C. (2003a) Mutant analyses define multiple roles for phytochrome C in *Arabidopsis* photomorphogenesis. *Plant Cell*, 15: 1981-1989.

Franklin K.A., Larner V.S. and Whitelam G.C. (2005) The signal transducing photoreceptors of plants. *Int. J. Dev. Biol*., 49: 653–64.

Franklin K.A., Praekelt U., Stoddart W.M., Billingham O.E., Halliday K.J. and Whitelam G.C. (2003b) Phytochromes B, D, and E act redundantly to control multiple physiological responses in *Arabidopsis*. *Plant Physiol.*, 131: 1340-1346.

Fujiwara S., Nakagawa M., Kamada H. and Mizoguchi T. (2005a) Circadian clock components in *Arabidopsis* III. *LHY/CCA1/GI* in regulating the floral integrator genes *LFY/SOC1/FT* to control flowering time and shoot architecture. *Plant Biotech*., 22: 327–331.

Fujiwara S., Oda A., Kamada H., Coupland G. and Mizoguchi T. (2005b) Circadian clock components in *Arabidopsis* II. *LHY/CCA1* regulate the floral integrator gene *SOC1* in both GI-dependent and -independent pathways. *Plant Biotech*., 22: 319–325.

Funk C. (2001) The PsbS protein: A Cab-protein with a function of its own, In E.M. Aro, B. Andersson, eds, Advances in Photosynthesis and Respiration-Regulation of Photosynthesis. Vol 11, Kluwer Academic Publishers, Dordrecht, The Netherlands, pp 453–467.

Funk C. and Vermaas W. (1999) A cyanobacterial gene family coding for single-helix proteins resembling part of the light-harvesting proteins from higher plants. *Biochem.*, 38: 9397-9404.

Furuya M. (1989) Molecular properties and biogenesis of phytochrome I and II. Adv. Biophys., 25: 133-167.

Furuya M. and Schafer E. (1996) Photoperception and signalling of induction reactions by different phytochromes. *Trends Plant Sci.*, 1: 301–307.

Furuya M., and Song P.-S. (1994) Assembly and properties of holophytochrome. In R.E. Kendrick and G.H.M. Kronenberg, eds, Photomorphogenesis in Plants. Dordrecht, Kluwer Academic Publishers, The Netherlands, pp. 105-140.

Gibson L.C.D., Marrison J.L., Leech R.M., Jenson P.E., Bassham D.C., Gibson M. and Hunter C.N. (1996) A putative Mg chelatase subunit from *Arabidopsis thaliana* cv C24. *Plant Physiol.*, 111: 61-71.

Gibson L.C.D., Willows R.D., Kannangara C.G., von Wettstein D. and Hunter C.N. (1995) Magnesium-protoporphyrin chelatase of *Rhodobacter sphaeroides*: reconstitiution of activity by combining the products of the *bchH-I* and *-D* genes expressed in *Escherichia coli*. *Proc.Natl.Acad. Sci. USA*, 92: 1941-1944.

Giovani B., Byrdin M., Ahmad M. and Brettel K. (2003) Light-induced electron transfer in a cryptochrome blue-light photoreceptor. *Nat. Struct. Biol*., 10: 489-490.

Giraudat J., Hauge B., Valon C., Smalle J., Parcy F. and Goodman H. (1992) Isolation of the *Arabidopsis ABI3* gene by positional cloning. *Plant Cell*, 4: 1251–1261.

Goslings D., Meskauskiene R., Kim C., Lee K.P., Nater M. and Apel K. (2004) Concurrent interactions of heme and FLU with Glu tRNA reductase (*HEMA1*), the target of metabolic feedback inhibition of tetrapyrrole biosynthesis, in dark- and light grown *Arabidopsis* plants. *Plant J.*, 40: 957–967.

Gosti F., Beaudoin N., Serizet C., Webb A.A.R., Vartanian N. and Giraudat J. (1999)

ABI1 protein phosphatase 2C is a negative regulator of abscisic acid signalling. *Plant Cell*, 11: 1897–1909.

Goto N., Kumagai T. and Koornneef M. (1991) Flowering responses to light-breaks in photomorphogenic mutants of *Arabidopsis thaliana*, a long day plant. *Physiologia Plantarum*, 83: 209-215.

Griffiths W.T. (1978) Reconstitution of chlorophyllide formation by isolated etioplast membranes. *Biochem.* J., 174: 681–692.

Griffiths W.T. (1991) Protochlorophyllide reduction. In, Scheer H., ed, Chlorophylls. Boca Raton, FL, CRC Press, pp 433-449.

Grossman A.R., Bhaya D., Apt K.E. and Kehoe D.M. (1995) Light-harvesting complexes in oxygenic photosynthesis: diversity, control, and evolution. Annu. Rev. *Genetics*, 29: 231–288.

Gruissem W. (1989) Chloroplast gene expression: How plants turn their plastids on. *Cell*, 56: 161-170.

Guo H., Yang H., Mockler T.C. and Lin C. (1998) Regulation of flowering time by *Arabidopsis* photoreceptors. *Science*, 279: 1360–1363.

Hajdukiewicz P.T.J., Allison L.A. and Maliga P. (1997) The two RNA polymerases encoded by the nuclear and the plastid compartments transcribe distinct groups of genes in tobacco plastids. Eur. *J. Mol. Biol.*, 16: 4041–4048.

Han L., Mason M., Risseeuw E.P., Crosby W.L. and Somers D.E. (2004) Formation of an SCFZTL complex is required for proper regulation of circadian timing. *Plant J.*, 40: 291–301.

Hanaoka M., Kanamaru K., Fujiwara M., Takahashi H. and Tanaka K. (2005) Glutamyl-tRNA mediates a switch in RNA polymerase use during chloroplast biogenesis. *Eur. J. Mol. Biol. Reports*, 6: 545–550.

Hangarter R.P. (1997) Gravity, light and plant form. *Plant, Cell and Environ.*, 20: 796-800.

Harmer S.L., Hogenesch J.B., Straume M., Chang H.S., Han B., Zhu T., Wang X., Kreps J.A. and Kay S.A. (2000) Orchestrated transcription of key pathways in *Arabidopsis* by the circadian clock. *Science*, 290: 2110–2113.

Harter, K., Kircher S., Frohnmeyer H., Krenz M., Nagy F. and Schäfer E. (1994) Light-regulated modification and nuclear translocation of cytosolic G-box binding factors in parsley. *Plant Cell* 6: 545–559.

Hay A., Barkoulas M., and Tsiantis M. (2006) *ASYMMETRIC LEAVES1* and auxin activities converge to repress *BREVIPEDICELLUS* expression and promote leaf development in *Arabidopsis*. *Development*, 133: 3955–3961.

Hazen S. P., Schultz T.F., Pruneda-Paz J.L., Borevitz J.O., Ecker J.R. and Kay S.A. (2005) *LUX ARRHYTHMO* encodes a Myb domain protein essential for circadian rhythms. *Proc. Natl. Acad. Sci. USA*, 102: 10387–10392.

Heddad M. and Adamska I. (2000) Light stress-regulated two-helix proteins in *Arabidopsis thaliana* related to the chlorophyll a/b-binding gene family. *Proc. Natl. Acad. Sci. USA*, 97: 3741–3746.

Hedtke B., Borner T. and Weihe A. (1997) Mitochondrial and chloroplast phage-type RNA polymerases in *Arabidopsis*. *Science*, 277: 809–811.

Hedtke B., Borner T. and Weihe A. (2000) One RNA polymerase serving two genomes. *Eur. J. Mol. Biol. Reports*, 1: 435–440.

Hennig L., Funk M.,Whitelam G.C. and Schafer E. (1999) Functional interaction of cryptochrome 1 and phytochrome D. *Plant J*., 20: 289–94.

Hennig L., Stoddart W. M., Dieterle M., Whitelam G. C. and Schafer E. (2002) Phytochrome E controls light induced germination of *Arabidopsis*. *Plant Physiol.*, 128: 194-200.

Hiltbrunner A., Tscheuschler A., Viczian A., Kunkel T., Kircher S. and Schafer E. (2006) FHY1 and FHL act together to mediate nuclear accumulation of the Phytochrome A Photoreceptor. *Plant Cell* Physiol., 47: 1023–1034.

Hiltbrunner A., Viczián A., Bury E., Tscheuschler A., Kircher S., Tóth R., Honsberger A., Nagy F., Fankhauser C. and Schafer E. (2005) Nuclear accumulation of the phytochrome A photoreceptor requires FHY1. *Curr. Biol.*, 15: 2125–2130.

Hiratsu K., Matsui K., Koyama T. and Ohme-Takagi M. (2003) Dominant repression of target genes by chimeric repressors that include the EAR motif, a repression domain, in *Arabidopsis. Plant J*., 34: 733–739.

Hirschi K.D., Zhen R.G., Cunningham K.W., Rea P.A. and Fink G.R. (1996) CAX1, an H+/Ca2+ antiporter from *Arabidopsis*. *Proc. Natl. Acad. Sci. USA*, 93: 8782-8786.

Hisada A., Hanzawa H., Weller J.L., Nagatani A., Reid J.B. and Furuya M. (2000) Light induced nuclear translocation of endogenous pea phytochrome A visualized by immunocytochemical procedures. *Plant Cell*, 12: 1063–1078.

Hofmann N.R. and Theg S.M. (2005) Chloroplast outer membrane protein targeting and insertion. *Trends Plant Sci.*, 10: 450–457.

Holm M., Ma L.-G., Qu L.-J. and Deng X.-W. (2002) Two interacting bZIP proteins are direct targets of *COP1*-mediated control of light-dependent gene expression in *Arabidopsis*. *Genes Dev.*, 16: 1247–1259.

Huala E., Oeller P.W., Liscum E., Han I.S., Larsen E. and Briggs W.R. (1997) *Arabidopsis NPH1*: a protein kinase with a putative redox-sensing domain. *Science*, 278: 2120–2123.

Huang C.J., Ayliffe M.A. and Timmis J.N. (2003) Direct measurement of the transfer rate of chloroplast DNA into the nucleus. *Nature*, 422: 72-76.

Hudson M. E., Lisch D. R. and Quail P. H. (2003) The *FHY3* and *FAR1* genes encode transposase-related proteins involved in regulation of gene expression by the phytochrome A-signaling pathway. *Plant J.*, 34: 453–471.

Hudson M., Ringli C., Boylan M. T. and Quail P. H. (1999) The *FAR1* locus encodes a novel nuclear protein specific to phytochrome A signalling. *Genes Dev.*, 13: 2017–2027.

Hulskamp M., Misera S. and Jurgens G. (1994) Genetic dissection of trichome cell development in *Arabidopsis*. *Cell*, 76: 555-566.

Hunter D.A., Ferrante A., Vernieri P. and Reid M.S. (2004) Role of abscisic acid in perianth senescence of daffodil (*Narcissus pseudonarcissus* ‘Dutch Master’). *Physiol. Plant*, 121: 313–321.

Huq E. and Quail P.H. (2002) PIF4, a phytochrome-interacting bHLH factor, functions as a negative regulator of phytochrome B signaling in *Arabidopsis*. *Eur. Mol. Biol. J.*, 21: 2441-2450.

Huq E., Al-Sady B. and Quail P.H. (2003) Nuclear translocation of the photoreceptor phytochrome B is necessary for its biological function in seedling photomorphogenesis. *Plant J.*, 35: 660–664.

Huq E., El-Sady B., Hudson M., Kim C., Apel K. and Quail P.H. (2004) *PHYTOCHROME INTERACTING FACTOR 1* is a critical bHLH regulator of chlorophyll biosynthesis. *Science*, 305: 1937-1941.

Ikeuchi M. and Murakami S. (1983) Separation and characterization of prolamellar bodies and prothylakoids from squash etioplasts. *Plant Cell* Physiol., 24: 71-80.

Ilag L.L., Kumar A.M. and Soll D. (1994) Light regulation of chlorophyll biosynthesis at the level of 5-aminolevulinate formation in *Arabidopsis*. *Plant Cell*, 6: 265–75.

Imaizumi T., Schultz T.F., Harmon F.G., Ho L.A. and Kay S.A. (2005) FKF1 F-box protein mediates cyclic degradation of a repressor of *CONSTANS* in *Arabidopsis*. *Science*. 309: 293–297.

Imaizumi T., Tran H.G., Swartz T.E., Briggs W.R. and Kay S.A. (2003) *FKF1* is essential for photoperiodic-specific light signalling in *Arabidopsis*. *Nature*, 426: 302–306.

Ishida T., Kurata T., Okada K. and Wada T. (2008) A genetic regulatory network in the development of trichomes and root hairs. *Annu. Rev. Plant Biol.*, 59: 365–86.

Ishikawa A., Okamoto H., Iwasaki Y. and Asahi T. (2001) A deficiency of coproporphyrinogen III oxidase causes lesion formation in *Arabidopsis*. *Plant J.*, 27: 89-99.

Isono K., Shimizu M., Yoshimoto K., Niwa Y., Satoh K., Yokota A. and Kobayashi H. (1997) Leaf-specifically expressed genes for polypeptides destined for chloroplasts with domains of r70 factors of bacterial RNA polymerases in *Arabidopsis thaliana*. *Proc. Natl. Acad. Sci. USA*, 94: 14948–14953.

Jakoby M., Weisshaar B., Dröge-Laser W., Vicente-Carbajosa J., Tiedemann J., Kroj T. and Parcy F. (2002) bZIP transcription factors in *Arabidopsis*. *Trends Plant Sci.*, 7: 106–111.

Jansson S. (1999) A guide to the Lhc genes and their relatives in *Arabidopsis. Trends Plant Sci*., 4: 236–240.

Jansson S., Andersson J., Jung Kim S. and Jackowski G. (2000) An *Arabidopsis thaliana* protein homologous to cyanobacterial high-light-inducible proteins. *Plant. Mol. Biol*., 42: 345-351.

Jarillo J.A., Capel J., Tang R.H., Yang H.Q., Alonso J.M., Ecker J.R. and Cashmore A.R. (2001b) An *Arabidopsis* circadian clock component interacts with both cry1 and phyB. *Nature*. 410: 487–490.

Jarillo J.A., Gabrys H., Capel J., Alonso J.M., Ecker J.R. and Cashmore A.R. (2001a) Phototropin-related *NPL1* controls chloroplast relocation induced by blue light. *Nature*, 410: 952–954.

Jarvis P. (2008) Targeting of nucleus-encoded proteins to chloroplasts in plants (Tansley Review). *New Phytol*., 179: 257-285.

Jarvis P. and Robinson C. (2004) Mechanisms of protein import and routing in chloroplasts. *Curr. Biol.*, 14: R1064–R1077.

Jensen P.E., Gibson L.C.D. and Hunter C.N. (1999) ATPase activity associated with the magnesium-protoporphyrin IX chelatase enzyme of *Synechocystis sp. PCC6803*: evidence for ATP hydrolysis during Mg2+ insertion, and the MgATP–dependent interaction of the ChlI and ChlD subunits. *Biochem. J*., 339: 127–134.

Jensen P.E., Gibson L.C.D., Henningsen K.W. and Hunter C.N. (1996) Expression of the *chlI*, *chlD*, and *chlH* genes from the cyanobacterium *Synechocystis PCC6803* in *Escherichia coli* and demonstration that the three cognate proteins are required for magnesium-protoporphyrin chelatase activity. *J. Biol. Chem*., 271: 16662–16667.

Jensen, P.E., Reid J.D. and Hunter C.N. (2000) Modification of cysteine residues in the ChlI and ChlH subunits of magnesium chelatase results in enzyme inactivation. *Biochem. J*., 352: 435–441.

Johanningmeier U. (1988) Possible control of transcript levels by chlorophyll precursors in Chlamydomonas. *Eur. J. Biochem.*, 177: 417-424.

Johanningmeier U. and Howell S.H. (1984) Regulation of light-harvesting chlorophyll

a/b binding protein mRNA accumulation in Chlamydomonas reinhardii: Possible involvement of chlorophyll synthesis precursors. *J. Biol. Chem*., 259: 13541-13549.

Johnsen E., Bradley M., Harberd N.P. and Whitelam G.C. (1994) Photoresponses of light-grown phyA mutants of *Arabidopsis*. *Plant Physiol.*, 105: 141-149.

Kagawa T. and Wada M. (2000) Blue light-induced chloroplast relocation in *Arabidopsis thaliana* as analyzed by microbeam irradiation. *Plant Cell Physiol*., 41: 84–93.

Kagawa T., Kasahara M., Abe T., Yoshida S. and Wada M. (2004) Function analysis of phototropin 2 using fern mutants deficient in blue light-induced chloroplast avoidance movement, *Plant Cell Physiol.*, 45: 416–426.

Kagawa T., Sakai T., Suetsugu N., Oikawa K., Ishiguro S., Kato T., Tabata S., Okada K. and Wada M. (2001) *Arabidopsis NPL1*: a phototropin homolog controlling the chloroplast high-light avoidance response. *Science*, 291: 2138–2141.

Karger G.A., Reid J.D. and Hunter C.N. (2001) Characterisation of the binding of deuteroporphyrin IX to the magnesium chelatase H subunit and spectroscopic properties of the complex. *Biochem.*, 40: 9291-9299.

Kato T., Murakami M., Nakamura Y., Ito S., Nakamichi N., Yamashino T. and Mizuno T. (2007) Mutants of circadian-associated PRR genes display a novel and visible phenotype as to light responses during de-etiolation of *Arabidopsis* thaliana seedlings. *Biosci. Biotechnol. Biochem*., 71: 834-839.

Khanna R., Huq E., Kikis E.A., Al-Sady B., Lanzatella C. and Quail P.H. (2004) A novel molecular recognition motif necessary for targeting photoactivated phytochrome signaling to specific basic helix-loop-helix transcription factors. *Plant Cell*, 16: 3033–3044.

Kikis E. A., Khanna R. and Quail P. H. (2005) *ELF4* is a phytochrome-regulated component of a negative feedback loop involving the central oscillator components *CCA1* and *LHY*. *Plant J.*, 44: 300–313.

Kim J., Yi H., Choi G., Shin B., Song P-S. and Choi G. (2003) Functional characterization of phytochrome interacting factor 3 in phytochrome-mediated light signal transduction. *Plant Cell*, 15: 2399–2407.

Kim W.Y., Fujiwara S., Suh S.S., Kim J., Kim Y., Han L., David K., Putterill J., Nam H.G. and Somers D.E. (2007) *ZEITLUPE* is a circadian photoreceptor stabilized by *GIGANTEA* in blue light. *Nature*, 449: 356–360.

Kinoshita T., Doi M., Suetsugu N., Kagawa T., Wada M. and Shimazaki K. (2001) Phot1 and phot2 mediate blue light regulation of stomatal opening. *Nature*, 414: 656–660.

Kircher S., Gil P., Kozma-Bognar L., Fejes E., Speth V., Husselstein-Muller T., Bauer D., Ádám E., Schäfer E. and Nagy F. (2002) Nucleocytoplasmic partitioning of the plant photoreceptors phytochrome A, B, C, D, and E is regulated differentially by light and exhibits a diurnal rhythm. *Plant Cell*, 14: 1541–1555.

Kircher S., Kozma-Bognar L., Kim L., Adam E., Harter K., Schafer E. and Nagy F. (1999) Light quality-dependent nuclear import of the plant photoreceptors phytochrome A and B. *Plant Cell*, 11: 1445–1456.

Klar T., Pokorny R., Moldt J., Batschauer A. and Essen L.-O. (2007) Cryptochrome 3 from *Arabidopsis thaliana*: structural and functional analysis of its complex with a folate light antenna. *J. Mol. Biol*., 366: 954-964.

Kleine, T., Lockhart P. and Batschauer A. (2003) An *Arabidopsis* protein closely related to *Synechocystis* cryptochrome is targeted to organelles. *Plant J.*, 35: 93–103.

Klimczak L.J., Schindler U. and Cashmore A.R. (1992) DNA binding activity of the *Arabidopsis* G-box binding factor GBF1 is stimulated by phosphorylation by casein kinase II from broccoli. *Plant Cell*, 4: 87–98.

Klimczak, L. J., Collinge M.A., Farini D., Giuliano G., Walker J.C. and Cashmore A.R. (1995) Reconstitution of *Arabidopsis* casein kinase II from recombinant subunits and phosphorylation of transcription factor *GBF1*. *Plant Cell*, 7: 105–115.

Koornneef M., Dellaert L.W.M. and Van der Veen J.H. (1982b) EMS and radiation-induced mutation frequencies at individual loci in *Arabidopsis thaliana*. *Mutat. Res*,. 93: 109-123.

Koornneef M., Jorna M.L., Brinkhorst-van der Swan D.L.C., and Karssen C.M.

(1982a). The isolation of abscisic acid (ABA) deficient mutants by selection of induced revertants in non-germinating gibberellin sensitive lines of *Arabidopsis thaliana* (L.), Heynh. *Theor. Appl. Genet*., 61: 385–393.

Koornneef M., Reuling G., and Karssen C.M. (1984). The isolation and characterization of abscisic acid–insensitive mutants of *Arabidopsis thaliana*. *Physiol. Plant*., 61: 377–383.

Koornneef M., Rolff E., and Spruit C. (1980) Genetic control of light-inhibited hypocotyl elongation in *Arabidopsis thaliana* (L.), Heynh. *Z. Pflanzenphysiol*., 100: 147-1 60.

Koussevitzky S., Nott A., Mockler T.C., Hong F., Sachetto-Martins G., Surpin M., Lim J., Mittler R. and Chory J. (2007) Multiple Signals from Damaged Chloroplasts Converge on a Common Pathway to Regulate Nuclear Gene Expression. *Science Express*, 316: 715-719.

Kovaleva L.V. and Zakharova E.V. (2003) Hormonal status of the pollen-pistil system at the progamic phase of fertilization after compatible and incompatible pollination in *Petunia hybrida L*. *Sex. Plant Reprod*., 16: 191–196.

Kropat J., Oster U., Rudiger W. and Beck C.F. (1997) Chlorophyll precursors are signals of chloroplast origin involved in light induction of nuclear heat-shock genes. *Proc. Natl. Acad. Sci. USA*, 94: 14168-14172.

Kropat J., Oster U., Rudiger W. and Beck C.F. (2000) Chloroplast signalling in the light induction of nuclear *HSP70A* genes requires the accumulation of precurors and their accessibility to the cytoplasm/nucleus. *Plant J.*, 24:523-531.

Kruse E., Grimm B., Beator J. and Kloppstech K. (1997) Developmental and circadian control of the capacity for 5-aminolevulinic acid synthesis in green barley. *Planta*, 202: 235-241.

Kruse E., Mock H.-P. and Grimm B. (1995) Reduction of coproporphyrinogen oxidase level by antisense RNA synthesis leads to deregulated gene expression of plastid proteins and affects the oxidative stress defense system, *Eur. J. Mol. Biol.*, 14: 3712–3720.

Kumar A.M. and Soll D. (2000) Antisense *HEMA1* RNA expression inhibits haem and

chlorophyll biosynthesis in *Arabidopsis*. *Plant Physiol.*, 122: 49-55.

Kumar A.M., Csankovszki G. and Soll D. (1996) A second and differentially expressed glutamyl-tRNA reductase gene from *Arabidopsis thaliana*. *Plant Mol. Biol*., 30: 419-426.

La Rocca N., Rascio N., Oster U. and Rudiger W. (2001) Amitrole treatment of etiolated seedlings leads to deregulation of tetrapyrrole synthesis and to reduced expression of *Lhc* and *RbcS* genes. *Planta*, 213: 101-108.

Laby R.J., Kincaid M.S., Kim D. and Gibson S.I. (2000) The *Arabidopsis* sugar-insensitive mutants *sis4* and *sis5* are defective in abscisic acid synthesis and response. *Plant J.*, 23: 587-596.

Lagarias D.M., Crepeau M.W., Maines M.D. and Lagarias J.C. (1997) Regulation of photomorphogenesis by expression of mammalian biliverdin reductase in transgenic *Arabidopsis* plants. *Plant Cell*, 9: 675–788.

Lagarias J.C. and Lagarias D.M. (1989) Self-assembly of synthetic phytochrome holoprotein *in vitro*. *Proc. Natl. Acad. Sci. USA*, 86: 5778-5780.

Lagarias J.C. and Rapoport H. (1980) Chromopeptides from phytochrome. The structure and linkage of the Pr form of the phytochrome chromophore. *J. Am. Chem. Soc*., 102: 4821–4828.

Lake V., Olsson U., Willows R.D. and Hansson M. (2004) ATPase activity of magnesium chelatase subunit I is required to maintain subunit D *in vivo*. *Eur. J. Biochem*., 271: 2182–2188.

Lamparter T., Esteban B. and Hughes J. (2001) Phytochrome Cph1 from the cyanobacterium *Synechocystis* PCC6803. Purification, assembly, and quaternary structure. *Eur. J. Biochem*., 268:4720–30

Larkin J. C., Oppenheimer D. G., Lloyd A. M., Paparozzi E. T. and Marks M. D., (1994) Roles of the *GLABROUS1* and *TRANSPARENT TESTA GLABRA* genes in *Arabidopsis* trichome development. *Plant Cell*, 6: 1065-1076.

Larkin R.M., Alonso J.M., Ecker J.R. and Chory J. (2003) *GUN4*, a regulator of chlorophyll synthesis and intracellular signalling. *Science*, 299: 902-906.

Lebedev N. and Timko M.P. (1998) Protochlorophyllide photoreduction. *Photosyn.*

Res., 58: 5–23.

Lee H., Fischer R.L., Goldberg R.B. and Harada J.J. (2003a) *Arabidopsis LEAFY COTYLEDON1* represents a functionally specialized subunit of the CCAAT binding transcription factor. *Proc. Natl. Acad. Sci. USA*, 100: 2152–2156.

Lee K.P., Kim C., Lee D.W. and Apel K. (2003b) *TIGRINA d*, requirewd for regulating the biosynthesis of tetrapyrroles in barley, is an ortholog of the *FLU* gene of *Arabidopsis thaliana*. *FEBS Letters*, 553: 119-124.

Leivar P., Monte E., Oka Y., Liu T., Carle C., Castillon A., Huq E. and Quail P.H. (2008) Multiple phytochrome-interacting bHLH transcription factors repress premature seedling photomorphogenesis in darkness. *Curr. Biol.*, 18: 1815-1823.

Leyser H.M.O., Lincoln C., Timpte C., Lammer D., Turner J. and Estelle M. (1993) The auxin-resistance gene *AXR1* of *Arabidopsis* encodes a protein related to ubiquitin-activating enzyme E1. *Nature*, 364:161–164.

Li Y., Rosso M.G., Viehoever P. and Weisshaar B. (2007) GABI-Kat SimpleSearch: an *Arabidopsis thaliana* T-DNA mutant database with detailed information for confirmed insertions. *Nucleic Acid Res.*, 35: 874-878.

Liang Y.-K., Dubos C., Dodd I.C., Holroyd G.H., Hetherington A.M. and Campbell M.M. (2005) *AtMYB61*, an R2R3-MYB transcription factor controlling stomatal aperture in *Arabidopsis thaliana*. *Curr. Biol.*, 15: 1201–1206.

Lichtenthaler H.K. (1987) Chlorophylls and carotenoids: Pigments of photosynthetic membranes. *Meth. Enzymol.*, 148: 350–382.

Lin C., Ahmad M. and Cashmore A.R. (1996) *Arabidopsis* cryptochrome 1 is a soluble protein mediating blue light-dependent regulation of plant growth and development. *Plant J.*, 10: 893–902.

Lin R.C., Ding L., Casola C., Ripoll D.R., Feschotte C. and Wang H.Y. (2007) Transposase-derived transcription factors regulate light signaling in *Arabidopsis. Science*, 318: 1302–1305.

Lin C., Yang H., Guo H., Mockler T., Chen J. and Cashmore A.R. (1998) Enhancement of blue-light sensitivity of *Arabidopsis* seedlings by a blue light receptor cryptochrome 2. *Proc. Natl. Acad. Sci. USA*, 95: 2686–2690.

Liscum E. and Hangarter R.P. (1993) Genetic evidence that the Pr form of phytochrome B plays a role in *Arabidopsis thaliana* gravitropism. *Plant Physiol.*, 103: 15-19.

Liscum E., and Briggs W.R. (1995) Mutations in the *NPH1* locus of *Arabidopsis* disrupt the perception of phototropic stimuli. *Plant Cell*, 7: 473–485.

Lister R., Chew O., Rudhe C., Lee M.N. and Whelan J. (2001) *Arabidopsis thaliana* ferrochelatase-I and -II are not imported into *Arabidopsis* mitochondria. *FEBS Letters*, 506: 291–295.

Liu X.-L., Covington M.F., Fankhauser C., Chory J. and Wagner D.R. (2001) *ELF3* encodes a circadian clock-regulated nuclear protein that functions in an *Arabidopsis* PHYB signal transduction pathway. *Plant Cell*, 13: 1293–1304.

Loeb MR (1995) Ferrochelatase activity and protoporphyrin IX utilization in *Haemophilus influenzae*. *J Bacteriol*., 177: 3613-3615

Lopez-Juez E. (2007) Plastid biogenesis: between light and shadows. *J. of Ex. Bot*., 58: 11-26.

Lopez-Juez E. and Pyke K.A. (2005) Plastids unleashed: their development and their integration in plant development. *Int. J. of Dev. Biol*., 49: 557–577.

Lopez-Juez E., Nagatani A., Tomizawa K., Deak M., Kern R., Kendrick R.E. and Furuya M. (1992) The cucumber long hypocotyl mutant lacks a light-stable PHYB-like phytochrome. *Plant Cell*, 4:241–51.

Makino S., Matsushika A., Kojima M., Yamashino T. and Mizuno T. (2002) The *APRR1/TOC1* quintet implicated in circadian rhythms of *Arabidopsis thaliana*: I. Characterization with APRR1-overexpressing plants. *Plant Cell* Physiol., 43: 58–69.

Mao J., Zhang J.C., Sang Y., Li Q.H. and Yang H.Q. (2005) A role for *Arabidopsis* cryptochromes and *COP1* in the regulation of stomatal opening. *Proc. Natl. Acad. Sci. USA*, 102: 12270–12275.

Martin W., Rujan T., Richly E., Hansen A., Cornelsen S., Lins T., Leister D., Stoebe B., Hasegawa M. and Penny D. (2002) Evolutionary analysis of *Arabidopsis*, cyanobacterial, and chloroplast genomes reveals plastid phylogeny and thousands of cyanobacterial genes in the nucleus. *Proc. Natl. Acad. Sci. USA*,

99: 12246–12251.

Martinez-Garcia J.F., Huq E. and Quail P.H. (2000) Direct targeting of light signals to a promoter element bound transcription factor. *Science*, 288: 859-863.

Mas P., Alabadi D., Yanovsky M.J., Oyama T. and Kay S.A. (2003a) Dual role of *TOC1* in the control of circadian and photomorphogenic responses in *Arabidopsis*. *Plant Cell*, 15: 223–236.

Mas P., Devlin P.F., Panda S. and Kay S.A. (2000) Functional interaction of phytochrome B and cryptochrome 2. *Nature*, 408: 207–211.

Más P., Kim W.-Y., Somers D.E. and Kay S.A. (2003b) Targeted degradation of TOC1 by ZTL modulates circadian function in *Arabidopsis thaliana*. *Nature*, 426: 567–570.

Masuda T. and Takamiya K. (2004) Novel insights into the enzymology, regulation and physiological functions of light-dependent protochlorophyllide oxidoreductase in angiosperms. *Photosyn. Res.*, 81: 1–29.

Masuda T., Ohta H., Shioi Y., Tsuji H. and Takamiya K. (1995) Stimulation of glutamyl-tRNA reductase activity by benzyladenine in greening cucumber cotyledons. *Plant Cell Physiol*., 36: 1237-1243.

Matsumoto F., Obayashi T., Sasaki-Sekimoto Y., Ohta H., Takamiya K. and Masuda T. (2004) Gene expression profiling of the tetrapyrrole metabolic pathway in *Arabidopsis* with a mini-array system. *Plant Physiol.*, 135: 2379-2391.

Matsumoto N., Hirano T., Iwasaki T. and Yamamoto N. (2003) Functional analysis and intracellular localization of rice cryptochromes. *Plant Physiol.*, 133: 1494–1503.

Matsushita T., Mochizuki N. and Nagatani A. (2003) Dimers of the N-terminal domain of phytochrome B are functional in the nucleus. *Nature*, 424: 571–574.

Maxwell D.P., Laudenbach D.E. and Huner N.P.A. (1995) Redox regulation of light-harvesting complex II and *CAB* mRNA abundance in Dunaliella salina. *Plant Physiol.*, 109: 787-795.

Mayer S.M. and Beale S.I. (1992) Succinyl-coenzyme A synthetase and its role in δ-aminolevulinic acid biosynthesis in Euglena gracilis. *Plant Physiol.*, 99: 482-

487.

McCormac A.C. and Terry M.J. (2002a) Light-signalling pathways leading to the co-ordinated expression of *HEMA1* and *Lhcb* during chloroplast development in *Arabidopsis thaliana. Plant J*., 32: 549–560.

McCormac A.C. and Terry M.J. (2002b) Loss of Nuclear Gene Expression during the Phytochrome A-Mediated Far-Red Block of Greening Response. *Plant Physiol.*, 130: 402-414.

McCormac A.C. and Terry M.J. (2004) The nuclear genes *Lhcb* and *HEMA1* are differentially sensitive to plastid signals and suggest distinct roles for the GUN1 and GUN5 plastid signalling pathways during de-etiolation. *Plant J.*, 40: 672-685.

McCormac A.C., Fischer A., Kumar A.M., Soll D. and Terry M.J. (2001) Regulation of *HEMA1* expression by phytochrome and a plastid signal during de-etiolation in *Arabidopsis thaliana*. *Plant J.*, 25: 549-561.

Meskauskiene R. and Apel K. (2002) Interaction of FLU, a negative regulator of chlorophyll biosynthesis, with glutamyl-tRNA reductase requires the tetratricopeptide repeat domain of FLU. *FEBS Letters*, 532: 27-30.

Meskauskiene R., Nater M., Goslings D., Kessler F., op den Camp R. and Apel K. (2001) FLU: a negative regulator of chlorophyll biosynthesis in *Arabidopsis thaliana*. *Proc. Natl. Acad. Sci. USA*, 98: 12826-12831.

Millar A.J. and Kay S.A. (1996) Intergration of circadian and phototransduction pathways in the network controlling *CAB* gene transcription in *Arabidopsis*. *Proc. Natl. Acad. Sci. USA*, 93: 15491-15496.

Miyamoto K., Tanaka R., Teramoto H., Masuda T., Tsuji H. and Inokuchi H. (1994) Nucleotide sequences of cDNA clones encoding ferrochelatase from barley and cucumber. *Plant Physiol.*, 105: 769–770.

Mizoguchi T., Wheatley K., Hanzawa Y., Wright L., Mizoguchi M., Song H.R., Carré I.A. and Coupland G. (2002) *LHY* and *CCA1* are partially redundant genes required to maintain circadian rhythms in *Arabidopsis*. *Dev. Cell*, 2: 629–641.

Mizoguchi T., Wright L., Fujiwara S., Cremer F., Lee K., Onouchi H., Mouradov A., Fowler S., Kamada H., Putterill J. and Coupland G. (2005) Distinct Roles of

GIGANTEA in Promoting Flowering and Regulating Circadian Rhythms in *Arabidopsis*. *Plant Cell*, 17: 2255–2270.

Mochizuki N., Brusslan J.A., Larkin R., Nagatani A. and Chory J. (2001) *Arabidopsis* genomes uncoupled 5 (gun5) mutant reveals the involvement of Mg-chelatase H subunit in plastid–to-nucleas signal transduction. *Proc. Natl. Acad. Sci. USA*, 98: 2053-2058.

Mochizuki, N., Susek, R., and Chory, J. (1996) An intracellular signal transduction pathway between the chloroplast and nucleus is involved in de-etiolation. *Plant Physiol.*, 112: 1465–1469.

Mochizuki N., Tanaka R., Tanaka A., Masuda T. and Nagatani A. (2008) The steady state level of Mg-protoporphyrin IX is not a determinant of plastid-to-nucleus signaling in *Arabidopsis. Proc. Natl. Acad. Sci. USA*, 105: 15184–15189.

Mock H.-P. and Grimm B. (1997) Reduction of uroporphyrinogen decarboxylase by antisense RNA expression affects activities of other enzymes involved in tetrapyrrole biosynthesis and leads to light-dependent necrosis. *Plant Physiol.*, 113: 1101–1112.

Mockler, T. C., Guo H., Yang H., Duong H. and Lin C. (1999) Antagonistic actions of *Arabidopsis* cryptochromes and phytochrome B in the regulation of floral induction. *Development*, 126: 2073–2082.

Mohan Ram I.I.Y. and Juiswal V.S. (1972) Induction of male flowers on female plants of *Canabis sativa* by gibberellins and its inhibition by abscisic acid. *Planta*, 105: 263–266.

Molina A., Volrath S., Guyer D., Maleck K., Ryals J. and Ward E. (1999) Inhibition of protoporphyrinogen oxidase expression in *Arabidopsis* causes a lesion-mimic phenotype that induces systemic acquired resistance. *Plant J*., 17: 667-678.

Møller S.G., Kunkel T. and Chua N.-H. (2001) A plastidic ABC protein involved in intercompartmental communication of light signalling. *Genes Dev.*, 15: 90-103.

Montane´ M.H. and Kloppstech K. (2000) The family of light-harvesting-related proteins (LHCs, ELIPs, HLIPs): Was the harvesting of light their primary function? *Gene*, 258: 1–8.

Monte E., Alonso J.M., Ecker J. R., Zhang Y., Li X., Young J., Austin-Phillips S. and Quail P.H. (2003) Isolation and characterization of phyC mutants in *Arabidopsis* reveals complex crosstalk between phytochrome signaling pathways. *Plant Cell*, 15: 1962-1980.

Monte E., Al-Sady B., Leivar P. and Quail PH (2007) Out of the dark: how the PIFs are unmasking a dual temporal mechanism of phytochrome signalling. *J. Exp. Bot*., 58: 3125-3133.

Monte E., Tepperman J.M., Al-Sady B., Kaczorowski K.A., Alonso J.M., Ecker J.R., Li X., Zhang Y. and Quail P.H. (2004) The phytochrome-interacting transcription factor, PIF3, acts early, selectively, and positively in light-induced chloroplast development. *Proc. Natl. Acad. Sci. USA*, 101: 16091–16098.

Montgomery B.L. and Lagarias J.C. (2002) Phytochrome ancestry: sensors of bilins and light. *Trends Plant Sci.*, 7: 357-366.

Moon J., Zhu L., Shen H. and Huq E. (2008) PIF1 directly and indirectly regulates chlorophyll biosynthesis to optimize the greening process in *Arabidopsis*. *Proc. Natl. Acad. Sci. USA*, 105: 9433-9438.

Moulin M., McCormac A.C., Terry M.J. and Smith A.G. (2008) Tetrapyrrole profiling in *Arabidopsis* seedlings reveals that retrograde plastid nuclear signalling is not due to Mg-protoporphyrin IX accumulation. *Proc. Natl. Acad. Sci. USA*, 105: 15178–15183.

Mudd E.A., Sullivan S., Gisby M.F., Mironov A., Kwon C.S., Chung W. and Day A. (2008) A 125 kDa RNase E/G-like protein is present in plastids and is essential for chloroplast development and autotrophic growth in *Arabidopsis*. *J. Exp. Bot*., 59: 2597-2610.

Mullen J.L., Weinig C. and Hangarter R.P. (2006) Shade avoidance and the regulation of leaf inclination in *Arabidopsis*. *Plant, Cell and Environ.*, 29: 1099-1106.

Mullet J. E. (1988) Chloroplast development and gene expression. Ann. Rev. *Plant Physiol. Plant Mol. Biol*., 39: 475-502.

Murashige T. and Skoog F. (1962) A revised medium for rapid growth and bioassays with tobacco cultures. *Physiol. Plant*, 15: 473-497.

Murphy M. J., Siegel L. M., Tove S. R. and Kamen, H. (1974) Siroheme: a new

prosthetic group participating in six-electron reduction reactions catalyzed by both sulfite and nitrite reductases. *Proc. Natl. Acad. Sci. USA*, 71: 612–616.

Nada A. and Soll J. (2004) Inner envelope protein 32 is imported into chloroplasts by a novel pathway. *J. of Cell Sci*., 117: 3975–3982.

Nagai S., Koide M., Takahashi S., Kikuta A., Aono M., Sasaki-Sekimoto Y., Ohta H., Takamiya K.-I. and Masuda T. (2007) Induction of Isoforms of Tetrapyrrole Biosynthetic Enzymes, *AtHEMA2* and *AtFC1*, under Stress Conditions and Their Physiological Functions in *Arabidopsis*. *Plant Physiol*., 144: 1039–1051.

Nagatani A., Reed J.W. and Chory J. (1993) Isolation and initial characterization of *Arabidopsis* mutants that are deficient in phytochrome A. *Plant Physiol.*, 102: 269-277.

Nagy F. and Schafer E. (2002) Phytochromes control photomorphogenesis by differentially regulated, interacting signalling pathways in higher plants. *Annu. Rev. Plant Biol.*, 53: 329–355.

Nakamichi N. Kita M., Ito S., Sato E., Yamashino T. and Mizuno T. (2005) The *Arabidopsis* pseudo-response regulators, *PRR5* and *PRR7*, coordinately play essential roles for circadian clock function. *Plant Cell Physiol*., 46: 609–619.

Nakamichi N., Kita M., Ito S., Yamashino T. and Mizuno T. (2005) *PSEUDO-RESPONSE REGULATORS*, *PRR9*, *PRR7* and *PRR5*, together play essential roles close to the circadian clock of *Arabidopsis thaliana*. *Plant Cell Physiol*., 46: 686–698.

Nakamura Y., Kaneko T. and Tabata S. (2000) CyanoBase, the genome database for Synechocystis sp. strain PCC6803: status for the year 2000. Nucleic Acids Res., 28: 72.

Neff M.M. and Chory J. (1998) Genetic interaction between phytochrome A, phytochrome B, and cryptochrome 1 during *Arabidopsis* development. *Plant Physiol.*, 118: 27–35.

Neff M.M. and Volkenburgh E. Van (1994) Light-stimulated cotyledon expansion in *Arabidopsis* seedlings. *Plant Physiol.*, 104: 1027-1032.

Nelson D.C., Lasswell J., Rogg L.E., Cohen M.A. and Bartel B. (2000) *FKF1*, a clock-controlled gene that regulates the transition to flowering in *Arabidopsis*. *Cell*,

101: 331–340.

Neuwald A.F., Aravind L., Spouge J.L. and Koonin E.V. (1999) AAA+: a class of chaperone-like ATPases associated with the assembly, operation, and disassembly of protein complexes. *Genome Res*., 9: 27–43.

Ni M., Tepperman J.M. and Quail P.H. (1998) PIF3, a phytochrome-interacting factor necessary for normal photoinduced signal transduction, is a novel basic helix-loop-helix protein. *Cell*, 95: 657–667.

Ni M., Tepperman J.M. and Quail P.H. (1999) Binding of phytochrome B to its nuclear signalling partner PIF3 is reversibly induced by light. *Nature*, 400: 781–784.

Niinuma K., Nakagawa M., Calvino M. and Mizoguchi T. (2007) Dance of plants with circadian clock. *Plant Biotech*., 24: 87–97.

Nott A., Jung H.S., Koussevitzky S. and Chory J. (2006) Plastid-to-nucleus retrograde signalling. *Ann. Rev. Plant Biol*., 57: 739-759.

Oda A., Fujiwara S., Kamada H., Coupland G. and Mizoguchi T. (2004) Antisense suppression of the *Arabidopsis PIF3* gene does not affect circadian rhythms but causes early flowering and increases *FT* expression. *FEBS Letters*, 557: 259–264.

Ogura Y., Komatsu A., Kazunori Z., Nanjo T., Tokutomi S., Wada M. And Kiyosue T. (2008) Blue light diminishes interaction of PAS/LOV proteins, putative blue light receptors in *Arabidopsis thaliana*, with their interacting partners. *J. Plant Res*., 121: 97-105.

Oh E., Kim J., Park E., Kim J-I., Kang C. and Choi G. (2004) *PIL5*, a phytochrome-interacting basic helix–loop–helix protein, is a key negative regulator of seed germination in *Arabidopsis thaliana*. *Plant Cell*, 16: 3045–3058.

Ohgishi M., Saji K., Okada K. and Sakai T. (2004) Functional analysis of each blue light receptor, Cry1, Cry2, Phot1, and Phot2, by using combinatorial multiple mutants in *Arabidopsis*. *Proc. Natl. Acad. Sci. USA*, 101: 2223–2228.

Ohta M., Matsui K., Hiratsu K., Shinshi H. and Ohme-Takagi M. (2001) Repression domains of class II ERF transcriptional repressors share an essential motif for active repression. *Plant Cell*, 13:1959–1968.

Onai K. and Ishiura M. (2005) *PHYTOCLOCK 1* encoding a novel GARP protein essential for the *Arabidopsis* circadian clock. *Genes Cells*, 10: 963–972.

Oster U., Brunner H. and Rudiger W. (1996) The greening process in cress seedlings. V. Possible interference of chlorophyll precursors, accumulated after thujaplicin treatment, with light-regulated expression of Lhc genes. *J. PhotoBiochem. Photobiol*., 36: 255-261.

Oster U., Tanaka R., Tanaka A. and Rudiger W. (2000) Cloning and functional expression of the gene encoding the key enzyme for chlorophyll b biosynthesis (CAO) from *Arabidopsis thaliana. Plant J*., 21: 305–310.

Pagnussat G.C., Yu H.J., Ngo Q.A., Rajani S., Mayalagu S., Johnson C.S., Capron A., Xie L.F., Ye D. and Sundaresan V. (2005) Genetic and molecular identification of genes required for female gametophyte development and function in *Arabidopsis. Development*, 132: 603–614.

Papenbrock J., Grafe S., Kruse E., Hanel F. and Grimm B. (1997) Mg-chelatase of tobacco: identification of a *ChlD* cDNA sequence encoding a third subunit, analysis of the interaction of the three subunits with the yeast two hybrid system, and reconstitution of the enzyme activity by co-expression of recombinant *CHLD*, *CHLH* and *CHLI*. *Plant J.*, 12: 981–990.

Papenbrock J., Mock H.-P., Kruse E. and Grimm B. (1999) Expression studies in tetrapyrrole biosynthesis: inverse maxima of magnesium chelatase and ferrochelatase activity during cyclic photoperiods. *Planta*, 208: 264-273.

Parcy F. and Giraudat J. (1997) Interactions between *ABI1* and the ectopically expressed *ABI3* genes in controlling abscisic acid responses in *Arabidopsis* vegetative tissues. *Plant J.*, 11: 693-702.

Park D.-H., Lim P.O., Kim J.S., Cho D.S., Hong S.H. and Nam H.G. (2003) The *Arabidopsis COG1* gene encodes a Dof domain transcription factor and negatively regulates phytochrome signalling. *Plant J.*, 34: 161–171.

Penfield S., Meissner R., Shoue D., Carpita N. and Bevan M. (2001) *MYB61* is required for mucilage deposition and extrusion in the *Arabidopsis* seed coat. *Plant Cell*, 13: 2777 -2791.

Penfield S., Rylott E.L., Gilday A.D., Graham S., Larson T.R. and Graham I.A. (2004)

Reserve mobilization in the *Arabidopsis* endosperm fuels hypocotyl elongation in the dark, is independent of abscisic acid, and requires *PHOSPHOENOLPYRUVATE CARBOXYKINASE1*. *Plant Cell*, 16: 2705–2718.

Perazza D., Vachon G. and Herzog M., (1998) Gibberellins Promote Trichome Formation by Up-Regulating GLABROUS1 in *Arabidopsis*. *Plant Physiol.*, 117: 375-383.

Perrotta G., Ninu L., Flamma F., Weller J.L., Kendrick R.E., Nebuloso E. and Giuliano G. (2000) Tomato contains homologues of *Arabidopsis* cryptochromes 1 and 2. *Plant Mol. Biol.*, 42: 765–773.

Peterson B.L., Moller M.G., Jensen P.E. and Henningsen K.W. (1999) Identification of the Xan-g gene and expression of the Mg-chelatase encoding genes Xan-f, -g and -h in mutant and wild type barley (Hordeum vulgare L.). *Hereditas*, 131: 165-170.

Petracek M.E., Dickey L.F., Nguyen T.T., Gatz C., Sowinski D.A., Allen G.C. and Thompson W.F. (1998) *Ferredoxin-1* mRNA is destabilised by changes in photosynthetic electron transport. *Proc. Natl. Acad. Sci. USA*, 95: 9009-9013.

Pfannschmidt T., Schutze K., Brost M. and Oelmuller R. (2001) A novel mechanism of nuclear phtosynthesis gene regulation by redox signals from the chloroplast during photosystem stoichiometry adjustment. *J. Biol. Chem*., 276: 36125-36130.

Pfannschmidt T., Schutze K., Fey V., Sherameti I. and Oelmuller R. (2003) Chloroplast redox control of nuclear gene expression- a new class of plastid signals in interorganellar communication. *Antiox. and Redox Signal*, 5: 95-101.

Platten J.D., Foo E., Foucher F., Hecht V., Reid J.B. and Weller J.L. (2005) The cryptochrome gene family in pea includes two differentially expressed *CRY2* genes. *Plant Mol. Biol.*, 59: 683–696.

Pogson B.J., Niyogi K.K., Björkman O. and DellaPenna D. (1998) Altered xanthophyll compositions adversely affect chlorophyll accumulation and nonphotochemical quenching in *Arabidopsis* mutants. *Proc. Natl. Acad. Sci. USA*, 95: 13324-13329.

Pontoppidan B. and Kannangara C.G. (1994) Purification and partial characterization of barley glutamyl-tRNA^{Glu} reductase, the enzyme that directs glutamate to chlorophyll biosynthesis. *Eur. J. Biochem.*, 225: 529–537.

Poppe C., Hangarter R.P., Sharrock R.A., Nagy F. and SchaÈfer E. (1996) The light-induced reduction of the gravitropic growth-orientation of seedlings of *Arabidopsis thaliana (L.) Heynh*. is a photomorphogenic response mediated synergistically by the far-red absorbing forms of phytochromes A and B. *Planta*, 119: 511-514.

Porra R.J. and Lascelles J. (1968) The enzymatic formation of haem in proplastids, chloroplasts and plant mitochondria. *Biochem. J.*, 108: 143-148.

Promnares K., Komenda J., Bumba L., Nebesarova J., Vacha F. and Tichy M. (2006) Cyanobacterial Small Chlorophyll-binding Protein ScpD (HliB) Is Located on the Periphery of Photosystem II in the Vicinity of PsbH and CP47 Subunits. *J. Biol. Chem.*, 281: 32705–32713.

Privat I., Hakimi M.A., Buhot L., Favory J.J. and Mache-Lerbs S. (2003) Characterization of Arabidopsis plastid sigma-like transcription factors SIG1, SIG2 and SIG3. *Plant Mol. Biol.*, 51: 385-399.

Pursiheimo S., Mulo P., Rintamaki E. and Aro E.-M. (2001) Coregulation of light-harvesting complex II phosphorylation and Lhcb accumulation in winter rye. *Plant J.*, 26: 317-327.

Quail P. (2007) Phytochrome-regulated gene expression. J. Integ. Plant Biol., 49: 11–20

Quail P.H. (1997) An emerging molecular map of the phytochromes. *Plant Cell Environ*., 20: 657-665.

Quail P.H. (2002) Phytochrome photosensory networks. *Nature Rev*., 3: 85-93.

Radin N. S., Rittenberg D. and Shemin D. (1950) The Role of Acetic Acid in the Biosynthesis of Heme. *J. Biol. Chem.*, 184: 755–767.

Razem F. A., Luo M., Liu J.-H., Abrams S. R. and Hill R. D. (2004) Purification and characterization of a barley aleurone abscisic acid-binding protein. *J. Biol. Chem.*, 279: 9922–-9929.

Razem F. A., El-Kereamy A., Abrams S. R. and Hill R. D. (2006) The RNA-binding protein FCA is an abscisic acid receptor. *Nature,* 439: 290–294.

Reed J.W., Nagatani A., Elich T.D., Fagan M. and Chory J. (1994) Phytochrome A and phytochrome B have overlapping but distinct functions in *Arabidopsis* development. *Plant Physiol.*, 104: 1139-1149.

Reid J.D. and Hunter C.N. (2004) Magnesium-dependent ATPase activity and cooperativity of magnesium chelatase from *Synechocystis sp. PCC6803*. *J. Biol. Chem*., 279: 26893–26899.

Reid J.D., Siebert C.A., Bullough P.A. and Hunter C.N. (2003) The ATPase activity of the ChlI subunit of magnesium chelatase and formation of a heptameric AAA+ ring. *Biochem.*, 42: 6912–6920.

Reinboth S., Reinboth C., Apel K. and Lebedev N. (1996) Evolution of chlorophyll biosynthesis – the challenge to survive photooxidation. *Cell*, 86: 703-705.

Robson P.R.H. and Smith H. (1996) Genetic and transgenic evidence that phytochromes A and B act to modulate the gravitropic orientation of *Arabidopsis thaliana* hypocotyls. *Plant Physiol.*, 110: 211-216.

Rock C.D. and Zeevaart J.A.D. (1991) The *aba* mutant of *Arabidopsis thaliana* is impaired in epoxy-carotenoid biosynthesis. *Proc. Natl. Acad. Sci. USA*, 88: 7496–7499.

Rockwell N.C., Su Y.S. and Lagarias J.C. (2006) Phytochrome structure and signaling mechanisms. *Ann. Rev. Plant Biol*., 57: 837–858.

Rosler J., Klein I. and Zeidler M. (2007) *Arabidopsis fhl/fhy1* double mutant reveals a distinct cytoplasmic action of phytochrome A. *Proc Natl Acad Sci USA*, 104: 10737–10742.

Rossini S., Casazza A.P., Engelmann E.C.M., Havaux M., Jennings R.C. and Soave C. (2006) Suppression of both *ELIP1* and *ELIP2* in *Arabidopsis thaliana* does not affect tolerance to photoinhibition and photooxidative stress. *Plant Physiol*., 141: 1264–1273.

Rosso M.G., Li Y., Strizhov N., Reiss B., Dekker K. and Weisshaar B. (2003) An *Arabidopsis thaliana* T-DNA mutagenized population (GABI-Kat) for flanking sequence tag-based reverse *Genetics*. *Plant Mol. Biol.*, 53: 247-259.

Rozen R. and Skaletsky H.J. (2000) Primer3 on the WWW for general users and for biologist programmers. In Krawetz S. and Misener S., eds, Bioinformatics Methods and Protocols: Methods in Molecular Biology. Humana Press, Totowa, NJ, pp 365-386.

Runge S., Sperling U., Frick G., Apel K. and Armstrong G.A. (1996) Distinct roles for light-dependent NADPH:protochlorophyllide oxidoreductases (POR) A and B during greening in higher plants. *Plant J.*, 9:513–523.

Ryberg M. and Sundqvist C. (1982) Characterization of prolamellar bodies and prothylakoids fractionated from wheat etioplasts. *Physiol. Plant*, 56: 125–132.

Ryberg, M. and Terry, M.J. (2002) Analysis of protochlorophyllide reaccumulation in the phytochrome chromophore-deficient aurea and yg-2 mutants of tomato by in vivo fluorescence spectroscopy. *Photosynth. Res*. 74, 195–203

Sakai T., Kagawa T., Kasahara M., Swartz T.E., Christie J.M., Briggs W.R., Wada T. and Okada K. (2001) *Arabidopsis nph1* and *npl1*: blue light receptors that mediate both phototropism and chloroplast relocation. *Proc. Natl. Acad. Sci. USA*, 98: 6969–6974.

Sakai T., Wada T., Ishiguro S. and Okada K. (2000) *RPT2*: A signal transducer of the phototropic response in *Arabidopsis*. *Plant Cell*, 12: 225–236.

Sakamoto K. and Briggs W.R. (2002) Cellular and subcellular localization of phototropin 1. *Plant Cell*, 14: 1723–1735.

Sakamoto K. and Nagatani A. (1996) Overexpression of a C-terminal region of phytochrome B. *Plant Mol. Biol.*, 31: 1079–1082.

Salomé P.A., Xie Q. and McClung C.R. (2008) Circadian timekeeping during early *Arabidopsis* development. *Plant Physiol.*, 147: 1110-1125.

Salomon M., Christie J.M., Knieb E., Lempert U. and Briggs W.R. (2000) Photochemical and mutational analysis of the FMN-binding domains of the plant blue light receptor, phototropin. *Biochem.*, 39: 9401–9410.

Sancar A. (1994) Structure and function of DNA photolyase. *Biochem.*, 33, 2–9.

Sang Y., Li Q.H., Rubio V., Zhang Y.C., Mao J., Deng X.W. and Yang H.Q. (2005) N-terminal domain-mediated homodimerization is required for photoreceptor

activity of *Arabidopsis CRYPTOCHROME 1*. *Plant Cell*, 17: 1569–1584.

Sasaki K., Ikeda S., Nishizawa Y. and Hayashi M. (1987) Production of 5-aminolevulinic acid by photosynthetic bacteria. *J. Ferment. Technol*., 65: 511–515.

Sato N., Terasawa K., Miyajima K. and Kabeya Y. (2003) Organization, developmental dynamics and evolution of plastid nucleoids. *Int. Rev. of Cyt*., 232: 217–262.

Sawa M., Nusinow D.A., Kay S.A. and Imaizumi T. (2007) *FKF1* and *GIGANTEA* Complex Formation Is Required for Day-Length Measurement in *Arabidopsis*. *Science*, 318: 261–265.

Schaffer R., Ramsay N., Samach A., Corden S., Putterill J., Carré I.A. and Coupland G. (1998) The late elongated hypocotyl mutation of *Arabidopsis* disrupts circadian rhythms and the photoperiodic control of flowering. *Cell*, 93: 1219–1229.

Schindler U., Menkens A. E., Beckmann H. Ecker J. R. and Cashmore A. R. (1992) Heterodimerization between light-regulated and ubiquitously expressed *Arabidopsis* GBF bZIP proteins. *Eur. J. Mol. Biol.*, 11: 1261–1273.

Schoefs B. and Franck F. (2003) Protochlorophyllide reduction: mechanisms and evolution. *Photochem. Photobiol.*, 78: 543–557.

Schuenemann D., Amin P., Hartmann E. and Hoffman N.E. (1999) Chloroplast SecY is complexed to SecE and involved in the translocation of the 33 kDa but not the 23 kDa subunit of the oxygen-evolving complex. *J. Biol. Chem*., 274: 12177–12182.

Schultz T.F., Kiyosue T., Yanovsky M., Wada M. and Kay S.A. (2001) A role for *LKP2* in the circadian clock of *Arabidopsis*. *Plant Cell*, 13: 2659–2670.

Seo, H.-S. Yang J.-Y., Ishikawa M., Bolle C., Ballesteros M.L. and Chua N.-H. (2003) *LAF1* ubiquitination by *COP1* controls photomorphogenesis and is stimulated by SPA1. *Nature*, 423: 995–999.

Sessions A., Burke E., Presting G., Aux G., McElver J., Patton D., Dietrich B., Ho P., Bacwaden J., Ko C., Clarke J.D., Cotton D., Bullis D., Snell J., Miguel T., Hutchison D., Kimmerly B., Mitzel T., Katagiri F., Glazebrook J., Law M. and

Goff S.A. (2002) A high-throughput *Arabidopsis* reverse *Genetics* system. *Plant Cell*, 14: 2985-2994.

Shalitin D., Yang H., Mockler T.C., Maymon M., Guo H., Whitelam G.C. and Lin C. (2002) Regulation of *Arabidopsis cryptochrome 2* by blue-light-dependent phosphorylation. *Nature*, 417: 763–767.

Sharp R.E. and LeNoble M.E. (2002) ABA, ethylene and the control of shoot and root growth underwater stress. *J. Exp. Bot*., 53: 33–37.

Sharrock R.A. and Clack T. (2002) Patterns of expression and normalized levels of the five *Arabidopsis* phytochromes. *Plant Physiol.*, 130: 442–456.

Sharrock R.A. and Quail P.H. (1989) Novel phytochrome sequences in *Arabidopsis thaliana*: structure, evolution, and differential expression of a plant regulatory photoreceptor family. *Genes Dev*., 3: 1745-1757.

Shen Y-Y. , Wang X-F., Wu F-Q, Du S-Y, Cao Z, Shang Y, Wang X-L, Peng C-C., Yu X-C., Zhu S-Y, Fan R-C, Xu Y-H & Zhang D-P. (2006) The Mg-chelatase H subunit is an ABA receptor. *Nature*, 443: 823-826.

Shepherd M., McLean S., Hunter C.N. (2005) Kinetic basis for linking the first two enzymes of chlorophyll biosynthesis. *FEBS Letters*, 272: 4532–4539.

Shiina T., Tsunoyama Y., Nakahira Y. and Khan M.S. (2005) Plastid RNA polymerases, promoters, and transcription regulators in higher plants. *Int. Rev. of Cyt*., 244: 1–68.

Shin J., Kim K., Kang H., Zulfugarov I. S., Bae G., Lee C. H., Lee D. and Choi G. (2009) Phytochromes promote seedling light responses by inhibiting four negatively-acting phytochrome-interacting factors. *Proc. Natl. Acad. Sci. USA*, 106: 7660-7665.

Shinomura T., Nagatani A., Hanzawa H., Kubota M., Watanabe M. and Furuya M. (1996) Action spectra for phytochrome A- and B-specific photoinhibition of seed germination in *Arabidopsis thaliana*. *Proc. Natl. Acad. Sci. USA*, 93: 8129-8133.

Shinomura T., Uchida K. and Furuya M. (2000) Elementary processes of photoperception by phytochrome A for highirradiance response of hypocotyl elongation in *Arabidopsis*. *Plant Physiol.*, 122: 147-156.

Singh D.V., Cornah J.E., Hadingham S. and Smith A.G. (2002) Expression analysis of the two ferrochelatase genes in *Arabidopsis* in different tissues and under stress conditions reveals their different roles in haem biosynthesis. *Plant Mol. Biol*., 50: 773–788.

Sharrock R.A. and Clack T. (2004) Heterodimerization of type II phytochromes in *Arabidopsis. Proc. Natl. Acad. Sci. USA*, 101: 11500–11505.

Shen H., Moon J. and Huq E. (2005) PIF1 is regulated by light-mediated degradation through the ubiquitin-26S proteasome pathway to optimize photomorphogenesis of seedlings in *Arabidopsis. Plant J*., 44: 1023–35.

Shen H., Zhu L., Castillon A., Majee M., Downie B. and Huq E. (2008) Light-induced phosphorylation and degradation of the negative regulator PHYTOCHROME-INTERACTING FACTOR1 from *Arabidopsis* depend upon its direct physical interactions with photoactivated phytochromes. *Plant Cell*, 20: 1586-1602.

Smillie R.M. and Hetherington S.E. (1999) Photoabatement by anthocyanin shields photosynthetic systems from light stress. *Photosynthetica*, 36: 451-463.

Smith A.G., Santana M.A., Wallace-Cook A.D.M., Roper J.M. and Labbe-Bois R. (1994) Isolation of a cDNA encoding chloroplast ferrochelatase from *Arabidopsis thaliana* by functional complementation of a yeast mutant. *J. Biol. Chem*. 269: 13405–13413.

Smith H., and Whitelam G.C. (1997) The shade avoidance syndrome: multiple responses mediated by multiple phytochromes. *Plant Cell Environ*., 20: 840-844.

Sokolove P. G. and Bushell W. N. (1978). The chi square periodogram: its utility for analysis of circadian rhythms. *J. Theoretical Biol*., 72: 131-160

Somers D.E., Kim W.Y. and Geng R. (2004) The F-Box Protein *ZEITLUPE* Confers Dosage-Dependent Control on the Circadian Clock, Photomorphogenesis, and Flowering Time. *Plant Cell*, 16: 769–782.

Somers D.E., Schultz T.F., Milnamow M. and Kay S.A. (2000) *ZEITLUPE* encodes a novel clock-associated PAS protein from *Arabidopsis*. *Cell*, 101: 319–329.

Somers D.E., Webb A.A.R., Pearson M. and Kay S. (1998) The shortperiod mutant, *toc1-1*, alters circadian clock regulation of multiple outputs throughout

development in *Arabidopsis thaliana*. *Development*, 125: 485–494.

Stephenson P.G., Fankhauser C. and Terry M.J. (2009) PIF3 is a repressor of chloroplast development, *Proc Natl. Acad. Sci. USA*, 106: 7654-7659.

Stracke R., Werber M. and Weisshaar B. (2001) The R2R3-MYB gene family in *Arabidopsis thaliana*. Curr. Opin. *Plant Biol*., 4: 447–456.

Strand A., Asami T., Alonso J., Ecker J.R. and Chory J. (2003) Chloroplast to nucleus communication triggered by accumulation of Mg-protoporphyrin IX. *Nature*, 421: 79–83.

Strayer C., Oyama T., Schultz T.F., Raman R., Somers D.E., Más P., Panda S., Kreps J.A. and Kay S.A. (2000) Cloning of the *Arabidopsis* clock gene *TOC1*, an autoregulatory response regulator homolog. *Science*, 289: 768–771.

Streatfield S.J., Weber A., Kinsman E.A., Husler R.E. Li J., Post-Beitenmiller D., Kaiser W.M., Pyke K.A., Flugge U.-I. and Chory J. (1999) The phosphenolpyruvate/phosphate translocator is required for phenolic metabolism, palisade cell development, and plastid-dependent nuclear gene expression. *Plant Cell*, 11: 1609-1621.

Su Y.S. and Lagarias J.C. (2007) Light-independent phytochrome signaling mediated by dominant GAF domain tyrosine mutants of *Arabidopsis* phytochromes in transgenic plants. *Plant Cell*, 19: 2124-2139.

Sundqvist C. and Dahlin C. (1997) With chlorophyll from prolamellar bodies to light-harvesting complexes. *Physiol. Plant*, 100: 748–759.

Susek R.E., Ausubel F.M. and Chory J. (1993) Signal transduction mutants of *Arabidopsis* uncouple nuclear *CAB* and *RBCS* expression from chloroplast development. *Cell*, 74: 787–799.

Suzuki G., Yanagawa Y., Kwok S.F., Matsui M. and Deng X.W. (2002a) *Arabidopsis* COP10 is a ubiquitin-conjugating enzyme variant that acts together with COP1 and the COP9 signalosome in repressing photomorphogenesis. *Genes Dev.*, 16: 554-559.

Suzuki J.Y., Ytterberg A.J., Beardslee T.A., Allison L.A., Wijk K.J. and Maliga P. (2004) Affinity purification of the tobacco plastid RNA polymerase and in vitro reconstitution of the holoenzyme. *Plant J.*, 40: 164–172.

Suzuki T., Masuda T., Singh D.P., Tan F.C., Tsuchiya T., Shimada H., Ohta H., Smith A.G. and Takamiya K. (2002b) Two types of ferrochelatase in photosynthetic and nonphotosynthetic tissues of cucumber: their difference in phylogeny, gene expression, and localization. *J. Biol. Chem.*, 277: 4731–4737.

Suzuki T., Tatsuru M., Hachiro I., Hiroshi S., Hiroyuki O. and Ken-ichiro T. (2000) Overexpression, enzymatic properties and tissue localization of a ferrochelatase of cucumber. *Plant Cell Physiol*., 41: 192–199.

Swarbreck D., Wilks C., Lamesch P., Berardini T.Z., Garcia-Hernandez M., Foerster H., Li D., Meyer T., Muller R., Ploetz L., Radenbaugh A., Singh S., Swing V., Tissier C., Zhang P. and Huala E. (2008) The *Arabidopsis* Information Resource (TAIR): gene structure and function annotation. *Nucleic Acids Res.*, 36: 1009-1014.

Takos A.M., Jaffe F.W., Jacob S.R., Bogs J., Robinson S.P. and Walker A.R. (2006) Light-induced expression of a MYB gene regulates anthocyanin biosynthesis in red apples. *Plant Physiol*., 142: 1216–1232.

Tamura K., Dudley J., Nei M. and Kumar S. (2007) MEGA4: molecular evolutionary genetics analysis (MEGA) software version 4.0. *Mol. Biol. Evol*., 24: 1596–1599.

Tanaka R. and Tanaka A. (2007) Tetrapyrrole biosynthesis in higher plants. *Annu. Rev. Plant Biol.*, 58: 321-346.

Tanaka R., Yoshida K., Nakayashiki T., Masuda T., Tsuji H., Inokuchi H. and Tanaka A. (1996) Differential Expression of Two hemA mRNAs Encoding Glutamyl-tRNA Reductase Proteins in Greening Cucumber Seedlings. *Plant Physiol.*, 110: 1223-1230.

Tanaka R., Yoshida K., Nakayashiki T., Tsuji H., Inokuchi H., Okada K. and Tanaka A. (1997) The third member of the *hemA* gene family encoding glutamyl-tRNA reductase is primarily expressed in roots in *Hordeum vulgare*. *Photosyn. Res.*, 53: 161-171.

Taylor B.L. and Zhulin I.B. (1999) PAS domains: internal sensors of oxygen, redox potential, and light. *Microbiol. Mol. Biol. Rev*., 63: 479–506.

Tepperman J. M., Hudson M.E., Khanna R., Zhu T., Chang S.H., Wang X. and Quail

P.H. (2004) Expression profiling of *phyB* mutant demonstrates substantial contribution of other phytochromes to red-light-regulated gene expression during seedling de-etiolation. *Plant J.*, 38: 725–739.

Tepperman J. M., Zhu T., Chang H.-S., Wang X. and Quail P. H. (2001) Multiple transcription-factor genes are early targets of phytochrome A signalling. *Proc. Natl. Acad. Sci. USA*, 98: 9437–9442.

Tepperman J.M., Hwang Y.S. and Quail P.H. (2006) phyA dominates in transduction of red-light signals to rapidly responding genes at the initiation of *Arabidopsis* seedling de-etiolation. *Plant J.*, 48: 728–742.

Terry M.J. and Kendrick R.E. (1999) Feedback inhibition of chlorophyll synthesis in the phytochrome chromophore deficient *aurea* and *yellow-green-2* mutants of tomato. *Plant Physiol.*, 119: 143–152.

Terry M.J., Ryberg M., Raitt C.E. and Page A.M. (2001) Altered etioplast development in phytochrome chromophore-deficient mutants. *Planta*, 214: 314–325.

Tiryaki I. and Staswick P.E. (2002) An *Arabidopsis* mutant defective in jasmonate response is allelic to the auxin-signaling mutant *axr1*. *Plant Physiol.*, 130:887–894.

Tissier A.F., Marillonnet S., Klimyuk V., Patel K., Torres M.A., Murphy G. and Jones J.D.G. (1999) Multiple Independent Defective *Suppressor-mutator* Transposon Insertions in *Arabidopsis*: A Tool for Functional Genomics. *Plant Cell*, 11: 1841-1852.

Toledo-Ortiz G., Huq E. and Quail P.H. (2003) The *Arabidopsis* basic/helix-loop-helix transcription factor family. *Plant Cell*, 15: 1749–1770.

Tzvetkova-Chevolleau1 T., Franck F., Alawady A.E., Dall'Osto L., Carriere F., Bassi R., Grimm B.,Nussaume L., and Havaux M. (2007) The light stress-induced protein *ELIP2* is a regulator of chlorophyll synthesis in *Arabidopsis thaliana*. *Plant J.*, 50: 795–809.

Ujwal M.J., McCormac A.C., Goulding A., Kumar A.M., Soll D. and Terry M.J. (2002) Divergent regulation of the *HEMA* gene family encoding glutamyl-tRNA reductase in *Arabidopsis thaliana*: expression of *HEMA2* is regulated by

sugars, but is independent of light and plastid signalling. *Plant Mol. Biol*., 50: 83-91.

Usami T., Mochizuki N., Kondo M., Nishimura M. and Nagatani A. (2004) Cryptochromes and phytochromes synergistically regulate *Arabidopsis* root greening under blue light. *Plant Cell Physiol*., 45: 1798–1808.

Valverde F., Mouradov A., Soppe W., Ravenscroft D., Samach A. and Coupland G. (2004) Photoreceptor regulation of *CONSTANS* protein in photoperiodic flowering. *Science*, 303: 1003–1006.

van Lis R., Atteia A., Nogaj L.A. and Beale S.I. (2005) Subcellular localization and light-regulated expression of protoporphyrinogen IX oxidase and ferrochelatase in *Chlamydomonas reinhardtii*. *Plant Physiol.*, 139: 1946–1958.

Vasileuskaya Z., Oster U. and Beck C.F. (2005) Mg-Protoporphyrin IX and heme control *HEMA*, the gene encoding the first specific step of tetrapyrrole biosynthesis, in Chlamydomonas reinhardtii. *Eukaryotic Cell*, 4: 1620-1628.

Verdecia M.A., Larkin R.M., Ferrer J.L., Riek R., Chory J. and Noel J.P. (2005) Structure of the Mg-Chelatase Cofactor *GUN4* Reveals a Novel Hand-Shaped Fold for Porphyrin Binding. *PLoS Biol*., 3: 777-789.

Verwoerd T.C., Dekker B.M., and Hoekema A. (1989) A small scale procedure for the rapid isolation of plant RNAs. *Nucleic Acids Res*, 17:2362.

Viczián A. Kircher S., Fejes E., Millar A.J., Schäfer E., Kozma-Bognár L. and Nagy F. (2005) Functional characterization of phytochrome interacting factor 3 for the *Arabidopsis thaliana* circadian clockwork. *Plant Cell Physiol*., 46: 1591–1602.

Vierstra R.D. and Quail P.H. (1986) The protein. In Kendrick R.E. and Kronenberg G.H.M., eds, Photomorphogenesis in plants. Martinus Nijhoff, Dordrecht, pp. 35-60.

Vinti G., Hills A., Campbell S., Bowyer J.R., Mochizuki N., Chory J. and Lopez-Juez E. (2000) Interactions between *hy1* and *gun* mutants of *Arabidopsis*, and their implications for plastid/nuclear signalling. *Plant J.*, 24: 883-894.

Von Arnim A.G. and Deng X.W. (1994) Light inactivation of *Arabidopsis* photomorphogenic repressor *COP1* involves a cell-specific regulation of its

nucleocytoplasmic partitioning. *Cell*, 79: 1035–1045.

Von Arnim A.G., Deng X.W. and Stacey M.G. (1998) Cloning vectors for the expression of green fluorescent protein fusion proteins in transgenic plants. *Gene*, 221: 35–43

Vothknecht U.C., Kannangara C.G. and von Wettstein D. (1998) Barley glutamyl $tRNA^{Glu}$ reductase: mutations affecting haem inhibition and enzyme activity. *Phytochem.*, 47: 513–519.

Walker C.J. and Willows R.D. (1997) Mechanism and regulation of Mg-chelatase. *Biochem. J.*, 327: 321–333

Walker C.J., Yu G.H. and Weinstein J.D. (1997) Comparative study of heme and Mg–protoporphyrin (monomethyl ester) biosynthesis in isolated pea chloroplasts: effects of ATP and metal ions. *Plant Physiol. Biochem.*, 35: 213–221.

Wang H. and Deng X.W. (2002b) *Arabidopsis FHY3* defines a key phytochrome A signaling component directly interacting with its homologous partner *FAR1*. Eur. *J. Mol. Biol.*, 21: 1339–1349.

Wang H. and Deng X.W. (2002a) Phytochrome signalling mechanism April 4, 2002. The *Arabidopsis* Book. Rockville, MD: American Society of Plant Biologists. doi: 10.1199/tab.0111, http://www.aspb.org/publications/*Arabidopsis*/

Wang H., Ma L.G., Li J.M., Zhao H.Y. and Deng X.W. (2001) Direct interaction of *Arabidopsis* cryptochromes with *COP1* in light control development. *Science*, 294: 154–158.

Wang Z.-Y. and Tobin E. (1998) Constitutive expression of the *CIRCADIAN CLOCK ASSOCIATED* (*CCA1*) gene disrupts circadian rhythms and suppresses its own expression. *Cell*, 93: 1207–1217.

Ward J. M., Cufr C. A., Denzel M. A. and Neff M. M. (2005) The Dof transcription factor *OBP3* modulates phytochrome and cryptochrome signaling in *Arabidopsis*. *Plant Cell*, 17: 475–485.

Waters M. and Pyke K. (2004) Plastid development and differentiation. In: Møller SG, ed, Plastids. Oxford, UK: Blackwell, pp 30–59.

Waters M.T., Moylan E.C. and Langdale J.A. (2008) GLK transcription factors

regulate chloroplast development in a cell-autonomous manner. *Plant J.*, 56: 432-444.

Wei N., Chamovitz D.A. and Deng X.W. (1994) *Arabidopsis COP9* is a component of a novel signaling complex mediating light control of development. *Cell*, 78: 117–124.

Wei, N., and Deng, X.W. (1996). The role of the COP/DET/FUS genes in light control of *Arabidopsis* seedling development. *Plant Physiol.* 112: 871-878.

Weisshaar B., Armstrong G.A., Block A., da Costa e Silva O. and Hahlbrock K. (1991) Light-inducible and constitutively expressed DNA-binding proteins recognizing a plant promoter element with functional relevance in light responsiveness. *Eur. J. Mol. Biol.*, 10: 1777–1786.

Weller J.L., Terry M.J., Rameau C., Reid J.B. and Kendrick R.E. (1996) The phytochrome-deficient *pcd1* mutant of pea is unable to convert heme to biliverdin IXa. *Plant Cell*, 8: 55–67.

Whatley J.M. (1978) A suggested cycle of plastid developmental interrelationships. *New Phytol*ogist, 80: 489–502.

Whitelam G.C., Johnson E., Peng J., Carol P., Anderson M.L., Cowl J.S. and Harberd N.P. (1993) Phytochrome A null mutants of *Arabidopsis* display a wild-type phenotype in white light. *Plant Cell*, 5: 757-768.

Wilde A., Mikolajczyk S., Alawady A., Lokstein H. and Grimm B. (2004) The *gun4* gene is essential for cyanobacterial porphyrin metabolism. *FEBS Letters*, 571: 119-123.

Willows R.D. and Beale S.I. (1998) Heterologous expression of the *Rhodobacter capsulatus BchI-D,* and *-H* genes that encode magnesium chelatase subunits and characterization of the reconstituted enzyme. *J. Biol. Chem.*, 273: 34206–34213.

Wu S.H. and Lagarias J.C. (2000) Defining the bilin lyase domain: lessons from the extended phytochrome superfamily. *Biochem.*, 39: 13487–13495.

Xie D.X., Feys B.F., James S., Nieto-Rostro M. and Turner J.G. (1998) *COI1*: An *Arabidopsis* gene required for jasmonate-regulated defense and fertility. *Science*, 280: 1091–1094.

Xu H., Vavilin D., Funk C. and Vermaas W. (2002) Small Cab-like proteins regulating tetrapyrrole biosynthesis in the cyanobacterium Synechocystis sp. PCC 6803. *Plant Mol. Biol.*, 49: 149–160.

Yadav V., Mallappa C., Gangappa S. N., Bhatia S. and Chattopadhyay, S. A (2005) basic helix-loop-helix transcription factor in *Arabidopsis, MYC2*, acts as a repressor of blue light-mediated photomorphogenic growth. *Plant Cell*, 17: 1953–1966.

Yamaguchi R., Nakamura M., Mochizuki N., Kay S.A. and Nagatani A. (1999) Light dependent translocation of a phytochrome B-GFP fusion protein to the nucleus in transgenic *Arabidopsis*. *J. Cell Biol*., 145: 437–445.

Yamashino T., Matsushika A., Fujimori T., Sato S., Kato T., Tabata S. and Mizuno T. (2003) A Link between circadian controlled bHLH factors and the *APRR1/TOC1* quintet in *Arabidopsis thaliana*. *Plant Cell Physiol*., 44: 619–629.

Yang H. Q., Tang R.H. and Cashmore A.R. (2001) The signalling mechanism of *Arabidopsis* Cry1 involves direct interaction with *COP1*. *Plant Cell*, 13: 2573–2587.

Yang H. Q., Wu Y.J., Tang R.H., Liu D., Liu Y. and Cashmore A.R. (2000) The C-termini of *Arabidopsis* cryptochromes mediate a constitutive light response. *Cell*, 103: 815–827.

Yanhui C., Xiaoyuan Y., Kun H., Meihua L., Jigang L., Zhaofeng G., Zhiqiang L., Yunfei Z., Xiaoxiao W., Xiaoming Q., Yunping S., Li Z., Xiaohui D., Jingchu L., Xing-Wang D., Zhangliang C., Hongya G. and Li-Jia Q. (2006) The MYB transcription factor superfamily of *Arabidopsis*: expression analysis and phylogenetic comparison with the rice MYB family. *Plant Mol. Biol*., 60: 107–124

Yanovsky M.J., and Kay S.A. (2003) Living by the calendar: how plants know when to flower. *Nat. Rev. Mol. Cell Biol*., 4: 265–275.

Yanovsky M.J., Luppi J.P., Kirchbauer D., Ogorodnikova O.B., Sineshchekov V.A., Adam E., Kirche S., Staneloni R.J., Schäfer E., Nagy F. and Casal J.J. (2002) Missense mutation in the PAS2 domain of phytochrome A impairs subnuclear

localization and a subset of responses. *Plant Cell*, 14: 1591–1603.

Yao D., Kieselbach T., Komenda J., Promnares K., Herna´ndez Prieto M.A., Tichy M., Vermaas W., and Funk C. (2007) Localization of the Small CAB-like Proteins in Photosystem II. *J. of Biol. Chem*., 282: 267–276.

Yeh K.C. and Lagarias J.C. (1998) Eukaryotic phytochromes: Light-regulated serine/threonine protein kinases with histidine kinase ancestry. *Proc. Natl. Acad. Sci. USA*, 95: 13976–13981.

Yi C. and Deng X.W. (2005) *COP1* - from plant photomorphogenesis to mammalian tumorigenesis. *Trends Cell Biol*., 15: 618–625.

Yoshida R., Umezawa T., Mizoguchi T., Takahashi S., Takahashi F. and Shinozaki K. (2006) The regulatory domain of SRK2E/OST1/ SnRK2.6 interacts with *ABI1* and integrates abscisic acid (ABA) and osmotic stress signals controlling stomatal closure in *Arabidopsis*. *J. Biol. Chem*., 281: 5310–5318.

Zeidler M., Bolle C. and Chua N.H. (2001) The phytochrome a specific signaling component PAT3 is a positive regulator of *Arabidopsis* photomorphogenesis. *Plant Cell Physiol*., 42: 1193–1200.

Zhou Q., Hare P.D., Yang S.W., Zeidler M., Huang L.F. Chua N.H. (2005) *FHL* is required for full phytochrome A signaling and shares overlapping functions with FHY1. *Plant J.*, 43: 356–370.

Zhu Y.,Tepperman J.M., Fairchild C.D. and Quail P.H. (2000) Phytochrome B binds with greater apparent affinity than phytochrome A to the basic helix-loop-helix factor PIF3 in a reaction requiring the PAS domain of PIF3. *Proc. Natl. Acad. Sci. USA*, 97: 13419–13424.

Zimmermann I. M., Heim M. A., Weisshaar B. and Uhrig J. F. (2004) Comprehensive identification of *Arabidopsis thaliana* MYB transcription factors interacting with R/B-like BHLH proteins. *Plant J.*, 40: 22–34.

Zimmermann P., Hennig L., and Gruissem W. (2005) Gene expression analysis and network discovery using Genevestigator. *Trends Plant Sci.*, 9: 407-409.